

The Interaction of Hepatitis C Virus and
Intracellular Lipid Metabolism

by

Jonathan Ramsay Hubb

A thesis presented for the degree of Doctor of
Philosophy

In

The Faculty of Biomedical and Life Sciences

At the

University of Glasgow

Infection and Immunity
University of Glasgow
120 University Place
Glasgow
G12 8TA

“I would like to dedicate this thesis to my parents, George and Gillian Hubb, who have given immense support through the years.”

Summary

Chronic hepatitis C virus (HCV) infection causes inflammation of the liver, which can lead to fibrosis and cirrhosis over time. Whether liver damage is a consequence of viral infection or is due to an immune mediated response is not clear. Steatosis is a histopathological feature often found in HCV infected patients. Steatosis is the accumulation of intracytoplasmic lipid droplets within hepatocytes. It has been linked to the progression of fibrosis (Adinolfi et al., 2001). Steatosis was found significantly more frequently in patients infected with HCV genotype 3 than those infected with genotype 1 (Mihm et al., 1997). Currently there is no cell-based method of investigating the life cycle of HCV genotype 3 and transgenic mice studies have been restricted to genotype 1 proteins.

Three chimpanzees experimentally infected with HCV showed differential regulation of genes encoding enzymes concerned with lipid metabolism. Treatment of HCV genotype 1b replicon containing cells with cerulenin, which inhibits fatty acid synthase, reduced replication of HCV RNA in a dose dependent manner (Su et al., 2002).

Polyunsaturated fatty acids (PUFAs) have recently been shown to inhibit replication of a genotype 1b sub-genomic replicon. PUFAs are essential and are known to down regulate lipogenic gene expression. However, the inhibitory effect of PUFAs on HCV RNA levels was thought to be independent of their inhibitory effect on fatty acid biosynthesis (Kapadia et al., 2005).

To assess the effects of cerulenin and fatty acids on HCV genome replication we measured replication by northern blot analysis of total HCV RNA and using a replicon expressing luciferase. HCV protein production was measured by western blot using an antibody to the NS5A protein. To examine the effect on long chain fatty acid synthesis, we measured incorporation of ^{14}C acetate into

total cellular lipids. Toxicity was assayed using mitochondrial enzyme activity assays.

Treating genotype 1b replicon cells with 30 μM cerulenin led to inhibition of fatty acid biosynthesis and a corresponding inhibition of HCV RNA replication. However, at this level of cerulenin, only 60 % of cells were viable. Inhibition of fatty acid biosynthesis was not observed at the lower non-toxic concentrations of 10 μM and 3 μM , although HCV replication was inhibited. These experiments were repeated using more frequent media changes and different suppliers of cerulenin. However, similar results were obtained. When a genotype 2a replicon expressing cell line (JFH1) was treated with cerulenin it was possible to inhibit both HCV RNA levels and fatty acid biosynthesis in a dose dependant manner. Furthermore cerulenin treatment of an alternative genotype 1b expressing cell line led to an inhibition of fatty acid synthesis in a dose dependent manner.

We have studied the effects of the PUFAs, docosahexaenoic acid (DHA) and eicosapentaenoic acid (EPA) on JFH1 replicon (genotype 2) replication using both constitutive and transiently expressing systems. For a control, we used oleic acid, a monounsaturated fatty acid. DHA and EPA administered from 3 to 100 μM concentration showed a dose responsive reduction in replication. Fatty acid biosynthesis was also inhibited; however at the higher concentrations there were reductions in cell viability. Oleic acid did not effectively inhibit JFH1 replication even though, at higher concentrations, there was a small reduction in ^{14}C acetate incorporation. Initial immunofluorescence data indicated that NS5A foci were not disrupted by treatment of cells with PUFAs and fluorescence recovery after photobleaching data indicated that PUFAs did not increase ER membrane fluidity.

A genotype 3 genome was amplified and sequenced using reverse-transcription polymerase chain reaction (RT-PCR) from the serum of an HCV genotype 3a-infected patient. A majority sequence was assembled and amplification products were ligated into vectors, which were sequenced and mutated back to the majority sequence. The genotype 3 genome was modified by the exclusion of the structural genes and non-structural (NS) protein 2. A bicistronic replicon was created in which the HCV internal ribosome entry site (IRES) controlled

expression of the selectable marker neomycin phosphotransferase and the encephalomyocarditis virus IRES controlled expression of the NS proteins. RNA replicons were transcribed and electroporated into HuH-7 cell lines. A transiently expressing replicon was made by replacing the neomycin gene with a firefly luciferase gene. Cells expressing neither the constitutively nor the transiently genotype 3 replicon sustained viral replication.

In conclusion cerulenin inhibited HCV replication at levels, which did not inhibit fatty acid biosynthesis and were not toxic. There was toxicity at cerulenin concentrations, which inhibited fatty acid biosynthesis. Cerulenin inhibited replication but by a mechanism other than inhibition of fatty acid biosynthesis. Cells with different passage histories were shown to behave differently to each other in their response to drugs.

The PUFAs, DHA and EPA exert an inhibitory effect on HCV replicon replication and fatty acid biosynthesis at non-toxic levels. Oleic acid did not inhibit HCV replication at equivalent concentrations. The mechanism behind PUFA inhibition of HCV RNA levels is still unknown.

An attempt to create genotype 3 constitutively and transiently expressing replicon HuH-7 cell lines failed.

Table of Contents

1	INTRODUCTION	1
1.1	Background	1
1.1.1	Viral hepatitis	1
1.1.2	Non-A, non-B hepatitis	4
1.1.3	Identification of hepatitis C virus genome	5
1.1.4	Morphology of HCV	6
1.1.5	Classification of HCV	6
1.2	HCV genome	7
1.2.1	Untranslated sequences	7
1.2.2	Structural proteins	14
1.2.3	Non-structural proteins	18
1.3	Model Systems for Investigating the HCV Life Cycle	23
1.3.1	HCV in cell culture	23
1.3.2	HCV infection of Chimpanzees	24
1.3.3	Establishing an HCV genotype 1b expressing cell line	25
1.3.4	Establishing an HCV 1a replicon expressing cell line	27
1.3.5	JFH1 genotype 2a isolate	28
1.4	HCV genotypes and quasispecies	29
1.5	HCV Infection	32
1.5.1	Acute and chronic infection	32
1.5.2	Treatment	32
1.6	Disease pathology	33
1.6.1	Steatosis	33
1.6.2	HCV and steatosis	36
1.7	Microarray analysis of livers from acutely HCV infected chimpanzees	39
1.7.1	Lipid metabolism and HCV replication	41
1.8	Lipid metabolism	47
1.8.1	Sterol Regulatory Element-Binding Proteins	47
1.8.2	Peroxisome proliferator activated receptor	49
1.8.3	Liver X Receptor and insulin	52
1.8.4	Lipid Transport	53
1.9	Aims and objectives of my project	55
2	MATERIALS AND METHODS	57
2.1	Materials	57
2.1.1	Bacterial Strains	57
2.1.2	Vectors	57
2.1.3	Enzymes and Kits for DNA modification	58
2.1.4	Mammalian cell lines and culture media	58
2.1.5	Human Serum	59
2.1.6	Radiochemicals	59
2.1.7	Antibodies and stains	59
2.1.8	Chemicals	60
2.1.9	Solutions	61
2.1.10	Other materials and apparatus	63
2.1.11	Synthetic Oligonucleotides	63
2.2	Manipulation of RNA and DNA	71
2.2.1	Extraction of viral RNA from serum	71
2.2.2	Extraction of cellular RNA	72

2.2.3	Reverse transcription of RNA	73
2.2.4	Quantification and Amplification of DNA	74
2.2.5	PCR reactions	76
2.2.6	Automated DNA sequencing	93
2.2.7	TA Cloning of PCR products	93
2.2.8	Small Scale preparation of plasmid DNA (minipreps)	94
2.2.9	Large scale preparation of plasmid DNA (midiprep)	95
2.2.10	Restriction enzyme digestion of DNA	96
2.2.11	Dephosphorylation of linearised plasmid DNA	97
2.2.12	Ligation reactions	97
2.2.13	Separation and purification of DNA fragments	98
2.2.14	Quantification of nucleic acids	100
2.2.15	Site-Directed Mutagenesis	101
2.2.16	In-vitro Transcription	102
2.2.17	Separation of RNA and Northern Blot Analysis	103
2.3	Preparation and transformation of <i>E.coli</i> DH5-α cells	107
2.3.1	Preparation of <i>E.coli</i> DH5- α competent cells	107
2.3.2	Transformation of competent <i>E.coli</i> cells	107
2.3.3	Making glycerol stocks	108
2.4	Maintenance of mammalian cell culture	108
2.4.1	Freezing of cells	108
2.5	Electroporation of mammalian cells	108
2.6	Transfection of mammalian cells	109
2.7	Luciferase assay	109
2.8	Lipid extraction and assay	110
2.8.1	Folch total lipid extraction	110
2.8.2	Measuring fatty acid biosynthesis	110
2.8.3	Conjugation of BSA to free fatty acids	111
2.9	MTT (3-(4,5-dimethylthiazol-2-yl) Assay	111
2.10	Protein analysis by SDS-PAGE and western blotting	112
2.10.1	Preparation of cell extracts	112
2.10.2	SDS-PAGE	112
2.10.3	Western Blotting	113
2.10.4	Immunodetection	113
2.11	Immunofluorescence	114
2.12	Fluorescence Recovery after photobleaching (FRAP)	115
2.13	Computer software	115
3	OPTIMISING TECHNIQUES	117
3.1	Enriching a 5-15 genotype 1b expressing cell line	117
3.2	Interferon “curing” of replicon expressing cells	119
3.3	Optimising the MTT (3-(4,5-dimethylthiazol-2-yl) assay	119
3.4	Optimisation of the fatty acid biosynthesis assay	121
4	THE EFFECT OF CERULENIN ON THE REPLICATION OF HCV EXPRESSING CELL LINES	126

4.1	Introduction	126
4.2	Cerulenin treatment of HCV genotype 1b replicon expressing cells	128
4.2.1	Cerulenin inhibition of HCV RNA replication did not correlate with its ability to inhibit fatty acid synthesis	128
4.2.2	Cerulenin was unable to inhibit fatty acid biosynthesis, even when media was changed every 8 hours	131
4.2.3	Cerulenin from different suppliers affected cells differently with respect to HCV replication, fatty acid synthesis and toxicity	132
4.3	Cerulenin treatment of HCV genotype 2a replicon expressing cells	135
4.3.1	Cerulenin inhibition of fatty acid biosynthesis appears to correlate with inhibition of HCV replication	135
4.3.2	Similar results were shown using cells transiently expressing replicon	141
4.4	Tandem treatment of 2 different HCV 1b replicon expressing cells was cell and not HCV type specific	146
4.5	NS5A localisation in cerulenin treated cells	148
4.6	Discussion	151
5	THE EFFECT OF FATTY ACIDS ON THE REPLICATION OF THE JFH1 HCV REPLICON	157
5.1	Introduction	157
5.2	Docosahexaenoic Acid (DHA) treatment cells expressing genotype 2a replicons	160
5.2.1	DHA treatment of cells constitutively expressing HCV 2a replicon	160
5.2.2	DHA treatment of cells transiently expressing HCV 2a replicon	163
5.3	Eicosapentaenoic Acid (EPA) treatment of cells expressing genotype 2a replicons	167
5.3.1	EPA treatment of cells constitutively expressing HCV 2a replicon	167
5.3.2	EPA treatment of cells transiently expressing HCV 2a replicon	170
5.4	Oleic Acid (OLA) treatment of cells expressing genotype 2a replicons	173
5.4.1	OLA treatment of cells constitutively expressing HCV 2a replicon	173
5.4.2	OLA treatment of cells transiently expressing HCV 2a replicon	177
5.5	NS5A localisation in fatty acid treated cells	180
5.5.1	PUFA treatment of cell constitutively expressing genotype 2a replicon	180
5.5.2	OLA treatment of cell constitutively expressing genotype 2a replicon	181
5.6	The effect of fatty acid treatment on ER membrane fluidity	186
5.7	Discussion	191
6	MAKING A GENOTYPE THREE EXPRESSING REPLICON HUH-7 CELL LINE	199
6.1	Introduction	199
6.2	Selection of a patient serum	200
6.3	Assembling a majority sequence	201
6.3.1	Amplification of the genome	201
6.3.2	Assembling majority sequence	205
6.4	Assembling a genotype 3 replicon that would express constitutively in cells	211
6.4.1	Cloning the genome	211
6.4.2	Modification of the isolate GM genome	218
6.4.3	Sequencing plasmid constructs and site directed mutagenesis	228
6.4.4	Cloning the genome into pSP64 Poly-A Vector	237

6.4.5	Incorporation of the NS5A adaptive mutation and NS5B null mutation	237
6.5	In-vitro transcription of constitutive replicons and electroporation into cells	240
6.6	Assembling a genotype 3 replicon that would transiently express in cells	245
6.6.1	Fusion of the 5'UTR to firefly luciferase	245
6.6.2	Removal of an internal Scal restriction enzyme site in the luciferase gene	249
6.6.3	Assembly of the transient replicon	249
6.7	In-vitro transcription of transient replicons and electroporation into cells	254
6.8	Discussion	254
7	FINAL DISCUSSION	263
7.1	Different cell responses to the fatty acid synthase inhibitor, cerulenin	263
7.2	Mechanisms by which PUFAs mediate inhibition of HCV replication	264
7.3	Variability between experiments	267
7.4	Assembling a genotype three replicon	267
7.5	Future experiments	268
7.6	Lipid metabolism and other viruses	269
8	APPENDIX	272
8.1	GM isolate sequence (appendix 1)	272
8.2	References	276

List of Figures and Tables

Figure		Page number
1.1	Phylogenetic tree indicating the relationship between hepatitis C virus and other <i>Flaviviridae</i> .	8
1.2	Diagrammatic representation of the HCV genome where gene products and function are shown below the genome.	9
1.3	Secondary structure of the 5'UTR.	10
1.4	Phylogenetic tree showing the HCV genotypes and subtypes.	31
1.5	Sections of a human liver with and without steatosis	34
1.6	Diagram of cholesterol and fatty acid biosynthesis	42
1.7	Spacefill representation of three fatty acids	46
1.8	Representation of the interaction between LXR, INSIG and SREBP-1c.	50
1.9	Diagrammatic representation of the interactions between PPAR, RXR, LXR and SREBP-1c.	54
3.1	Enrichment of a 5-15 genotype 1b expressing cell line.	118
3.2	Interferon alpha 2b treatment of 5-15 1b cells.	120
3.3	Optimisation of MTT assay for cell seeding number.	122
3.4	Cellular and media lipid extractions following incubation with radiolabelled acetate.	123
3.5	Effect of increasing the amount of radiolabelled acetate on incorporation.	125
4.1	Effect of cerulenin treatment on 1b and 1b-C expressing cell lines.	130
4.2	Effect of frequent cerulenin medium changes on 1b and 1b-C expressing cell lines.	134
4.3	Effect of cerulenin treatment obtained from a different supplier on 1b and 1b-C expressing cell lines.	137
4.4	Effect of cerulenin treatment on 2a and 2a-C expressing cell lines.	140
4.5	Effect of cerulenin on a transient JFH1 and JFH1 GND expressing replicon.	143
4.6	Absolute luciferase values for cerulenin treated transient replicon.	145
4.7	Effect of cerulenin treatment on another 1b expressing cell line.	147
4.8	Effect of cerulenin treatment for 3 days on NS5A localisation in 2a cells using immunofluorescence.	150
4.9	Diagrammatic representation of the fatty acid biosynthesis pathway.	154
5.1	Treatment of 2a and 2a-C expressing cell lines with Docosahexaenoic Acid (DHA): BSA conjugates.	162
5.2	Treatment with DHA:BSA conjugates on transient JFH1 and JFH1 "GND" replicons.	166
5.3	Treatment of 2a and 2a-C expressing cell lines with Eicosapentaenoic Acid (EPA): BSA conjugates.	169
5.4	Treatment with EPA:BSA conjugates on transient JFH1 and JFH1 "GND" replicons.	172
5.5	Treatment of 2a and 2a-C expressing cell lines with Oleic Acid (OLA): BSA conjugates.	176

5.6	Treatment with OLA:BSA conjugates on transient JFH1 and JFH1 “GND” replicons.	179
5.7	Effect of DHA treatment for 3 days on NS5A localisation in 2a cells using indirect immunofluorescence.	183
5.8	Effect of EPA treatment for 3 days on NS5A localisation in 2a cells using indirect immunofluorescence.	185
5.9	Effect of OLA treatment for 3 days on NS5A localisation in 2a cells using indirect immunofluorescence.	188
5.10	Fluorescence recovery after photobleaching (FRAP) analysis on the effect of fatty acids on ER membrane mobility.	190
6.1	Diagrammatic representation of RTs, and PCRs performed on GM genotype 3 genome.	204
6.2	Agarose gel electrophoresis of diagnostic PCRs	206
6.3	Agarose gel electrophoresis of PCR optimisation	207
6.4	Multiple sequence alignment and electropherograms of sequencing products	210
6.5	Diagrammatic representation of cDNAs and PCRs performed on GM genotype 3 genome.	213
6.6	Diagrammatic representation of plasmid diagrams for pCR2.1(5’GT3), pCR2.1(3’GT3) and pGEM linker.	214
6.7	Agarose gel electrophoresis of GM genotype 3 HCV 5’ and 3’ ends of the genome.	215
6.8	Agarose gel electrophoresis of an restriction enzyme digest of pCR2.1(3’GT3).	217
6.9	Multiple sequence alignment 3’ UTR sequences.	220
6.10	Electropherogram of sequence of a pGEM T7(5’GT3)	221
6.11	Diagrammatic representation of the cloning of pGEMT7-emcv.	223
6.12	Diagrammatic representation of the cloning of pGEMT7-emcv-NS3.	224
6.13	Diagrammatic representation of the cloning of pGEM(3’GT3)-X.	226
6.14	Diagrammatic representation of the cloning of pUC18T7-NS3.	227
6.15	Diagrammatic representation of the cloning of pUC18(3’GT3).	229
6.16	Electropherograms of sequence obtained from site-directed mutagenesis of mutation 4.	233
6.17	Diagrammatic representation of the cloning of pUC18T7-NS3 Mut1-2.	234
6.18	Diagrammatic representation of the cloning of pUC18(3’GT3)Mut3-7.	236
6.19	Diagrammatic representation of the cloning of pSP64GM-NS3.	238
6.20	Diagrammatic representation of the cloning of pSP64GM.	239
6.21	Diagrammatic of representation of the RNA of genotype 3 replicons (GM, GM* and GM GND).	241
6.22	Agarose gel electrophoresis of in-vitro transcribed RNA.	242
6.23	Colony formation assay for HuH7 electroporated with genotypes 1 and 3 replicons.	244
6.24	Diagrammatic representation of PCRs used to fuse the coding sequence of isolate GM to the firefly luciferase gene.	247
6.25	Diagrammatic representation of the cloning of pGEMT7-luc-emcv.	248
6.26	Diagrammatic of representation of the removal of the <i>ScaI</i> restriction enzyme site in the firefly luciferase gene	251

6.27	Diagrammatic representation of the cloning of pSP64lucNS3.	252
6.28	Diagrammatic representation of the cloning of pSP64GM-luc.	253
6.29	Diagrammatic of representation of the RNA of genotype 3 transient replicons (GM, GM* and GM GND).	255
6.30	Graphs showing luciferase activity for electroporation for JFH1 and GM replicons into HuH7.	257
Table		Page
6.1	Position of non-synonymous mutations and their location in the genome.	206

Acknowledgements

Firstly, I would like to thank my supervisor, Dr Liz McCrudden, for her patience, encouragement and advice during the course of my project and more recently for her help proof reading this thesis. I would also like to extend my thanks to Dr John McLauchlan for his advice during helpful discussions and his scientific expertise as well as providing help with various techniques and supplying with reagents and cell lines.

I would like also to thank my other supervisor, Prof Victor Zammit, for his knowledge and advice on lipid metabolism and providing me with techniques specialised to this area, which without would have made the project impossible.

I am indebted to Dr Paul Target-Adams for his help with showing me the luciferase assay which he had developed and Dr Steeve Boulant for his help using the infectious system and immunofluorescence.

I would also like to thank the lab members, past and present, of Liz and John's labs for their help during the course of my project, particularly Carol Anne Smith and Dr Graham Hope.

Finally, I would like to thank all the friends (Sarah, Ali, Tanya, Amanda B, Louise, David and James) I have made in the MRC virology unit and the University of Glasgow for their support and companionship during the week, especially on a Friday night after work. Last but not least I would like to thank the huge support from Ross and my flatmates (Lynsay, Zoe and Jen) who have allowed me to come home to a happy environment, which has made the hard work of this PhD possible.

Author's Declaration

Unless otherwise stated, all the work presented in this thesis is by the author's own effort.

Jonathan Ramsay Hubb

August 2007

Abbreviations

%	percentage
¹⁴ C	Carbon isotope (14)
³² P	Phosphate isotope (32)
ALT	Alanine transaminase
A	Wavelength absorbance
AA	Arachidonic Acid
ACC	Acetyl Co carboxylase
AOX	Acetyl Co oxidase
Apolipoprotein B	ApoB
Apolipoprotein E	ApoE
B	Base(s)
BMI	Body mass index
C-	Carboxy-
CoA	Co enzyme A
cDNA	Copy deoxyribonucleic acid
Cpm	Counts per minute
CPT-1	Carnitine palmitoyl transferase-I
DHA	Docosahexaenoic acid
DMF	Dimethylformamide
DMSO	Dimethyl sulfoxide
DNA	Deoxyribonucleic acid
<i>E. coli</i>	<i>Escherichia coli</i>

EDTA	Ethylenediamine tetraacetic acid
EPA	Eicosahexaenoic acid
ER	Endoplasmic reticulum
FAS	Fatty Acid Synthase
FTase	Farnesyltransferase
GAPDH	glyceraldehyde-3-phosphate dehydrogenase (GAPDH),
GGTase	Geranylgeranyltransferase
GM	Glasgow Male
HAV	Hepatitis A virus
HBV	Hepatitis B virus
HCV	Hepatitis C Virus
HDL	High Density lipoprotein
HDV	Hepatitis D virus
HEV	Hepatitis E virus
HGV	Hepatitis G virus
HIV	human immunodeficiency virus
HMG	3-hydroxy-3-methyl-glutaryl
Hrs	Hours
HuH-7	Human hepatoma cells
IFN- α	Pegelated Interferon-alpha 2b
INSIG	Insulin induced gene
IRES	Internal ribosome entry site
K	Kilodalton

Kb	Kilobase
Kg	Kilogram(s)
L	Litre(s)
LDL	Low density lipoprotein
Mg	Milligram
MGB	Minor groove binding
MHC	Major histocompatibility complex
Min	Minute(s)
ml	Millilitre(s)
MTP	Microsomal transfer protein
MTT	(3-(4,5-dimethylthiazol-2-yl)
N-	Amino-
NANBH	Non-A, non-B hepatitis
NAFLD	Non-alcoholic fatty liver disease
NASH	Non-alcoholic steatohepatitis
Nm	Nanometre(s)
NS	Non-structural
°C	Degrees Celsius
OLA	Oleic acid
ORF	Open reading frame
PCR	Polymerase chain reaction
PPAR	Peroxisome proliferators activated receptor
PUFA	Polyunsaturated fatty acid

RNA	Ribonucleic acid
ROS	Reactive oxygen species
RXR	Retanoid X receptor
RT	Reverse transcription
RT	Reverse transcription
SCAP	SREPB cleavage-activating protein
SDS	Sodium dodecyl sulphate
SRB-1	Scavenger receptor class B type 1
SREBP	Sterol regulatory element binding protein
ss	Single stranded
SSC	Sodium chloride sodium citrate
SVR	Sustained viral response
TAG	Triacylglycerol
TOFA	5-(Tetradecyloxy)-2-furoic acid
UTR	Untranslated region
μCu	Microcurrie(s)
Mg	Microgram(s)
ml	Microlitre(s)
μM	Micromolar
VLDL	Very low density lipoprotein
ZA	Zaragozic acid

Chapter one

1 Introduction

1.1 Background

The liver has vascular, metabolic, secretory and excretory functions. Therefore, if it becomes diseased, the effects can be experienced throughout the body. Liver disease can have many causes including drugs, alcohol, viral infection, autoimmune disease, toxins or be congenital. Signs of liver disease include; jaundice, cholestasis (reduced or stopped bile flow), liver enlargement, portal hypertension (increased blood pressure in the portal blood vessels which supply the liver with blood from the intestine), ascites (a build up of fluid in the abdominal cavity due to leakage from the liver and intestine) and hepatic encephalopathy (the deterioration of brain function due to toxins not being removed from the blood by the liver). Of these, jaundice is the most common sign of acute liver disease and sometimes is the only one. Jaundice is caused by high levels of bilirubin in the bloodstream leading to yellowing of the skin and the whites of the eyes. However, jaundice is not common in chronic liver disease.

Hepatitis or inflammation of the liver caused by viral infection was first described in the 1900s. The group of viruses associated with hepatitis are called the hepatitis viruses. These are not related taxonomically but by their primary disease site. They cause inflammation of the liver and the hepatocyte is their major target host cell.

1.1.1 Viral hepatitis

Hepatitis A virus (HAV) was described in the early 1900s by its clinical symptoms and faecal oral route of transmission. However, virus particles were first

isolated from a faecal sample only in 1973 (Alter et al., 1975). During the incubation period, the virus replicates within the liver but is undetected by the immune system. Clinical symptoms of infection are manifested only when an immune response occurs. The virus is efficiently removed by the adaptive immune system. An increased risk of exposure occurs in people living in developing countries, illicit drug users, actively homosexual men and patients who require treatment with clotting factors. The HAV genome was cloned and sequenced in 1987, which allowed its classification in the *Picornaviridae* family of viruses. HAV is a positive-sense, single-stranded (ss) RNA non-enveloped virus. Its 7500 nucleotide genome is packaged into an icosahedral protein capsid. The genome contains a single open reading frame (ORF) which encodes a polyprotein flanked by 5' and 3' untranslated regions (UTR). The polyprotein is cleaved to produce structural proteins, which make up the capsid of the virus, and non-structural (NS) proteins concerned with replication (Martin A, 2006).

Hepatitis B virus (HBV) first came to notice in 1883 when patients developed jaundice after inoculation with a contaminated batch of smallpox vaccine (Shepard et al., 2006). The route of infection is by blood or body fluid percutaneously (through the skin) or contact with mucosal surfaces leading to an acute or chronic infection. HBV has a circular, partially double-stranded DNA genome of 3200 bp, which encodes 7 known viral proteins. It has been classified in the *Hepadnaviridae* family of viruses. Currently, the World Health Organisation estimates that there are 350 million people infected worldwide (WHO, 2007). It is estimated that 500,000 - 700,000 people die each year from HBV infection. HBV causes one third of all cases of liver cirrhosis and a half of all cases of hepatocellular carcinoma. Methods for combating the virus rely on prevention more than treatment as an effective vaccine is available. Unfortunately, treatment of infected patients is complicated by development of viral resistance to drugs and is expensive (Shepard et al., 2006).

Hepatitis D virus (HDV) was first discovered in 1977 after the recognition of the delta antigen in patients with HBV infection. Initially, delta antigen was thought to be an HBV antigen but was found to be the core of another virus (Taylor J, 2006). Like HBV, HDV infection occurs by percutaneous or mucosal surface contact with blood or blood products. HDV infection can occur only in the presence of a helper HBV, as it requires the HBV surface antigen (HBsAg) for

envelopment. The two viruses have unrelated genomes. HDV is a ss circular RNA virus with a genome of 1679 bases, which shows similarities in genome structure and replication to plant virioids. Patients who are infected with HBV and HDV at the same time are said to be “co-infected”. If a patient already chronically infected with HBV becomes infected with HDV, it is termed “super infection”. Acute HDV “super-infection” causes an increase in the rate of liver disease and increases the chance of fulminant hepatitis. Fulminant hepatitis is a clinical syndrome in which necrosis of large numbers of liver cells causes a severe impairment of hepatic function resulting in liver failure and encephalopathy. Of HBV infected patients worldwide, it is roughly estimated that 20 million people are infected with HDV. Treatment of chronic HDV infections is ineffective and prevention is based on vaccination against HBV.

Hepatitis E virus (HEV) is a waterborne disease found mostly in developing countries. HEV shows a similar epidemiological spread to HAV. However, it was first identified that this was another enteric hepatitis virus in the early 1990's. Initially known as enterically transmitted non-A, non-B hepatitis, the genome of HEV was eventually cloned and was classified in a new genus, *Hepeviridae*. It is transmitted via the faecal oral route. HEV causes acute hepatitis in young adults with most risk to pregnant woman. HEV is a non-enveloped, spherical ss RNA virus similar to caliciviruses. The genome is 7500 bases in length and contains three overlapping ORFs used to produce viral proteins. The 5' and 3' ends of the genome contain short UTRs (Subrat K, 2006).

Hepatitis G virus (HGV) was first reported in 1995 by Genelabs, Inc after being isolated from patients with chronic hepatitis but no other viral hepatitis infection. This was later followed by the isolation of another similar virus called GBV-C by Abbott laboratories. Both HGV and GBV-C were different isolates of the same virus and were classified in the *Flaviviridae* family of viruses. However, HGV is now referred to as GBV-C as further epidemiological studies revealed it has no association with liver disease. GBV-C is a positive ss RNA virus which produces a polyprotein of approximately 3000 amino acid. Interest in GBV-C is because it has a similar gene organisation and shares amino acid homology with HCV. Although not pathogenic, surprisingly it has been shown epidemiologically that GBV-C co-infection with human immunodeficiency virus

(HIV) improves the life expectancy of patients by an unknown mechanism (Stapleton et al., 2004).

1.1.2 Non-A, non-B hepatitis

With the discovery of HAV and HBV, serological markers were developed, which allowed their diagnosis. However, it became clear that a form of hepatitis clinically indistinguishable from HAV and HBV infection, occurred without the presence of serological markers for HAV or HBV (Feinman et al., 1980). This type of hepatitis was called non-A, non-B hepatitis (NANBH). The evidence for another hepatitis virus mounted over the 1970s. With the advent of highly sensitive radioimmunoassay, which was used to detect HAV and HBV infections, it soon became apparent that many patients who had developed hepatitis after blood transfusion were HAV and HBV negative. A reduction in post-transfusion hepatitis was achieved by the elimination of blood donors who were positive for HBV. However, 11 % of the remaining patients developed hepatitis, which was serologically unrelated to HAV or other hepatotropic viruses such as Epstein-Barr virus or human cytomegalovirus. Although 4 cases were identified later as HBV infections, the remaining 89 % of patients with hepatitis developed the disease by an unknown agent. The study suggested that another virus was causing hepatitis in these patients (Alter et al., 1975).

As there was no laboratory test for NANBH, diagnosis relied on exclusion of other causes of hepatitis. The infectious nature of NANBH was demonstrated by the intravenous inoculation of chimpanzees with serum from patients presumed to be infected with NANBH. It was possible to take infected serum from the first chimpanzee and infect another resulting in the second chimpanzee displaying alanine transaminase (ALT) levels, which were twice that of what would be considered to be the upper limit of normal (40 IU/L). ALT is a liver enzyme, which can be used to assess damage to the liver by measuring increased levels in the serum. Inactivation of NANBH infectivity with chloroform suggested that the infectious agent might have a lipid envelope (Feinstone et al., 1983).

1.1.3 Identification of hepatitis C virus genome

Viral antigens and antibodies associated with NANBH failed to be identified using all conventional immunological methods. However, Choo et al (1989) used recombinant DNA cloning technologies to identify the infectious agent of NANBH. They believed that a lack of antigen had led to the failure to identify the virus so they created a cDNA library to isolate the NANBH sequence.

Initially, chimpanzee plasma was obtained that had displayed a high infectious titre. The plasma was subjected to extensive ultracentrifugation to allow the pelleting of even small viruses and nucleic acid. The resultant pellet was denatured after which cDNA was made using either DNA polymerase or reverse transcriptase and random primers since the nature of the viral nucleic acid was unknown. A cDNA expression library was then made by cloning the cDNAs into bacteriophage λ gt11 and expression in *Escherichia coli* (*E.coli*). The cDNA libraries were then screened for clones expressing viral antigens with serum from “pedigreed” chronically-infected NANBH patients. After screening 10^6 clones, a positive cDNA clone (clone 5-1-1) was identified along with a larger clone (clone 81) which overlapped clone 5-1-1.

Both these clones failed to hybridise to DNA from extracted human and chimpanzee cells, indicating that neither was derived from the host genome. Furthermore, the cDNA clones hybridised to total RNA extracted from infectious chimpanzees but not RNA extracted from uninfected chimpanzees. This signal was lost on ribonuclease treatment but not on deoxyribonuclease treatment indicating it was an RNA molecule. It was estimated that this hybridised RNA was 0.00001 % (w/w) of that of the total liver RNA. The maximum size of the RNA was estimated to be 10,000 nucleotides after gel electrophoresis of RNA derived from an infected chimpanzee and hybridisation to clone 81. Further analyses showed the genome to be ss, contain a single open reading frame, and be of positive-sense. Thus, the infectious agent of NANBH had been isolated and was called hepatitis C virus (HCV).

1.1.4 Morphology of HCV

The exact morphology of the HCV virion is not known. Virus-like particles associated with NANBH had been described as early as 1975 (Feinman et al., 1980). The lack of cell-based infectious systems has meant slow progress in characterising the HCV virion. Initial filtration experiments had indicated that the infectivity of an inoculum was not reduced on passage through an 80 nm filter. The use of smaller filters indicated the diameter of the virion to be approximately 30-60 nm (He et al., 1987). In fact, various diameters have been reported ranging from 20-100 nm. This suggests that there may be different forms of the virion. The different structural forms of the virion might also alter its association with host immunoglobulins and lipoproteins resulting in differences in the buoyant density of the virion (Diedrich G., 2006). Separation of serum by density centrifugation found HCV RNA to be associated with fractions containing very low density lipoprotein (VLDL), low density lipoprotein (LDL), and high density lipoprotein (HDL). HCV RNA was found with buoyant gradients of $\leq 1.06 \text{ g}\cdot\text{mL}^{-1}$ associated with LDL and VLDL and $1.06 - 1.17 \text{ g}\cdot\text{mL}^{-1}$ associated with HDL (Nielsen et al., 2006). Chimpanzees infected with separated fractions showed infectious particles to be present in the lowest density ($< 1.10 \text{ g}\cdot\text{mL}^{-1}$). The study indicated that HCV particles associated with lipoproteins were the most infectious (Hijikata et al., 1993).

More recently, virus-like particles have been produced directly from transfection of cells with full-length HCV genotype 2a genomes (Wakita et al., 2005). The density of these particles was found to be between $1.15 - 1.17 \text{ g}\cdot\text{mL}^{-1}$ and they had a diameter of 55 nm.

1.1.5 Classification of HCV

Originally, Choo et al (1989) had described a positive-sense, ss RNA enveloped virus, which could be classified in the *Togaviridae* or *Flaviviridae* family of viruses. Analysis of derived amino acid sequences found similarities in non-structural protein 3 between HCV and dengue type 2 virus, a member of the *Flaviviridae* family. Furthermore, HCV contained some protein sequence similarity to members of this family within the pestivirus group. Based on these features, HCV was classified into the *Flaviviridae* family of viruses (Miller et al.,

1990). Although some sequence similarity was present, this classification was based mainly on genome organisation. Gene organisation and hydrophobicity profiles suggested HCV was closer to the pestivirus genus than the flaviviruses (Choo et al., 1991). Currently, the *Flaviviridae* family contains 3 genera with HCV classified in its own genus, Hepacivirus. This had been decided based on sequence and phylogenetic analysis, which showed the HCV sequence was too divergent from either pestivirus or flavivirus to be assigned to either genus (Figure 1.1) (Robertson et al., 1998).

1.2 HCV genome

The HCV genome is approximately 10 kb in length (Figure 1.2). It comprises a single open reading frame (ORF), which is flanked by two UTRs. There are 10 gene products with structural genes found at the 5' end of the ORF and non-structural (NS) genes at the 3' end.

1.2.1 Untranslated sequences

1.2.1.1 5' UTR

The 5' terminus of the HCV genome was described as being highly conserved between genotypes with similarity to pestivirus 5' sequences (Choo et al., 1991; Han et al., 1991). The structure of the HCV 5'UTR, was described, based on primary sequence, as stem-loop structures which may act as a platform for ribosome binding (Figure 1.3).

Studies with picornaviruses had determined a similar highly conserved structure in the 5' UTR, which was responsible for directing translation of viral genes (internal ribosome entry site - IRES) (Brown et al., 1992; Reynolds et al., 1995). IRES elements were first discovered in the picornavirus, polio, where a *cis*-acting element found in the 5' end of the genome was responsible for translation of the internal ORF (Pelletier et al., 1988). The IRES allowed translation of viral proteins in a cap-independent manner. There were some subtle differences between the HCV IRES and those of polioviruses. A comparison of the HCV IRES with other viral IRES structures found similarities with pestivirus IRES elements, which consist of 2 main stem loops. However, picornavirus IRES

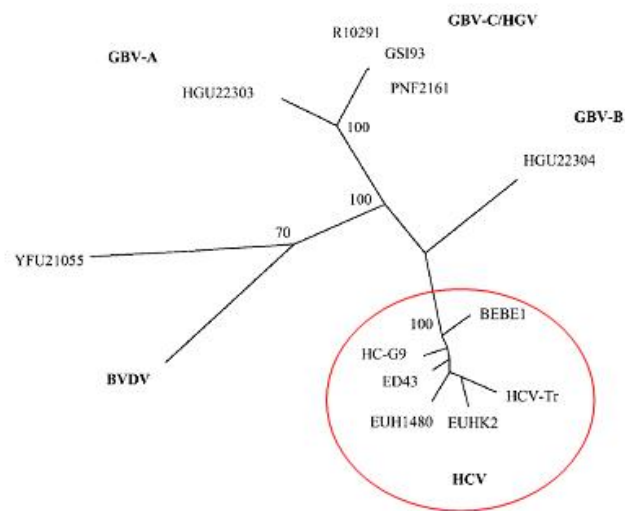


Figure 1.1. A phylogenetic tree indicating the relationship between hepatitis C virus (HCV) isolates which are members of hepacivirus, yellow fever virus (YFU21055) which is a flavivirus, bovine viral diarrhoea (BVDV) which is a pestivirus and the related GBV viruses (GBV-A, GBV-C and GBV-B). HCV isolates are encircled where all genotypes are represented: genotype 1 (HC-G9), genotype 2 (BEBE1), genotype 3 (HCV-Tr), genotype 4 (ED43), genotype 5 (EUH1480) and genotype 6 (EUHK2) (B. Robertson 1998)

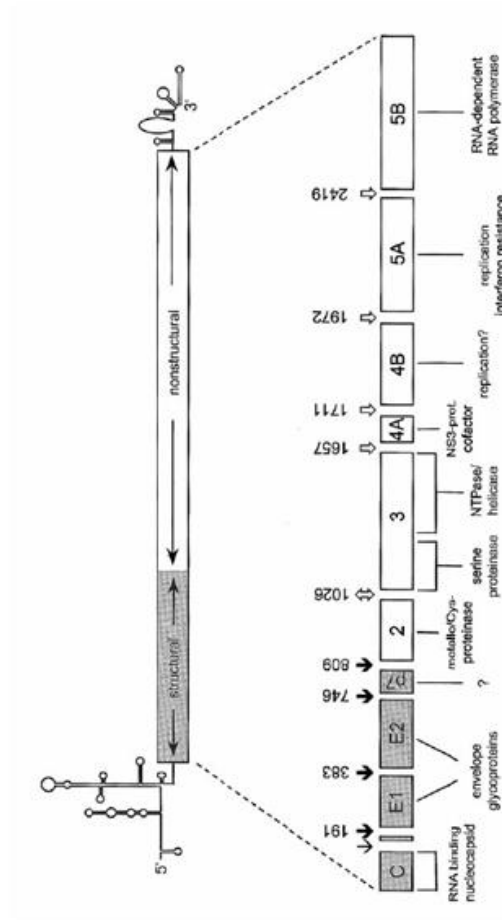


Figure 1.2. A diagrammatic representation of the HCV genome where gene products and function are shown below the genome. Structural genes are located at the 5' end of the genome and non-structural genes are located at the 3' end of the genome. The open reading frame is flanked by two untranslated regions. Polyprotein cleavage sites for (↓) host cell signalases, the host (↕) signal peptide peptidase, (↕) the NS2-3 protease and (↕) the NS3/4A protease complex are marked. Numbers above the arrows refer to the P1 positions of the corresponding cleavage sites (numbering according a genotype 1) (Bartenschlager *et al.*, 2001).

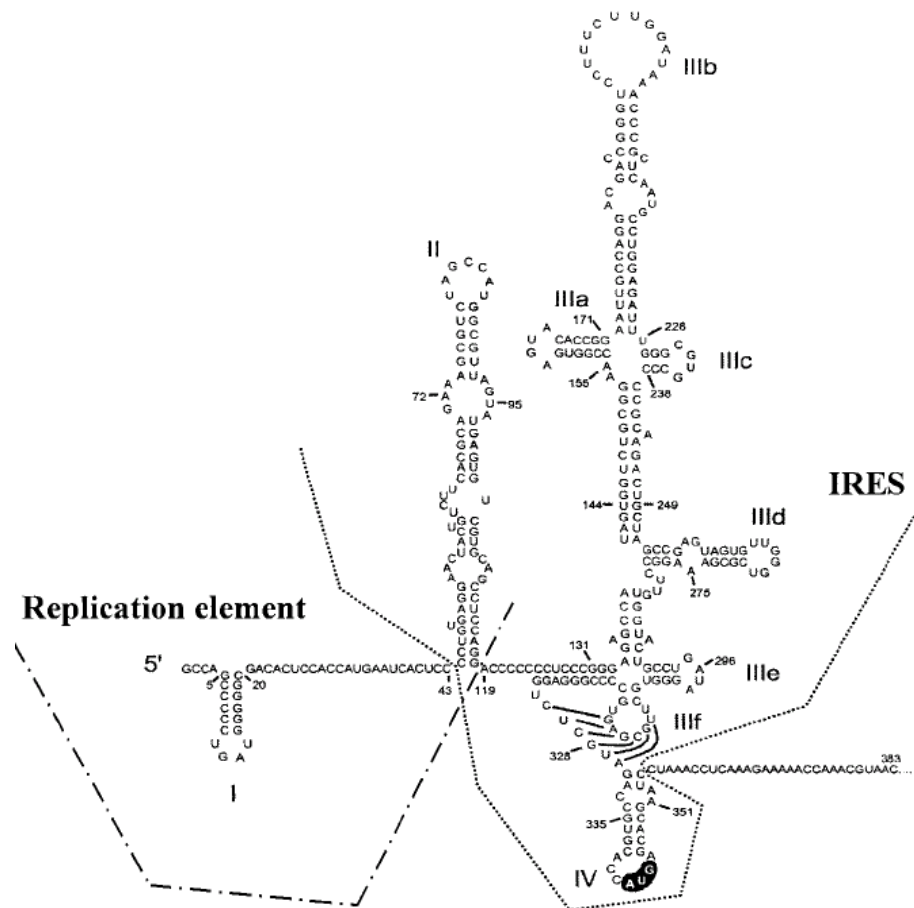


Figure 1.3. The secondary structure of the 5'UTR indicating the replication element, the IRES and the start of the downstream ORF. The replication element comprises domains I and II and the IRES, domains II to domain IV. The start codon of the ORF is highlighted (Kim et al., 2001).

elements, although similar to each other, were morphologically different to pestivirus IRES elements. They were generally larger and required more direct interactions between domains (Beales et al., 2003).

Studies by Reynolds et al (1995) showed that nucleotides 40 - 370 were required for IRES function. Bicistronic mRNAs containing the HCV IRES were used to control translation of a slightly truncated form of an influenza NS protein. Deletion of sequences 3' to the start of the ORF, at nucleotide 342, reduced protein expression (Reynolds et al., 1995).

A combination of thermodynamic, phylogenetic and biochemical methods were used to obtain the secondary structure of the HCV IRES (Brown et al., 1992). The HCV 5' UTR was proposed to comprise 4 domains (I, II, III and IV). Domain I contained a small stem loop structure, which along with domain II, was essential for replication (Kim et al., 2002). Domain II was also involved in translation. Domains II and III contained numerous complex stem loop structures, which were necessary for ribosome binding. Domain III had much secondary structural homology with the pestiviruses even though there was little primary sequence homology (Brown et al., 1992). It also contained a pseudoknot, which was essential for translation at the base of the stem loop situated just 5' of the initiation codon (Wang et al., 1995). Domain IV had a short stem loop structure, which contained the initiation codon. This stem loop could be destabilised with little effect on translation. However, a mutation, which stabilised the structure, caused a decrease in translation efficiency (Honda et al., 1996).

Most mRNAs are translated by association of the cap binding protein complex to mRNA at its 5' terminus after recognition of the guanine cap (a methylated guanine in reverse polarity). This complex then recruits the 43S ribosome to the mRNA, which scans along the transcripts to the initiation codon. Binding of a 40S ribosome unit directly to the IRES without ribosome scanning was described as a unique feature of IRES elements (Honda et al., 1996). Translation of the HCV IRES is thought to be mediated by the interaction of stem loops, pseudoknots and the initiation codon with the 40S ribosomal protein. Ribosomal protein S5/S9, the guanine exchange factor eIF-2B and eIF-2 γ have all been shown to be co-factors for HCV translation (Fukushi et al., 2001; Kruger et al., 2000).

1.2.1.23' Untranslated region

The 3' UTR is described as a tripartite structure containing a variable region after the stop codon, a poly (U) tract and a highly conserved element termed the X tail. Originally, the 3' UTR was described as a short 54 base structure, which consisted of some direct and inverted repeats followed by a short poly(U) stretch (Takamizawa et al., 1991). However, the 3' UTR was found to be longer by Tanaka et al (1995) when primer extension experiments revealed a 98 base structure at the 3' end. The sequence was able to form stem loop secondary structures and was termed the X tail. The X tail was confirmed as being the authentic 3' end of the genome after its presence was found in serum samples from infected patients with no additional sequence beyond it (Tanaka et al., 1996). Sequence conservation of the X tail between genotypes was high with between 98 -100 % homology (Kolykhalov et al., 1996; Yamada et al., 1996). The structure of the X tail suggested that the 3' terminal 42 nucleotides formed a stable stem loop structure, which had high thermodynamic stability. This indicated that the structure might be involved in important interactions for the viral life cycle. The 56 nucleotides 5' to these nucleotides were able to form multiple conformations and therefore were suggested to have multiple possible protein or RNA interactions (Blight et al., 1997).

RNA/protein interactions with polypyrimidine tract protein (PTB), involved in RNA processing and translation, were described between the X tail and the poly(U) tract by performing UV cross-linking experiments (Ito et al., 1997; Luo G, 1999; Tsuchihara et al., 1997). Both primary RNA sequence and the stem-loop structures of the 3' UTR were shown to be important for this interaction. However, some studies showed an interaction only with the poly(U) tract (Gontarek et al., 1999). The ability of PTB to bind to the 5' UTR suggested that it may be able to control translation through interactions between the two UTRs. Initially, PTB was suggested to enhance translation of the 5' UTR. A *cis*-acting X tail was shown to enhance translation through its interaction with PTB. Removal of the X tail or mutation of the PTB binding site decreased but did not abolish translation (Ito et al., 1998). In contrast, another study found that the 3' UTR down-regulated IRES-dependent translation of viral RNA (Murakami et al., 2001). Murakami et al (2001) found that PTB could down-regulate IRES function although through another binding site thought to be situated in the coding region.

Furthermore, mutational studies of the X region indicated PTB does not participate in 3' UTR mediated enhanced IRES translation (Brocard et al., 2006).

Other proteins have been implicated in interactions with the 3' UTR. La protein, which recognises oligouridylate sequences, was able to bind the HCV poly(U) and protect it from RNA degradation by ribonucleases (Spangberg et al., 2001). Heterogeneous nuclear ribonucleoprotein C (hnRNP C) was also found to interact with the poly(U) tract of the 3' UTR. The exact function of this protein is not known but is thought to be important for viral replication possibly modulating RNA secondary and tertiary structure (Gontarek et al., 1999; Murakami et al., 2001). The HCV X tail also interacts with ribosomal proteins L22, L3, S3 and mL3. Furthermore, L22 protein and La protein enhanced translation efficiency of the HCV IRES in mono- and bi-cistronic replicons (Wood et al., 2001).

There is little information on RNA-RNA interactions between the 3' UTR and other RNA structures. However, an important RNA interaction between a *cis*-acting element in NS5B and the X tail was essential for replication of a replicon. The structure, rather than primary sequence, was necessary for the kissing-loop interaction, which was thought to be important for NS5B RNA polymerase priming (Friebe et al., 2005; You et al., 2004).

Chimpanzees experimentally inoculated intra-hepatically with *in vitro* transcribed full length HCV RNA which had deletions in all or part of the X tail and poly(U) tract did not become infected (Kolykhalov et al., 2000; Yanagi et al., 1999). In contrast, deletions in the variable region had no noticeable effect on viral infection (Yanagi et al., 1999). In fact, HCV replicon studies have shown that the complete deletion of the variable region reduces but does not abolish replication (Friebe et al., 2002). Similar deletion studies have shown that deletion of the X tail or poly(U) abolishes replication. Deleted poly(U) mutants could be rescued by the insertion of, a minimum, poly(U) of 50 - 62 nucleotides of poly (U/UC) (Yi et al., 2003). However, other studies showed at least 26 nucleotides of poly (U/UC) were required for replication (Friebe et al., 2002).

1.2.2 Structural proteins

1.2.2.1 Core

HCV core is a highly conserved basic protein, which is presumed to make up the viral capsid (Bukh et al., 1994). The protein consists of the first 191 amino acids of the nascent polyprotein and three different isoforms have been isolated. The first isoform called p23, based on its approximate molecular weight in a polyacrylamide gel, acts as a precursor for the other isoform p21. However p16 has only ever been found in one strain of HCV, HCV-1 (Lo et al., 1995). p21 is the major isoform and is thought to be the mature core viral capsid protein as it has been found in infected patients' sera (Yasui et al., 1998). Mutational analysis placed the cleavage site of p23 between amino acids 191 and 192 by a cellular signal peptidase. Originally, studies failed to identify the exact cleavage site for the p21 isoform placing it between amino acid 172 - 174 (Hüssy et al., 1994). Recently, it has been proposed that cleavage occurs between amino acids 179 -180 by an intramembrane cleaving signal peptide peptidase (SPP) (McLauchlan et al., 2002).

Core can be divided into three domains based on its hydrophobicity. Domain 1 (amino acids 1 - ~117) contains mainly basic residues with two short hydrophobic regions. Domain 2 (amino acids 118 - 174) is less basic and more hydrophobic and its C -terminus is at the end of p21. Domain 3 (amino acids 175 - 191) is highly hydrophobic and acts as a signal sequence for E1 envelope protein (Bukh et al., 1994).

Core is a cytosolic membrane-bound protein, which has been found to associate with the endoplasmic reticulum (ER), lipid droplets, mitochondria and the nucleus. Association of mature core with lipid droplets and mitochondria was found only after cleavage to produce the p21 isoform (Barba et al., 1997; Schwer et al., 2004). After SPP cleavage, mature core is able to transfer from the ER membrane to lipid droplets and mitochondrial surface membranes. Core has also been reported to be found in the nucleus implicating a regulatory function. However, nuclear localisation has been associated only with the p16 isoform of core or truncated versions of expressed core (Lo et al., 1995; McLauchlan J, 2000).

As mentioned, mature core is thought to form the viral capsid. Core protein can bind viral RNA (Santolini et al., 1994) via domain 1 (amino acids 1 - 74) and also multimerises (Matsumoto et al., 1996). The ability of a capsid protein to interact with itself is important for capsid formation. The domain of core involved with self-interaction was mapped to domain 1 (amino acids 1 - 115).

Many other protein-protein interactions involving core have been identified by the yeast two-hybrid system and biochemical analysis. Only domain 1 has been implicated in these interactions but the wide range of proteins with which core can associate suggests its multifunctional role in infection. Core has been suggested to interact with apolipoproteins on the surface of lipid droplets (Barba et al., 1997). Also core was found to interact with the Lymphotoxin- β receptor whose exact function is not known (Chen et al., 1997). Core interaction with RNA helicases of the DEAD box family of proteins has been described (Mamiya et al., 1999; Patel et al., 1999). Finally core can interact with hnRNP K, which suggests a regulatory role for core in transcription or viral replication. Interestingly, core was shown to suppress not only cellular transcription but also HBV gene expression (Chen et al., 2003).

The interaction of core with cellular proteins allows for the deregulation of many cellular processes leading to suppression of apoptotic pathways (Ray et al., 1996), an induction of cell proliferation (Erhardt et al., 2002) and cellular transformation (Yoshida et al., 2002).

Recently, p16, a ribosomal frameshift protein called protein F was identified, which was made from a +1 frameshift in the region encoding core. It displayed a similar subcellular localisation to core (Cristina et al., 2005) and F protein specific antibodies have been found in patients who are chronically infected. However, little is known about its function although it has been found to interact with prefoldin 2 disrupting the microtubule cytoskeleton (Tsao M-L, 2006).

1.2.2.2 Envelope proteins

HCV has two envelope proteins, E1 and E2, which are glycosylated and mediate viral entry into the cell. They form non-covalently bound heterodimers. The proteins each contain an ectodomain, which is targeted to the lumen of the ER

after translation and a transmembrane domain. The ectodomain of E1 is targeted to the ER lumen by a signal sequence in the C-terminus of core protein and the ectodomain of E2 is targeted to the ER lumen by a signal sequence in the C-terminus of E1 (Santolini et al., 1994). In the ER membrane, E1 and E2, are glycosylated at 5 and 11 glycosylation sites, respectively. However, the number of glycosylation sites can vary between different HCV genotypes. The addition of these glycan groups is essential for proper folding of the proteins and is mediated by the ER protein calnexin (Dubuisson et al., 1996; Merola et al., 2001). It was thought that slow E1 folding represents the limiting step in the E1E2 oligomerisation process with calnexin retaining misfolded complexes in the ER (Dubuisson et al., 1996). Mutation analysis of charged residues within the transmembrane domains of the envelope proteins found possible ER retention signals. Transmembrane domains with charged amino acid residues prevent translocation from the membrane and tether envelope proteins to the membrane (Cocquerel et al., 2000). Deletion studies and domain swapping showed the transmembrane domains of HCV envelope proteins were essential for their heterodimerisation (Owsianka et al., 2001).

The envelope proteins are thought to mediate cell entry by recognition of cellular membrane receptor proteins. However, until recently, research in this area was difficult due to the lack of infectious cell based systems. The development of cells, which produce infectious HCV pseudotype particles (HCVpp) by the use of a retroviral vector for assembly of the virus pseudoparticle has helped the identification of cellular receptors (Bartosch et al., 2003). Furthermore, HCVpp could be neutralised by anti-E2 monoclonal antibodies (Hsu et al., 2003).

Various putative cellular receptors have been suggested as mediating interactions with HCV envelope proteins. Truncated forms of E2 have been shown to interact with CD81, scavenger receptor type B class 1 protein (SRB-1) and high density lipoprotein (HDL) binding molecule (Scarselli et al., 2002; Pileri et al., 1998). Soluble forms of CD81 can inhibit entry of HCVpp to cells (Hsu et al., 2003). Ectopic expression of CD81 in CD81-negative cells does not permit HCVpp entry indicating that CD81 is a co-receptor. Another proposed HCV receptor is the low density lipoprotein (LDL) receptor, which was shown to help endocytosis of the virus. Viral entry could be prevented in a number of cell

types using an anti-LDL monoclonal antibody (Agnello et al., 1999). Mannose binding proteins (DC-SIGN and L-SIGN) have been suggested as having interactions with E2 but their contribution to viral entry is not known (Gardner et al., 2003).

E2 contains two hypervariable regions (HVR), HVR1 and HVR2, which are under constant selection for mutation probably because they are targets for neutralising antibodies. Numerous studies have highlighted the genetic heterogeneity of the HVR1, which may enable virus to evade the immune system and facilitate establishment of chronic infection (Boulestin et al., 2002; Polyak et al., 1998). However, chronic infection has been reported in an experimentally infected chimpanzee even though there was no variation in HVR (van Doorn et al., 1995).

1.2.2.3 p7

The p7 protein is a small, 62 amino acid, hydrophobic polypeptide thought to be a viroporin (Lin et al., 1994). Analysis of the primary sequence predicted it to contain two hydrophobic transmembrane regions connected by a short hydrophilic segment. Alkaline extraction confirmed p7 as an integral membrane protein and membrane localisation showed some p7 to localise to the plasma membrane while most remained in an earlier ER-derived secretory compartment (Carrere-Kremer et al., 2002). The localisation of p7 to mitochondrial membranes further indicated the different functions the protein may have (Griffin et al., 2005). It has been proposed that p7 may have a role in production of viral progeny. Recently, p7 has been shown to oligomerise with itself and form ion channels in artificial membranes. Interestingly, the use of the anti-influenza drug amantadine, which can block ion channels, was shown to block HCV p7 ion channel formation (Griffin et al., 2003). More recently, using the JFH1 infectious cell system, p7 has been shown to be essential for virus particle assembly and release of infectious virions in a genotype specific manner (Steinmann et al., 2007).

1.2.3 Non-structural proteins

1.2.3.1 NS2

NS2 protein is a 217 amino acid transmembrane protein that is an essential component of the NS2-3 autoprotease. Studies have found that NS2 is not needed for RNA replication (Lohmann et al., 1999). NS2 was found to contain signal sequences in its multiple transmembrane domains, which cross from the cytosol to the lumen of the ER, that target it to the ER membrane. Its N-terminus and C-terminus are found in the ER lumen (Yamaga et al., 2002). This is contrary to previous reports which indicated that the C-terminus was found in the cytosol (Santolini et al., 1995). The NS2-3 metalloprotease protein contains autoproteolytic activity, which is able to cleave the junction between NS2 and NS3 in a zinc dependent manner (Pallaoro et al., 2001; Santolini et al., 1995). The domain required for this cleavage was mapped between amino acids 827 and 1207 of the polyprotein at the C-terminus of NS2 (Grakoui et al., 1993a). NS2-3 was called a metalloprotease based on observations that exogenous zinc stimulated protease activity and chelating agents, like EDTA, were able to inhibit protease activity. The zinc, which is known to be essential, may act structurally to stabilise the NS3 structure at the active site. Analysis of the region showed that amino acid requirements for effective NS2-3 cleavage vary between HCV strains but deletion was required in both NS2 and NS3 to inhibit cleavage (Reed et al., 1995).

1.2.3.2 NS3

The NS3 protein is a hydrophilic multifunctional protein, which contains an N-terminal serine protease domain and a C-terminal NTPase/helicase domain. The mature protein has a molecular weight of 67 kDa (Gallinari et al., 1998) and is bound to the ER membrane by its association with NS4A protein. When expressed on its own, NS3 protein showed a diffuse cytoplasmic and nuclear staining pattern. The co-expression of NS4A and NS3 localised NS3 protein to the ER (Wolk et al., 2000). Interestingly, the enzymatic activity of either the serine protease domain or the NTPase/helicase domain showed differences when expressed as part of the whole recombinant enzyme or individually as independent domains (Gallinari et al., 1998).

The identification of the serine protease domain was based initially on comparison with NS3 protein function and gene arrangement from other related flaviviruses and pestiviruses. The related pestivirus NS3 protein contained serine protease activity, which was catalysed by a triad of amino acid residues (Eckart et al., 1993). HCV NS3 protease is contained within the last 185 amino acids at the N-terminus and is involved in cleavage between NS3-4A, 4A-4B, 4B-5A and 5A-5B (Bartenschlager et al., 1993). The exact order in which the NS3 cleaves the polyprotein is complex. An initial cleavage between NS3-4A is thought to occur, however NS3-5A intermediates have been found indicating that there can be variation. Cleavage between NS5A and 5B was rapid with both NS3-4A and NS5A-5B cleavages occurring cotranslationally (Bartenschlager et al., 1994). The proposed catalytic triad in HCV NS3 is positioned at amino acid residues His-1083, Asp-1107 and Ser-1165. Replacement of His-1083 and Ser-1165 with alanine abolished NS3 cleavage of the HCV polyprotein without affecting protein structure of NS3 (Bartenschlager et al., 1994; Grakoui et al., 1993a). Furthermore, NS2 sequences were not required for NS3 cleavages. X-ray crystallography has shown a zinc ion to be tetrahedrally coordinated by three cysteine residues and a histidine (via a water molecule) bound tightly to NS3 where it may provide a structural rather than enzymatic role (Kim et al., 1996).

The NTPase/helicase domain of NS3 resides in the C-terminal 465 residues of the NS3 protein. Initial sequence analysis indicated that the region contained RNA helicase motifs (Gallinari et al., 1998). The helicase contained a consensus sequence common to the DEAD box family of proteins and could be placed in the DEXH subfamily (Kim et al., 1995). The presence of helicase and NTPase domains was confirmed after expression of recombinant forms of NS3 and biochemical analysis (Suzich et al., 1993). Biochemical analysis of the helicase domain showed double-stranded RNA could be unwound and denatured in an ATP and divalent ion dependent manner (Gallinari et al., 1998). Also the helicase domain was able to unwind double-stranded DNA and DNA-RNA hybrids (Tai et al., 1996). Furthermore, both the 5' and 3' UTRs of HCV have been shown to interact with the helicase domain. However, presence of a ss region was necessary for this interaction. These studies indicated that the helicase had 3' to 5' activity (Tai et al., 1996). Recently, the stem loop structures in the X tail were found to be important for binding of the helicase domain to negative-

stranded HCV RNA whereas the whole 3' UTR was required for binding to positive-sense HCV RNA (Banerjee et al., 2001).

The NS3 protein also contained a short consensus sequence, which interacted with the catalytic subunit of protein kinase A (PKA). This interaction led to retention of the catalytic subunit of PKA in the cytoplasm preventing it entering the nucleus. PKA modifies intracellular proteins by adding phosphate groups altering target protein function. Therefore, NS3/PKA interactions may deregulate intracellular signalling (Borowski et al., 1997).

1.2.3.3 NS4A

NS4A is a 54 amino acid protein, which acts as a cofactor for NS3 protein. Little is known about NS4A protein function other than its interaction with NS3. The NS4A protein has an N-terminus which is highly hydrophobic and deletion analysis showed it to be involved in targeting NS3 to the ER membrane (Wolk et al., 2000). It was proposed the last 20 amino acids form a transmembrane helix, which anchors the NS3/NS4A complex on the ER membrane. The interaction between NS4A and NS3 is mediated between residues within the core of NS3 and the C-terminus of NS4A. This interaction allows activation of the NS3 active site and more efficient protease cleavage (Kim et al., 1996).

NS4A is also required for the phosphorylation of NS5A and can directly interact with NS5A. Deletion analysis indicated that a region of amino acids in the centre of NS5A (amino acids 2135 to 2139) was essential for NS4A-dependent phosphorylation of NS5A (Asabe et al., 1997).

1.2.3.4 NS4B

NS4B is a small hydrophobic 27 kDa protein, which may act as a "platform" for recruitment of other viral proteins. Topology studies have found NS4B contains 4 transmembrane domains. The C-terminus of NS4B faces the cytoplasm and the N-terminus has a dual topology where most faces the ER lumen (Lundin et al., 2006). NS4B interacts with NS4A and therefore indirectly with NS3 and NS5A (Lin et al., 1997). The NS4B protein was found to be an integral membrane protein which was targeted to the ER and colocalised with other non-structural proteins at foci in the ER membrane (Hugle et al., 2001). Electron microscopy studies

indicated that NS4B induced morphological changes to the ER forming a structure termed the membranous web. All viral proteins were localised to this area suggesting a site for replication complex formation (Egger et al., 2002). Additional immunofluorescence studies indicated that NS4B has reduced mobility in these foci which may be due to oligomerisation (Gretton et al., 2005). NS4B can interact with lipids where it is palmitylated at two residues in the C-terminus, which are important for oligomerisation (Yu et al., 2006). NS4B protein failed to show cytopathic or oncogenic effects in the livers of transgenic mice (Wang et al., 2006).

1.2.3.5 NS5A

NS5A is a hydrophilic phosphoprotein, which contains no transmembrane domains. Localisation studies have indicated that it associates with the ER through an amphipathic helix in the N-terminal 30 residues, which lies parallel to the membrane and is essential for replication (Brass et al., 2002). NS5A localised to the nucleus when N- and C-termini were deleted. Furthermore, production of this nuclear product could be achieved by cleavage by a cellular caspase-like protein (Shinya et al., 2000). This might have interesting consequences for nuclear functions of NS5A. However, the cleavage product was only found when NS5A was expressed alone and not in the context of the full polyprotein. NS5A associated with lipid droplets when expressed alone or as part of the polyprotein (Shi et al., 2002). Structural analysis of the N-terminus showed NS5A contained an essential zinc-coordination motif, required for structural integrity (Moradpour et al., 2005).

NS5A is present as two phosphorylated forms based on its electrophoretic mobility, p56 and p58. The p56 isoform is basally phosphorylated between residues 2200 and 2250 and near the C-terminus by cellular kinases (Tanji et al., 1995). Replicon studies have shown that active NS3, NS4A, NS4B and NS5A are required in the same polyprotein in order for NS5A phosphorylation to occur (Neddermann et al., 1999). Kinase inhibitor studies failed to identify those kinases responsible for NS5A phosphorylation, however the CMGC family of kinases were suggested to be involved (Reed et al., 1997). CMGC is an acronym for the best known members of this group CDK, MAPK, GSK3 and CKII. As mentioned previously, hyperphosphorylation of NS5A to the p58 isoform requires

NS3, NS4A and NS4B production from the same polyprotein (Neddermann et al., 1999). Furthermore, Asabe et al (1997) described direct interaction of NS4A with NS5A was needed for hyperphosphorylation. Hyperphosphorylation occurred in the centre of NS5A at three serine residues (S-2197, S-2201 and S-2204).

NS5A has been implicated as being important in viral replication. Recently, it was found to bind to 3' synthetic positive and negative HCV RNA strands, showing a preference for the poly(U) of the 3' positive strand (Wang et al., 2005). Initial studies, which indicated the association of NS5A with other viral proteins suggested its presence in replication complexes (Neddermann et al., 1999). Mutation of the amphipatic helix disrupted membrane association and prevented formation of replicon-harboring cells (Elazar et al., 2003). Mutation in NS5A was essential for viral replication and establishing a replicon cell line (Lohmann et al., 1999). Interestingly, a highly adaptive mutation, which improved replication efficiency of the replicon occurred at the hyperphosphorylated residue S-2204, changing it to an isoleucine residue and prevented hyperphosphorylation. Although the presence of a hyperphosphorylated serine was required for successful infection of a chimpanzee with HCV, hyperphosphorylation was not required in the replicon system (Bukh et al., 2002).

NS5A has also been proposed to contain a region, which confers resistance of the virus to interferon treatment (Gale et al., 1997). This region, called the interferon- α sensitivity-determining region (ISDR), was later found to interact directly with an IFN- α stimulated gene product, PKR protein kinase. PKR protein kinase is activated by binding to double-stranded RNA resulting eventually in cessation of protein synthesis. It was proposed that sequences in the ISDR could be used to predict sensitivity or resistance of HCV to IFN- α treatment (Enomoto et al., 1995). However, these Japanese studies were contradicted by a European study which found no correlation between sequence type and the response to IFN- α treatment (McKechnie et al., 2000). NS5A has been proposed as having numerous interactions with proteins affecting cell signalling. However, the exact contribution of each interaction to viral infection is unclear. NS5A can modulate the three main MAPK pathways involved in host cell mitogenic signalling, which regulate growth and activation. It is able

differentially to regulate members of the MAPK family of kinases leading to perturbation of host cell cycle, decreased cap-dependant translation and perturb apoptosis. NS5A is able to regulate cellular signalling by both pro- and anti- apoptotic mechanisms. It has also been implicated in interfering with ROS pathways and phosphatidylinositol 3-kinase signalling pathways, which may lead to hepatocyte transformation and HCC formation (Macdonald et al., 2004).

1.2.3.6 NS5B

The NS5B protein is a 65 kDa, RNA dependent RNA polymerase (RdRp) and forms the major component of the replication complex (Behrens et al., 1996). Sequence analysis had identified an amino acid motif GDD, common to RdRp's and critical for polymerase activity (Yamashita et al., 1998). The crystal structure of NS5B has been solved, revealing it to have a "fingers-palm-thumb" conformation in which the catalytic domain is found in the palm domain. The RNA template lies between the fingers and thumb on the palm domain (Lesburg et al., 1999).

The NS5B protein is a cytosolic ER membrane-bound protein, which is tethered by a transmembrane alpha-helix located in C-terminal 21 amino acid residues (Schmidt-Mende et al., 2001). It forms a vital part of the replication complex via interactions with NS5A and therefore indirectly to all other non-structural proteins (Shirota et al., 2002).

1.3 Model Systems for Investigating the HCV Life Cycle

1.3.1 HCV in cell culture

Viruses are obligate intercellular parasites that require the presence of a host cell in order to multiply. Research into HCV has been hampered by the lack of a susceptible cell culture system. Conventional virological methods involving inoculation of cell lines failed to initiate productive HCV infection. Initial attempts to establish HCV infection used primary cells from humans and chimpanzees. One study found that low levels of infection were possible in chimpanzee but not baboon primary hepatocytes, although efficiency was poor (Lanford et al., 1994). In a study by Iacovacci et al. (1997), primary human

foetal hepatocytes were infected with HCV-containing sera. Although small increases in HCV positive-strand RNA were detected, the overall efficiency of the system was low.

As there can be difficulties associated with primary cell culture due to contamination problems and short passage life, other systems have been tried using immortalised human hepatoma cell types and human B- and T-cells. A human hepatocyte cell line, PH5CH, which was immortalised with simian virus 40 large antigen, was extensively studied. Although found to be more susceptible to HCV infection than others, the system was still inefficient (Kato et al., 1996). Studies looking at hepatoma cell lines HepG2 and HuH-7 gave poor results even though conditions were changed extensively to try to optimise the approach (Seipp et al., 1997). Mizutani et al. (1996) looked at infection of the human T-cell line, MT-2, which harbours human T-cell leukaemia virus-1 (HTLV-1). Although susceptible to HCV infection, it was not possible to produce long-term infection. Infection of Daudi cells, a B-lymphoplastoid cell line, managed to produce long-term infection for up to 1 year (Shimizu et al., 1998) but addition of the virus led to cellular cytopathic effects. It was possible to infect a chimpanzee with supernatant obtained after 58 days of culturing in Daudi cells, but infectivity was low.

Other attempts were made to culture virus directly from cells of infected liver biopsies from persistently infected patients (Ito et al., 1996). However, replication efficiency was low and reproducibility of the system poor.

1.3.2 HCV infection of Chimpanzees

Cell culture studies have highlighted the narrow host range of HCV in that infection was possible only in human and chimpanzee cells. Baboon and porcine cell lines did not permit viral infection (Lanford et al., 1994; Seipp et al., 1997). Chimpanzees offer the only animal model for HCV infection. However, there are inherent difficulties in using these animals as they are expensive, the ethics of their use is debatable and it is difficult to sustain their use. Nevertheless, chimpanzee work has been extremely useful in identifying the components required for infection. Firstly, a cDNA clone was made that corresponded to the entire sequence of an HCV isolate. RNA transcripts were then made, which were

infected into chimpanzees by intrahepatic injection. The advantages of this technique are that the HCV genome was well defined and homogenous. As the sequence of the cDNA clone was known any changes in infected viral RNA sequence could quickly be identified and defined. Also RNA could be produced in large quantities to optimise the infection process and the cDNA clone was easily manipulated genetically (Yanagi et al., 1997).

Based on the above approach, a cDNA clone was constructed with a consensus sequence derived from the sequence of six full-length variants of the same H77 (genotype 1a) isolate. From the resultant consensus cDNA genome, RNA transcripts were produced, which were intrahepatically injected into a chimpanzee and resulted in serum HCV RNA levels of approximately 1×10^6 copies/ml (Kolykhalov et al., 1997). Other studies have found that many viral variants may actually be defective in causing infection. For example, studies using the H77 strain found two initial full-length cDNA clones were unable to cause infection. However, a chimeric full length cDNA clone containing a consensus constructed from four full length clones was able to infect chimpanzees (Yanagi et al., 1997). Sequence analysis indicated that null mutations may be responsible but it was unclear whether this was due to the error-prone NS5B viral protein or *Taq* polymerase error when amplifying the clones. Infectious cDNA clones have been made for genotype 1b and 2a (Beard et al., 1999; Yanagi M, 1999). Furthermore, chimeras between genotypes 2a and 1a were unable to cause infection (Yanagi M, 1999). Mutational analysis was used to assess the contribution of non-structural genes and the 3' UTR to infection. Mutation of NS2, NS3, NS5B or removal of the 3' terminus prevented viral infection (Kolykhalov et al., 2000). Other studies have shown that the structural protein p7 was necessary for infection. Also p7 chimeras, which had N- and C-termini swapped for different genotypes, were non viable (Sakai et al., 2003). Therefore, the use of chimpanzees as an animal model has provided important knowledge of viral gene function in infection.

1.3.3 Establishing an HCV genotype 1b expressing cell line

A major breakthrough towards a system for productive infection of tissue culture cells was the development of HCV replicon systems. This approach relies on hepatoma cell lines, which express an autonomously replicating modified HCV

genome. This was first achieved by Lohmann et al. (1999) after the modification of Con1, an HCV genotype 1b strain, creating HuH-7 cell lines that harbor replicons. Initially the coding region was amplified in two overlapping segments. This was then mutated to a consensus sequence based on the sequence of several clones from each overlapping fragment. The UTRs were amplified separately and assembled with the ORF. A truncated T7 promoter oligonucleotide was ligated to the 5' flank of the 5' UTR to allow synthesis of RNA transcripts. A *ScaI* restriction site was engineered at the 3' terminus of the 3' UTR to allow digestion of plasmid DNA and the synthesis of transcripts lacking vector sequence. The HCV genome was modified by the deletion of structural genes as far as NS2 or NS3. The incorporation of a selectable marker, the neomycin phosphotransferase gene, under the control of the HCV 5' UTR allowed the selection of cells with actively replicating genomes. A bi-cistronic replicon was created with the inclusion of an encephalomyocarditis virus (EMCV) IRES before the HCV non-structural genes. A negative control was made by creating a 10 amino acid in-frame deletion at the active site of the NS5B gene. Two variant 5' UTRs were used which contained either nucleotides 1 - 377 or 1 - 389. Transcribed RNA was extensively treated with DNase1 to ensure removal of the DNA template and then transfected into HuH-7 cells. Colonies from the initial experiments were then isolated and passaged to obtain clonal cell lines. Most cells died during this procedure and only nine clonal cell lines were obtained. A replicon-harboring cell line was defined as cells, which contained a replicon of correct size and conferred G418 resistance. The frequency of stable replicon cell clones was low for the first generation of sub-genomic replicons (Lohmann et al., 2003).

A combination of adaptation by both host cells and the acquisition of mutations by the replicon were required for successful and higher levels of RNA replication (Lohmann et al., 2003). Replicons containing a luciferase gene to replace the neomycin phosphotransferase gene were used in transient assays to identify adaptive mutations required for growth in cell culture. The highly adapted 5.1 replicon contained three adaptive mutations (two in NS3 and one in NS5A), which were necessary to detect replication in transient assays. Blight et al. (2000) also characterised culture adaptive mutations in NS5A in the Con1 replicon. Two occurred in serine residues used to produce the hyperphosphorylated form of NS5A. Of these, a mutation of S-2204 to

isoleucine, which totally blocked p58 NS5A isoform formation, was found to be highly advantageous for replication. This suggested that hyperphosphorylation was not required for efficient replication. Mutations could be divided into two groups: those that had little impact on replication alone but could increase replication when combined with a highly adaptive mutation and those mutations that were highly adapted but incompatible with each other. A highly adaptive mutation was defined as a single mutation, which resulted in approximately 4-fold increase in replication compared to the wild type 1b replicon. Therefore, a replication deficient replicon could be produced by the combination of the two highly adaptive mutations in NS5A, S-2204 and S2197 (Lohmann et al., 2003).

Cellular factors were also important for replicon establishment in cell culture. Replicons in HuH-7 cells of passage 128 replicated more efficiently than those of passage 80 or 142. Indeed, replicons of passage number 128 replicated 100-fold more efficiently than those in cells at passage number 15 (Lohmann et al., 2003).

Characterisation of cells that harboured replicons showed that they were able to maintain autonomously replicating RNA for over one year. Furthermore, viral RNA was still detectable 10 months after removal of selection by neomycin. Replicon-bearing cells showed no obvious signs of cytopathogenicity. Viral proteins were localised to ER membranes and replication and expression were linked to the cell cycle (Pietschmann et al., 2001). Other studies showed that treatment of replicon expressing cells with IFN- α reduced expression and replication in a dose-dependent manner (Frese et al., 2001; Guo et al., 2001). Long term treatment of replicon-harboring cells with IFN- α effectively removed or “cured” cells of the replicon (Blight et al., 2003).

1.3.4 Establishing an HCV 1a replicon expressing cell line

The genotype 1a replicon system was based on the infectious H77 isolate. The genome was specifically modified using the mutations observed with the Con1 genotype 1b system as a guide. In order for successful replicon establishment, the previously described adaptive mutation of the hyperphosphorylated serine residues in NS5A was incorporated. In addition, the cell line HuH-7.5 was used for replicon uptake (Blight et al., 2003). Previously, this cell line had been

noted to be highly permissive for the establishment of Con1 genotype 1b replicon harbouring cell line. Using the hypothesis that this permissive environment would be maintained in an IFN- α replicon “cured” cell line, the Con1 genotype 1b replicon was removed with IFN- α treatment (Blight et al., 2002). Successful replicon harbouring cells acquired additional adaptive mutations in NS3 similar to those NS3 mutations in the 1b replicon (Blight et al., 2003).

1.3.5 JFH1 genotype 2a isolate

A recent breakthrough in HCV research has been the development of an infectious cell culture system, based on the JFH1 genotype 2a isolate. This sequence was isolated from a 32 year old male patient with fulminant hepatitis. The patient had elevated serum alanine amino transferase levels, as is normally seen in HCV infection indicating liver damage. Unusually, the patient developed jaundice and encephalopathy, the latter being extremely rare in acute HCV infection. Based on sequence analysis, the JFH1 genome clustered with genotype 2a although it was found to be slightly divergent in its 5' UTR, core, NS3 and NS5A sequences (Takanobu et al., 2001).

1.3.5.1 Subgenomic replicon

Initially, the JFH1 replicon was made in the same manner as previous replicons. The genome was amplified in 12 fragments, which were cloned into vectors. A majority sequence was assembled based on the consensus of 5 sequences for each fragment. Notably, no adaptive mutations were required in JFH1 sequences prior to successful transfection. JFH1 replicons produced over 50 times more colonies than the Con1 replicon in colony forming assays and could be transfected into naïve HuH-7 cells. Analysis of JFH1 replicon sequences from clones showed that all but one had acquired cell culture adaptive mutations. Most were found in NS5A and NS5B and were able to increase colony formation efficiency when introduced into the original replicon (Takanobu et al., 2003). Furthermore, replicons could be established in HepG2 cells and IMY-N9 cells (hepatocyte cells fused with a HepG2 cells). However, the overall efficiency was lower than that found in HuH-7 cells (Date et al., 2004). More recently, the JFH1 replicon was shown to replicate efficiently in non-hepatic cells lines e.g.

Hela and HEK293 cells (Kato et al., 2005) and U2OS human osteosarcoma cells (Targett-Adams et al., 2005). These studies used transiently expressing systems with measurement of luciferase activity as an indirect measure of replication. The ability of JFH1 to replicate in other cells types and the improved efficiency of the transient JFH1 replicon when compared to the Con1 replicon highlighted its improved replication capacity. JFH1 was also found to be sensitive to IFN- α treatment (Targett-Adams et al., 2005).

1.3.5.2 Infectious system

The JFH1 isolate has been shown to be infectious in cell culture. Transfection of HuH-7 cells with full length JFH1 RNA results in the production of infectious particles described in section 1.1.4. The cell culture particles can be neutralised using CD81 specific antibodies. The infectious system was inefficient with a limited spread of infection between HuH-7 cells. However, it was possible to infect chimpanzees intrahepatically using particles obtained from cell culture (Wakita et al., 2005). Recently, this system was improved by the use of another HuH-7 derived cell line to yield viral titres of 10^4 - 10^5 infectious units per ml of culture supernatant. This study indicated that HCV particles rapidly enter cells and expressed from input genomes within the first 24 hrs and found that limitations with naïve HuH-7 cells may be due to an innate antiviral response. The derived HuH-7 cell line, discussed above, contained an inactivating mutation in the retinoic acid inducible gene-I (RIG-I), which is a component of a double stranded RNA antiviral pathway. This suggested that, in naïve HuH-7 cells, this pathway transiently impedes HCV replication (Zhong et al., 2005). Furthermore, these results were confirmed, where HCV infected HuH-7 cells produced 10^8 copies of HCV viral RNA per ml of culture supernatant and infection of HuH-7.5 cells showed high levels of HCV protein and RNA expression. These studies showed HCV infection could be inhibited by treatment with monoclonal antibodies for CD81, E1 and E2 (Cai et al., 2005).

1.4 HCV genotypes and quasispecies

After the isolation of the HCV genome by Choo et al (1989), other isolates were found which were similar to the original sequence but also distinctly different. In general, sequence variability is distributed equally throughout the genome

except in the 5' UTR, core and the HVRs of the envelope proteins (Zein et al., 2000). Initially, attempts to classify genotypes led to the formation of 4 different classification systems. However, this was later clarified by the creation of a new system, which classified genotypes according to their nucleotide similarity. The system numbered the genotypes in order of their discovery. A total of six genotypes were designated (Figure 1.4). Strains which were closely related to a genotype were classified as a subtype. Normally, a genotype is defined by the genetic heterogeneity between it and other HCV isolates and will share only between 65.7 % to 68.9 % sequence similarity with other genotypes. A subtype will share 76.9 % to 80.1 % sequence similarity with other closely related isolates within the same genotype and a variant within a "quasispecies" will share 90.8 % to 99 % sequence similarity with other variants within the same isolate (Simmonds et al., 1994). Any RNA viral population, "quasispecies", within a patient derived from the same infectious population has a sequence which is dominant (the master sequence) and a number of variants differing from this (Forns et al., 1999). HCV genotypes 1, 2 and 3 are distributed worldwide; however there appears to be some regional differences in prevalence. HCV 1a and 1b are prevalent in the USA and in Europe (Zein et al., 1996). However, the main subtype found in Japan is 1b. HCV subtypes 2a and 2b are found in the USA, Europe and Japan. Patients with genotype 3a are frequently intravenous drug users in the USA and Europe (Zein et al., 2000). Genotype 4 is found predominantly in North Africa and the Middle East and genotypes 5 and 6 are found only in South Africa and Hong Kong, respectively (Cha et al., 1992; McOmish et al., 1994).

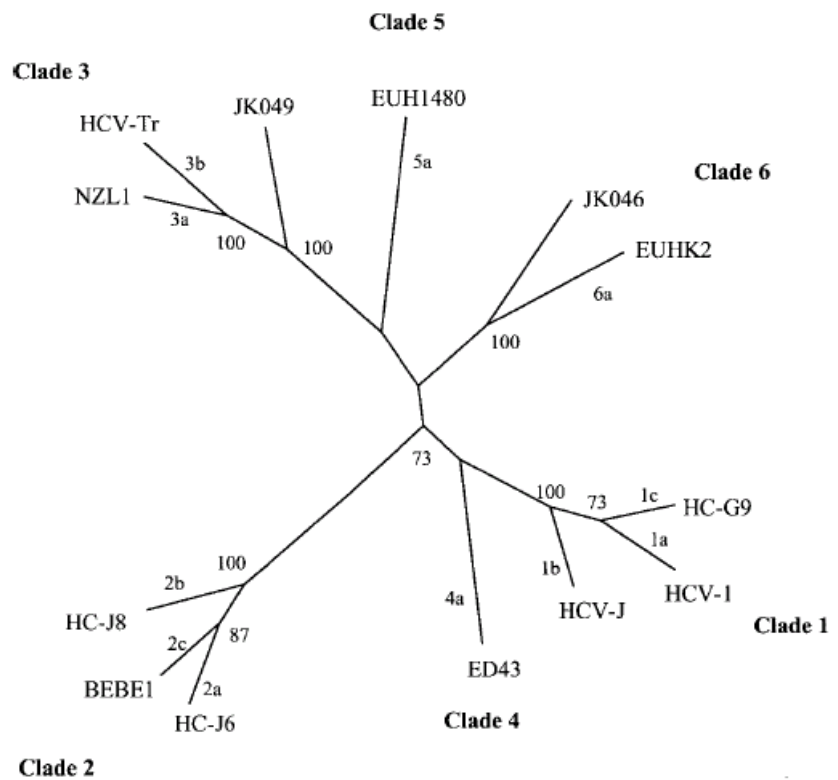


Figure 1.4. A phylogenetic tree of complete virus genome nucleotide sequences compared using parsimony analysis. They are classified into six clades (genotypes) and subtypes a, b, etc (Robertson *et al.*, 1998)

1.5 HCV Infection

1.5.1 Acute and chronic infection

In most cases acute HCV infection is asymptomatic and is therefore poorly characterised (Seeff L, 1997). Non-specific symptoms include fatigue, discomfort in the upper right quadrant of the abdomen and pruritis. 50 % - 80 % of acutely infected patients with HCV develop a chronic infection. Approximately 25 % of patients with chronic infection will have fibrosis depending on the population studied (Pawlotsky J, 2004). This can lead to cirrhosis and, in a small proportion of patients, hepatocellular carcinoma (HCC). Of the approximately 20 % of chronically infected patients who had developed cirrhosis, between 1.9 % and 6.7 % of HCV-infected patients will develop HCC. However, these figures can vary between different studies (Bisceglie A, 1997). An important study in Germany of 2867 women accidentally infected with HCV contaminated Rhesus anti-D immunoglobulin allowed an unbiased assessment of the natural history of the infection. The study revealed that 1833 women were positive for HCV antibodies. However, only 46 % had developed chronic infection and of these, 683 were untreated over a 25 year period. During this period, only 9 developed cirrhosis and 1 developed hepatocellular carcinoma (Wiese et al., 2005). The proportion of woman from this study who developed chronic infection was lower than had previously been described.

1.5.2 Treatment

The treatment of HCV is dependent on genotype and follows a treatment regime plan in an attempt to obtain a sustained viral response (SVR) to therapy. The current treatment is pegylated IFN- α 2a or 2b in combination with ribavirin. Treatment length varies according to genotype; genotype 1 infected patients receive a 48 week course and patients with genotypes 2 and 3 receive 24 weeks. An SVR is achieved with 42 % to 46 % of genotype 1 infected patients compared to 78 % to 82 % of patients with genotypes 2 and 3 (Flamm S, 2003). Currently, there is no vaccine to prevent HCV infection. However, non-structural proteins are a target for the production of viral inhibitors. The main targets for the drug therapy are the NS3/4A serine protease and the NS5B RdRp. Although some drugs are in clinical trials it is believed a similar approach to HIV therapy will

need to be adopted using a combination of drugs which target different viral mechanisms to avoid escaping viral mutation (Zhuhui H, 2006).

1.6 Disease pathology

The pathology of liver disease as a result of hepatitis infection is not fully understood. Whether liver damage is a consequence of viral infection or due to immune responses is still not known. Immune-mediated pathways leading to liver damage are more likely since it has been shown there is no correlation between viral RNA titres and liver damage (Wejstal R, 1995).

It has been recognised that liver histology may vary according to HCV genotype. A study by Mihm et al. (1997) showed that patients with genotype 3a frequently manifested more steatosis of the liver and bile duct lesions than patients with genotype 1a. However, it has not been shown conclusively that progression to cirrhosis is more likely with any one genotype.

1.6.1 Steatosis

Steatosis is the accumulation of intracytoplasmic lipid droplets within hepatocytes (Figure 1.5). Lipid droplets are spherical organelles in which neutral lipids are stored. They contain a core of neutral triacylglycerols and cholesterol esters, which are formed in the ER and then coated in a phospholipid monolayer (Shi et al., 2002). An external proteinaceous coat prevents fusion with other lipophilic surfaces. Proteins within this coat are poorly described. Known proteins, which localise to the surface of lipid droplets include the perilipin family of proteins, adipocyte differentiation related protein (ADRP) (Lu et al., 2001) and caveolin (Pol et al., 2001). ADRP has been proposed as possible marker of steatosis and has been used to observe lipid droplet biogenesis and behaviour in live cell analysis (Targett-Adams et al., 2003).

The mechanism by which steatosis occurs is unknown. However, there are numerous risk factors, which may predispose a patient to acquire the condition. These include an increased body mass index (BMI), increasing age, alcohol abuse, insulin resistance, HCV infection and drugs. Assessing the contribution of individual factors to the progression to steatosis is difficult (Quadri et al., 2001).

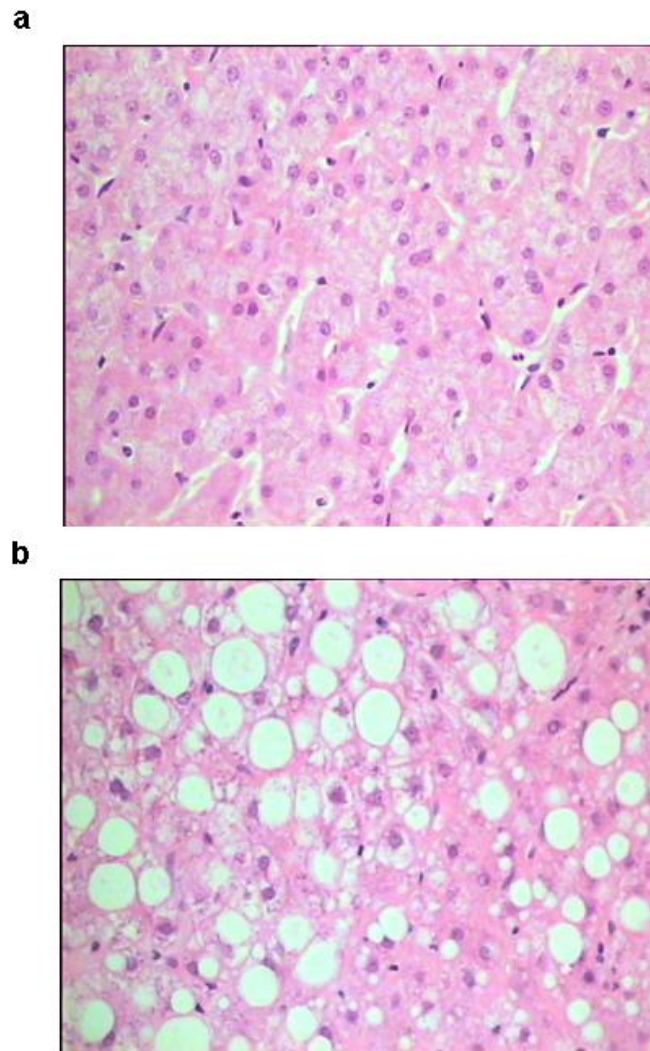


Figure 1.5. Sections taken from a human liver with either very minor steatosis (a) or moderate to severe steatosis (b). The large vacuolar structures would have been lipid-filled but this is removed during the fixation process. It is thought that they would be made of small lipid-filled compartments whose membranes are disrupted during fixation and staining (Mills P, unpublished: obtained from Glasgow Regional Virus laboratory)

Fatty liver disease can be divided into two main groups; alcoholic fatty liver disease and non-alcoholic fatty liver disease (NAFLD). NAFLD varies from the less serious steatosis to more serious non-alcoholic steatohepatitis (NASH). Although steatosis itself is not thought to lead to fibrosis, NASH has been shown to develop into fibrosis and cirrhosis, end stage liver disease and hepatocellular carcinoma. Steatohepatitis is steatosis accompanied by lipid peroxidation to produce reactive oxygen species and inflammation. This can lead to fibrosis and liver disease over time (Green R, 2003; Tarantino et al., 2007). Recent studies have found an association of NASH with metabolic syndrome which is characterised by abdominal obesity, insulin resistance, dyslipidemia (disruption of lipids in the blood) and hypertension (high blood pressure) (Green R, 2003).

NASH is thought to develop in steatotic livers that undergo a secondary pathogenic stimulus, which results in oxidative stress and lipid peroxidation resulting in steatohepatitis. Highlighting the importance of oxidative stress in the formation of fibrosing steatohepatitis, Ip et al. (2003) investigated the contribution of peroxisome proliferator-activated receptor- α (PPAR- α). PPAR- α is a transcription factor that induces expression of hepatic cytochrome P450 enzymes, which contribute to reactive oxygen species (ROS) and oxidative stress. Mice fed a lipid rich diet, both methionine and choline deficient (MCD), displayed an increase in cytochrome P450 expression and steatohepatitis. However, activation of PPAR- α with an agonist reduced hepatic triacylglycerol content and ROS. It was thought that the PPAR- α activation of genes involved in mitochondrial β -oxidation of fatty acids reduced the amount of the cellular fatty acid substrate for production of ROS.

Another study examined the effect of inhibiting microsomal transfer protein (MTP)(Lettéron et al., 2003). MTP is important in the formation of very low density lipoprotein (VLDL). VLDL particles are secreted into plasma and used to transport lipids in the blood. The particle consists of a core of triacylglycerols surrounded by a phospholipid layer, which itself is surrounded by apolipoprotein B (ApoB). MTP acts to lipidate ApoB co-translationally in the lumen of the ER. Complete lipidation of ApoB is crucial for the assembly of VLDL and its correct secretion. Incomplete lipidation of ApoB causes it to translocate to the cytosol for degradation (Shelness et al., 1999).

In the study by Lettéron et al. (2003,) drugs were used that were able to induce steatosis in mice by their inhibitory effect on MTP activity. The most steatogenic drugs were those which were able to inhibit both MTP and mitochondrial β -oxidation. Inhibition of MTP alone led only to steatosis in this study. However, the accumulation of triacylglycerols (TAG) in the cytosol can lead to lipid peroxidation, such that reactive by-products cause DNA damage and interfere with mitochondrial respiratory pathways (Lettéron et al., 2003). Interestingly, mice fed diets deficient in choline display only steatosis not steatohepatitis. Choline is an important substrate used in the synthesis of phospholipids and therefore diets deficient in it may affect VLDL formation and thereby lead to steatosis (Green R, 2003). An MCD fed mouse could be rescued from liver disease by dietary supplementation with methionine (Chawla et al., 1998). This further suggests the two hit hypothesis mentioned previously in which steatosis itself may be benign but an additional metabolic or pathogenic insult results in steatohepatitis.

1.6.2 HCV and steatosis

An estimate of the proportion of the general population with NAFLD is 25 % and up to 20 % - 30 % of these patients may develop steatohepatitis, leading to cirrhosis. Steatosis is present in approximately 50 % of patients with chronic HCV infection (Hickman et al., 2002). Therefore, the proportion of HCV patients with steatosis is greater than in the general population. In chronic HCV infection, steatosis could occur as a direct result of viral infection or as a secondary effect of viral infection.

Multivariate statistical analysis is used when investigating the contribution of individual predisposing factors to the development of disease. This statistical method allows multiple factors to be considered at the same time. Multivariate analysis has indicated that there was an association between HCV genotype 3 infection and steatosis, which was not found in genotype 1 infected patients (Mihm et al., 1997). Adinolfi et al (2001) found a measure of visceral fat rather than BMI itself was associated with steatosis in patients infected with genotype 3 and the degree of steatosis was associated with the level of HCV RNA. In contrast, in genotype 1 infected patients the degree of steatosis was associated with BMI not with genotype 1 infection. This study suggested that steatosis may

be present as “metabolic fat” or “viral fat”. Thus in genotype 1 infections, steatosis may be found but it is not associated with the virus but rather BMI is the predisposing factor to steatosis. By contrast, in genotype 3 infections, the virus is associated with moderate to severe grades of steatosis independent of other risk factors.

In a study of 254 chronic HCV patients attempting to identify the risk factors associated with steatosis, there was a significant association between genotype 3 and moderate to severe steatosis (30 to 60 % steatotic hepatocytes). 70.5 % of patients with genotype 3 had steatosis whereas it was present in only 34.2 % of patients with other genotypes. Patients with genotype 3 had a 10-fold increase in the probability of having steatosis. A history of alcohol abuse was often associated with steatosis but there was no correlation between a history of intravenous drug addiction (IVDA) and increased steatosis (Rubbia-Brandt et al., 2001).

Steatosis is associated with an increased rate of fibrosis progression over time. Adinolfi et al., (2001) suggested that steatosis together with even a small amount of alcohol accelerated the progression of liver fibrosis. Furthermore, hepatic steatosis together with aging, cirrhosis and no prior interferon treatment were all independently significant risk factors for hepatocellular carcinoma (Zhu A, 2003). Recently, the effect of weight loss in patients chronically infected with HCV genotypes 1 and 3 was investigated for its effect on liver histology and biochemistry (Hickman et al., 2002). A diet and exercise regime, which led to weight loss, was accompanied by a reduction in steatosis irrespective of viral genotype. The effect of this on serum HCV RNA levels was not investigated however an improvement of fibrosis was found.

A sustained viral response after anti-viral treatment significantly reduced steatosis in patients with genotype 3 HCV infection. An improvement in steatosis was not found in patients with genotype 3 infection who did not respond to treatment and patients who achieved a SVR with a genotype 1 infection (Kumar et al., 2002). Additionally, these results were supported by another retrospective study. Patients with genotype 1 infection and steatosis responded poorly to anti-viral treatments compared to genotype 1 infected patients without steatosis (Patton et al., 2004). There was no relationship

between steatosis and inflammation although steatosis and fibrosis were associated. This might indicate that fibrosis in HCV infection occurs by a mechanism, which does not invoke steatohepatitis. However, other studies have found an association between steatosis and inflammation (Adinolfi et al., 2001; Mihm et al., 1997; Westin et al., 2002).

HCV may be able to induce fibrosis via a number of mechanisms. HCV proteins may induce steatosis, which leads to the production of ROS and the activation of hepatic stellate cells and fibrosis. Alternatively, ROS may be produced directly by HCV infection causing stellate cell activation. Immune-mediated responses to the virus may lead to necroinflammation and fibrosis (Asselah et al., 2006).

Recently, the contribution of insulin resistance to fibrosis has been investigated. Insulin resistance is commonly associated with chronic HCV infection and often leads to type II diabetes mellitus and the metabolic syndrome. In fact, insulin resistance has been implicated in the causation of steatosis and is a risk factor for progression of fibrosis in genotype 1 patients (Fartoux et al., 2005). A recent study looked at the contribution of steatosis and insulin resistance to fibrosis in patients with NAFLD and chronic HCV genotype 3 infection. Although both NAFLD and chronic HCV genotype 3 infection were associated with fibrosis, steatosis was associated with advanced fibrosis only in NAFLD. "Viral steatosis", in chronically infected HCV genotype 3 patients, was not associated with advanced fibrosis (Bugianesi et al., 2006).

1.6.2.1 Transgenic mice studies

Transgenic mice expressing HCV core protein displayed an increase in the accumulation of fatty acids and formation of lipid droplets within the liver. Both β -oxidation and secretion of TAGs from the liver was impaired (Moriya et al., 2001). Furthermore, transgenic mice expressing HCV core protein have lower MTP activity and decreased secretion of VLDL suggesting a mechanism for steatosis of the liver by core protein. Therefore, it has been suggested that core protein may induce steatosis in the livers of infected patients (Perlemuter et al., 2002). Transient expression of HCV core protein in mice led to dysregulation of lipid metabolism genes and an increase in hepatic TAG and ROS (Yamaguchi et al., 2005). Other genes involved in β -oxidation that have been implicated in having a role in steatosis were downregulated i.e. PPAR- α , acyl-CoA oxidase

(AOX) and carnitine palmitoyl transferase-1 (CPT-1). However, the problem with many mice studies is that the core protein used is derived from genotype 1, which would be contrary to the results obtained from clinical studies. As discussed, patients chronically infected with genotype 1b display steatosis, which is associated with metabolic causes, whereas genotype 3 is the only genotype with evidence for direct involvement in steatosis. Therefore, the finding in the mouse model that genotype 1 core causes steatosis is possibly irrelevant to the disease in humans. Moreover, levels of core expression may be greater in transgenic mice compared to that of HCV-infected cells and core is not expressed in the context of the whole viral polyprotein (Quadri et al., 2001).

Although no transgenic animal studies have been performed with genotype 3 core protein, expression of a genotype 3 core protein induced greater levels of accumulation of TAG in HuH-7 cells compared to core protein derived from genotype 1b (Abida et al., 2005).

Nevertheless, steatosis is most likely not as simple as being caused by one single viral protein. Other viral proteins may be involved and in fact NS5A was shown to interact with lipid droplets (Shi et al., 2002).

Transgenic mice expressing HCV core protein have increased hepatic levels of tumour necrosis factor- α (TNF- α). This finding was also seen in the livers of HCV infected patients (Neuman et al., 2002). Increased TNF- α levels have been shown to induce insulin resistance in transgenic mice (Uysal et al., 1997).

1.7 Microarray analysis of livers from acutely HCV infected chimpanzees

Microarray analysis of host cellular gene expression after acute infection of three chimpanzees with HCV genotype 1 found three groups of genes with altered expression patterns. Initially, one chimpanzee (1590) was intrahepatically infected with RNA transcribed from a full-length clone of the H77 strain (genotype 1a), which lacked the hypervariable region 1 (Su et al., 2002). This strain has previously been characterised as being able to cause infection but was somewhat attenuated compared to the wild type virus (Xavier Forns, 2000). Four weeks after inoculation, a second chimpanzee (Ch96A008)

was inoculated with infectious plasma from chimpanzee 1590. Another chimpanzee (1581) was inoculated with plasma from a patient with acute fulminant HCV infection. Chimpanzee 1590 developed a persistent infection with no antiviral or IFN- γ response. Chimpanzee Ch96A008 cleared the virus in response to a strong IFN- γ response and chimpanzee 1581 initially cleared the virus in response to an IFN- γ induction but then became persistently infected (Su et al., 2002).

Gene expression analysis using microarrays was performed for selected time points during infection of each chimpanzee. Three groups of genes were found to have altered expression: IFN- α stimulated genes, IFN- γ stimulated genes and genes involved in lipid metabolism (Su et al., 2002). Alterations in the first two groups of genes would be expected as they are involved in the immune response. Interestingly, IFN- α stimulated genes were induced on viral infection, however this had no effect on viral titre. A predictor of outcome of infection was the up-regulation of IFN- γ stimulated genes involved in antigen presentation by major histocompatibility complexes (MHC) class I and T-cell recruitment. Altered expression of IFN genes confirmed data obtained from a previous study, which looked at HCV acute infection in chimpanzees (Bigger et al., 2001).

An unexpected group of genes with altered gene expression were those involved in lipid metabolism. The study had sought to find genes, which could be used as predictors for the outcome of infection. Of these, up-regulation of 45 genes had positive impacts on the onset of detection of viral RNA within the blood (viremia) and down-regulation of 10 genes were negative indicators of viremia. Genes involved in lipid metabolism were found in both these groups. Genes, which were found to be repressed early in the onset of viremia, were PPAR- α , Flotillin (a lipid raft protein important in vesicular trafficking and signal transduction) and hepatic lipase C (involved in hydrolysis of lipoprotein TAGs and phospholipids). Genes which were up-regulated early during the onset of viremia were UDP-glucose ceramide glucosyltransferase (involved in membrane lipid synthesis), sterol regulatory binding protein (SREBP)(transcription factor activating lipogenic gene expression), lipase A (involved in the hydrolysis of membrane lipids) and ATP citrate lyase (maintains cytosolic levels of acetyl CoA). These results indicated that genes involved in the synthesis of fatty acids were induced and those involved in their breakdown were being repressed.

However, levels of fatty acid synthase, (FAS) a key enzyme involved in the synthesis of fatty acids did not show any correlation with HCV RNA levels. However, FAS expression was at a consistently high level in chimpanzees with sustained and temporary viral clearance (Su et al., 2002).

Another microarray study of livers from 10 chimpanzees chronically infected with HCV genotypes 1b, 1a and 3a showed that IFN-stimulated genes displayed altered gene expression compared with livers from uninfected animals. Although some genes from the previous study had similar expression patterns in chronically infected and acutely-resolving chimpanzees, this pattern was not found in all animals. This highlighted differences between chronic and acutely infected chimpanzees indicating that up-regulation of specific lipid metabolism genes was not absolute for chronic infection (Bigger et al., 2004).

1.7.1 Lipid metabolism and HCV replication

These studies were extended from the in-vivo chimpanzee animal model to observe the effect of lipid metabolism on the in-vitro HCV replicon system. Replication in replicon-expressing cells could be prevented in a dose-dependent manner by specific inhibitors of lipid metabolism, cerulenin (inhibits FAS) and 25-hydroxycholesterol (inhibits cholesterol biosynthesis). Use of a lipid metabolism inducer, nystatin, increased replication (Su et al., 2002). These effects were reported as independent of the effects on cell cycle and cell toxicity.

The ability of inhibitors of lipid metabolism to reduce HCV replicon levels indicated that products or enzymes within the pathway or affected by the pathway could alter viral RNA abundance. Lipid biosynthesis can be divided into two separate branches: one branch leading to the synthesis of cholesterol and one branch leading to the synthesis of fatty acids (Figure 1.6). The small molecule inhibitors used affected the two different branches of lipid metabolism suggesting that both cholesterol and fatty acid biosynthesis play roles in HCV replication.

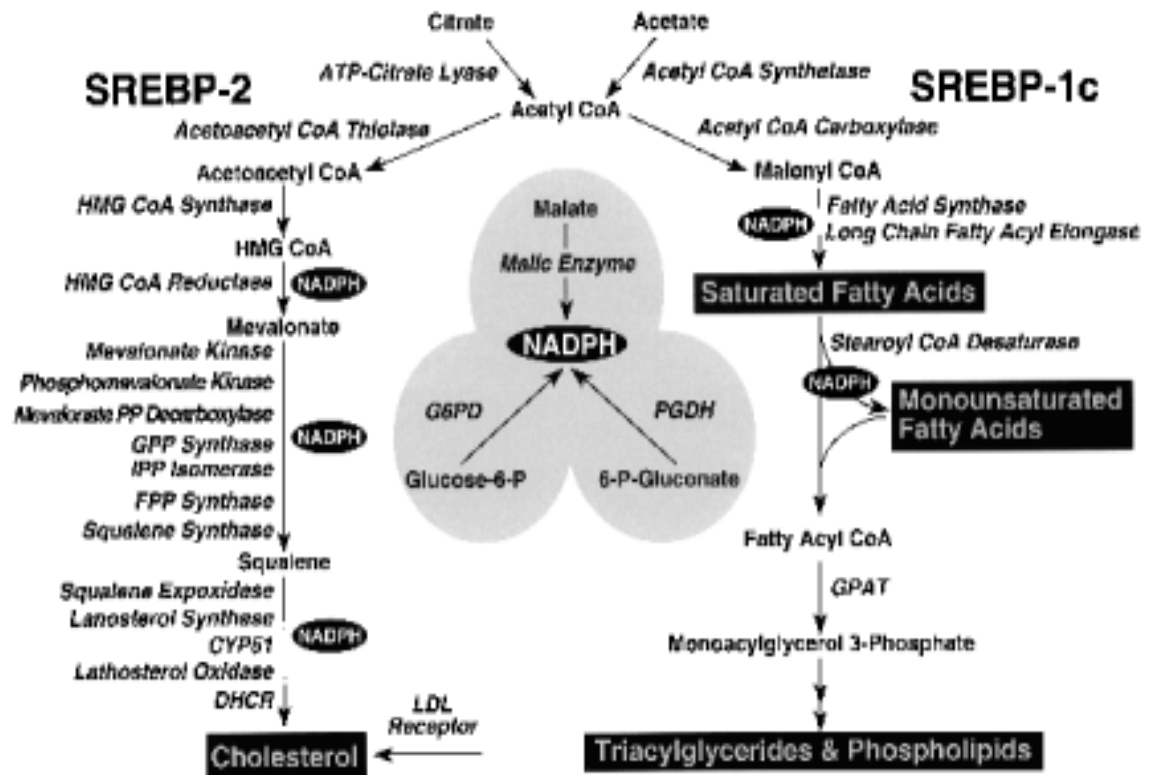


Figure 1.6. shows the main genes regulated in SREBP cholesterol and lipid biosynthetic pathways. SREBP-1c is concerned with regulating genes involved in FA synthesis and SREBP-2 is concerned with regulating genes involved in cholesterol synthesis and transport (diagram taken from Horton et al., 2002)

1.7.1.1 Cholesterol biosynthesis and HCV replication

Several other studies have investigated the effect on HCV replication of cholesterol inhibitors, which target specific stages in cholesterol biosynthesis. These studies found that it was possible to inhibit cholesterol biosynthesis using lovastatin leading to a reduction in replicon RNA levels (Kapadia et al., 2005; Ye et al., 2003). Lovastatin is a specific inhibitor of 3-hydroxy-3-methyl-glutaryl (HMG) CoA reductase that converts HMG CoA to mevalonate, which are both cholesterol precursors (Figure 1.6). Rescue of lovastatin-treated replicon expressing cells with mevalonate gave a dose-dependent increase in HCV RNA levels. This was enhanced by the treatment of the replicon expressing cell line with LDL in addition to other treatments. Supplying cells with LDL, an exogenous cholesterol source, directed metabolites destined for cholesterol biosynthesis to be used to make non-steroid isoprenoids. These “off-shoots” of the cholesterol pathway are synthesised prior to the conversion to the end product, cholesterol (Ye et al., 2003). Furthermore, treatment of cells with zarogozic acid (ZA) induced HCV RNA levels. ZA is a specific inhibitor of squalene synthesis, a metabolite produced after the geranyl and farnesyl sub-pathways but before cholesterol synthesis. This induction was not affected by the addition of cholesterol supplied in LDL. This confirmed that induction was not due to lack of downstream products but the presence of more upstream products. Lovastatin-reduced HCV replication could be restored by treatment in a dose-dependent fashion with geranylgeraniol but not farnesol or oleate (Kapadia et al., 2005).

Prenylation of host cellular proteins facilitates membrane association and can be important for function. Lovastatin reduces downstream isoprenoids and therefore prenylation. After lovastatin-treatment of replicon-expressing cells immunofluorescence studies showed a relocalisation of NS5A foci to display a diffuse cellular distribution. This and previous results suggested membrane association may be altered. The cellular enzymes farnesyltransferase (FTase) and geranylgeranyltransferase I (GGTase I) are involved in the addition of the isoprenoid lipids, farnesyl pyrophosphate and geranylgeranyl pyrophosphate, respectively, to host cellular proteins. A GGTase I inhibitor, GGTI-286, reduced

HCV RNA levels, however an equivalent inhibitor of FTase had no effect (Kapadia et al., 2005). The host cellular geranylgeranylated protein, FBL2, was identified which interacted with NS5A and was essential for viral replication (Wang et al., 2000). Three possible proteins were identified; but only the FBL2 protein interacted with NS5A. FBL2 is an F-box protein known to interact with other F box proteins and may be involved in ubiquitination reactions. The prenylation of FBL2 occurs at geranylgeranylation sequences (CVIL motif) at its C-terminus. Mevalonate labelling of wild type protein produced a radiolabelled band. However, mutants that lack the CVIL motif were unable to be prenylated. Treatment with the GGTI-286 inhibitor abolished FBL2 membrane association. FBL2 bound specifically to NS5A and less efficiently to NS5B. Mutational analysis of both FBL2 and NS5A showed that the N-terminus of NS5A and the geranylgeranylated CVIL motif (CAAX box) were essential for their association. Furthermore, the F-box of FBL2 was required to allow RNA replication in cells expressing the replicon. In other F-box proteins, this domain is required for the interaction with ubiquitin ligase complexes. SiRNA knockdown of FBL2 reduced its expression by 70 % and reduced HCV RNA replicon levels by 60 %. The exact reason for the FBL2 interaction with NS5A is not understood but it may either direct NS5A for ubiquitination or direct it to the membrane.

1.7.1.2 Fatty acid biosynthesis and HCV replicon

Fatty acid biosynthesis can be inhibited by the drug cerulenin, which directly inhibits the enzyme FAS (Su et al., 2002). FAS is a key enzyme in the synthesis of long chain fatty acids using malonyl CoA as a substrate for the sequential elongation of the fatty acid chain to produce a 16 carbon end product, palmitic acid (Figure 1.6). A dose-dependent decrease in the HCV RNA levels was found on treatment with cerulenin in both constitutively expressing and transiently expressing replicon cell lines. This was reported to be independent of toxic effects of the drug (Su et al., 2002). Furthermore 5-(Tetradecyloxy)-2-furoic acid (TOFA), an inhibitor of Acetyl CoA carboxylase (ACC), the rate limiting enzyme in fatty acid biosynthesis, was reported to reduce HCV RNA levels and HCV NS3, NS5A and NS5B protein levels.

Analysis of host cellular gene expression in replicon-expressing cells showed that ATP citrate lyase and acetyl CoA synthetase were induced compared to cells,

which had been cured of replicon. Both these enzymes are concerned with the synthesis of cytosolic acetyl CoA. This is the substrate, which is used to make either cholesterol or fatty acids. Interestingly, FAS expression was not altered compared to cured cells (Kapadia et al., 2005). This was in contrast to in-vivo studies in which FAS was expressed highly in acutely infected chimpanzees with increased viremia. However, no correlation could be found between the high levels of FAS and increasing viremia (Su et al., 2002).

1.7.1.3 Fatty acids and HCV replication

Fatty acids are the product of fatty acid biosynthesis. They consist of a hydrocarbon chain with a methyl group at one end and a carboxyl group at the other, which gives them their acidic nature. The number of carbons in the hydrocarbon tail can vary. Carbon atoms are joined together by a single bond or a double bond. If a fatty acid contains no double bonds they are called “saturated” e.g. palmitic acid. This is because all carbon atoms are involved in the maximum number of carbon hydrogen bonds. A fatty acid with a single double bond is called “monounsaturated” e.g. oleic acid (OLA). Fatty acids with more than one double bond are termed “unsaturated” e.g. linoleic acid. Polyunsaturated fatty acids (PUFAs) e.g. eicosapentaenoic acid (EPA) and docosahexaenoic acid (DHA) contain 2 or more double bonds and cannot be produced in humans directly from acetyl CoA. PUFAs must be supplied through diet or alternatively, via a substrate e.g. linoleic acid that can be converted into a PUFA. As Figure 1.7 shows, the number of double bonds in a fatty acid can drastically alter its structure. This can have important consequences for function where the saturation of fatty acids creates a diverse group of chemicals, which have varied functions.

The effect of fatty acids on HCV RNA levels varies according to the degree of saturation in the hydrocarbon tail. Studies have indicated that saturated fatty acids and monounsaturated fatty acids increase HCV replication (Kapadia et al., 2005; Leu et al., 2004). Furthermore, increasing unsaturated fatty acid levels reduced HCV RNA levels. The degree of unsaturation was an indicator of their ability to inhibit HCV. PUFAs were the most efficient at reducing HCV RNA levels. The PUFA, arachidonic acid, acted synergistically in the presence of

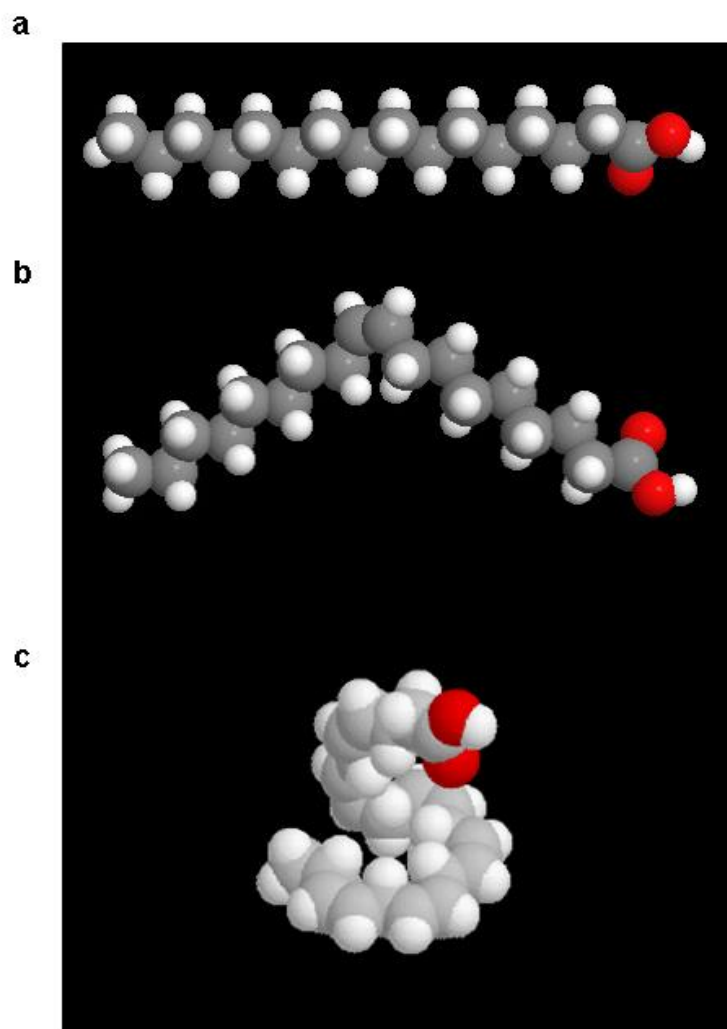


Figure 1.7. A spacefill representation of three fatty acids; saturated palmitic acid (a), monounsaturated oleic acid (b) and polyunsaturated docosahexaenoic acid (c) containing 6 double bonds. Carbons are represented as grey, hydrogens in white and oxygen in red. A double bond is signified by a bend in the hydrocarbon backbone.

IFN- α treatment in inhibiting HCV replication (Leu et al., 2004). PUFAs inhibit fatty acid biosynthesis through their inhibition of SREBP activated gene expression by antagonising its transcriptional partner, liver X receptor (LXR). Treatment of replicon expressing cells with several PUFAs (EPA and DHA) reduced HCV RNA levels as well as SREBP-1c and FAS RNA levels. However, replicon expressing cells could be rescued from inhibition of fatty acid biosynthesis by treatment with the LXR agonist, T0901317. Restoring fatty acid biosynthesis did not rescue PUFA-mediated HCV inhibition. Therefore, PUFA inhibition of HCV was thought to be by a pathway other than the inhibition of fatty acid biosynthesis via SREBP-1c and LXR (Kapadia et al, 2005). This suggests that cerulenin and PUFA inhibition of HCV are mediated by different pathways.

1.8 Lipid metabolism

1.8.1 Sterol Regulatory Element-Binding Proteins

Sterol regulatory element-binding proteins (SREBPs) are a family of transcription factors that are involved in the control of cholesterol and fatty acid metabolism. Fatty acid and cholesterol pathways are controlled nutritionally at the transcriptional level (Shimano H, 2001). There are three isoforms of SREBP; SREBP-1a, SREBP-1c and SREBP-2. SREBP-1a and -1c are derived from the same gene on human chromosome 17p11.2 using alternative transcriptional start sites (Brown M, 1997), resulting in two proteins, which are exactly the same, apart from SREBP-1c having a shorter transactivation domain. The SREBP-2 isoform is transcribed from a separate gene located on human chromosome 22q13.

The different isoforms have distinctly different regulation profiles. SREBP-1c is more involved with the regulation of lipogenic genes and SREBP-2 is involved in the regulation of cholesterologenic genes. SREBP-1a is thought to be involved in maintaining basal levels of both cholesterol and lipid synthesis and transport (Horton et al., 2002; Pai et al., 1998). Tissue expression patterns show SREBP-1c may be expressed 10-fold more abundantly than SREBP-1a and twice as abundantly as SREBP-2, although this varies according to tissue (Shimomura et al., 1997).

Structurally SREBPs belong to the basic-helix-loop-helix-leucine zipper (bHLH-Zip) family of transcription factors. SREBPs are produced as protein precursors bound to the ER and contain several structural domains with two membrane-spanning regions positioned such that the C- and N-terminals of protein project into the cytoplasm. The N-terminal region contains the bHLH-Zip region. On release from the ER membrane, the bHLH-Zip region (nSREBP) of the protein is able to enter the nucleus to activate target genes. nSREBP is released in a two-step proteolytic process (Horton et al., 2002). On entry to the nucleus, nSREBP binds to specific DNA recognition sequences in target genes. These regulatory sequences have been termed sterol regulatory elements (SREs). Other sequences that nSREBP binds are the classic palindromic E-boxes. nSREBPs activate a range of genes involved in cholesterol and lipid metabolism. Genes involved in cholesterol synthesis have an SRE closely similar to the classic SRE. Lipogenic genes show a more divergent SRE sequence (Mater et al., 1999). The varying length in transactivation domains of the SREBP isoforms dictates which type of gene is activated. The shorter transactivation domain of SREBP-1c means it is only concerned with regulating lipogenic genes. It is thought that the shorter length of transactivation domain reduces its overall activation ability. However, SREBP-1a retains the long transactivation domain and is able to activate all SREBP responsive genes (Horton et al., 2002; Pai et al., 1998).

The C-terminus of SREBP is thought to interact with SREBP cleavage activating protein (SCAP) and is also involved in sterol regulation (Hua et al., 1996; Sakai et al., 1997). SCAP is both an escort protein and a sterol sensor. The mechanism by which it senses increased lipid demand is unknown. However, SCAP associates with SREBP through its C-terminus and escorts it from the ER to the golgi for proteolytic cleavage (Horton et al., 2002; Shimano H, 2001). In the presence of sterols, SCAP-SREBP complexes interact with insulin-induced gene (INSIG), which retains them in the ER (Yabe et al., 2002). However, when sterols are depleted SCAP undergoes a conformational change, which stops its interaction with INSIG and allows translocation to the golgi for cleavage to the nuclear form. Originally, this mechanism was thought to apply to all SREBP isoforms. However, *in vivo* studies indicated that something quite opposite happens with SREBP-1c. In rodents, sterol depletion led to mature forms of SREBP-1c being reduced and this was mainly regulated by nutritional status (Horton et al., 1998).

Regulation of SREBP-1c is mainly thought to occur at the transcriptional level through control by insulin and the transcription factor liver X receptor (LXR). Agonists of LXR are able to activate lipogenic gene expression and induce SREBP-1c expression (Hegarty et al., 2005). LXR will be discussed in more detail later in section 1.8.3. Insulin as well as LXR activation of SREBP-1c was required for cleavage of the precursor SREBP-1c and activation of lipogenic gene expression (Figure 1.8). However, LXR induced expression of SREBP-1c without insulin poorly activated lipogenic gene expression. Interestingly, LXR activates expression of both INSIG and SREBP-1c. This would appear to be counterproductive in that activation of the mature SREBP-1c isoform would be prevented by expression of INSIG. It is thought that this mechanism protects in

times of low glucose availability and prevents the production of fatty acids from glucose. LXR activation of SREBP-1c would not activate lipogenic gene expression until blood glucose levels are sufficiently high that insulin is produced. This mechanism would allow a rapid response to increased glucose levels for the conversion to fatty acid (Hegarty et al., 2005).

Overexpression of SREBP-1c in transgenic mice leads to steatosis and increases in lipogenic gene expression (Shimomura et al., 1998). Furthermore, increased SREBP-1c levels are associated with insulin resistance by inhibition of IRS-2 signalling (Ide et al., 2004).

1.8.2 Peroxisome proliferator activated receptor

Peroxisome proliferator activated receptor (PPARs) proteins are members of the superfamily of ligand activated nuclear transcription factors. Their transcriptional effect is directly at the gene level where they affect genes involved in fatty acid oxidation and storage. PPARs themselves act as lipid sensors controlling lipid metabolism according to fatty acid fluctuations. There are three subtypes, PPAR α , PPAR δ (PPAR β) and PPAR γ (Smith S, 2002). PPARs contain several modular domains with functions including DNA binding, protein binding and ligand binding.

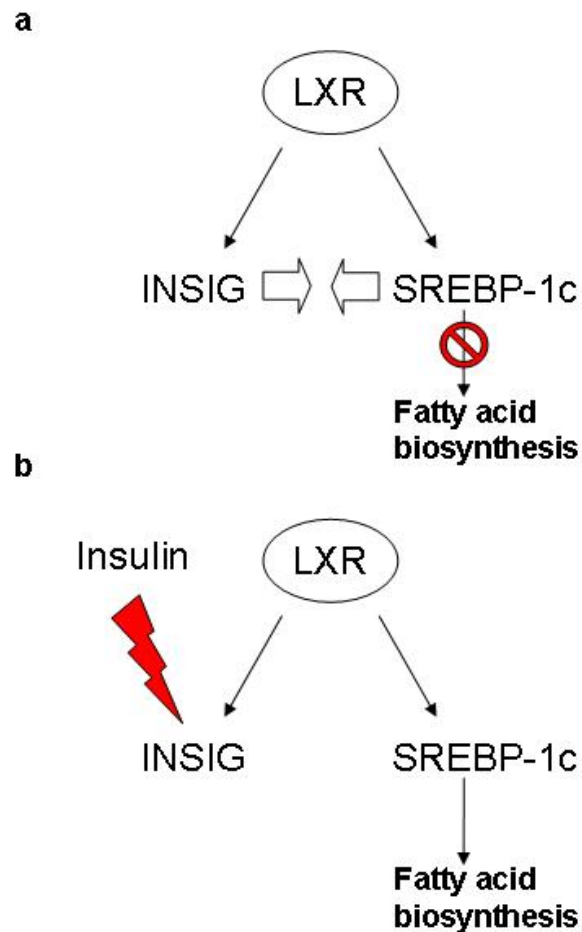


Figure 1.8. A representation of the interaction between LXR, INSIG and SREBP-1c. Panel a) shows that LXR transactivates INSIG and SREBP-1c. SREBP1c and INSIG interact with each other on the ER preventing nuclear SREBP-1c formation and lipogenic gene expression. Panel b) shows in the presence of insulin INSIG undergoes a conformational change releasing SREBP-1c for processing and leads to the activation of lipogenic gene expression.

For transcriptional activation, PPARs must heterodimerise with activated retinoid X receptor (RXR) (Kliewer et al., 1992). RXR is part of the same ligand dependent nuclear receptor super family as PPARs. PPAR-RXR heterodimers without ligand form large complexes with associated repressors. Ligand binding causes a conformational change releasing repressors and activating the transactivation domain. PPARs are able to bind a range of endogenous ligands that include all fatty acids except short-chain fatty acids (<C10), very long chain monounsaturated fatty acids and dodecanedioic acid (12 carbon fatty acid). Exogenous substances, which induce peroxisome proliferation, can also activate PPARs. These include hypolipidemic fibrate drugs, phthalate ester plasticizers and herbicides (Schoonjans et al., 1996). Fatty acids are trafficked to the nucleus by liver fatty acid binding protein (L-FABP) where a direct interaction with PPAR isoforms and L-FABP is observed (Wolfrum et al., 2001).

PPAR-RXR activated heterodimers are able to bind to specific DNA sequences within target genes. These PPAR response elements (PPREs) are a direct repeat (DR) with a consensus of six bases (TGACCT), followed by an irrelevant spacer base (termed the DR-1 element) and followed by a further six base repeat (Smith S, 2002).

The different isoforms of PPAR are expressed heterogeneously in different tissues. Where a tissue has higher lipid oxidation levels, for instance the heart, liver and skeletal muscle, the dominant isoform of PPAR, is PPAR α . In white and brown adipose tissue where lipids are stored, the predominant isoform is PPAR γ . There are two types of PPAR γ , PPAR γ 1 and PPAR γ 2 (Elbrecht et al., 1996). Reports on the expression of these two isoforms are conflicting in human studies but rodent studies have indicated that PPAR γ 2 is adipose tissue specific (Smith S, 2002). PPAR δ is expressed fairly ubiquitously in tissues (Kliewer et al., 1992).

It is possible to induce peroxisome proliferation and PPAR-induced proteins by treatment with exogenous PPAR ligands. Peroxisomes are subcellular organelles, which have a single membrane and carry out many important anabolic and catabolic enzymatic processes (Schoonjans et al., 1996). Fibrate activation of PPAR α in rodents leads to hepatic peroxisome proliferation and increased expression of enzymes involved in fatty acid peroxisomal and microsomal oxidation pathways. However, this activation is noted only in rodents and not in

humans. PPARs have low ligand specificity and although PUFAs have a higher affinity than saturated FAs, there is no difference in activation properties. This has meant that elucidating the exact role of PPAR α is difficult. It may act merely as a sensor to prevent excess triacylglycerols from accumulating, although a role in regulating energy supply for vascular and cardiac tissues has been proposed (Schiffrin et al., 2003; Smith S, 2002).

The biological function of PPAR δ remains undefined. It can be activated in a similar manner to PPAR α . Knockout mice experiments have indicated that it may have some role in FA uptake, brain development and skin epidermal cell differentiation (Smith S, 2002). Other studies have indicated a role as an anti-atherosclerosis and anti-inflammatory agent. It is up-regulated in activated macrophages (Haraguchi et al., 2003; Schiffrin et al., 2003).

Insulin sensitising agents (e.g. thiazolidinediones) activate PPAR γ when insulin resistance is found, allowing the selective activation of PPAR-responsive genes. As mentioned earlier, of the two isoforms, PPAR γ 2 plays an important role in adipocyte differentiation and adipose storage in rodents. In both humans and rats, a sustained activation of PPAR γ leads to altered adipose tissue distribution (Smith S, 2002).

When looking at genes involved in PPAR regulation, many studies utilise transgenic rodents but it should be appreciated that the action of specific PPAR isoforms may differ between rodent and human forms. For instance, human PPAR α is present at lower levels and does not induce the enzymatic cascades to the same extent as does murine PPAR α (Palmer et al., 1998).

1.8.3 Liver X Receptor and insulin

PUFAs are able to inhibit genes involved in lipogenesis such as FAS and steroyl-CoA desaturase (Clarke S, 2001). This is due to down-regulation of SREBP-1c mediated by the interaction of the transcription factor LXR (Kersten S, 2002).

LXR is a member of a family of nuclear receptors, which form obligate heterodimers with RXRs. They are activated by oxysterols. There are two subtypes LXR α (expressed in the liver, spleen, kidney, adipose and small intestine) and LXR β (expressed ubiquitously). LXR-RXR heterodimers recognise

specific sequences within target genes called LXR response elements (LXRE). They have also been shown to be dominant activators of the SREBP-1c promoter (Hu et al., 2003). Although LXR- α in hepatocytes is a potent activator of SREBP-1c expression and transcription, insulin is required to induce the mature nuclear form.

The activation of PPAR α to form PPAR-RXR heterodimers, could reduce the available RXR for the LXR-SREBP-1c pathway by reducing the cellular levels of LXR-RXR heterodimers and therefore limit activated LXR formation (Figure 1.9) (Yoshikawa et al., 2003). LXR inhibits PPAR α and lipid degradation. This is partially explained by competition between PPAR and LXR for RXR. It has, however, been shown that, in presence of its ligand, LXR can also bind to PPAR α to form a heterodimer which, not only inhibits the LXR-SREBP-1c lipid biosynthesis pathway, but also the PPAR α -RXR lipid degradation pathway. PUFAs which act as PPAR ligands are also able to inhibit LXR by binding and preventing LXR-RXR heterodimerisation. Interaction between pathways leads to a mutual regulation of lipid degradation and lipolysis (Ide et al., 2003).

1.8.4 Lipid Transport

Lipids are transported in the blood in the form of lipoproteins, ketone bodies or conjugated to BSA. As mentioned there are various forms of lipoproteins. Proteins which are needed for lipoprotein formation are called apolipoproteins and these are specific to the type of lipoprotein. Lipids absorbed by the gut are released into the blood flow as large chylomicrons in a process, which requires apolipoprotein B-48. Chylomicrons contain an internal TAG store that is hydrolysed to produce free fatty acid and glycerol, which is mainly absorbed by the liver. The liver releases endogenous lipids in the form of VLDL in a process which requires apolipoprotein B-100 (Kwiterovich P, 2000). As previously discussed, complete lipidation of apolipoproteins is required for VLDL secretion (Perlemuter et al., 2002). VLDL is hydrolysed in the blood to produce intermediate density lipoprotein (IDL), which is further hydrolysed to produce low density lipoprotein (LDL). VLDL and LDL are associated with atherogenesis. PUFA treatment of patients with atherogenesis may have a positive effect reducing circulating VLDL and LDL and increasing high density lipoprotein (HDL) levels (Kwiterovich P, 2000).

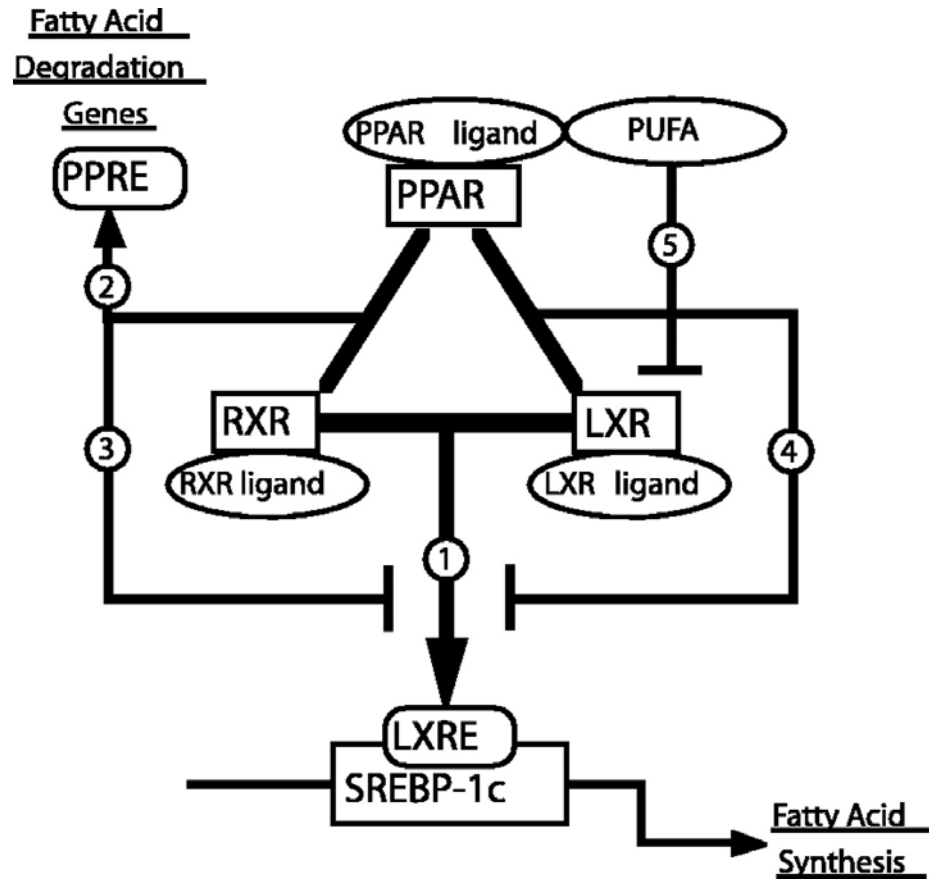


Figure 1.9. A diagrammatic representation of the interactions between PPAR, RXR, LXR and SREBP-1c. 1. LXR and RXR dimerise transactivating SREBP-1c transcription from the LXRE in the SREBP-1c promoter. 2. Ligand activated PPAR- α /RXR transactivate expression of genes involved in lipid β -oxidation. 3 and 4, The formation of PPAR/RXR and PPAR/LXR inhibits SREBP-1c expression and down-regulates fatty acid biosynthesis. 5. PUFAs, which are PPAR ligands, down-regulate fatty acid biosynthesis by antagonising LXR (Yoshikawa et al., 2003).

A role for VLDL in HCV viral assembly and secretion has recently been identified where two agents, which reduce VLDL formation were able to reduce HCV particle production. Using an inhibitor of MTP or siRNA directed against apoB HCV particle release was reduced without affecting HCV replication. Furthermore, HCV replication complexes were isolated in membrane fractions enriched in MTP, apoB and apoE, which are all involved in VLDL formation. These results suggested that HCV particles are associated with or incorporated into VLDL particles and VLDL assembly is important for viral particle release (Huang et al., 2007). Yao et al (2008) showed that an inhibitor of long chain acyl-CoA synthetase 3, a protein required for VLDL secretion, could inhibit HCV particle release. VLDL formation can be reduced by treatment of cells with PUFAs. PUFAs activate a post-ER presecretory proteolysis pathway, which targets apoB for degradation and thereby reduces VLDL formation (Pan et al., 2004). Further work would be required to ascertain whether PUFA treatment of HCV infected cells would reduce particle assembly and release. However, it does not go to explain why PUFAs are also able to reduce HCV replication. As the study above indicated that a reduction of VLDL formation had no impact of HCV replication.

1.9 Aims and objectives of my project

There were three parts to the project each with their own aims:

- The aim of the first two parts of the project were to treat HCV genotypes 1b and 2a replicon expressing cells with inhibitors of fatty acid biosynthesis and measure the effects on HCV RNA and protein levels while also measuring the effect of cellular fatty acid biosynthesis and cell viability. The two methods chosen were cerulenin mediated inhibition, which directly inhibits fatty acid synthase and PUFA mediated inhibition, which inhibits the transcription of genes involved with fatty acid biosynthesis. Following on from this the objective was to ascertain the mechanism for the inhibition of HCV RNA levels that was occurring.
- The third part of the project was to amplify an HCV genotype 3 isolate and assemble genotype 3 replicon-expressing cells, which was of isolate majority sequence. This genotype 3 replicon-expressing cell line was to

be used to observe the effect of genotype 3 on the accumulation of intracytoplasmic lipid droplets.

Chapter two

2 Materials and Methods

2.1 Materials

2.1.1 Bacterial Strains

Escherichia (E.coli) strain

Phenotype

DH5 α

F' / *endA1 hsdR17 (r_k⁻m⁺) supE44 thi1
recA1 gyrA (Nal^r) relA1 Δ (*lacZYA-argF*)
U169 (Φ 80*dlac(lacZ)*M15)*

2.1.2 Vectors

pCR[®]2.1-TOPO[®]

Invitrogen, Paisley, UK

pGEM[®] T-Easy

Promega, Southampton, UK

pUC18

Roche Applied Sciences, Burgess Hill,
UK

pSP64 Poly A

Promega, Southampton, UK

2.1.3 Enzymes and Kits for DNA modification

QIAmp Viral RNA Mini Kit, Ominscript™ Qiagen, Crawley, UK

RT Kit, QIAprep® Miniprep Kit,

QIAprep® Midiprep Kit, QIAquick® Spin

Kit, QIAquick® Gel Extraction Kit

Superscript™ II Reverse transcriptase, Invitrogen, Paisley, UK

ThermoScript™ RT-PCR system, *Taq*

DNA Polymerase, Platinum® *Pfx* DNA

Polymerase, Deoxyribonuclease I, DNA

Polymerase I Large (Klenow) Fragment

dNTPs

Advantage™ HF 2 PCR, Advantage™ 2

PCR

BD Biosciences, Oxford, UK

SP6/T7 Transcription Kit, Phosphatase

Alkaline Shrimp (SAP), RNase H,

Restriction Enzymes

Roche Applied Sciences, Burgess Hill,

UK

RNasin® Rnase inhibitor, T4 DNA Ligase, Promega, Southampton, UK

rNTPs

Restriction Enzymes

New England Biolabs, Hitchin, UK

Taqman® Universal PCR master mix,

SYBR® green PCR master mix

Applied Biosystems, Warrington, UK

2.1.4 Mammalian cell lines and culture media

Human hepatocellular carcinoma (HuH-7) cells, 5-15 HCV genotype 1b expressing clonal cell line 12 (Bartenschlager et al., 1999), HCV genotype 2a JFH1 expressing cell line (Kato et al., 2003), interferon cured replicon cell lines for the 1b and 2a genotypes.

Dulbecco's Modified Eagles Medium (DMEM), foetal calf serum, L-glutamine, non-essential amino acids (MEM) and penicillin/streptomycin were supplied by Invitrogen life technologies. Phosphate Buffered Saline (PBSA and PBS complete), versene, Luria Bertani (LB) broth, LB agar were produced "in house" by the media department of the Institute of Virology.

2.1.5 Human Serum

Human serum in this study was obtained from a HCV genotype 3 infected patient. The serum was collected at Gartnavel General Hospital, Glasgow, after informed consent had been obtained from the patient. Ethical approval was obtained from West Glasgow Ethics committee. Serum was separated by Carol-Anne Smith. Samples were stored at -80°C.

2.1.6 Radiochemicals

³² P-dCTP	10 µCi/µl	Amersham, Little Chalfont, UK
1- ¹⁴ C Acetic acid	1 µCi/µl	MP Biomedicals, Illkirch, France

2.1.7 Antibodies and stains

R1065 Rabbit Polyclonal antiserum raised against NS5A	Made by J. McLauchlan and G. Hope. Raised against NS5A derived against the H77 sequence corresponding to 3 synthetic peptides from amino acid 197-212, 255-264 and 289-303
Sheep Polyclonal antiserum raised to NS5A	Made by Macdonald et al (2003)
Anti-adipocyte differentiation related protein monoclonal antibody	Made by Target-Adams et al (2003)

Anti-calnexin monoclonal antibody	Chemicon, http://www.millipore.com
Anti-GAPDH monoclonal antibody	AMS Biotech, Milton Abingdon, UK
Anti-mouse HRP, Anti sheep HRP, Protein A- Peroxidase Conjugate from <i>Staphylococcus aureus</i> /horseradish, TRITC Goat Anti-rabbit IgG (Alexis 488), TRITC donkey anti-rabbit IgG (Alexis 488), FITC goat anti-mouse IgG (Alexis 568), FITC donkey anti-goat IgG (594)	Sigma-Aldrich, Gillingham, UK

2.1.8 Chemicals

All chemicals were purchased from Sigma-Aldrich Co., unless stated.

Hybond Nitrocellulose membrane, ECL reagent	Amersham, Little Chalfont, UK
Nylon membrane, 30% Acrylamide/Bis solution, ammonium persulphate	Bio-Rad, Hemel Hempstead, UK
Dried skimmed milk	“Marvel” (Cadburys), London, UK
Viraferon (pegylated interferon alpha-2b)	Zymed Laboratories, San Francisco, USA
C75, Cerulenin	Axxora Biochemicals, Sigma Aldrich Ltd
Cerulenin	Sigma-Aldrich, Gillingham, UK

2.1.9 Solutions

4MGT solution	4 M Guanidinium thiocyanate, 750 mM Sodium citrate pH 7 (with citric acid), 10 % N-lauroylsarcosine sodium salt
Agarose gel loading buffer	100 mM EDTA, 50 % sucrose, 1 µg/ml bromophenol blue.
Alkaline hydrolysis solution	50 mM NaOH, 1.5 M NaCl
Boiling mix	31 % stacking gel buffer, 31 % glycerol, 21 % sodium dodecyl sulphate (SDS)(25 %), 9 % β-mecaptoethanol, 1 µg/ml bromophenol blue, 8 % water.
Denhardt's solution	10 g Ficoll 400, 10 g polyvinylprrolidone, 10 g bovine serum albumin in 500 ml H ₂ O
Gel running buffer	40 mM Tris, 186 mM Glycine, 0.1 % SDS
Hybridisation buffer	50 % formamide, 5 x sodium chloride sodium citrate (SSC), 1 x Denhardt's solution, 0.1 % SDS, 100 µg/ml herring sperm DNA
LB Agar	LB broth plus 1.5 % (w/v) agar
LB Broth	10 g tryptone, 5 g yeast extract, 10 g NaCl in 1 L H ₂ O
Low stringency wash	2 x SSC, 0.1 % SDS
Lysis Buffer (solution II)	0.2 M NaOH, 1 % SDS

Neutralisation Buffer (solution III)	60 ml $\text{KC}_2\text{H}_3\text{O}_2$ (5 M), 11.5 ml glacial acetic acid, 28.5 ml water
Neutralisation solution	500 mM Tris (HCl pH 7.4), 1.5 M NaCl
Moderate stringency wash	0.2 x SSC, 0.1 % SDS
MOPS buffer	200 mM MOPS [3-(<i>N</i> -morpholino)-propanesulfonic acid] pH 7.0, 50 mM sodium acetate, 10 mM EDTA
PBS	PBS(A) plus 6.8 mM $\text{CaCl}_2 \cdot 2\text{H}_2\text{O}$ and 4 mM $\text{MgCl}_2 \cdot 6\text{H}_2\text{O}$
PBS(A)	170 mM NaCl, 3.4 mM KCl, 10 mM Na_2HPO_4 , 1.8 mM KH_2PO_4 , 25 mM Tris-HCl (pH 7.2).
PBST	PBS(A) plus 0.05 % (v/v) Tween 20
Prehybridisation buffer	50 % formamide, 5 x SSC, 5 x Denhardt's solution, 0.1 % SDS, 100 $\mu\text{g}/\text{ml}$ herring sperm DNA
Resolving gel buffer	1.5 M Tris-HCl (pH 8.9), 0.4 % SDS
Resuspension buffer (solution I)	50 mM Glucose, 10 mM EDTA, 25 mM Tris pH 8.0 (HCl)
RNA loading buffer	100 μl MOPS, 178 μl formaldehyde pH 4, 222 μl DEPC water, 500 μl pure formamide
RNA running buffer	50 % glycerol, 0.1 % bromophenol blue, 0.1 % xylene cyanol

SSC 20x	3 M NaCl, 300 mM Na ₃ Citrate·2H ₂ O, pH 7.0 with 1 M HCl
Solution D	50 ml 4M GT solution, 0.36 ml 2 M β- mercaptoethanol
Stacking gel buffer	0.5 M Tris-HCl (pH 6.8), 0.4 % SDS
Stripping buffer	62.5 mM Tris (pH 6.8), EDTA 100 mM, 2 M β-mercaptoethanol, 2% SDS
TBE x10	890 mM Tris, 890 mM Boric acid, 20 mM EDTA (pH 8.0)
TE buffer	10 mM Tris·Cl (pH 7.5), 1 mM EDTA
Towbin buffer	25 mM Tris-HCl (pH8.3), 192 mM glycine, 20 % (v/v) methanol
Versene	0.6 mM EDTA in PBS(A), 0.002 % (w/v) phenol red

2.1.10 Other materials and apparatus

Bacterial and tissue culture plasticware was supplied by Nunc. Taqman[®] plates and lids were purchased from VWR. Ecoscint[™] A was obtained from National Diagnostics. X-Omat UV film, developer and fixer for the Dynex, were purchased from KONICA.

2.1.11 Synthetic Oligonucleotides

Oligonucleotides were ordered from Sigma-Genosys.

Primer	Primer name	Use	Sense/ Antisense	Primer sequence (5'- 3')
Primer 1	PP-AC5- GT1/3	Sequencing (A1F)	Sense	GCGACACTCCACCATG
Primer 2	PP-AC8- GT1/3	Sequencing (A1R)	Antisense	GATGTACCCCATGAGG
Primer 3	MSQ1	Sequencing (A2F)	Sense	AAAGTCATCGATACCCT
Primer 4	MSQ10	Sequencing (A2R)	Antisense	GCCATTCGATGTCCTGAG AG
Primer 5	MSQ15	Sequencing (A3F)	Sense	AAGCCTTCACGTTCCAGAC CT
Primer 6	MSQ9	Sequencing (A3R)/PCR	Antisense	AGGTGCGTAGTGCCAGC AGT
Primer 7	MSQ13	Sequencing (B1F)/PCR	Sense	ACCAATGGCTCGTGGCAC ATC
Primer 8	MS2	Sequencing (B1R)/PCR	Reverse	TGATAAGGTAAAGAAGCC G
Primer 9	MSQ7	Sequencing (B2F)	Sense	GTCTGCGGCCCTGTGTAC TG
Primer 10	MSQ16	Sequencing (B2R)	Antisense	GGGGGAGCTCCGCACGT CTTG
Primer 11	MSQ12	Sequencing (C1F)/PCR	Sense	CGCTGAACGCCGTCGCTG CT

Primer	Primer name	Use	Sense/ Antisense	Primer sequence (5'- 3')
Primer 12	a4935gt3	Sequencing (C1R)/PCR	Antisense	CGAGCAGCCCGCGTCATA GC
Primer 13	s3990gt3	Sequencing (C2F)	Sense	TCTGACAATTCAACTCCT CCTG
Primer 14	a4098gt3	Sequencing (C2R)	Antisense	GTGCTACCATAAGCGGCC GGGAC
Primer 15	s3471gt3	Sequencing (C3F)/	Sense	GGGCCTTCTTGGGACTAT TG
Primer 16	a3550gt3-SpeI	Sequencing (C3R)/PCR	Antisense	GCGCACTAGTCGTGGAAA GCACCTGCACTT
Primer 17	s4935gt3	Sequencing (D1F)/PCR	Sense	GCTATGACGCGGGCTGC TCG
Primer 18	a6120gt3-SpeI	Sequencing (D1R)/PCR	Antisense	GCGCACTAGTCGCGATGA GCCTGTTCATCCACT
Primer 19	s5475gt3	Sequencing (D2F/I1F)	Sense	CGATGAGATGGAGGAGT GCT
Primer 20	a5548gt3	Sequencing (D2R/J1R)	Antisense	CCTTGA ACTGGTGGGCTA T
Primer 21	s4586gt3	Sequencing (J1F)/PCR	Sense	GATGAGATAGCGTCCAAA CTCAGAGGCA
Primer 22	3a5aAO31	Sequencing (I1R)	Antisense	ACATGTTAGCACATGTAC GC

Primer	Primer name	Use	Sense/ Antisense	Primer sequence (5'- 3')
Primer 23	3a5aA032	Sequencing (G1F)/PCR	Sense	AGCGACGATTGGCTGCG TAT
Primer 24	3aAnti	Sequencing (G2F)/PCR	Antisense	GGAGGTTTCTTGAAACAC TC
Primer 25	35a6	Sequencing (H1F)	Sense	CCCTGTGAGCCAGAACCA GA
Primer 26	3a5aA035	Sequencing (H1R)/PCR	Antisense	AGCAGCAGACCACGCTCT GT
Primer 27	3a5aA038	Sequencing (F1F)/PCR	Sense	AGGAAGAGAATAGCTCAT AA
Primer 28	PP6-Gt2/3Rev	Sequencing (F2R)/PCR	Antisense	ACACGCTGTGATAAATGT CG
Primer 29	s8308gt3	Sequencing (F2F)	Sense	CTGTCACTGAACAGGACA TCA
Primer 30	a8343gt3	Sequencing (F2R)	Antisense	CTCCTCTTCCACCCTGAT GT
Primer 31	s8818gt3	Sequencing (F3F)	Sense	GGGAAACAGCTCGTCACA CT
Primer 32	a8878gt3	Sequencing (F3R)/PCR	Antisense	GCGCGTACATGATGATGT T
Primer 33	s7466gt3	Sequencing (F4F)PCR	Sense	GTCCAGCACTACTTCCAA GGT

Primer	Primer name	Use	Sense/ Antisense	Primer sequence (5'- 3')
Primer 34	semcv2	Sequencing (semcv)	Sense	CCGCTATCAGGACATAGC GTT
Primer 35	aemcv2	Sequencing (aemcv)	Antisense	GGTTGCGGTCAGCCCATT
Primer 36	3a5aA032	PCR	Sense	AGCGACGATTGGCTACGT AT
Primer 37	5-15-neo emcv-BglII	PCR	Antisense	AGATCTCAAAGGAAAACC ACGTCCCCGT
Primer 38	NS3GT3-BglII	PCR	Sense	AGATCTACGAATGGCTCC GATCACAGCATA
Primer 39	aXtailGT3- SpeI	PCR	Antisense	GCACTAGTAGTACTTGAT CTGCAGAGAGGCCAGTA
Primer 40	aluc-NotI	PCR	Antisense	AAACTTACACGGCGATCT TTCCGC
Primer 41	sluc-gt3(2)	PCR	Sense	GCGTCTTCCATGCGGCCG CTGGCGCGCCCGTTGGT CTT
Primer 42	aluc-NotI(2)	PCR	Antisense	AGCGGCCGCATGGAAGA CGCCAAAAACATAAAGA
Primer 43	alucPme1	PCR	Antisense	TCTGTTTAACTTACACG GCGATCTTTCCGC

Primer	Primer name	Use	Sense/ Antisense	Primer sequence (5'- 3')
Primer 44	Vtag940	PCR	Sense	GTGGTCAAGACGCCTAGA GCTTCACGCAGA AAGCGTCTAG
Primer 45	Vtag3	PCR	Sense	GTGGTCAAGACGCCTAGA GC
Primer 46	NCR4	PCR	Antisense	CACTCTCGAGCACCTAT CAGGCAGT
Primer 47	EMCVHCVF	PCR	Sense	TCTGCGGAACCGGTGAG TAC
Primer 48	EMCVHCVR	PCR	Antisense	GCACTCGCAAGCACCTA TC
Primer 49	PP-GT3- 5'UTR	PCR	Sense	TGCGGATCCACCTGCCTC TTACGAGGCGACACTCCA CCA
Primer 50	T7-5UTR-GT3	PCR	Sense	TAATACGACTCACTATAG ACCTGCCTCTTACGAGGC GAC
Primer 51	sGAPDH1	PCR	Sense	ATCTTCTTTTTCGTCGCC AG
Primer 52	SGAPDH2	PCR	Sense	ACCACAGTCCATGCCATC AC
Primer 53	aGAPDH1	PCR	Antisense	CCCACAGCCTTGGCAG

Primer	Primer name	Use	Sense/ Antisense	Primer sequence (5'- 3')
Primer 54	3a5aA034	PCR	Sense	CACGGTACTTTCCCCATC AA
Primer 55	sG225Tgt3	Site-directed mutagenesis	Sense	CTCAATACCCAGAAATTT GGGCGTGCCCC
Primer 56	aG225Tgt3	Site-directed mutagenesis	Antisense	GGGGCAGCCCAAATTTTC TGGGTATTGAG
Primer 57	sA4820Tgt3	Site-directed mutagenesis	Sense	GTTTCTCGCAGCCAACGT CGTGGCCGTACGG
Primer 58	aA4820Tgt3	Site-directed mutagenesis	Antisense	CCGTACGGCCACGACGTT GGCTGCGAGAAAC
Primer 59	sD6290EGT3	Site-directed mutagenesis	Sense	GTTGCGTACCATCTGGGA ATGGGTTTGCACTG
Primer 60	aD6290EGT3	Site-directed mutagenesis	Antisense	CAGTGCAAACCCATTCCC AGATGGTACGCAAC
Primer 61	sA7792Vgt3	Site-directed mutagenesis	Sense	CTTCGACAGGCTGCAGGT GCTCGACGACCATTACAA GAC
Primer 62	aA7792Vgt3	Site-directed mutagenesis	Antisense	GTCTTGTAATGGTCGTCC AGCACCTGCAGCCTGTCC AAG
Primer 63	sI8302Tgt3	Site-directed mutagenesis	Sense	CTGCTTTGACTCGACTGT CACTGAACAGGACATCAG

Primer	Primer name	Use	Sense/ Antisense	Primer sequence (5'- 3')
Primer 64	aI8302Tgt3	Site-directed mutagenesis	Antisense	CTGATGTCCTGTT CAGTG ACAGTCGAGTCAAAGCAG
Primer 65	sT8967Agt3	Site-directed mutagenesis	Sense	GACTTTGAAATGTACGGG GCCACTTACTCTGTCACT C
Primer 66	aT8967Agt3	Site-directed mutagenesis	Antisense	GAGTGACAGAGTAAGTG GCCCCGTACATTTCAAAG TC
Primer 67	sC9098Igt3	Site-directed mutagenesis	Sense	GAAGCTTGGGTGCCCCCC CCTACGGGCTTG
Primer 68	aC9098Igt3	Site-directed mutagenesis	Antisense	CAAGCCCGTAGGGGGGG GCACCCAAGCTTC
Primer 69	sS2204Igt3	Site-directed mutagenesis	Sense	GCTAGCTCATCCGCCATT CAACTATCGGCTCC
Primer 70	aS2204Igt3	Site-directed mutagenesis	Antisense	GGAGCCGATAGTTGAAT GGCGGATGAGCTAGC
Primer 71	sGNDgt3	Site-directed mutagenesis	Sense	CCCGGACTTTCTTGTCTG CGGAAATGATCTAGTCGT GGTGGC
Primer 72	aGNDgt3	Site-directed mutagenesis	Antisense	GCCACCACGACTAGATCA TTTCCGCAGACAAGAAAG TCCGGG

Primer	Primer name	Use	Sense/ Antisense	Primer sequence (5'- 3')
Primer 73	sΔBglIlgT3	Site-directed mutagenesis	Sense	CGTGGTTTTTCCTTTGAAA AACACGAATGGCTCCGAT CACAGC
Primer 74	aΔBglIlgT3	Site-directed mutagenesis	Antisense	GCTGTGATCGGAGCCATT CGTGTTTTTTCAAAGGAAA ACCACG
Primer 75	slucΔScal	Site-directed mutagenesis	Sense	GTGGACATCACTTACGCT GAATACTTCGAAATGTCC GTTCG
Primer 76	alucΔScal	Site-directed mutagenesis	Antisense	CGAACGGACATTTTGAAG TATTCAGCGTAAGTGATG TCCAC
Primer 77	a9425gt3	PCR	Antisense	GCTCCCCGTTACCCGAGC
Primer 78	PP-AC6-GT3	PCR	Antisense	CGGGAACGACATTTATC
Primer 79	3a5aAO33	PCR	Antisense	AATATGCGGCCTTTAGG
Primer 80	PM3 2AS	PCR	Antisense	GTAGTACTTGATCTGCAG AGAGGCCAGTA

2.2 Manipulation of RNA and DNA

2.2.1 Extraction of viral RNA from serum

Viral RNA was extracted from serum using the QIAamp Viral RNA Mini Kit. Samples were first brought to 15 - 25°C. A 560 µl aliquot of buffer AVL containing carrier RNA was placed into a 1.5 ml micro-centrifuge tube. An

aliquot of 140 μ l of serum was added to the buffer AVL and mixed by pulse vortexing. The sample was incubated at room temperature for 10 min. Any drops were removed from the lid by centrifuging briefly. A 560 μ l aliquot of absolute ethanol was added to the sample and mixed by pulse-vortexing for 15 secs. Any drops were again removed from the lid by centrifuging briefly. The sample was bound to the column by applying 630 μ l of the solution to a QIAamp spin column in a 2 ml collection tube. The sample was centrifuged at 6800 g for 1 min and the collection tube was discarded. Then another 630 μ l of the solution was applied to the spin column and the process was repeated. The spin column was placed in a fresh 2 ml collection tube and washed after 500 μ l of AW1 buffer was applied. The column was centrifuged at 6800 g for 1 min and the collection tube discarded. In a fresh collection tube, a second wash was performed by the addition of 500 μ l of buffer AW2. The sample was centrifuged at 17,900 g for 3 min and the collection tube was discarded. The sample was placed in a new collection tube and centrifuged at full speed for 1 min to remove all buffer AW2. The QIAamp spin column was placed in a clean 1.5 ml microcentrifuge tube and 60 μ l of buffer AVE, equilibrated to room temperature, was applied. The column was incubated at room temperature for 1 min and the RNA was eluted by centrifuging at 6800 g for 1 min.

2.2.2 Extraction of cellular RNA

This extraction technique was adapted from Chomezynski *et al* (1987). First cells (1×10^7 to 1×10^8 cells) were lysed by the addition of 500 μ l solution D. To this was added 0.1 volume 2 M sodium acetate (pH 4). The mixture was mixed thoroughly. Then a further 1 volume of phenol was added and mixed. Finally 0.2 volume of chloroform:isoamyl (49:1) was added and the mixture was vortexed for 10 sec. The mixture was incubated on ice for 15 min and then centrifuged 10,000 g for 20 min at 4°C. The upper aqueous phase was then placed in a fresh micro centrifuge tube. To this was added 1 volume of isopropanol. The RNA was allowed to precipitate for 4 hrs or overnight at -20°C. The RNA was pelleted by centrifuging at 17,900 g for 20 min at 4°C. The supernatant was removed and the wet pellet was resuspended in 300 μ l solution D. Two volumes of absolute ethanol was added to this. The mixture was vortexed and incubated at -20°C for 2 hrs. The RNA was pelleted by centrifuging at 17,900 g for 20 min at 4°C and the supernatant was removed. The pellet was washed in 75 % absolute ethanol

twice. After the second wash, the alcohol was removed and the pellet allowed to air dry briefly. The pellet was resuspended in 100 µl water. In order to resuspend the pellet completely it was heated for 10 min at 65°C. RNA was stored at -20°C for short term storage or -80°C for longer term storage (Chomczynski P, 1987).

2.2.3 Reverse transcription of RNA

2.2.3.1 Omniscript reverse transcription

For the purpose of quantification and amplification of DNA, Omniscript reverse transcription kit was used to produce a first strand cDNA template. First 3 µl of RNA was added to 9.7 µl water and heated to 65°C for 5 min. Meanwhile the mastermix was mixed on ice. The mastermix contained 2 µl 10 x RT buffer (Qiagen), 2 µl dNTPs (5 mM each dNTP), 2 pmoles RT primer, 12 U of RNasin inhibitor and 4 U of Omniscript RT enzyme. The mastermix was added to the denatured RNA and incubated for 60 min at 37°C and then heated to 95°C for 5 min before being cooled to 4°C.

2.2.3.2 Superscript reverse transcription

For synthesis of cDNA for RNAs with a high degree of secondary structure SuperscriptTM II RNase H⁻ Reverse Transcription was used. First 3 µl of RNA, 1 µl dNTPs (10 mM each dNTP), 2 pmol RT primer and sterile distilled water to 12 µl volume were mixed in a micro centrifuge tube. This mixture was heated to 65°C for 5 min and chilled rapidly to 4°C. Then to this was added 4 µl 5 x First strand buffer, 2 µl 0.1 M DTT and 1 µl RNaseOUTTM Recombinant ribonuclease inhibitor (40 units/µl). The contents were mixed and then incubated for 2 min at 42°C. Then 1 µl of superscriptTM II RT was added and mixed by gently pipetting up and down. The reaction was then incubated at 42°C for 50 min and it was inactivated by heating at 70°C for 15 min. RNA template was removed by the addition of 1 µl (2U) *E.coli* RNase H and incubation for a further 37°C for 20 min.

2.2.3.3 ThermoScript RT-PCR System

For templates with a high degree of secondary structure ThermoScriptTM reverse transcription was used. Briefly 3 µl RNA template was mixed with 1 µl gene

specific RT primer (10 μ M) and 2 μ l dNTPs (10 mM). This mixture was incubated at 65°C for 5 min to denature the RNA and cooled on ice. To this was added 4 μ l 5 x cDNA synthesis buffer, 0.1 M DTT, 1 μ l RNaseOUT™ (40 U/ μ l), 1 μ l DEPC treated water and 1 μ l Thermoscript™ RT (15 U/ μ l). The reaction was mixed and incubated 65°C for 60 min. The reaction was inactivated by heating to 85°C for 5 min. The RNA template was removed by addition of 1 μ l RNase H and incubation for 20 min at 37°C.

2.2.4 Quantification and Amplification of DNA

2.2.4.1 Polymerase chain reaction (PCR) amplification of cDNA

PCR was used for the amplification of HCV cDNA for quantification, cloning and sequencing purposes. Amplification of HCV sequences required a “nested” or “semi-nested” approach to allow more specific and a higher yield of products. Two sets of primers were used. The second set was internal (nested) or partially (semi-nested) internal to the first set of primers. Primers were designed which covered the whole of the HCV GT3 genome allowing amplification of all coding and non-coding regions. All PCRs were carried out on the Biometra TRIO-Thermoblock

2.2.4.2 BD Advantage™ 2 and HF-2 PCR Enzyme system

The BD Advantage™ 2 and HF-2 PCR enzyme systems were used for amplifying large segments of DNA or high fidelity PCRs, respectively. BD Advantage™ 2 polymerase mix could amplify long distances of DNA (up to 18kb). Both systems contained a BD Titanium™ Taq DNA polymerase plus a BD™ Taqstart antibody as well as a small amount of proof reading enzyme. The BD™ Taqstart antibody prevents synthesis of DNA until antibodies which are bound to the polymerase, are inactivated on heating. This is called “hotstart” PCR. This allowed increased range, fidelity and greater yields of amplification product. A standard 25 μ l reaction mixture included either 1 x BD advantage 2 PCR buffer or 1 x HF-2 buffer, 1 x dNTP mix (10 mM each nucleotide), 1 μ l each primer (10 μ M each), 1 μ l DNA template and 1 x BD advantage 2 polymerase mix or 1 x HF-2 polymerase. The reaction was carried out under the following conditions: a 95°C denaturing step for 1 minute, then 25 - 35 cycles of a 95°C strand separation step for 30 secs and a 68°C primer annealing and strand elongation step for 2 -

10 min depending on the template size. The elongation allowed for 1 min per kilobase of DNA. These cycles were followed by a further elongation step, before the reaction was held at 4°C.

2.2.4.3 *Pfu* Polymerase PCR system

Pfu DNA polymerase has proof-reading ability due to the presence of 3' to 5' exonuclease activity. Due to its increased fidelity compared to that of *Taq* it was preferentially used when sequencing directly from PCR product. A standard 25 µl reaction contained 1 x *Pfu* DNA Polymerase Buffer, 1 µl dNTPs mix (10 mM each), 1 µl each primer (10 µl) and 1 unit *Pfu* DNA Polymerase. The reaction was processed as follows: a 95°C denaturing step for 2 min, then 25 - 35 cycles of a 95°C strand separation step for 30 sec, a 50°C - 65°C primer annealing step for 30 sec and a 72°C strand elongation step for 2 - 4 minutes. Extension steps were designed allowing 2 min per kilobase of DNA. This was followed by a 72°C final elongation step for 5 min and the reaction was held at 4°C.

2.2.4.4 *Taq* Polymerase PCR system

Taq DNA polymerase was used for diagnostic PCR where sequence fidelity did not matter. There were also occasions where proof-reading enzymes were unable to amplify regions of DNA. In these cases *Taq* was used. A standard 25 µl reaction contained 1 x *Taq* buffer, 0.75 µl MgCl₂ (50 mM), 0.5 µl dNTPs (10 mM each), 1 µl each PCR primer and 1 unit *Taq* DNA Polymerase. For problematic templates amplification could be improved by the addition 0.5 µl of DMSO. The reaction was carried out under the following conditions: a 95°C denaturing step for 4 min, 25 - 35 cycles of a 95°C strand separation step for 30 sec, a 50°C - 65°C primer annealing step for 30 sec and a 72°C strand elongation step for 1 - 3 min. A final elongation step for 10 min was performed before the reaction was held at 4°C.

2.2.4.5 Platinum[®] *Pfx* PCR system

Platinum[®] *Pfx* DNA polymerase was used for amplification for cloning purposes due to its increased fidelity compared to that of *Pfu*. It has a fast chain elongation capability and is supplied in an inactive form due to the presence of the Platinum[®] antibody. This allows "hot start" PCR which increases yield, specificity and sensitivity. A standard reaction was set up as follows: 1 x *Pfx*

amplification buffer, 1 μ l dNTP mixture (10 mM), 1 μ l $MgSO_4$ (50 mM), 1 μ l each primer (10 μ M), 1 μ l DNA template, 1 unit Platinum[®] Pfx DNA polymerase. The reaction was processed as follows: a 94°C denaturing step for 2 min, 25 - 35 cycles consisting of a 94°C strand separation step for 15 sec, a 55°C - 65°C primer annealing step for 30 sec, a 68°C elongation step for 1 - 4 min. These cycles were followed by a final elongation step before the reaction was held at 4°C.

2.2.4.6 Real-time PCR of HCV cDNA

Detection a small quantities of HCV cDNA used real-time PCR using the Perkin Elmer Applied Biosystems 5700 sequence detection system and reagents from Applied Biosystems. A 25 μ l reaction was set up as follows: 12.5 μ l Universal PCR mastermix (AmpliTaqGold DNA polymerase and dNTPs), 7 pmol EMC HCVF primer (Primer 47), 1.2 pmol EMC HCVR primer (Primer 48), 5.1 pmol minor groove binding (MGB) probe (CGAAAGGCCTTGTGGTACTGCCT) and 1 μ l cDNA template. The MGB probe was complementary to a short consensus sequence in the HCV 5'UTR and was able to bind all genotypes. In some cases 12.5 μ l SYBR green PCR master mix was used instead of Universal PCR mastermix. This allowed for the non-specific detection of any double stranded DNA products to detect the loading control GAPDH. Detection of GAPDH sequences used the primers, 52 and 53 in the same reaction described below. In these cases MGB probe was omitted and 1 μ l each gene specific primer (10 μ M) was used instead of HCV primers. The following thermal cycling product was used for amplification of PCR product: a 50°C step for 2 min, a 95°C denaturing step for 10 min, 40 cycles consisting of a 95°C denaturing step for 40 sec and a 60°C primer annealing/strand elongation step for 1 min. In reactions where SYBR green was used an additional dissociation step was included at the end of the 40 cycles. The reaction was held at 4°C for up to 24 hrs.

2.2.5 PCR reactions

The various PCR conditions are described in the following section where the PCRs performed during the project are shown.

2.2.5.1 Diagnostic PCRs**PCR 1: Diagnostic PCR****1 (First Round/P1)****Cycle number**

Stage 1	95°C	4 min	X 1
Stage 2	95°C	30 secs	} X 30
	76°C	30 secs	
	72°C	30 secs	
Stage 3	72°C	1 min	X 1
Stage 4	4°C	Hold	

Primers: Primer 43 + PP-AC6-GT3

Polymerase: *Taq* Polymerase**PCR 2: Diagnostic PCR****1 (Second Round/P2)****Cycle number**

Stage 1	95°C	4 min	X 1
Stage 2	95°C	30 secs	} X 30
	55°C	30 secs	
	72°C	45 secs	
Stage 3	72°C	7 min	X 1
Stage 4	4°C	Hold	

Primers: Primer 45 + Primer 46

Polymerase: *Taq* Polymerase

PCR 3: Diagnostic PCR**2 (P1)****Cycle number**

Stage 1	95°C	4 min	X 1
Stage 2	95°C	30 secs	} X 30
	58°C	30 secs	
	72°C	1 min 30 secs	
Stage 3	72°C	1 min	X 1
Stage 4	4°C	Hold	

Primers: Primer 26 + Primer 23

Polymerase: *Taq* Polymerase**PCR 4: Diagnostic PCR****2 (P2)****Cycle number**

Stage 1	95°C	4 min	X 1
Stage 2	95°C	30 secs	} X 30
	55°C	30 secs	
	72°C	45 secs	
Stage 3	72°C	1 min	X 1
Stage 4	4°C	Hold	

Primers: Primer 54 + Primer 24

Polymerase: *Taq* Polymerase

2.2.5.2 PCR of Fragments 1-7**PCR 5: P1/P2 PCR****Fragment 1****Cycle number**

Stage 1	95°C	1 min	X 1
Stage 2	95°C	30 secs	} X 30
	68°C	6 min 30 secs	
Stage 3	68°C	10 min	X 1
Stage 4	4°C	Hold	

Primers: Primer 49 + Primer 18

Polymerase: BD Advantage Polymerase

PCR 6: P1/P2 PCR**Fragment 2****Cycle number**

Stage 1	95°C	1 min	X 1
Stage 2	95°C	30 secs	} X 30
	68°C	5 min	
Stage 3	68°C	10 min	X 1
Stage 4	4°C	Hold	

Primers: Primer 49 + Primer 12

Polymerase: BD Advantage Polymerase

PCR 7: P1/P2 PCR**Fragment 3****Cycle number**

Stage 1	95°C	1 min	X 1
Stage 2	95°C	30 secs	} X 30
	68°C	4 min 30 secs	
Stage 3	68°C	10 min	X 1
Stage 4	4°C	Hold	

Primers: Primer 17 + Primer 77

Polymerase: BD Advantage Polymerase

PCR 8: P1 PCR**Fragment 4****Cycle number**

Stage 1	95°C	4 min	X 1
Stage 2	95°C	30 secs	} X 30
	55°C	30 secs	
	72°C	2 min	
Stage 3	72°C	4 min	X 1
Stage 4	4°C	Hold	

Primers: Primer 19 + Primer 79

Polymerase: *Pfu* Polymerase

PCR 9: P1 PCR**Fragment 5****Cycle number**

Stage 1	95°C	4 min	X 1
Stage 2	95°C	30 secs	} X 30
	58°C	30 secs	
	72°C	1 min 30 secs	
Stage 3	72°C	4 min	X 1
Stage 4	4°C	Hold	

Primers: Primer 23 + Primer 26

Polymerase: *Pfu* Polymerase

PCR 10: P1 PCR**Fragment 6****Cycle number**

Stage 1	95°C	4 min	X 1
Stage 2	95°C	30 secs	} X 30
	45°C	30 secs	
	72°C	1 min 20 secs	
Stage 3	72°C	4 min	X 1
Stage 4	4°C	Hold	

Primers: Primer 27 + Primer 28

Polymerase: *Pfu* Polymerase

PCR 11: P1 PCR**Fragment 7****Cycle number**

Stage 1	95°C	1 min	X 1
Stage 2	95°C	30 secs	} X 30
	68°C	10 secs	
Stage 3	68°C	12 min	X 1
Stage 4	4°C	Hold	

Primers: Primer 49 + Primer 77

Polymerase: BD Advantage Polymerase

PCR 12: Linker**Fragment PCR****Cycle number**

Stage 1	95°C	1 min	1
Stage 2	95°C	15 secs	} X 35
	68°C	4 min	
Stage 3	68°C	4 min	1
Stage 4	4°C	Hold	

Primers: Primer 11 + Primer 18

Polymerase:

HF-2 Polymerase + 1 in 12.5 HF-2 Buffer + 1 in 50 Advantage Buffer

2.2.5.3 P2 PCR Fragments A-J**PCR 13: P2 PCR****Fragment A****Cycle number**

Stage 1	95°C	4 min	X 1
Stage 2	95°C	30 secs	} X 30
	60°C	30 secs	
	72°C	1 min 40 secs	
Stage 3	72°C	4 min	X 1
Stage 4	4°C	Hold	

Primers: Primer 1 + Primer 6

Polymerase: *Pfu* Polymerase**PCR 14: P2 PCR****Fragment B****Cycle number**

Stage 1	95°C	4 min	X 1
Stage 2	95°C	30 secs	} X 30
	55°C	30 secs	
	72°C	1 min 40 secs	
Stage 3	72°C	4 min	X 1
Stage 4	4°C	Hold	

Primers: Primer 7 + Primer 8

Polymerase: *Pfu* Polymerase

PCR 15: P2 PCR**Fragment C****Cycle number**

Stage 1	95°C	4 min	X 1
Stage 2	95°C	30 secs	} X 30
	68°C	30 secs	
	72°C	2 min 30 secs	
Stage 3	72°C	4 min	X 1
Stage 4	4°C	Hold	

Primers: Primer 11 + Primer 12

Polymerase: *Pfu* Polymerase

PCR 16: P2 PCR**Fragment D****Cycle number**

Stage 1	95°C	4 min	X 1
Stage 2	95°C	30 secs	} X 30
	66°C	30 secs	
	72°C	1 min 30 secs	
Stage 3	72°C	4 min	X 1
Stage 4	4°C	Hold	

Primers: Primer 21 + Primer 18

Polymerase: *Pfu* Polymerase

PCR 17: P2 PCR**Fragment F****Cycle number**

Stage 1	95°C	4 min	X 1
Stage 2	95°C	30 secs	} X 30
	58°C	30 secs	
	72°C	1 min 20 secs	
Stage 3	72°C	4 min	X 1
Stage 4	4°C	Hold	

Primers: Primer 27 + Primer 28

Polymerase: *Pfu* Polymerase**PCR 18: P2 PCR****Fragment G****Cycle number**

Stage 1	95°C	4 mins	X 1
Stage 2	95°C	30 secs	} X 30
	45°C	30 secs	
	72°C	1 min 20 secs	
Stage 3	72°C	4 min	X 1
Stage 4	4°C	Hold	

Primers: Primer 23 + Primer 54

Polymerase: *Pfu* Polymerase

PCR 19: P2 PCR**Fragment H****Cycle number**

Stage 1	95°C	4 mins	X 1
Stage 2	95°C	30 secs	} X 30
	55°C	30 secs	
	72°C	1 min	
Stage 3	72°C	4 min	X 1
Stage 4	4°C	Hold	

Primers: Primer 25 + Primer 26

Polymerase: *Pfu* Polymerase

PCR 20: P2 PCR**Fragment I****Cycle number**

Stage 1	95°C	4 mins	X 1
Stage 2	95°C	30 secs	} X 30
	60°C	30 secs	
	72°C	1 min	
Stage 3	72°C	4 min	X 1
Stage 4	4°C	Hold	

Primers: Primer 19 + Primer 26

Polymerase: *Pfu* Polymerase

PCR 21: P2 PCR**Fragment J****Cycle number**

Stage 1	95°C	4 min	X 1
Stage 2	95°C	30 secs	} X 30
	65°C	30 secs	
	72°C	1 min	
Stage 3	72°C	4 min	X 1
Stage 4	4°C	Hold	

Primers: Primer 20 + Primer 21

Polymerase: *Taq* Polymerase + DMSO

PCR 22: P2 PCR**Fragment 3'stop****Cycle number**

Stage 1	95°C	4 min	X 1
Stage 2	95°C	30 secs	} X 30
	65°C	30 secs	
	72°C	1 min	
Stage 3	72°C	4 min	X 1
Stage 4	4°C	Hold	

Primers: Primer 31 + Primer 77

Polymerase: *Taq* Polymerase + DMSO

2.2.5.4 PCR of HCV 3'UTR

PCR 23: PCR of the 3'UTR			Cycle number
Stage 1	95°C	4 min	X 1
Stage 2	95°C	30 secs	} X 30
	65°C	30 secs	
	72°C	1 secs	
Stage 3	72°C	4 min	X 1
Stage 4	4°C	Hold	

Primers: Primer 31 + Primer 39

Polymerase: *Taq* Polymerase + DMSO

2.2.5.5 Modification of the GM genome PCR

PCR 24: T7 Promoter PCR			Cycle number
Stage 1	95°C	2 min	X 1
Stage 2	95°C	15 secs	} X 30
	58°C	30 secs	
	68°C	5 min	
Stage 3	68°C	7 min	X 1
Stage 4	4°C	Hold	

Primers: Primer 50 + Primer 16 Polymerase: *Pfx* Platinum Polymerase

PCR 25: EMCV IRES

PCR			Cycle number
Stage 1	95°C	4 min	X 1
Stage 2	95°C	30 secs	} X 30
	55°C	30 secs	
	72°C	1 min 20 secs	
Stage 3	72°C	4 min	X 1
Stage 4	4°C	Hold	

Primers: Primer 44 + Primer 37

Polymerase: *Taq* Polymerase

PCR 26: NS3-GT3

PCR			Cycle number
Stage 1	95°C	2 min	X 1
Stage 2	95°C	15 secs	} X 30
	60°C	30 secs	
	68°C	3 min	
Stage 3	68°C	4 min	X 1
Stage 4	4°C	Hold	

Primers: Primer 38 + Primer 18

Polymerase: *Pfx* Platinum Polymerase

2.2.5.6 Site-Directed Mutagenesis PCR

PCR 27: Mutagenesis PCR			Cycle number
Stage 1	95°C	1 min	X 1
Stage 2	95°C	30 secs	} X 25
	68°C	Varied (1min/kb)	
Stage 3	68°C	10 min	X 1
Stage 4	4°C	hold	

Primers: Sense and Antisense mutagenesis primer for desired mutation

Polymerase: BD Advantage Polymerase

2.2.5.7 Luciferase PCR**PCR 28: Luciferase****PCR 1****Cycle number**

Stage 1	95°C	4 min		1
Stage 2	95°C	15 secs	}	X 30
	60°C	30 secs		
	68°C	2 min		
Stage 3	68°C	4 min		1
Stage 4	4°C	hold		

Primers: Primer 42 + Primer 43 Polymerase: *Pfx* Platinum Polymerase

PCR 29: Luciferase**PCR Fragment 2****Cycle number**

Stage 1	95°C	4 min		1
Stage 2	95°C	15 secs	}	X 30
	50°C	30 secs		
	68°C	1 min		
Stage 3	68°C	4 min		1
Stage 4	4°C	hold		

Primers: Primer 44 + Primer 40

Polymerase: *Pfx* Platinum Polymerase

PCR 30: Luciferase**PCR Fragment 3****Cycle number**

Stage 1	95°C	4 min		X 1
Stage 2	95°C	15 secs	}	X 8
	60°C	30 secs		
	68°C	2 min		
Stage 3	Add Primers: Vtag940 + aluc-Pmel			
Stage 4	Repeat Stage 2 for 25 cycles			
Stage 5	4°C	hold		

Initially luciferase PCR fragments 1 and 2 were used in a self priming reaction
 Polymerase: *Taq* Polymerase + DMSO

2.2.5.8 GAPDH PCR**PCR 31: GAPDH PCR****Cycle number**

Stage 1	95°C	4 min		1
Stage 2	95°C	30 secs	}	X 30
	60°C	30 secs		
	72°C	1 min		
Stage 3	72°C	4 min	1	
Stage 4	4°C	hold		

Primers: Primer 51 + Primer 53

Polymerase: *Taq* Polymerase

2.2.6 Automated DNA sequencing

Automated DNA sequencing was performed by The Sequencing Service (School of Life Sciences, University of Dundee, Scotland) using Applied Biosystems Big-Dye Ver 3.1 chemistry. The sequencing was performed on an Applied Biosystem model 3730 automated capillary DNA sequencer. This system uses a fluorescent dye terminator where all four nucleotides are present in the same reactions each with a different dye group attached. The dye terminator becomes incorporated at the end of the synthesised DNA chain producing many different length fluorescent DNA molecules. The complementary nature of the synthesised new strand DNA to its template means that the fluorescent dye terminator represents the other half to the base pair at that position in the DNA template strand. By separating strands according to molecular size in a polyacrylamide gel the DNA sequence can be plotted.

2.2.7 TA Cloning of PCR products

2.2.7.1 *Taq* 3' adenine addition

Cloning of PCR using the TA system required a 3' adenine to be present on the amplification product. *Taq* DNA polymerase leaves a 3' single base overhang at the end of a PCR product after amplification. Proof-reading enzymes do not leave this overhang creating blunt ended products. Where TA cloning was being performed with a PCR product originating from proof-reading enzyme amplification, the addition of a 3' adenine was required. A 25 µl reaction was set up as follows: 1 x buffer, 1.5 mM MgCl₂, 1 µl dATP (10 mM), 1 unit of *Taq* DNA polymerase, 15 µl purified PCR product. The reaction was incubated at 72°C for 15 min before being held on ice.

2.2.7.2 TOPO TA Cloning[®] system

The TOPO TA cloning[®] system is a highly efficient system which uses topoisomerase I from *Vaccinia* virus to create a covalent bond between the 3' thymine on the vector DNA and PCR product. The reaction is possible without the need for ligase. A standard 6 µl reaction included: 4 µl PCR product (containing 3' adenine overhang), 1 µl salt solution and 1 µl pCR2.1 TOPO[®] vector. The reaction was incubated on the bench for 5 min at room temperature

(22°C - 23°C). The ligation was stored at -20°C until it was needed for transformation into chemically competent *E.coli* cells. Cells were transformed with 2 µl of ligation mixture.

2.2.7.3 pGEM[®] T-Easy TA Cloning system

The pGEM[®] T-Easy TA cloning kit uses a linearised pGEM T-Easy vector which contains a 3' thymine. A 10 µl standard reaction contained 1 x rapid ligation buffer, 1 - 2 µl ligase, 1 µl pGEM[®] T-Easy and 2 µl PCR product (containing 3' adenine overhang). The reaction was mixed and incubated for 1 hr at room temperature. Alternatively for maximum transformants, ligations could be incubated overnight at 4°C before being transformed into competent *E.coli* cells.

2.2.8 Small Scale preparation of plasmid DNA (minipreps)

2.2.8.1 Step-wise alkaline lysis method

The alkaline lysis method of plasmid extraction was used when plasmid DNA was being used for restriction digest analysis and ligations. A single colony of transformed bacteria was inoculated into 2 ml LB broth containing 100 µg/ml ampicillin. This was incubated overnight on a shaking incubator at 37°C. A 1.5 ml aliquot of the culture was centrifuged for 5 min at 17,900 g. The LB broth supernatant was discarded ensuring that none was left in the tube. The cell pellet was resuspended in 100 µl chilled solution I and placed on ice. Then a 200 µl aliquot of solution II was added to this and the solutions mixed immediately by inverting gently 3 - 4 times. The solution was then incubated on ice for 5 min allowing lysis of the cells. After this the solution was neutralised and protein was precipitated by the addition of 150 µl chilled solution III. The solutions were mixed immediately, to avoid localised precipitation, by inverting sharply. They were incubated on ice for a further 5 min before being centrifuged at 17,900 g for 5 min. The supernatant was removed to a fresh 1.5 ml microcentrifuge tube and 400 µl phenol:chloroform:isoamyl alcohol (24:24:1) was added. The tube was vortexed for 10 sec and centrifuged for 3 min at 17,900 g. The upper aqueous phase was placed in a fresh 1.5 ml microcentrifuge tube. To this was added 800 µl chilled ethanol and the mixture was kept on ice for 20 min. The plasmid DNA was pelleted by centrifuging at 17,000 g for 10 min. The supernatant was discarded and the pellet was washed

in 1 ml 70 % absolute ethanol. The pellet was centrifuged for 5 min at 17,900 g and the supernatant discarded. The pellet was allowed to air dry at room temperature for 30 min and then resuspended in 50 µl molecular grade water or TE buffer.

2.2.8.2 QIAprep[®] Miniprep Kit

“QIAprep[®] Miniprep Kit” was used for the extraction of plasmid DNA when it was to be used for sequencing or site-directed PCR methods. A single colony was picked, inoculated into 3 ml LB broth containing ampicillin (100 µg/ml) and incubated overnight at 37°C. The culture was split into two 1.5 ml centrifuge tubes and cells were pelleted by centrifuging at 17,900 g for 5 min. The LB broth supernatant was discarded and the pellet was resuspended in 250 µl chilled buffer P1 (RnaseA 100 µg/ml). To this was added 250 µl buffer P2 and the solutions were mixed by inverting gently 3 - 4 times. The lysis step was not allowed to proceed for longer than 5 min. Then a 350 µl aliquot of buffer NS3 was added and the solutions were mixed immediately by inverting sharply 4 - 5 times. The mixture was then centrifuged for 10 min at 17,900 g. The supernatant was then transferred to a QIAprep[®] spin column and centrifuged for 1 min at 17,900 g. The flow through was discarded and then the supernatant from the second 1.5 ml microcentrifuge was applied to the same column. The column was centrifuge at 17,900 g for 1 min and the flow through discarded. Then 750 µl of wash buffer PE was applied to the column. The column was centrifuged for 1 min at 17,900 g. The flow through was discarded and the column was centrifuged at 17,900 g for a further two minutes to remove trace amounts of wash buffer. The discard tube was discarded and the column was placed in a 1.5 ml microcentrifuge tube with lid cut off. The plasmid DNA was then eluted by the addition of 50 µl of buffer EB to the centre of the filter and centrifuged for 2 min at 17,900 g.

2.2.9 Large scale preparation of plasmid DNA (midiprep)

The large scale preparation of plasmid DNA was performed using the “Qiagen[®] plasmid midi kit”. This was used for propagating high concentrations of plasmid DNA that could be used for in-vitro transcriptions. A single colony was picked from transformed *E.coli* bacteria and inoculated into 100 ml LB broth containing

ampicillin (100 µg/ml). The culture was inoculated overnight in a shaking incubator at 37°C. The cells were harvested by centrifuging at 6000 g for 15 min at 4°C. The supernatant was then completely removed and the bacterial pellet was resuspended in 4 ml chilled buffer P1 (containing RNase). The cells were then lysed by the addition of 4 ml buffer P2 and mixed by inverting 3 - 4 times. The lysis reaction was incubated for 5 min at room temperature. To this was added 4 ml chilled buffer P3 and the tube immediately inverted 4 - 6 times. The solution was then incubated on ice for 15 min. Precipitated material was removed by centrifuging at 20,000 g for 30 min at 4°C. The supernatant was placed in a fresh centrifugation tube and was recentrifuged at 20,000 g for 15 min at 4°C. Meanwhile, a QIAGEN-tip column was equilibrated by the addition of 4 ml buffer QBT and allowed to empty by gravity flow into a conical flask to collect the waste. Once the column had drained completely the supernatant was applied to the column and allowed to drain through by gravity. Once all the supernatant was added the column was washed by the addition of 10 ml buffer QC. This was allowed to drain through and then a further 10 ml buffer QC applied. The column was placed in a centrifuge tube and the plasmid DNA was eluted by the addition of 5 ml buffer QF. The DNA was precipitated by the addition of 3.5 ml isopropanol to the eluted DNA. It was mixed and centrifuged immediately at 17,900 g for 30 min at 4°C. The supernatant was discarded and the pellet was washed with 2 ml 70 % ethanol. The tube was centrifuged at 17,900 g for 10 min at 4°C and the supernatant was completely discarded. The pellet was allowed air dry for 5 - 10 min and resuspended in 100 µl buffer TE (pH 8.0) or molecular grade water.

2.2.10 Restriction enzyme digestion of DNA

Restriction enzyme digests were performed as was described in Sambrook et al. (1989). 15 - 50 µl total reaction volume was incubated at 37°C for 1 ½ - 4 hrs. The reaction contained 10 U of enzyme per 1 µg of DNA in a buffer as advised by manufacture. Reactions were stopped by the addition of a ¼ volume of gel running buffer and digested DNA was analysed by agarose gel electrophoresis as described in section 2.2.13.1 (Sambrook J, 1989).

2.2.11 Dephosphorylation of linearised plasmid DNA

For the purposes of cloning linearised plasmid vector, DNA had 5' terminal phosphates removed by the use of shrimp alkaline phosphatase. A total volume of 20 µl consisted 1 x SAP dephosphorylation buffer, 2 µl Shrimp Alkaline phosphatase, 15 µl DNA. The reaction was incubated for 1 hr at 37°C, after which the enzyme was inactivated by heating for 65°C for 15 min.

2.2.12 Ligation reactions

Ligation reactions were performed as manufactures instructions using DNA obtained from restriction digests. When restriction digests produced “sticky ends” and the vector and insert were of similar size, a 1:3 molar ratio was used. When the restriction digest produced “blunt ends” a 1:1 molar ratio was used. The total concentration of DNA used in a reaction did not exceed 1 µg. In a 10 µl reaction, vector DNA and insert DNA were mixed with 1 x reaction buffer and 10 U T4 ligase. “Sticky end” ligations were incubated for 4 - 16 hr at 22°C. “Blunt end” ligations were incubated at 16°C for 16 hr.

2.2.12.1 Mung Bean nuclease treatment

Mung bean nuclease treatment was used to remove 5' overhangs left from restriction enzyme digest. A standard 30 µl reaction contained 1 x Mung bean nuclease, 1 U/µg DNA and x µg DNA. The reaction was heated at 30°C for 30 min. The reaction was stopped by phenol:chloroform extraction followed by ethanol precipitation as described in section 2.2.13.4 & 5.

2.2.12.2 Random priming

Random priming was used to make DNA probes for northern blot analysis using Klenow fragment (large subunit of DNA polymerase I). A DNA fragment complementary to a target sequence was first purified from an agarose gel (Section 2.2.13.2). 1 - 40 ng of the DNA was heated to 95°C for 7 min before being cooled to 4°C. To this was added 1 x NEB buffer 2, 1 x BSA, 1 mM dNTPs (dGTP, dATP & dTTP), 1 U random primer, 2.5 µl ³²P dCTP and 2 µl Klenow fragment. The reaction was heated for 1 ½ hrs at 37°C after which the radio labelled probe was purified by phenol:chloroform extraction and ethanol

precipitation (Section 2.2.13.4 & 5). Precipitated DNA pellets were resuspended in 20 µl molecular grade water. Before use, probes were denatured by heating at 95°C for 7 min.

2.2.12.3 *Optimisation of probes for northern blots*

Detection of the 5-15 1b replicon RNA was initially attempted using probes designed against NS4B sequences. RNA probes were transcribed from linearised pGEM T-Easy NS4B 1b plasmid (McLauchlan unpublished). Non-specific binding of NS4B probes to ribosomal bands prevented detection of replicon. Therefore a plasmid construct containing an NcoI/SphI fragment, derived from pGEM neoemcv, comprising half the neomycin gene and a portion of the 1b 5'UTR was cloned into pGEM T-Easy vector. This was used to make probes for detecting HCV 1b RNA. The housekeeping gene, glyceraldehyde-3-phosphate dehydrogenase (GAPDH), was used to normalise HCV RNA levels for loading. The GAPDH cellular control plasmid was made by PCR amplifying a GAPDH RT product. Oligonucleotides were designed from GAPDH sequences (Accession number M33197) and PCR product was resolved by agarose gel electrophoresis. An annealing temperature of 60°C was chosen for optimal amplification and purified products were cloned into pGEM T-Easy.

Initially RNA probes were used to detect HCV and GAPDH sequences. However HCV probes still failed to give high resolution of HCV RNA bands. Alternatively random primed DNA probes bound HCV RNA more stringently and were therefore used for detection in northern blot hybridisation. JFH1 genotype 2a sequences were detected by synthesising DNA probes from an internal NS3 NcoI/PmeI fragment, which was obtained directly from pSGR-Luc-JFHI plasmid (Targett-Adams et al., 2005).

2.2.13 *Separation and purification of DNA fragments*

2.2.13.1 *Agarose gel electrophoresis*

DNA fragments produced from restriction enzyme digests and PCRs were separated according to their electrophoretic mobility in an agarose gel. A standard 1 % gel contained 1 % agarose melted in 1 x TBE buffer and 0.05 µg/ml ethidium bromide. In cases in which samples were 100 - 500 bases in length,

“Metaphore” agarose was used. Samples were mixed with agarose loading buffer before being loaded onto the gel. Molecular weight markers were used as standards to indicate size of DNA. The agarose gel was run in 1 x TBE buffer at 40 - 100 V for 1 ½ - 4 hrs. DNA was visualised under short wave UV light for a standard gel. If gel extraction of fragments was required long wave UV light was used to minimise damage to the DNA. A “Bio-Rad Gel Doc 2000” Imaging system and software was used for photography.

2.2.13.2 Purification of DNA from agarose gels

Purification of DNA from agarose gels was performed using “QIAquick® Gel Extraction Kit”. Appropriate bands were cut from agarose gel. They were dissolved in 3 volumes Buffer QG to 1 volume gel slice at 50°C for 10 min. Once completely dissolved 1 volume of isopropanol was added. The mixture was then applied to a QIAquick® column to bind DNA by centrifugation at 17,900 g for 1 min. The DNA was washed with 750 µl Buffer PE and the centrifugation was repeated. The flowthrough was discarded and a further centrifugation was repeated for 2 min to remove completely all traces of Buffer PE. The DNA was eluted by addition of 30 µl Buffer EB to the centre of the QIAquick membrane. This was incubated for 1 min at room temperature before the flowthrough was collected in a 1.5 ml microcentrifuge tube after centrifugation at 17,900 g for 2 min.

2.2.13.3 Purification of DNA from PCR and restriction digests

The purification of linear DNA and PCR fragments was performed using “QIAquick® PCR Purification Kit”. DNA was bound to a column by the addition of 5 volumes Buffer PB to 1 volume reaction mixture. This was applied to a column and centrifuged at 17,900 g for 1 min. The DNA was washed and eluted as described in 2.2.13.2.

2.2.13.4 Phenol/Chloroform extraction

This was used for the removal of proteins from nucleic acid. For volumes over 100 µl, an equal volume of 25:24:1 phenol:chloroform:isoamyl alcohol solution was added. The mixture was vortexed vigorously for 10 sec and centrifuged at 17,900 g for 3 min. The upper aqueous phase was removed to a fresh centrifuge

tube, careful not to remove any of the interphase or lower phase. Further phenol extraction could be performed to remove any interphase contaminants. Residual phenol was removed by the addition of an equal volume of 24:1 chloroform:isoamyl alcohol solution and centrifugation. The upper aqueous phase was removed and nucleic acids precipitated as described below in 2.2.13.5.

2.2.13.5 Ethanol precipitation

Nucleic acids were precipitated by the addition of 1/10 3 M sodium acetate and 2 ½ volumes of absolute ethanol. The alcohol/nucleic acid 'slurry' was mixed and incubated on dry ice for 20 min. Nucleic acids were pelleted by centrifugation at 17,900 g for 10 min. The pellet was washed with 70 % ethanol and centrifuged at 17,900 g for 5 min. The pellet was allowed to air dry briefly for 5 - 10 min before being resuspended in 20 - 50 µl molecular grade water.

2.2.14 Quantification of nucleic acids

Nucleic acids were quantified using the "Eppendorf BioPhotometer". Optical densities of nucleic acid at 1 in 100 dilutions were compared to that of a blank. The absorption of light by nucleic acids at 260 nm giving 1 OD corresponds to 50 µg/ml DNA or 40 µg/ml RNA. The concentration of nucleic acid was given automatically using the following equations:

$$\text{DNA concentration } (\mu\text{g/ml}) = (\text{OD}_{260}) \times (\text{dilution factor}) \times (50 \mu\text{g DNA/ml}) / (1 \text{ OD}_{260} \text{ unit})$$

$$\text{RNA concentration } (\mu\text{g/ml}) = (\text{OD}_{260}) \times (\text{dilution factor}) \times (40 \mu\text{g RNA/ml}) / (1 \text{ OD}_{260} \text{ unit})$$

Impurities in the sample were detected from the ratios of 260 nm/280 nm for proteins and 260 nm/230 nm for carbohydrates, peptides, phenols and aromatic compounds. Pure DNA should give a value of 2 and RNA a value of 1.8 for protein free contamination. Protein contamination will decrease these values. The 260/230 ratio should be higher than 2 for pure samples. Turbidity of the solution was corrected for, where pure samples should give a value of zero at

320 nm. At this wavelength neither protein nor DNA absorbs light so it allows for background correction.

2.2.15 *Site-Directed Mutagenesis*

A site-directed mutagenesis technique was adapted from a “Quikchange II Site” directed mutagenesis kit from Stratagene. Specific mutations could be introduced using a long PCR based method. Primers containing specific mutations were designed as described in the user manual for sense and antisense amplification as described below:

- Both sense and antisense primers contained the desired mutation.
- Primers were 25 - 45 nucleotides long with a melting temperature (T_m) of $\geq 78^\circ\text{C}$. T_m was calculated using the following equation:
 - $T_m = 81.5 + 0.41 (\%GC) - 675/n - \% \text{ mismatch}$
 - N is primer length in nucleotides
 - %GC and % mismatch are whole numbers
- The mutation should be in the centre of the primer with 10 -15 bases on either side.
- There should be a minimum GC content of 40 %.

The system uses a parental plasmid template obtained from bacterial mini or midi prep plasmid extraction. After a number of cycles of PCR with the mutagenic primers, the parental DNA is digested with *DpnI* removing all *dam* methylated DNA. Dam methylation is mediated by the methylase of the *dam* gene (Dam methylase) which transfers a methyl group from S-adenosylmethionine to the N⁶ position of the adenine residue in the sequence GATC. In *E.coli* which are *dam* positive, plasmid DNA will be *dam* methylated. Therefore, using *DpnI*, which cuts only *dam* methylated recognition sequences allows digestion of plasmid DNA only. The PCR product could then be transformed into DH5- α competent cells and plasmid DNA examined by DNA

sequencing for the presence of the desired mutation. A standard 50 µl PCR reaction contained: 1 x BD advantage 2 PCR buffer, 1 x dNTP mix (10 mM each nucleotide), 5 µl each primer (10 µM each), 1 µl DNA template (5 - 50 ng) and 1 x BD advantage 2 polymerase mix. The reaction was carried out under the following conditions: a 95°C denaturing step for 1 minute, then 18 cycles of a 95°C strand separation step for 30 sec and a 55°C primer annealing step for 1 min and strand elongation step for 7 - 11 min depending on the template size. A further elongation step was included and the reaction was held at 4°C. After the PCR the template plasmid DNA was digested with 1 µl *DpnI* for 2 hrs at 37°C. 20 µl of this reaction was transformed in 100 µl DH5-α competent *E.coli* as in section 2.4. The cells were resuspended in 500 µl LB broth for the expression step and half of this was plated onto 100 µg/ml ampicillin LB agar plates. These were incubated at 37°C overnight and colonies streaked onto fresh media. Single colonies were picked and grown overnight in LB broth containing 100 µg/ml ampicillin. Plasmid DNA was extracted using Qiagen kits as in section 2.2.8. Any mutation was confirmed by direct DNA sequencing.

2.2.16 In-vitro Transcription

In-vitro transcriptions were performed from a linearised DNA template. Care was taken to ensure that plasmid DNA was completely digested as circularised plasmid inhibited the transcription reaction. Digested DNA was phenol/chloroform extracted and ethanol precipitated (sections 2.2.13.4 and 2.2.13.5).

2.2.16.1 T7 and SP6 RNA Polymerase

T7 and SP6 RNA polymerases were used to transcribe RNA from T7 and SP6 promoter sites within linearised plasmid sequences. A standard 20 µl reaction contained: 1 x transcription buffer, 2 µl rNTPs (ribonucleotides) (10 mM each), 1 µg linearised plasmid DNA, 0.4 µl RNasin (40 U/µl) and 2 µl T7 or SP6 RNA polymerase. Reactions were incubated at 37°C for 2 hrs and purified by phenol/chloroform extraction and ethanol precipitation. When 'hot' reactions were being performed to make an RNA probe radiolabelled ³²P rUTP was included. The reaction contained the following: 1 x transcription buffer, 2 µl rNTPs (10 mM rATP, rCTP and rGTP), 2 µl rUTP (200 µM), 5 µl ³²P rUTP, 1 µg

linearised plasmid DNA, 0.4 µl RNasin (40 U/µl) and 2 µl T7 or SP6 RNA polymerase. Samples were processed as before.

2.2.16.2 *Ambion MEGAscript® T7 Kit*

For electroporation of RNA into mammalian cells, the Ambion MEGAscript® T7 Kit was used because of its ability to produce a high yield of RNA. A standard 20 µl reaction contained 1 x reaction buffer, 2 µl each rNTP, 2 µl enzyme mix and 1 µg linearised plasmid DNA. The reaction was incubated at 37°C for 2 ½ hrs. If the RNA was to be used for luciferase assays, 1 µl of the reaction was visualised on an agarose gel to check the integrity of the RNA. In some cases, it was necessary to remove the DNA template before using the RNA. This was achieved by treatment with 1 µl “Ambion Turbo DNase I” for 30 min at 37°C. Then 15 µl ammonium acetate and 115 µl DEPC treated molecular grade water was added to stop the reaction and the RNA was phenol:chloroform extracted. After centrifugation, the upper phase was removed to a fresh microcentrifuge tube and 1 volume of isopropanol added. The RNA was precipitated at -20°C for a minimum of 15 min before being pelleted at 17,900 g for 15 min at 4°C. The supernatant was removed and the pellet resuspended in an appropriate volume of DEPC treated molecular grade water.

2.2.17 *Separation of RNA and Northern Blot Analysis*

2.2.17.1 *Preparation of RNA samples*

Before total cellular RNA was run on a gel it was denatured. 4 µl total RNA (5 - 20 µg) was added to 16 µl RNA loading buffer. It was then heated to 68°C for 10 min and 2 µl RNA running buffer added. Samples were kept on ice before loading.

2.2.17.2 *Formaldehyde Gel*

RNA obtained from cellular RNA extractions was separated on a formaldehyde denaturing gel. A 100 ml gel was made as follows: 1 g of agarose was melted in 84.8 ml DEPC water. Then 10 ml of 10 x MOPS buffer was added. Just before pouring the gel, 5.2 ml formaldehyde was added. Samples were loaded onto the gel and run in 1 x MOPS buffer at 4°C at 80 V for 2 - 3 hrs.

2.2.17.3 Staining of gel and preparation for blotting

The formaldehyde was removed from the gel by soaking in sufficient 0.5 M ammonium acetate to cover the gel for 20 min. The solution was poured off and the gel soaked for a further 20 min. The solution was discarded and the gel stained for visualisation of bands by soaking in 0.5 M ammonium acetate with 0.5 µg/ml ethidium bromide for 30 min. Total RNA was visualised under UV light. rRNA bands were used as a cellular molecular weight marker showing RNA integrity and cellular loading such that 28S corresponded to 4718 nucleotides and 18S corresponded to 1874 nucleotides. A ruler was placed at the side of the gel to indicate where each marker corresponded to on the actual gel. The stain was removed by soaking the gel for 45 min in 0.5 M ammonium acetate.

To improve transfer of longer RNA molecules, the gel was soaked in 100 ml alkaline hydrolysis solution for 20 min. The solution was removed and the gel neutralised by the addition of 100 ml neutralisation solution for 20 min. The neutralisation solution was removed and the gel prepared for blotting by soaking in 100 ml 20 x SSC for 45 min.

2.2.17.4 Northern blotting

The blot was assembled on a plastic stand sitting in a larger plastic dish. The dish was filled with enough 20 x SSC to half submerge the plastic stand. Three long lengths of Whatman 3 mm paper were cut and used as wick to cover the plastic stand and were partially submerged in the 20 x SSC in the dish. Three 20 x SSC soaked pieces of Whatman were cut to the size of the plastic stand. They were placed on top of the stand. Next the gel was placed on the stand and the air bubbles were removed by rolling a glass pipette over its surface. The edges of the gel and stand were covered with cling film to prevent short circuiting in the system. A nitrocellulose membrane was cut to the size of the gel and placed on the surface of some 20 x SSC to soak for 10 min. After soaking, it was carefully placed on top of the gel and air bubbles removed again. The surface of the blot was flooded with 20 x SSC and five more sheets of Whatmann paper placed on top of the membrane. On top of this was placed 4 cm of paper towels cut to the size of the membrane and a glass plate with a small weight on it. The RNA was left to transfer onto the nitrocellulose membrane overnight by capillary action.

2.2.17.5 *Preparation of membrane for hybridisation*

The stack was disassembled and the blot marked with pencil to indicate its orientation. When hybridising with two probes annealing to targets of different size, the blot was cut in two across its width. The ruler measurements taken earlier in the gel visualisation section (sect 2.2.17.3) allowed estimation of where to cut. The two halves were briefly rinsed in 2 x SSC and placed on a sheet of Whatmann paper to dry briefly. The RNA was immobilised to the blot by UV cross-linking using the Stratagene Stratalinker. The RNA was irradiated, RNA side showing, at 254-nm UV light for 30 sec.

2.2.17.6 *Hybridisation of probe to target*

The membrane was placed in a hybridisation tube, RNA facing up, with 1 ml pre hybridisation buffer per 10 cm² of membrane and incubated at 42°C for 3 hrs in a rotating incubator. After this, the buffer was discarded and an equal volume of hybridisation buffer added. To this, 20 µl random primed probe (section 2.2.12.2 & 3), specific to target, was added directly and mixed. The blot was incubated for 16 - 48 hrs with the probe at 42°C in a rotating incubator.

2.2.17.7 *Washing and exposure of the blot*

After hybridisation the blot was washed in an excess volume of low stringency wash at room temperature for 5 min agitating gently. The wash was discarded safely and the step repeated twice. After the last wash, an excess of pre-warmed moderate stringency wash was added and the blot incubated at 42°C for 15 min in a rotating incubator. This was repeated twice. After the final wash, the membrane was removed from the tube and the excess wash buffer blotted onto Whatmann paper. It was then wrapped in UV transparent plastic wrap and placed in a blank phosphorimager cassette with the RNA facing the screen. The cassette was incubated for 4 - 48 hrs at room temperature before the image was visualised on a phosphorimager using the Bio-Rad Gel Doc 2000 Imaging system software.

2.2.17.8 Calculation of HCV RNA levels

Radioactive RNA bands were detected by the phosphorimager, which assigned an arbitrary figure for photon emission that was detected after exposure to the phosphorimager laser. The level of HCV RNA was calculated by normalising according to the GAPDH control. The following equation was used to obtain a normalised HCV value:

$$\frac{\text{GAPDH Control RNA Value - Background}}{\text{GAPDH Test RNA Value - Background}} \times \text{HCV RNA Value - Background}$$

The GAPDH control, which was represented either by a BSA or DMSO control depending on the experiment, represented 100 % and HCV RNA levels were normalised according to the ratio of the control GAPDH and test GAPDH levels. Therefore, if the HCV GAPDH value was less than the control GAPDH value the HCV RNA value would be increased accordingly.

These normalised HCV test RNA values were represented as a percentage of that of the normalised HCV control RNA values using the following equation:

$$\frac{\text{Normalised Test HCV RNA Value}}{\text{Normalised Control HCV RNA Value}} \times 100 \%$$

The normalised RNA values obtained from northern blots were confirmed using luciferase (described in section 2.7) assays. These two techniques had previously been compared by Tanabe et al (2004), who found that northern and

luciferase RNA levels correlated well with each other. Our results supported these findings. Figure 4.5 shows that HCV RNA levels obtained from either northern blots or luciferase assays were equivalent.

2.3 Preparation and transformation of *E.coli* DH5- α cells

2.3.1 Preparation of E.coli DH5- α competent cells

Chemically competent *E.coli* DH5- α cells were used for transformation of plasmid DNA. A single colony was inoculated into 10 ml LB broth and incubated overnight at 37°C on a shaking incubator. The following day a sub-culture of this was made by taking 200 μ l of the overnight culture and inoculating into 20 ml LB broth. The sub-culture was grown at 37°C for 2 - 2 ½ hrs on a shaking incubator or until it had reached a growth density of 0.6 absorbance at OD 600 nm. At this point, the culture was placed on ice immediately for 15 min after which it was centrifuged at 6000 g for 10 min at 4°C to pellet the cells. The supernatant was discarded and the cell pellet resuspended in 10 ml 100 mM CaCl₂ and incubated on ice for 30 min. The cells were then pelleted by centrifugation at 6000 g for 5 min at 4°C. The supernatant was discarded and the pellet resuspended in 1 ml 100 mM CaCl₂. The cells were incubated for a further 30 min before use.

2.3.2 Transformation of competent E.coli cells

Transformation of chemically competent *E.coli* DH5- α with plasmid DNA and ligations were performed by heat shock transformation. Bacterial competent cells and DNA were incubated at 4°C for ½ hr before use. DNA was added to 100 μ l competent cells in a microcentrifuge tube and mixed by flicking the tube. The mixture was incubated at 4°C for ½ hr gently agitating every 5 min. The cells were heat shocked for the uptake of the DNA by placing in a 42°C water bath for 2 ½ min. After this they were immediately placed on ice for 5 min before 900 μ l of LB broth was added and incubation at 37°C with a shaking for 1 hr. Transformed bacteria were selected for by spreading 100 - 200 μ l transformants onto a suitable antibiotic selective LB agar plate. In all cases, selection for uptake of plasmid DNA was achieved with 100 μ g/ml ampicillin in LB media. In some cases blue/white selection was used to identify if successful

ligation had taken place. In this case, 200 μM IPTG and 40 $\mu\text{g}/\text{ml}$ X-Gal was added to the selective agar LB media.

2.3.3 Making glycerol stocks

E. coli stocks containing successfully transformed plasmid were stored at -80°C as glycerol stocks. A 1 ml culture was grown overnight at 37°C in a shaking incubator. 700 μl of culture was placed in a 1.5 ml cryovial and mixed with 300 μl 50 % glycerol. Vials were then placed at -80°C till required.

2.4 Maintenance of mammalian cell culture

All mammalian cells lines were cultured in Dulbecco's Modified Eagles Medium (DMEM) containing 10 % foetal calf serum, 4 mM L-Glutamine, and 6 ml non-essential amino acids. In some cases 100 units/ml penicillin/streptomycin was included. Replicon containing cell lines were selected using G418 (1 mg/ml). Cultures were incubated at 37°C in 5 % CO_2 until growth was confluent. At this point cells, were trypsinised from the flask and proportion of cells used to seed a new flask of cells. G418 selection was removed at least two passages before experiment to prevent any selection for the replicon during the experiment.

2.4.1 Freezing of cells

Mammalian cell lines were stored in liquid nitrogen. A large 175 cm^2 tissue culture flask was trypsinised and cells counted using a haemocytometer. Cells were centrifuged at 900 rpm for 5 min. The supernatant was discarded and the cells resuspended in sufficient DMEM media to give 5×10^6 per 0.5 ml media. A 0.5 ml aliquot of cells was mixed with 0.5 ml foetal calf serum and 0.25 ml glycerol in a 2 ml cryovials. Vials were frozen at -80°C overnight and then transferred to long-term storage in liquid nitrogen

2.5 Electroporation of mammalian cells

HuH-7 cells were used for the electroporation of RNA produced from in-vitro transcription, as described in section 2.2.16.2. Cells were cultured in 175 cm^2

tissue culture flasks till confluent. Media was discarded and cells washed with 20 ml versene at room temperature. Cells were collected by trypsin treatment and resuspended in 10 ml media. The cells were pipetted up and down to achieve a single cell suspension and counted using a haemocytometer. Each electroporation required 1×10^6 cells to seed four 35 mm tissue culture dishes. Sufficient cells were removed to a fresh centrifuge tube for one electroporation and centrifuged at 400 g for 5 min. The medium was discarded and the cells washed in 10 ml PBSA. Cells were centrifuged again and the PBSA was discarded. The cells were resuspended in 0.8 ml PBSA and placed in an electroporation cuvette (0.4 cm gap, CLP-direct) with 5 μ g in-vitro transcribed RNA. The cell/RNA suspension was mixed by gently tapping and electroporated using a Bio-Rad Gene Pulser II with the following conditions: Volts of 0.36 K and High capacitance of 0.96 F. The cells were immediately transferred to 8 ml DMEM media and mixed. Each 35 mm dish was seeded with 2 ml electroporated cells. Cells were incubated at 37°C at 5 % CO₂.

In some cases 10 μ g in-vitro transcribed RNA was electroporated into 2×10^6 cells which were seeded onto a 90 mm tissue culture dish.

2.6 Transfection of mammalian cells

Mammalian cells were transfected with DNA using an “Invitrogen lipofectamine transfection kit”. One day prior to transfection HuH-7 cells ($0.5 - 2 \times 10^5$ cells) were seeded into a 35 mm dish. DNA-Lipofectamine complexes were assembled for each transfection. Initially, 1 μ g of green fluorescent protein tagged (GFP)-DnaseX expression plasmid was mixed with 250 μ l Opti-MEM[®]. At the same time 10 μ l of Lipofectamine[™] 2000 was mixed with 240 μ l Opti-MEM[®] and incubated for 5 min at room temperature. The diluted DNA was added to the Lipofectamine[™] 2000, mixed gently and incubated for 20 min at room temperature. The DNA-lipofectamine complexes were added to the seeded mammalian cells and incubated for 10 hrs at 37°C (5 % CO₂).

2.7 Luciferase assay

The Promega luciferase assay system was used as measure of replicon replication. In-vitro transcribed RNA was electroporated into naïve HuH-7 cells

as described above (Section 2.5) and luciferase assays performed at 4 hrs, 24 hrs, 48 hrs and 72 hrs. First medium was removed from the dish and the cells washed with 1 ml PBS. The PBS was discarded and the well washed again. Once all PBS was removed, the cells were lysed in 100 μ l Promega 1 x passive lysis buffer. The lysed cells were removed from the dish and placed in a 1.5 ml microcentrifuge tube. The lysed supernatant could be frozen at -20°C or used in a luciferase assay. A 100 μ l aliquot of luciferase assay reagent was placed in a 1.5 ml microcentrifuge tube and 40 μ l of the lysis supernatant added. The solutions were mixed briefly and luciferase activity assayed immediately by measurement in a Promega "20/20ⁿ luminometry system".

2.8 Lipid extraction and assay

2.8.1 Folch total lipid extraction

Total lipids were extracted from mammalian cells by the use of the Folch extraction technique in 35 mm dishes. The first medium was removed and cells were washed with versene. The cells were treated with 1 ml 1 x trypsin for 1 min. The trypsin was removed and cells lysed in 1 ml chilled methanol. The cells were scraped off the bottom of the well and added to 4 ml chilled chloroform in a glass test-tube. Another 1 ml of chilled methanol was used to remove all cell extract from the dish before being added to the chloroform. The methanol:chloroform mixture was vortexed for 30 sec and incubated on ice for 20 min. After lysis, the mixture was washed with 1.75 ml 0.88 % potassium chloride and placed in the cold room on a rocker for 30 min. The extraction was then centrifuged for 6000 g for 5 min to separate. The upper aqueous phase was discarded and the bottom hydrophobic layer (containing most lipids) transferred to a glass scintillation vial. The sample could be stored at -20°C or dried down to lipid components under nitrogen (Folch J, 1957).

2.8.2 Measuring fatty acid biosynthesis

Fatty acid biosynthesis was measured using ^{1-14}C Acetic acid as a substrate for the fatty acid elongation. A 35 mm dish of confluent cells was used in a ^{14}C pulse experiment. A 0.2 μCi aliquot of ^{1-14}C Acetic acid was mixed in 30 μ l (10 mM sodium acetate). This was incubated at 37°C for $\frac{1}{2}$ hr and was mixed

with the media in the dish to give a final concentration of 1 mM sodium acetate, 0.2 μCi ^{14}C Acetic acid per dish. The cells were incubated at 37°C in 5 % CO_2 for 3 hrs and after 3 hrs a total lipid extraction was performed as described in section 2.8.1. The chloroform layer was allowed to evaporate overnight in a fume hood. The lipids were resuspended in 10 ml Ecoscint™ A by being vortexed for 30 sec. Radioactive decays were measured as counts per minute on a scintillation counter.

2.8.3 Conjugation of BSA to free fatty acids

Treatment of mammalian cells with fatty acids first required them to be conjugated to fatty acid free BSA. A 10 % BSA/5 mM fatty acid complex was made as follows: 50 μl 100 mM free fatty acid in ethanol was added dropwise to 950 μl 10 % fatty acid free BSA. The mixture was vortexed for 2 min and incubated at 37°C for 2 hrs. The resultant BSA-FA complex was used on the day of making and added directly to DMEM media containing 5 % foetal calf serum.

2.9 MTT (3-(4,5-dimethylthiazol-2-yl) Assay

The MTT cell viability method measured the toxicity of compounds to mammalian cell lines. The method relies on the ability of living cells to reduce MTT (yellow) to purple insoluble formazan crystals catalysed by mitochondrial succinate dehydrogenase. A 96-welled plate was used in the assay. All outside wells were filled with 100 μl media to prevent evaporation in test wells. 100 μl aliquots of 2 x test media was placed in wells 2B-2G. 50 μl of untreated media was placed in all empty wells. A serial dilution of 2 x test media was made in lanes 3 - 9 using a multi pipetter. A 50 μl aliquot containing 2.5×10^4 cells was seeded into each of the test wells. Each assay was performed in triplicate. Lane 10 was used a control for the test solvent and lane 11 contained untreated cells.

Cells were incubated with test media at 37°C in 5 % CO_2 for 72 hrs. The medium was changed daily to avoid degradation of test compounds. At 72 hrs the medium was removed and then replaced with 100 μl DMEM containing 0.5 mg/ml MTT. The plate was incubated at 37°C in 5 % CO_2 for 3 hrs. The MTT medium was then removed and replaced with 100 μl isopropanol (0.4 M HCl). The plate

was wrapped in tin foil and placed at 4°C overnight. The following day, the absorbance of the formazan crystals was measured at 595 nm and background at 630 nm using the Dynex plate reader with “Revelation” software. Cell viability was obtained using the following equation:

Percentage cell viability =

$$(\text{Test 595 nm} - \text{test 630 nm} / \text{Control 595 nm} - \text{Control 630 nm}) * 100$$

The values obtained were used to create a dose response curve of cell viability against concentration of compound.

2.10 Protein analysis by SDS-PAGE and western blotting

2.10.1 Preparation of cell extracts

Cell extracts were prepared from confluent cell growth in 35 mm dishes. Media was removed from the well and the cells washed twice in PBS. The cells were lysed by the addition of 150 µl 1 x boiling mix at room temperature. Extracts were placed in a 1.5 ml microcentrifuge tube and boiled at 100°C for 10 min. Cellular extracts were stored at -80°C. Samples were boiled before use.

2.10.2 SDS-PAGE

Proteins were separated by SDS polyacrylamide gel electrophoresis (Laemmli, 1970) in a Bio-Rad Miniprotein II apparatus. In all cases, a 10 % polyacrylamide gel was made for resolving proteins. The gel was made by mixing 8 ml of 30 % acrylamide Bis-solution (consisting of acrylamide and *N,N'* methylene bisacrylamide (ratio 37.5:1)), 6 ml resolving gel buffer, 10 ml water and 200 µl 10 % ammonium persulphate (APS). The solution was mixed and 25 µl TEMED added as catalyst for polymerisation. The solution was immediately poured between the assembled gel plates to approximately 4 cm from the top of the smaller plate. 200 µl butan-2-ol was placed on top of the resolving gel solution to allow a smooth interface between the two parts of the gel. After polymerisation of the gel, the stacking gel was made. This was achieved as follows: 4 ml 30 % acrylamide bis solution, 6 ml stacking gel buffer, 14 ml water

and 200 µl 10 % APS. The solution was mixed and 25 µl TEMED added. The buton-2-ol was removed and the interface washed several times with water. All water was removed with paper towel. The stacking gel was immediately poured on top of the resolving gel, to the top of the glass plate and a 1.5 mm comb inserted for loading samples. Once the gel had polymerised, the comb removed and the gel placed in the electrophoresis tank and the tank was filled with gel running buffer.

Protein extracts were denatured by boiling prior to gel loading. A 20 - 25 µl aliquot of cellular extract was loaded into each well. An Amersham protein molecular weight marker (rainbow marker) was used to estimate size of loaded samples. Any empty wells had 20 µl boiling mix loaded into it. The gel was run at 120 V for 1 ½ hrs, until the bromophenol blue had run off the end of the gel.

2.10.3 Western Blotting

Proteins resolved by SDS-PAGE were transferred to nitrocellulose membrane using the western blotting technique in the Bio-Rad mini transblot apparatus as described by Towbin et al. (1979). The gel was removed from the electrophoresis tank and the stacking gel discarded. A blotting sandwich was made where the gel was placed with a piece of nitrocellulose membrane in contact with it between two pieces of 3 MM Whatman paper and two fibre pads. The sandwich was held together in a cassette and was placed into the transblot apparatus and immersed in Towbin buffer (Towbin H, 1979). Electrotransfer was carried out at 100 mA (for 1 gel) or 200 mA (for 2 gels) for 2 hrs or 25 mA at 4°C overnight.

2.10.4 Immunodetection

After transfer, the sandwich was dismantled and the blot recovered for immunodetection. First the blot was incubated in 3 % BSA prepared in PBS(A) for 1 hr at room temperature or overnight at 4°C. Next, the blot was incubated on an orbital shaker with primary antibody, 1 % BSA and 0.05 % Tween 20 in PBS(A) for 2 hrs at room temperature. If an overnight incubation was required, 0.01 % sodium azide was included. The primary antibody was removed by washing in excess PBSA/0.05 % Tween 20 (PBST) twice for 15 min. The secondary antibody

(either protein A conjugated to horseradish or anti-sheep IgG HRP or anti-mouse IgG HRP) and 2 % Marvel milk were prepared in PBST and incubated with the blot at room temperature on an orbital shaker at room temperature for 1 - 4 hrs. The secondary antibody was removed and the blot was washed twice in PBST for 15 min. The proteins were detected using Amersham enhanced chemiluminescence (ECL) reagents. The blot was placed between two sheets of mellanine with the two reagents placed directly on the proteins of the blot in a 1:1 ratio. After a short incubation the proteins were visualised by exposing the blot to a sheet of Kodak XS-1 film for 10 - 120 sec in a dark room. The film was developed in an Xomat Kodak developer.

2.11 Immunofluorescence

For the purpose of viewing protein expression in cells immunofluorescence was used. Replicon cells were seeded on coverslips in a 24-welled plate and grown overnight at 37°C 5 % CO₂. The medium was removed and the cells fixed by the addition of 0.5 ml methanol (-20°C) at -20°C for 20 min. The methanol was aspirated and cells were washed in 1 ml PBS(C) for 10 min. The PBSA was removed and cells incubated in 1 ml PBS/2 % foetal calf serum for 10 min. Next, 200 µl of primary antibody in PBS/2 % foetal calf serum was added for 1 ½ hrs at room temperature. The primary antibody was removed and the cells were washed three times in 1 ml PBS/2 % foetal calf serum. 200 µl secondary antibody (conjugated with TRITC or FITC) in PBS/2 % foetal calf serum was added. The plate was wrapped in foil and it was incubated for 1 hr at room temperature. The secondary antibody was removed and the cells were washed twice in 1 ml PBS/2 % foetal calf serum. This wash was followed by a single wash in 1 ml PBS. During the washes the plate remained wrapped in the tin foil to prevent degradation of the secondary antibody fluorescent group. All steps were performed at room temperature on the orbital shaker.

Coverslips were mounted onto a slide cell side down on a drop of CITI FLUOR. The edges of the coverslip were sealed with nail varnish and the slides were stored in the dark at 4°C till use. Slides were viewed using the ZEISS LSM 510 confocal microscope using the accompanying software.

2.12 Fluorescence Recovery after photobleaching (FRAP)

FRAP analyse was used to analysis the mobility of proteins bound to the ER membrane. Previously, cells were transfected with GFP tagged DNaseX (GFP-DNaseX). Initially test medium was removed and replaced with prewarmed DMEM (1 % foetal calf serum) that did not contain phenol red. Cells were kept in a 37°C at 5 % CO₂. When required, cell dishes were moved to the live cell chamber on the ZEISS LSM 510 confocal microscope. FRAP experiments observed the movement of GFP tagged DNaseX protein on the ER. First a defined area (38 μm²) on the ER membrane was irreversibly bleached by a high power focused laser beam (100% laser power, 488 nm laser line). The movement of non bleached protein into the bleached area allowed the recovery to be observed. In addition to measuring the movement of GFP tagged proteins into the bleached area, another defined area of the same size measured the loss of GFP tagged proteins from an unbleached part of the ER membrane. By taking into account the background, the recovery of GFP tagged proteins could be calculated using the following equation:

$$\frac{\text{The recovery of fluorescence into the bleached area} \times \text{The background fluorescence}}{\text{The starting fluorescence prior to bleaching in the unbleached area}}$$

Once the recovery of fluorescence had been calculated a percentage of fluorescence recovery could be obtained.

2.13 Computer software

TaqMan PCR products that were produced in the Perkin Elmer Applied Biosystems 5700 sequence detection system were detected using Perkin-Elmer sequence detector software. Agarose gels and phosphoimaging screens were viewed using Bio-Rad's Gel Doc system and software. Multiple sequence alignments were performed using a UNIX server and the GCG GEL START

programs or an internet based program called BCM launcher. Text files produced from BCM launcher multiple sequence alignments were then viewed using Boxshade programs. Toxicity assays were performed on a DYNEX plate reader using the Revelation software. Endnote 5.0 was used to create the bibliography. Vector diagrams were drawn using a freeware program called BioEdit. Computer analytical restriction enzyme digests were performed by NEB Cutter (www.neb.com).

Chapter 3

3 Optimising techniques

3.1 Enriching a 5-15 genotype 1b expressing cell line

The 5-15 genotype 1b replicon cell line was derived from a single colony of HuH-7 cells transfected with a Con1 genotype 1b sub-genomic replicon (Lohmann et al., 1999). Analysis of transfected HuH-7 cells had revealed that only 10 - 50% of cells displayed HCV protein expression (Lohmann et al., 2003). This emphasised the differences in expression of HCV non-structural proteins between cells within an apparent homogeneous population of cells. These variations in expression were possibly due to heterogeneity of HuH-7 cells or cell cycle effects (Pietschmann et al., 2001). The 5-15 clonal cell line had increased HCV RNA levels compared to other clonal cell lines derived from the same initial transfection.

To minimise the heterogeneity of HCV replicon expression in HuH-7 cells, we selected a clonal cell line with robust expression on which to test inhibitors of lipid metabolism by serially diluting a stock of cells and isolating single cell colonies and growing-up. To obtain the highest expressing 5-15 genotype 1b clonal cell line, individual clones from single cells were grown and selected on the basis of NS5A expression, initially using indirect immunofluorescence and then Western blot analysis. Two highly expressing clonal cell lines were obtained, clones 12 and 15 (Figure 3.1a). Although immunofluorescence analysis was useful in visualising the proportion of expressing cells, Western blot analysis was necessary to quantify total NS5A expression. Indirect immunofluorescence highlighted the variations in NS5A protein expression within populations of cells where there was a range of expression (Figure 3.1b). All future experiments on the 1b sub genomic replicon were performed using clone 12 (1b).

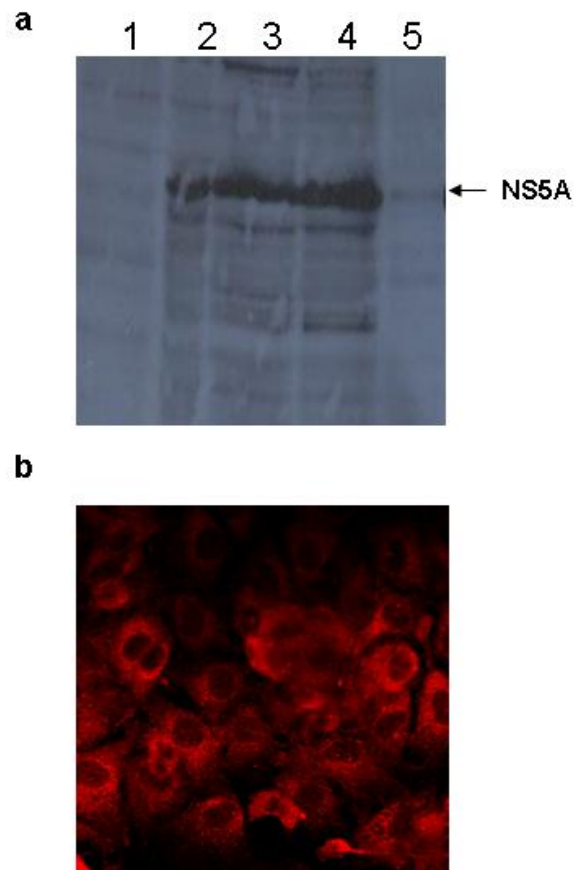


Figure 3.1. Enrichment of a 5-15 genotype 1b expressing cell line. Western blot analysis (a) and indirect immunofluorescence (b). Two high expressing cells lines were obtained, clones 12 and 15. Cells were seeded at an equivalent number (10^6 cells) per well. Protein extracts from HuH-7 (lane 1), 1b positive control (lane 2), 5-15 1b clonal cell lines 12, 15 (lanes 3 and 4 respectively) and a low expressing 5-15 1b clone (lane 5) were separated on a 10 % polyacrylamide gel. NS5A was detected using the polyclonal R1065 rabbit anti-serum (McLauchlan et al., unpublished). Panel (b) shows immunofluorescence results for 5-15 1b clonal 12 cells. NS5A was detected using the polyclonal R1065 rabbit anti-serum.

3.2 Interferon “curing” of replicon expressing cells

Previous reports had indicated that the Con1 1b subgenomic replicon acquired specific mutations for achieving higher levels of replication (Lohmann et al., 2003). IFN- α treatment blocks HCV replication, thereby progressively clearing the replicon from cells (Blight et al., 2003; Frese et al., 2001; Guo et al., 2001). The resultant cells, cured with IFN- α , often give a slightly more permissive cellular environment for replication than naïve HuH-7 cells.

Here, replicon containing cells were cured of HCV RNA using pegylated interferon alpha-2b (Blight et al., 2003). “Cured” cells could then be used as a permissive host for the electroporation of subgenomic RNA for attempts to establish a genotype 3 replicon. They could also be used as a negative control, which would better represent the cellular properties of replicon cells than naïve HuH-7 cells. Figure 3.2 shows loss of NS5A expression in replicon-bearing cells by Western blot analysis. Over a 120 hour period the expression of NS5A was abolished (Figure 3.2). Furthermore, Figure 3.2 shows that by removing G418 selection, there was no effect on NS5A expression. This indicated that the replicon was lost due to IFN treatment and not due to the removal of G418 from the medium. Cells were grown in the presence of IFN- α for a total of four passages. Removal of replicon was confirmed by culturing in G418 containing media. All future experiments used 1b “cured” HuH-7 cells (1b-C) as a negative control.

3.3 Optimising the MTT (3-(4,5-dimethylthiazol-2-yl) assay

The treatment of tumour cells with drugs or metabolites that interfere with lipid metabolism can reduce cell viability by inducing apoptosis and/or reducing cell proliferation (Kuhajda, 2000). Drugs which inhibit fatty acid synthase induce apoptosis in breast cancer cells (Menendez JA, 2004). Polyunsaturated fatty acids (PUFAs), which can globally effect the transcription of genes involved in lipid metabolism, reduce cell viability in breast cancer cells (Schley, 2005). It was therefore important to ensure that any effect seen following treatment of cells with drugs or compounds was a specific effect and not the result of general

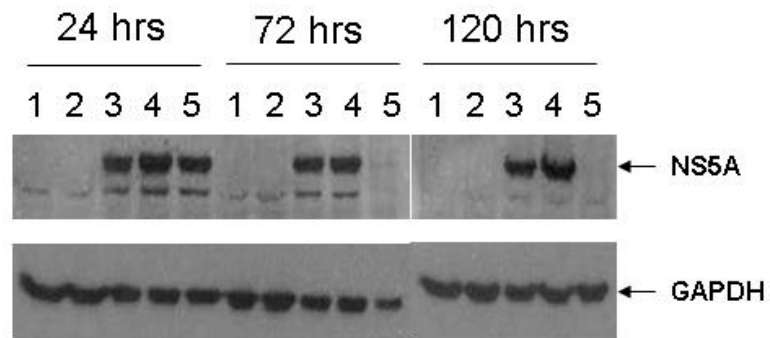


Figure 3.2. Interferon alpha 2b treatment of 5-15 1b cells. Loss of replicon was determined by Western blot analysis. HuH-7 (lanes 1 & 2) and 1b replicon (lanes 3, 4, & 5) cells were treated with IFN- α (lanes 2 & 5), as described by Blight *et al* (2002) and without IFN- α and (1, 3, & 4). G418 was present only in the replicon positive control (lane 3). Samples were taken at 24 hrs, 72 hrs and 120 hrs. Proteins were separated on a 10 % polyacrylamide gel. NS5A was detected using the polyclonal R1065 rabbit anti-serum (McLauchlan *et al.*, unpublished) and GAPDH was detected using a monoclonal antibody.

toxicity. Cytotoxicity was measured using an MTT cell viability assay adapted from Mossman (1983). MTT is a yellow tetrazolium salt, which is cleaved by dehydrogenase activity in active mitochondria to produce purple insoluble formazan crystals. The absorbance of the resuspended formazan crystals is proportional to the number of living cells present (Mosmann, 1983). The original method was modified slightly to measure absorbance of the formazan at a wavelength absorbance of 590 nm (A_{590}) because cell number is directly proportional to absorbance over a wider range of cells/well at this wavelength (Tada et al., 1986). In this study, the optimal seeding numbers varied between cell types because of differing metabolic activities. Optimal cell seeding number was obtained by growing serial dilutions of replicon and cured cells for three days in microplates and performing an MTT assay at 72 hrs. This allowed the relationship between MTT formazan production and cell number to be represented in a graph (Figure 3.3). The optimal cell seeding number occurred approximately half way along the linear phase of absorbance. This gave an optimal cell seeding number of approximately 25,000 cells/well for all cell lines.

3.4 Optimisation of the fatty acid biosynthesis assay

The effect of inhibitors on fatty acid biosynthesis can be measured by supplying cells with radiolabelled (^{14}C) acetate, which becomes incorporated into all cellular lipids. To measure the uptake and incorporation of radiolabelled acetate, total lipid extractions were performed at intervals over 3 hours. Replicon and cured cells (seeded with 5×10^5 cells per dish), which had been grown overnight to 80 % confluency were incubated with radiolabelled (^{14}C) acetate (0.2 $\mu\text{Ci}/\text{well}$) for three hours. Lipid extractions were performed, at 5 time points, on cells and medium separately to measure the difference between incorporation of acetate into secreted and cellular lipids. Figure 3.4 shows that there was an increase in acetate incorporated into cellular lipids but secretion of radiolabelled lipids into the medium did not increase over this period. Based on these results, all future lipid extractions were performed only on cells, not on media.

To confirm that the ^{14}C was not being exhausted during the 3 hrs of the assay, an experiment was carried out using two different concentrations of label (0.2

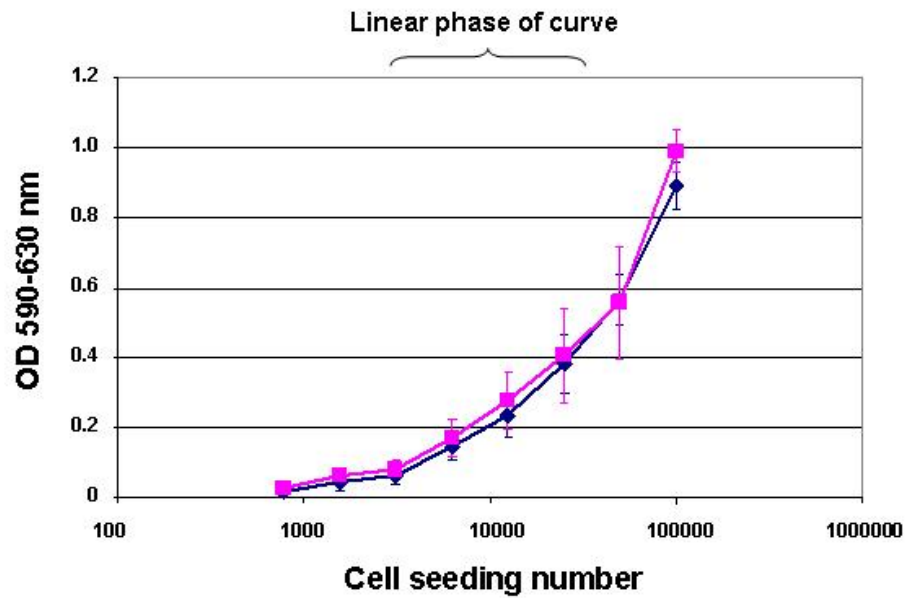


Figure 3.3. Optimisation of MTT assay for cell seeding number. 1b replicon and cured cells were serially diluted and grown for 72 hrs. MTT assay was performed and formazan absorbance (A590) and background absorbance (A630) were measured. Absorbance obtained from 1b replicon (pink) and cured (1b-C)(blue) cells has been corrected for background.

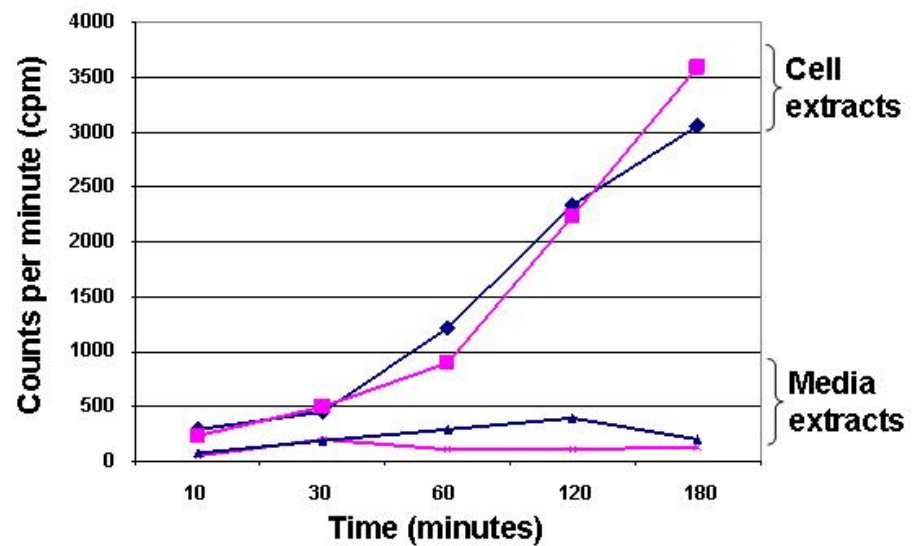


Figure 3.4. Cellular and media lipid extractions following incubation with radiolabelled acetate. Radiolabelled acetate was added at 0 mins. Total cellular and medium lipid extractions were performed at five time points over a three hour period on 1b (pink) and 1b-C (blue). Radioactivity was measured by scintillation counting.

$\mu\text{Ci}/\text{well}$ & $0.4 \mu\text{Ci}/\text{well}$). Cerulenin was used to assess the effect of inhibitors of fatty acid biosynthesis on acetate incorporation in 1b replicon harbouring (1b) and 1b cured (1b-C) cells. Again, as above, cells which had been grown overnight were incubated with the two concentrations of radiolabelled (^{14}C) acetate for three hrs and then total cellular lipid extractions were performed. Figure 3.5a shows actual values for untreated controls, DMSO controls and cerulenin-treated cells. As expected, incorporation of acetate into extracted lipids approximately doubled when adding twice the amount of radiolabel, $0.4 \mu\text{Ci}/\text{well}$ (Figure 3.5a). Furthermore, normalised data showed that the proportion of incorporation compared to that of the DMSO controls remained the same between the two concentrations (Figure 3.5b). This indicated that the label was not exhausted at the lower concentration. Future experiments used $0.2 \mu\text{Ci}/\text{well}$ radiolabelled acetate. Treatment of both replicon and “cured” cells with cerulenin reduced fatty acid biosynthesis at $30 \mu\text{M}$ and minimally at $10 \mu\text{M}$.

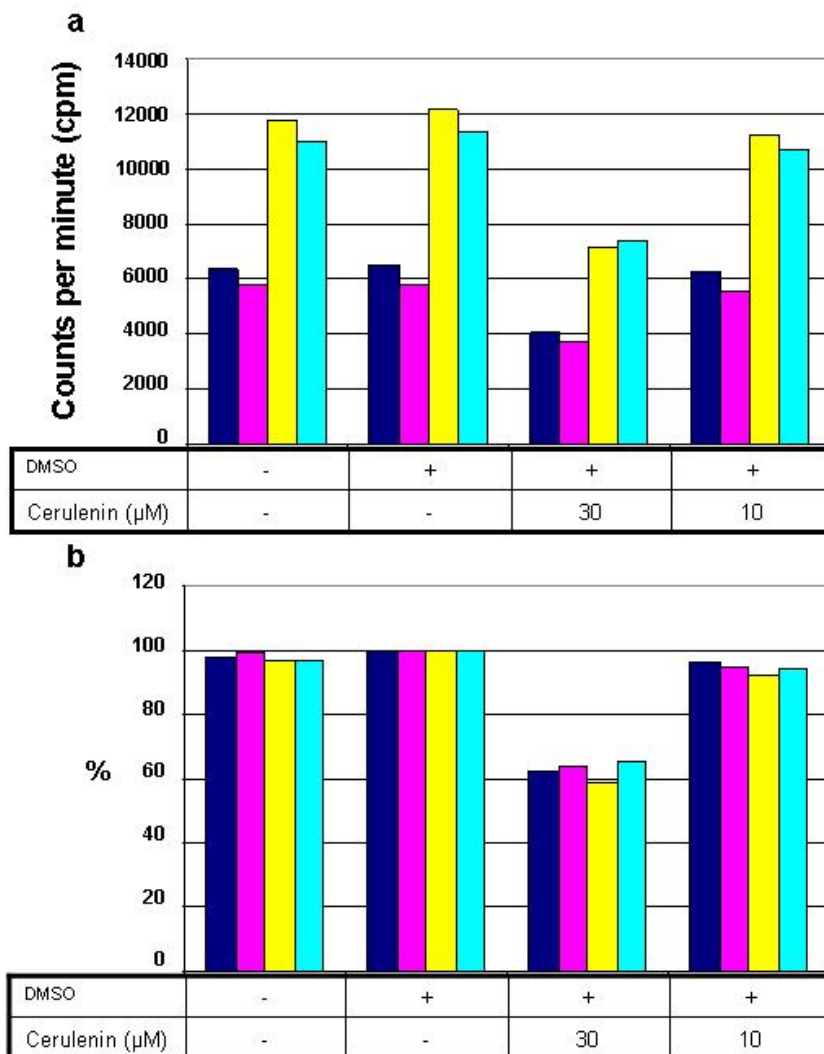


Figure 3.5. The effect of increasing the amount of radiolabelled acetate on incorporation. 1b-C (dark blue and yellow) and 1b (pink and light blue) cell lines were incubated for 15 min in the presence of DMSO or Cerulenin at 30 μM and 10 μM . DMSO concentration was kept constant in test and DMSO wells. Pulse labelling with ^{14}C acetate was performed at 0.2 $\mu\text{Ci/well}$ (dark blue and pink) and 0.4 $\mu\text{Ci/well}$ (yellow and light blue) and cellular lipids were extracted. Panel (a) shows actual values obtained from scintillation counting. Panel (b) shows the data represented as a percentage of that of the DMSO control.

Chapter 4

4 The effect of cerulenin on the replication of HCV expressing cell lines

4.1 Introduction

Microarray analysis of mRNA levels of host cellular genes from three chimpanzees acutely infected with HCV genotype 1a, highlighted three groups of genes with perturbed expression (Su et al., 2002). Genes which had altered mRNA levels were IFN- α activated genes, IFN- γ stimulated genes and genes encoding enzymes involved in lipid metabolism. In some viral infection, IFN- α activation of genes can aid viral clearance. However, the study by Su et al. (2002) indicated that expression of IFN- α stimulated genes had little or no effect on HCV viral titre or outcome. Another group of genes that showed perturbed expression were IFN- γ stimulated genes concerned with antigen presentation. Several genes in this group, which explicitly process antigen for presentation to T-cells in the adaptive immune system, were up-regulated. Up-regulation of these genes was associated with sustained or transient viral clearance.

The observed increased mRNA levels of some lipid metabolism genes associated with the early onset of virus detection in the blood (viremia) was unexpected. The genes concerned encoded proteins or enzymes involved with the synthesis of endogenous cholesterol and fatty acids and their modification into complex lipid. The mechanisms directing changes in such genes during viremia were not understood. A second micorarray study on 10 chronically infected chimpanzees also revealed perturbed expression of genes concerned with lipid metabolism (Bigger et al., 2004). There were some differences however between the two studies. Up-regulation of some genes associated with the onset of viremia in the study of acute infection was not found in the chronically infected animals. Also

the fatty acid synthase (FAS) gene was more highly expressed in acutely infected animals that had a sustained or transient clearance of virus than those which displayed a persistent infection. FAS expression in chronically infected chimpanzees was decreased in four animals. Differences between these two studies may be due to differences between acute and chronic infections. The inconsistencies between these studies may also suggest that altered expression of genes concerned with lipid metabolism is not a prerequisite for successful viral infection.

Further analysis was performed on cells harbouring HCV replicons and showed an altered cellular abundance of mRNA for some essential lipid metabolism genes. ATP citrate lyase and acetyl Co-A synthetase, were up-regulated in HuH-7 cells containing full-length genotype 1b HCV replicon (Kapadia et al., 2005). ATP citrate lyase, which synthesises acetyl CoA in the cytosol, was also up-regulated in acutely and chronically infected chimpanzees (Bigger et al., 2004; Su et al., 2002). However, one difference between replicon and HCV infected chimpanzee studies was the lack of any change on FAS transcript levels in replicon-bearing cells.

The importance of lipid metabolism to viral replication was further shown when drugs that interfere with lipid metabolism affected replication by the HCV replicon (Kapadia et al., 2005; Su et al., 2002). Studies failed to identify the mechanism, which reduced replicon RNA levels after inhibition of fatty acid biosynthesis. Induction of fatty acid biosynthesis by cholesterol sequestration using nystatin increased HCV replication (Su et al., 2002). HCV replicon RNA was reduced by cerulenin, an inhibitor of fatty acid biosynthesis (Su et al., 2002). However, the effect of cerulenin, on fatty acid production was never investigated. Cerulenin ([2S,3R]2,3-epoxy-4-oxo-7E10E-dodecadienamide), is an antibiotic product made by the fungus *Cephalosporium ceruleans* (Ronnett et al., 2005). It acts by binding irreversibly to the the ketoacyl synthase domain in the active site of FAS and modifies an active site cysteine preventing fatty acid chain elongation and consequently fatty acid biosynthesis (Knowles et al., 2004). A number of non-specific effects other than its inhibitory effect on FAS have been attributed to cerulenin (Schlesinger et al., 1982).

4.2 Cerulenin treatment of HCV genotype 1b replicon expressing cells

4.2.1 Cerulenin inhibition of HCV RNA replication did not correlate with its ability to inhibit fatty acid synthesis

In order to ascertain whether inhibition of HCV replication was a consequence of cerulenin's inhibitory effects on FAS, we measured both fatty acid biosynthesis and HCV replication. Cerulenin has been reported to reduce cell viability in tumour cell lines. Thus, toxicity assays were used simultaneously to confirm that any effects seen were not due to cytopathic effects of the drug. To maintain as much continuity as possible between our study and that of Su et al. (2002) a genotype 1b expressing cell line was used. As previously described (Chapter 3.1) a highly expressing 5-15 genotype 1b cell line called clone 12 had been selected. Clone 12 or "1b" was cured with IFN- α (chapter 3.2) to produce a cell line (1b-C) that could be used as a negative control in experiments. 1b and 1b-C cells were incubated in the presence and absence of DMSO and at four concentrations of cerulenin (30 μ M, 10 μ M, 3 μ M and 1 μ M). DMSO was kept constant at 0.00003%. 1b and 1b-C cells were grown for 72 hrs under these experimental conditions. As the manufacturer advised that the stability of cerulenin in the aqueous medium could not be guaranteed for longer than 24 hrs, the medium was changed daily. Assays and extractions were performed at 72 hrs. The results shown are from three experiments.

Figure 4.1a shows that cerulenin was able to reduce fatty acid biosynthesis at the highest concentration of 30 μ M giving inhibitory levels of 50-60 % in both 1b and 1b-C cells. At other cerulenin concentrations, inhibition was either not seen or fatty acid biosynthesis continued at greater than 80 % of that of the DMSO control. For reasons that are unknown there appeared to be slightly more variation in results obtained from 1b experiments. At 10 μ M cerulenin, fatty acid biosynthesis was not inhibited. However at the lower concentrations of 3 μ M and 1 μ M a slight inhibition was seen. Why no inhibition of fatty acid biosynthesis was seen at the higher concentration of 10 μ M while there was slight inhibition at lower concentrations could not be explained but was found consistently.

Figure 4.1. The effect of cerulenin treatment on 1b (pink) and 1b-C (blue) expressing cell lines. Assays were performed to measure cellular fatty acid biosynthesis (a) and cellular toxicity (b). HCV RNA replication is shown as a normalised percentage of that of the DMSO control (c) obtained using Northern blot analysis (d) where RNA was resolved in a 1 % formaldehyde gel. RNA extracts were obtained from experiments with 1b cells treated only with DMSO solvent (lane 1) or treated at 4 concentrations of cerulenin 30 μM , 10 μM , 3 μM and 1 μM (lanes 2, 3, 4 and 5 respectively). DMSO was kept constant at 0.00003 %.

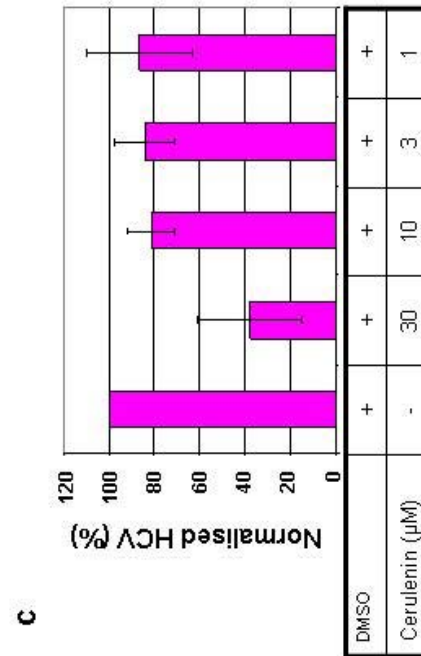
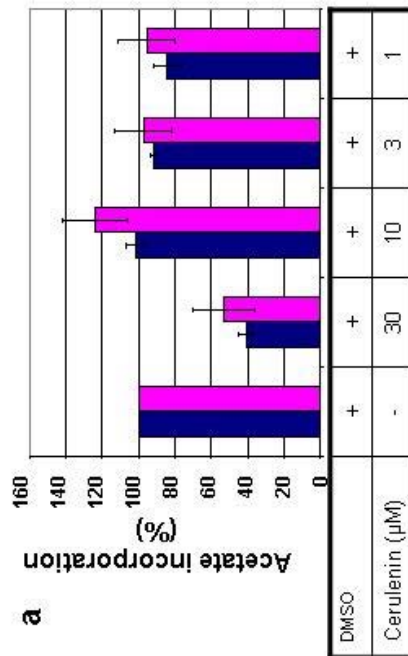
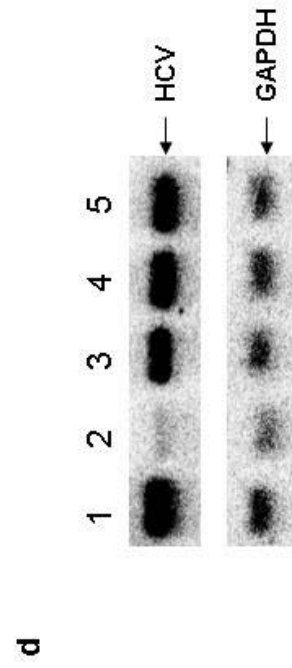
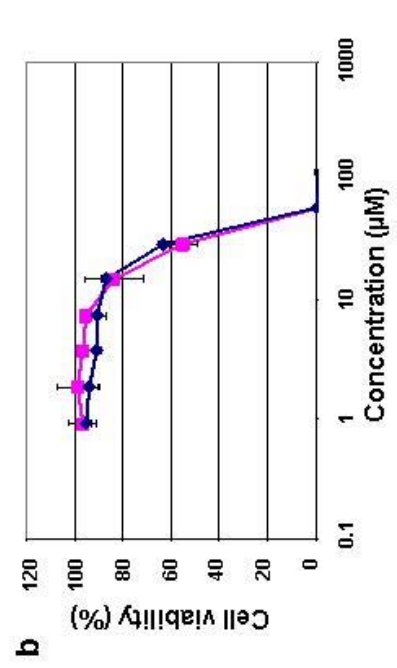


Figure 4.1b shows treatment with lower concentrations of 10 μM , 3 μM , and 1 μM cerulenin resulted in cell viability which were comparable to that of the DMSO control. At higher concentrations of 60 μM and 120 μM cerulenin, the drug is completely lethal. At 30 μM cell viability is approximately 60 % of that of the DMSO control.

Figure 4.1c & d show that HCV replication was inhibited at all concentrations of cerulenin. Effects at the upper concentration of 30 μM may be due to the toxic effects of the drug as cell viability was reduced by 20-30 %. However, lower, non-toxic concentrations of cerulenin had a slight inhibitory effect on HCV RNA levels. At 10 μM and 3 μM , HCV RNA dropped to 81 % and 84 % of that of the DMSO control respectively.

The results indicated that cerulenin did not inhibit fatty acid biosynthesis without a corresponding effect on cell viability nor did it inhibit fatty acid biosynthesis in a dose dependent manner. However, HCV replication was inhibited by cerulenin treatment at all concentrations, although this was minimally at non-toxic concentrations.

4.2.2 Cerulenin was unable to inhibit fatty acid biosynthesis, even when media was changed every 8 hours

The treatment of 1b with cerulenin had resulted in a slight drop in HCV RNA levels. However, experiments failed to show inhibition of fatty acid biosynthesis. Cerulenin is well established as a direct inhibitor of FAS. It therefore came as a surprise to find that it did not inhibit fatty acid biosynthesis. One possibility was that cerulenin was not stable and was degraded in the aqueous solution. Our initial hypothesis was that cerulenin acted on fatty acid biosynthesis and this action led to the drop in HCV replicon RNA levels. Over time, as the compound degraded, fatty acid biosynthesis would recover. In order to test this possibility, experiments were repeated with cerulenin being replaced every 8 hours. It was hoped this approach would minimise effects of degradation of cerulenin and enhance the impact on fatty acid biosynthesis. The experiment was also modified to include a final cerulenin replacement just before the fatty acid biosynthesis assay. This additional step

was performed in all future experiments. Fresh cerulenin would better show the effect on fatty acid biosynthesis directly after its addition.

The first notable difference between the experiments was that the toxicity (figure 4.2b) of cerulenin increased. An initial experiment found 30 μM was more toxic with a cell viability of only 20 %. Therefore, 3 subsequent experiments were performed at 10 μM , 3 μM and 1 μM . A 50 % cell viability or toxic dose 50 (TD_{50}) was found at approximately 20 μM . This compared to the previous experiment which had a TD_{50} of approximately 40 μM . Thus by changing the medium more often, the toxicity cerulenin had increased.

Figure 4.2a shows that by changing the medium more often, there was still no appreciable effect on fatty acid biosynthesis. Therefore, the effect of cerulenin on fatty acid biosynthesis was equivalent irrespective of whether media was changed every 24 hours or every 8 hours.

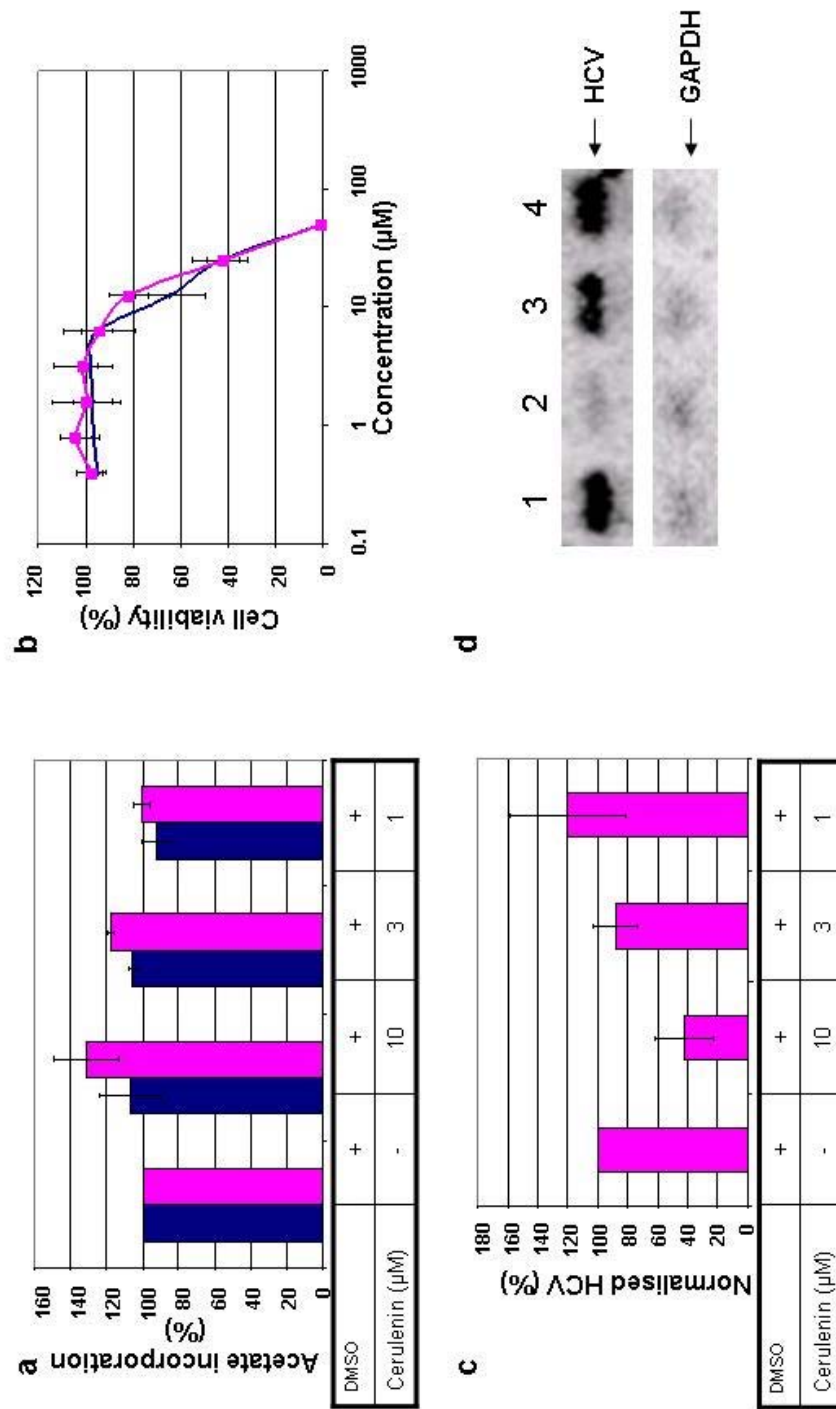
HCV replication was inhibited as before although the effect at 10 μM was more potent in that HCV RNA levels were 42 % of that of the control. This was half that seen when changing the medium daily. Therefore by changing the medium more frequently cerulenin's effects on HCV replication and toxicity were increased however there was no change in fatty acid biosynthesis.

4.2.3 Cerulenin from different suppliers affected cells differently with respect to HCV replication, fatty acid synthesis and toxicity

The lack of any effect on fatty acid biosynthesis with cerulenin treatment of 1b and 1b-C cell lines was unexpected. Results had indicated that the inability of cerulenin to inhibit FAS activity was unlikely to be due to the stability of the drug given the toxicity observed. To investigate whether similar trends in the effects of cerulenin were obtained from an alternative source for the compound, the experiment in section 4.1.1 was repeated with cerulenin obtained from Axxora Ltd (Cayman Biochemicals) with drug being replenished every 24 hrs.

Treatment of 1b and 1b-C cells with cerulenin obtained for Axxora Ltd showed a slightly different response from previous experiments. The inhibitory effect of

Figure 4.2. The effect of frequent cerulenin medium changes on 1b (pink) and 1b-C (blue) expressing cell lines. Assays were performed to measure cellular fatty acid biosynthesis (a) and cellular toxicity (b). HCV RNA replication is shown as a normalised percentage of that of the DMSO control (c) obtained using Northern blot analysis (d) where RNA was resolved in a 1 % formaldehyde gel. RNA extracts were obtained from experiments with 1b cells were treated only with DMSO solvent (lane 1), or treated at 3 concentrations of cerulenin 10 μM , 3 μM and 1 μM (lanes 2, 3, and 4 respectively). DMSO was kept constant at 0.00003 %.



cerulenin on fatty acid biosynthesis (Figure 4.3a) was far more pronounced at 30 μM than that seen in Figure 4.1a (cerulenin supplied by Sigma-Aldrich Ltd). At this concentration fatty acid biosynthesis was less than 10 % of that of the DMSO control. This compared to 40 % with cerulenin from Sigma. At 10 μM there was slight inhibition of fatty acid biosynthesis to 80-90 % but virtually no inhibition at the two lower concentrations of 3 μM and 1 μM .

Figure 4.3b shows the toxicity result for this experiment. There was also a slight difference in the toxicity of cerulenin from these two manufacturers. A TD_{50} was obtained at approximately 35 μM with cerulenin from Axxora. At 30 μM of cerulenin from Axxora, 58-62% cell viability was found. This compared to 70-80 % cell viability with cerulenin from Sigma-Aldrich Ltd. Again all lower concentrations of cerulenin were non-toxic. Comparing the data in Figures 4.3a and b, the compound was still unable to inhibit fatty acid biosynthesis effectively at non-toxic levels.

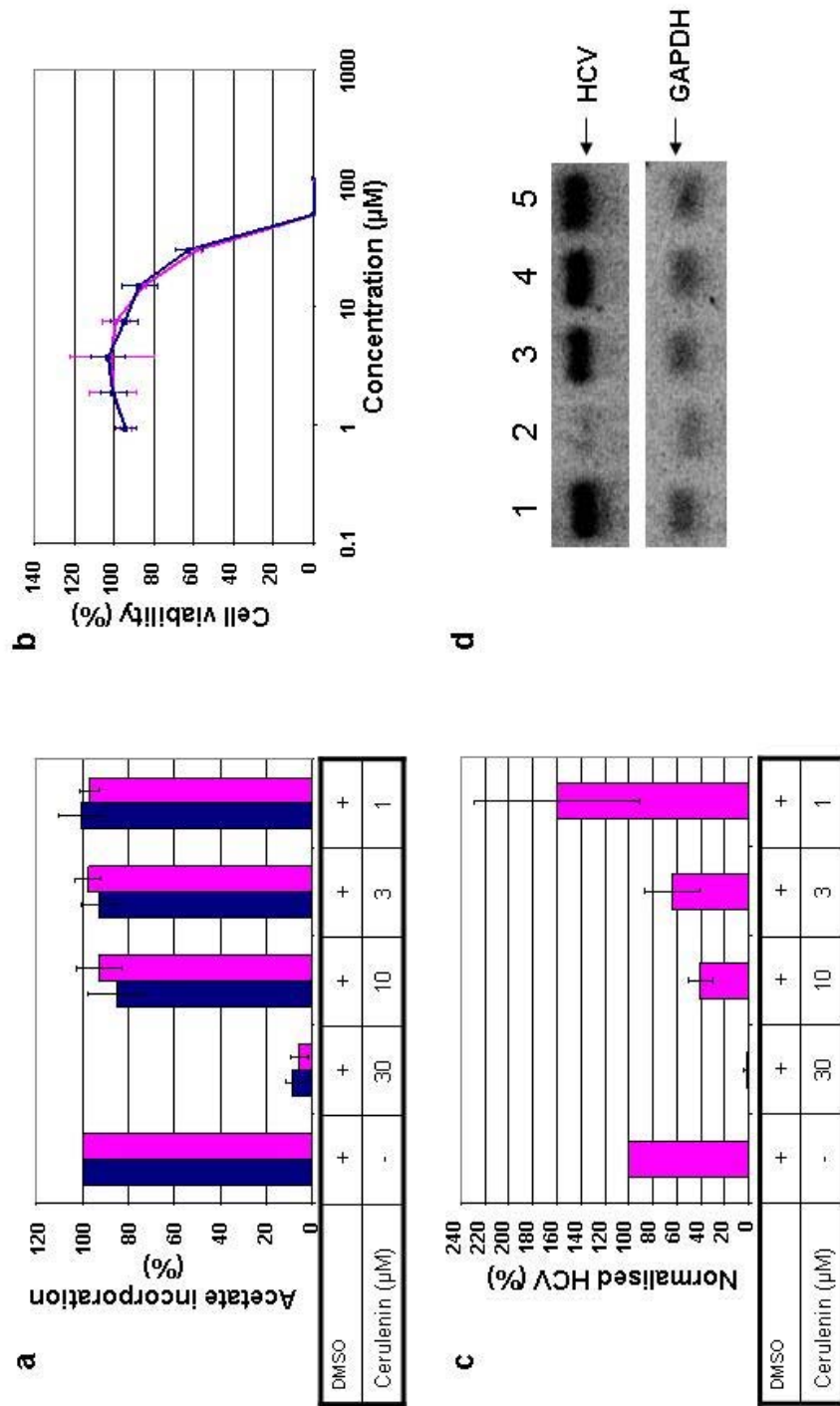
Cerulenin obtained from Axxora was more potent in reducing HCV RNA replication than that obtained from Sigma Aldrich. Figure 4.3c & d shows replication was inhibited at 30 μM , 10 μM and 3 μM to 2 %, 40 % and 60 % of that of the DMSO control, respectively. As previously, discussed toxicity may contribute to the inhibition seen at 30 μM however HCV RNA levels were reduced at non-toxic concentrations.

4.3 Cerulenin treatment of HCV genotype 2a replicon expressing cells

4.3.1 Cerulenin inhibition of fatty acid biosynthesis appears to correlate with inhibition of HCV replication

In order to ascertain whether the effects seen with the 1b and 1b-C cell line was a response to either the HCV genotype or cell line used, experiments were repeated using an HuH-7 cell line expressing the JFH1 genotype 2a replicon (2a). A cured derivative had also previously been made (supplied by Paul Targett-Adams) and this was used as a negative control. Experiments were repeated as in section 4.1.1, using cerulenin obtained from Axxora Ltd.

Figure 4.3. The effect of cerulenin treatment obtained from a different supplier on 1b (pink) and 1b-C (blue) expressing cell lines. Assays were performed to measure cellular fatty acid biosynthesis (a) and cellular toxicity (b). HCV RNA replication is shown as a normalised percentage of that of the DMSO control (c) obtained using Northern blot analysis (d) where RNA was resolved in a 1 % formaldehyde gel. RNA extracts were obtained from experiments with 1b cells were treated only with DMSO solvent (lane 1) or treated at 4 concentrations of cerulenin 30 μM , 10 μM , 3 μM and 1 μM (lanes 2, 3, 4 and 5 respectively). DMSO was kept constant at 0.00003 %.



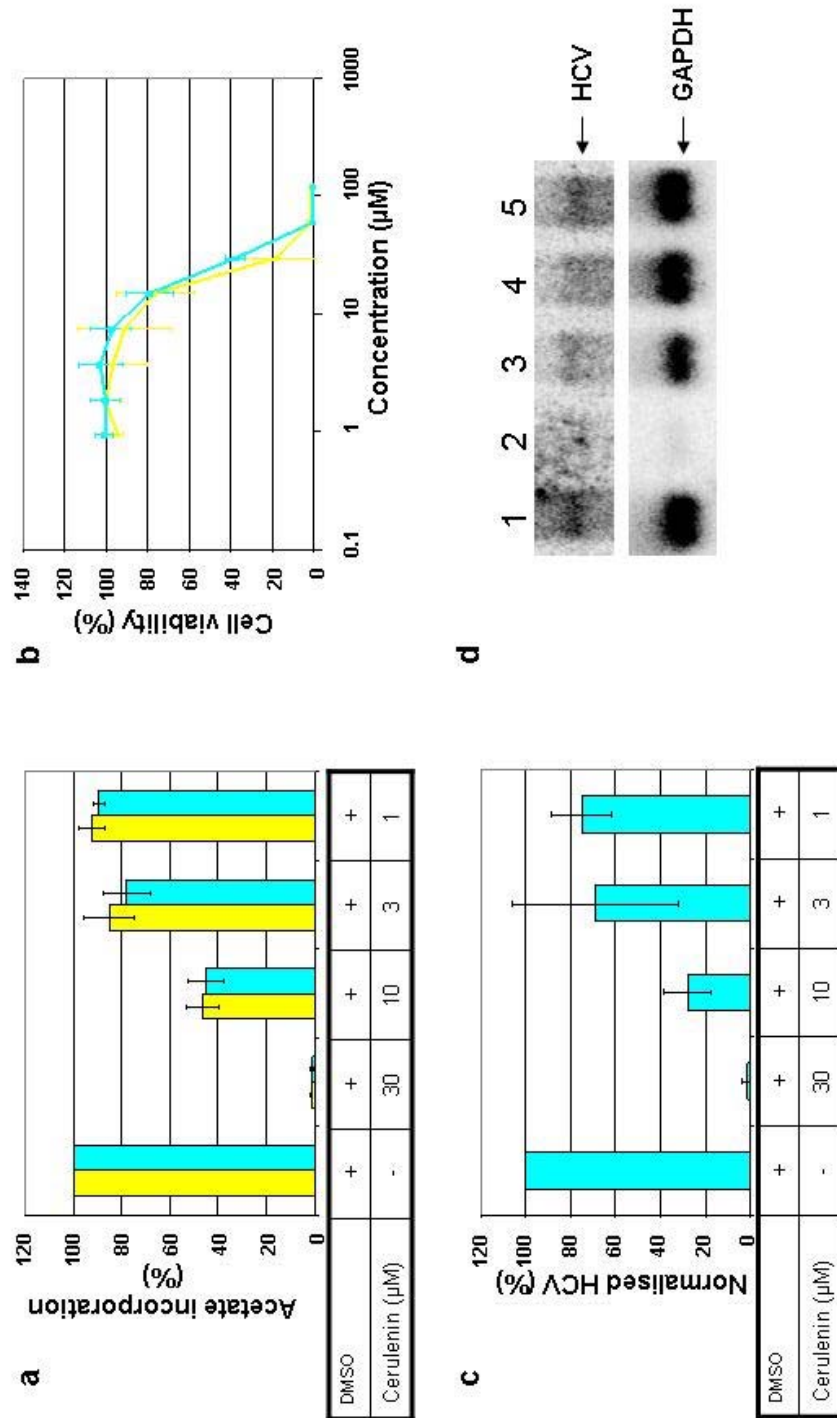
Unexpectedly, Figure 4.4a shows that cerulenin inhibited fatty acid biosynthesis in 2a and 2a-C cells in a dose dependent manner. At 30 μM , fatty acid biosynthesis was less than 5 % of that of the DMSO control. This compared to 10 % in 1b and 1b-C cells. Furthermore, cerulenin inhibited fatty acid biosynthesis at all concentrations. Fatty acid biosynthesis was approximately 45 %, 81 % and 90 % of that of the DMSO control at 10 μM , 3 μM and 1 μM , respectively.

Figure 4.4b shows that toxicity of cerulenin on 2a and 2a-C cells was slightly greater than that with 1b and 1b-C cells. A TD_{50} was found at 22-28 μM cerulenin and the upper concentration of 30 μM had a cell viability of only 18 - 38 % of that of the DMSO control. There appeared some variation between results obtained from 2a and 2a-C cells which were reflected in the standard deviations within 2a-C results. This could be explained by one 2a-C toxicity result, which behaved slightly different from the others. This led to an increased difference between 2a and 2a-C toxicity curves and greater variation, which was echoed in the standard deviations within the 2a-C curve itself. If this toxicity value was omitted then the 2a-C cells follow a similar pattern to the 2a cells.

Inhibition of HCV replicon RNA levels was found at all concentrations of cerulenin used (Figure 4.4c & d). Furthermore, HCV RNA levels were less than 2 % of that of the DMSO control at the upper concentration of 30 μM . However as discussed, at this concentration cerulenin was toxic which may contribute to its effect on HCV RNA levels. At 10 μM , cell viability was approximately 90 % of that of the DMSO control and fatty acid biosynthesis and HCV RNA levels were both less than 50 %. However, there was a large amount of variation seen in HCV RNA levels at 3 μM , which could be explained by a single experiment which varied from the other 2 experiments and was reflected in the standard deviation values. Even at 1 μM cerulenin, fatty acid biosynthesis and HCV RNA levels were approximately 90 % and 75 % of that of the DMSO control respectively.

In conclusion, cerulenin acted in distinctly different manner on treatment of 2a and 2a-C cells. Fatty acid biosynthesis was inhibited in a dose dependent fashion at all concentrations as were HCV RNA levels. Although toxicity slightly increased, this did not account for the different response to the drug.

Figure 4.4. The effect of cerulenin treatment on 2a (blue) and 2a-C (yellow) expressing cell lines. Assays were performed to measure cellular fatty acid biosynthesis (a) and cellular toxicity (b). HCV RNA replication is shown as a normalised percentage of that of the DMSO control (c) obtained using Northern blot analysis (d) where RNA was resolved in a 1 % formaldehyde gel. RNA and protein extracts were obtained from experiments with 2a cells were treated only with DMSO solvent (lane 1) or treated at 4 concentrations of cerulenin 30 μM , 10 μM , 3 μM and 1 μM (lanes 2, 3, 4 and 5 respectively). DMSO was kept constant at 0.00003 %.



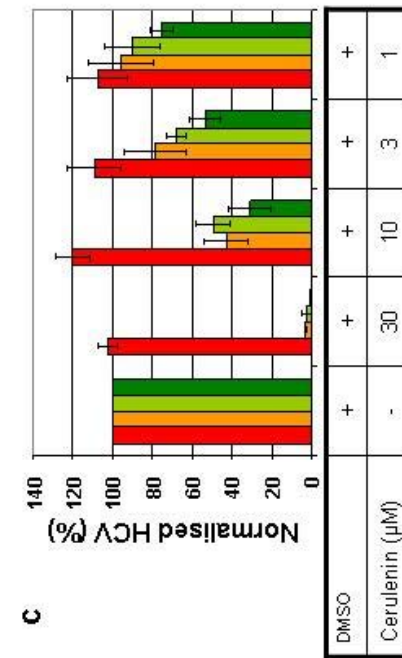
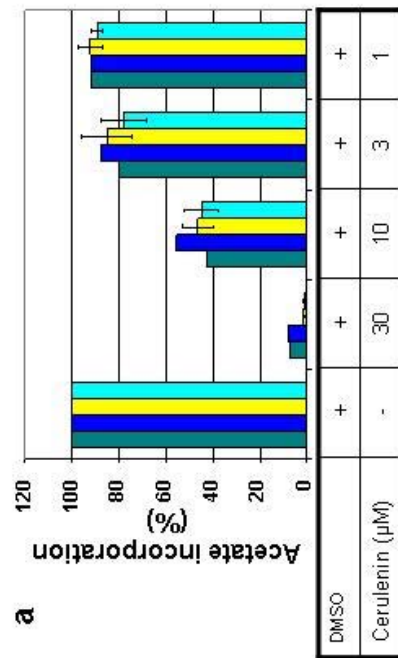
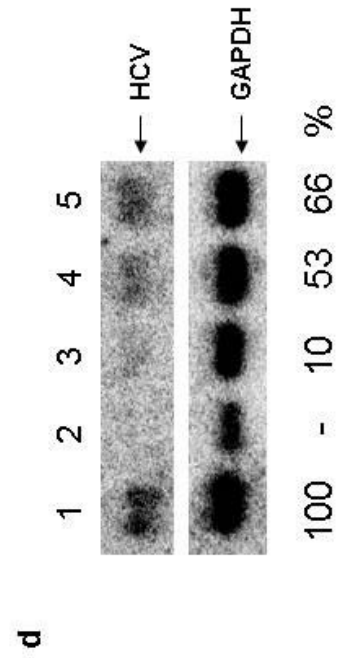
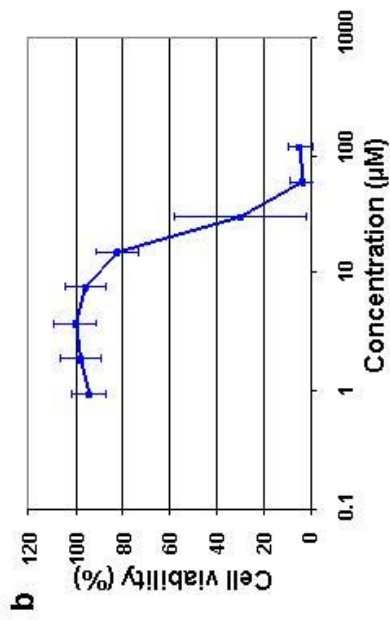
4.3.2 Similar results were shown using cells transiently expressing replicon

To confirm the results found with the cell line constitutively expressing JFH1 genotype 2a, experiments were repeated using the transient JFH1 genotype 2a replicon (Targett-Adams et al., 2005). This replicon was derived from the constitutive replicon but had been modified by the replacement of the neomycin phosphotransferase resistance gene with a firefly luciferase gene. Thus measuring luciferase values would reflect the extent of HCV replication. The experiments were performed as with the constitutive replicon at four concentrations of cerulenin and replication assayed every 24 hrs over 72 hrs. A NS5B “GND” mutant defective in replication was used as a negative control. To confirm that the transiently expressing cells responded in a similar manner to the constitutively expressing cell line, fatty acid biosynthesis was assayed for one of the triplicate experiments. RNA was also extracted from this experiment for Northern blot analysis.

Figure 4.5a shows that cerulenin’s inhibitory effect on FAS was virtually equivalent between HuH-7 cells expressing the transient replicon and HuH-7 cells expressing the constitutive replicon. Fatty acid biosynthesis in cells electroporated with both JFH1 and JFH1 GND luciferase replicon RNAs was inhibited in a dose dependent manner. The results indicated that fatty acid biosynthesis responded in a similar manner between transient and constitutively expressing cell lines.

The toxicity of cerulenin on cells containing the transient JFH1 replicon (Figure 4.5b) was also similar to that found with 2a and 2a-C cells. A TD_{50} at approximately 20 μM was obtained and 30 % at 30 μM . However the standard deviation between experiments is very large at this point in the graph. This could be explained by a single value, which deviated from the others at this concentration. Had this value been omitted the dose response curve would have a TD_{50} at approximately 28 μM . This would suggest that cerulenin was less toxic at this concentration than that seen with the 2a and 2a-C experiments. Had this been the case, this might have answered why at the upper concentration of 30 μM , cerulenin was slightly less effective at inhibiting fatty acid biosynthesis

Figure 4.5. The effect of cerulenin on a transient JFH1 (dark green) and JFH1 GND (dark blue) expressing replicon. Assays were performed to measure cellular fatty acid biosynthesis (a) and cellular toxicity (b). The fatty acid biosynthesis assay (a) also shows 2a (light blue) and 2a-C (yellow) results for comparison. HCV RNA replication was measured luciferase activity (c) and Northern blot analysis (d) where RNA was resolved in a 1 % formaldehyde gel. Luciferase activity (c) of transient replicons was assayed for untreated, DMSO treated and at 4 concentrations of cerulenin 30 μM , 10 μM , 3 μM and 1 μM . DMSO was kept constant at 0.00003 %. Luciferase assays were performed at 4 time points 4 hrs (orange), 24 hrs (yellow), 48 hrs (light green) and 72 hrs (dark green). RNA extracts obtained at the 72 hrs time point for the above conditions were resolved on a 1 % formaldehyde gel and analysed by Northern blot.



when treating transient replicon expressing cells. At 10 μM , 3 μM and 1 μM cerulenin was non toxic to the cells.

Figure 4.5c shows that over a 3 day period, all concentrations of cerulenin were able to reduce replication of the transient 2a replicon expressing cells. Even after 20 hrs of cerulenin treatment, a dramatic inhibition of HCV replication was found at 30 μM . However, this concentration was toxic at 72 hrs indicating that effects seen at all time points at this concentration might merely be a consequence of toxic effects on the cell. At 72 hrs HCV replication was 31 %, 53 % and 76 % of that of the DMSO control at 10 μM , 3 μM and 1 μM , respectively. These replication levels were similar to those results found with the 2a and 2a-C results. Figure 4.5d shows that replicon RNA levels behaved in a similar manner to luciferase values with HCV RNA levels at 10 %, 53 % and 66 % of that of the DMSO control at 10 μM , 3 μM and 1 μM .

Figure 4.6 shows that absolute luciferase values in untreated and DMSO controlled JFH1 replication increased initially over the first 48 hrs till it levelled off at the 72 hrs period. The graph shows an initial burst of luciferase activity at the 4 hr time point in both JFH1 and JFH1 GND replicons. This was considered to be expression of electroporated RNA. The signal then increased for the replication competent JFH1 and gradually decreased for the replication deficient JFH1 GND replicon. The graph shows there was a dose dependant decrease in cerulenin treated JFH1 replication. Cerulenin treatment most noticeably reduced absolute luciferase values at 30 μM . However, at this concentration cerulenin was toxic. At 10 μM there was almost a one log drop in luciferase actual values.

A reduction in luciferase activity might have been caused by a direct inhibitory effect of cerulenin on luciferase rather than inhibition of replicon RNA. To confirm that the effect seen was due to an inhibition of replicon, Northern blots were used to visualise replicon RNA.

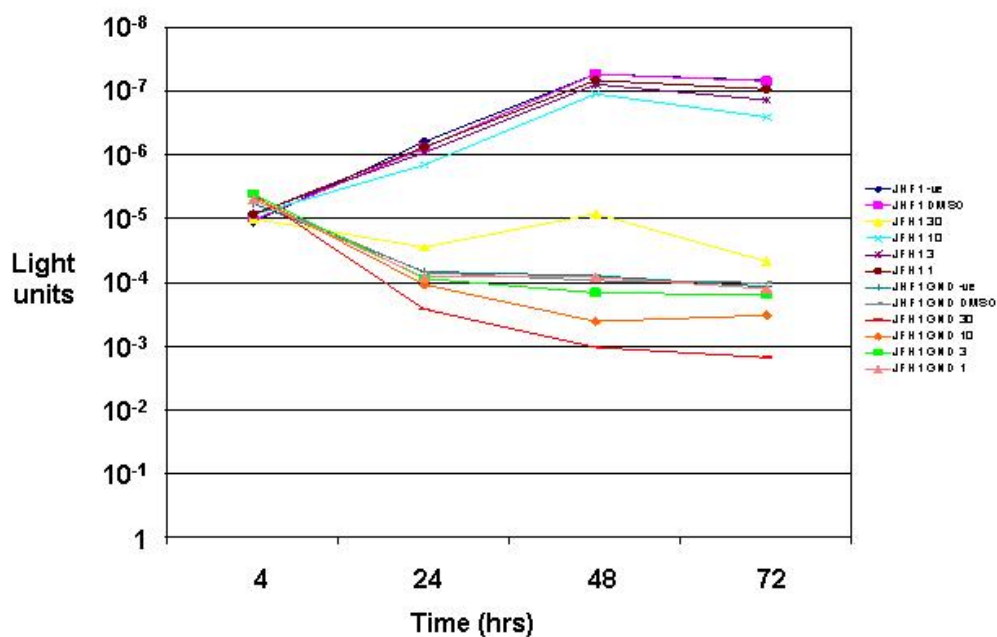


Figure 4.6. The effect of cerulenin on a transient JFH1 and JFH1 GND expressing replicon over a 72hrs period. 0.25×10^{-6} HuH-7 cells were electroporated with 1 μ g RNA. Luciferase assays were performed at 4 hrs, 24 hrs, 48 hrs and 72 hrs. Cerulenin was incubated with cells after the 4 hrs period and medium was changed daily. Cerulenin was treated at 30 μ M, 10 μ M, 3 μ M and 1 μ M.

4.4 Tandem treatment of 2 different HCV 1b replicon expressing cells was cell and not HCV type specific

Treatment of JFH1 2a constitutive and transient replicon expressing cells with cerulenin inhibited both fatty acid biosynthesis and HCV replication. Although cerulenin was toxic at the upper concentration of 30 μM , inhibition was also seen at lower concentrations. This inhibitory effect of cerulenin on fatty acid biosynthesis had not been found using the previous 1b and 1b-C cell lines. The reason cerulenin inhibition of FAS did not lead to a reduction in fatty acid biosynthesis in 1b and 1b-C cells was not clear. It was likely that cell-type specific differences were the source of the variation in responses. For example, 1b expressing cells may have an altered cellular environment, becoming resistant to the action of the drug. This resistant cellular environment may then be maintained in cured cells. All HuH-7 cells containing genotype 2a constitutive and transient replicons were derived from the same initial HuH-7 source (cells originally from J.Dubuisson, University of Lille) and had a similar passage history. In contrast 1b and 1b-C cells were derived from the 5-15 genotype 1b expressing cell line (Lohmann et al., 1999). HuH-7 cells containing and "cured" of the 1b replicon had an unknown passage history and had been obtained from a different source (cells originally from R. Bartenschlager, University of Heidelberg).

In order to clarify whether responses seen on cerulenin treatment of the 1b and 1b-C cells were due to the different sources of HuH-7 cells and not a consequence of HCV genotype, another line expressing the 1b replicon was used. This contained the 5.1 genotype 1b subgenomic replicon transfected into HuH-7 cells that originated from the University of Lille (supplied by S.Gretton). The 5.1 subgenomic replicon was originally derived from the 5-15 subgenomic replicon but it had several different adaptive mutations (Krieger et al., 2001). Tandem fatty acid biosynthesis assays were performed on cells treated with various concentrations of cerulenin. The cell lines tested were 1b, 1b-C, 2a, 2a-C and the 5.1 1b cell line. Unfortunately no 5.1 cured cells were available. However, previous experiments had shown that cured cells behaved as replicon cells on cerulenin treatment. Figure 4.7 shows that the 5.1 1b cell line behaved in a similar manner to the 2a and 2a-C cells in its response to cerulenin treatment. Fatty acid biosynthesis was inhibited in a dose-dependent

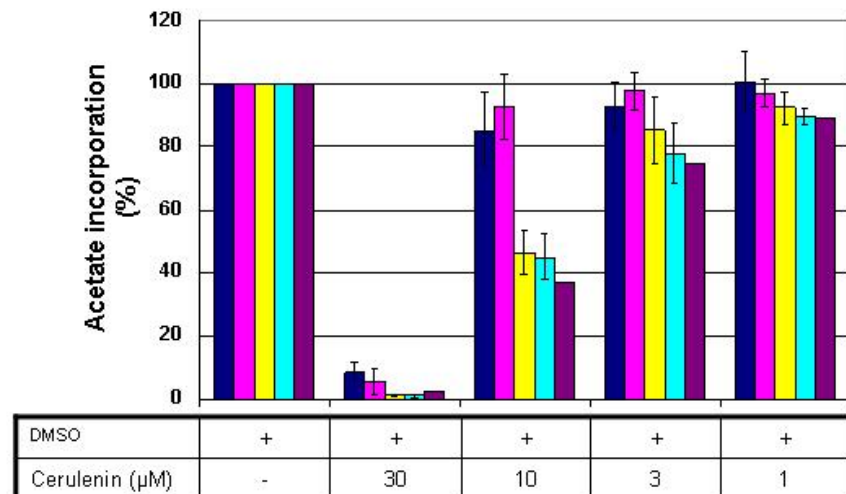


Figure 4.7. The effect of cerulenin treatment on another 1b expressing cell, the 5.1 cell line. A fatty acid biosynthesis assay was performed to measure the effect of cerulenin treatment on fatty acid production. Cells were treated in the presence and absence of cerulenin and DMSO. Cerulenin was supplied to cells dissolved in DMSO at 30 μM , 10 μM , 3 μM and 1 μM . 1b (pink), 1b-C (dark blue), 2a (yellow), 2a-C (light blue) and 5.1 1b (purple) cells were treated for 3 days in test medium. Medium was changed daily.

manner at all concentrations. At 30 μM , 10 μM , 3 μM and 1 μM cerulenin, the effect seen between the 5.1 cells and the 2a and 2a-C was equivalent. However, there remained distinct differences in FAS response to cerulenin between these cell lines derived from the same University of Lille HuH-7 stock and the 1b and 1b-C cells, which were derived from a different HuH-7 stock.

4.5 NS5A localisation in cerulenin treated cells

The above experiments identified a stock of HuH-7 cells, containing the 5-15 1b replicon, that behaved differently in their response to cerulenin compared to HuH-7 cells from a different source. Initial attempts had failed to reveal a strong correlation between inhibitory effects of cerulenin on fatty acid biosynthesis and HCV replication. It has been shown that cerulenin treatment of MCF-7 human breast cancer cells can deplete phospholipids from membranes (Zhou et al., 2003). Although in this case it was suggested as a possible apoptotic mechanism, it could also have consequences on viral replication in HuH-7 cells. The significance of membranes to the HCV life cycle has been demonstrated where viral proteins can cause morphological changes to the ER membrane forming a “membranous web” (Egger et al., 2002). Our hypothesis was that changes in membrane constituents by FAS inhibition may change ER morphology and viral protein localisation. HCV NS proteins are normally found to associate with one another on the ER membrane forming replication complexes.

NS5A is found both as punctuate sites on the ER membrane and on lipid droplets. By staining for NS5A it was possible to observe small punctate spots that had an ER localisation. These are thought to be sites where viral NS proteins associate to form replication complexes. In order to determine whether cerulenin treatment of cells affected localisation of the NS5A protein, immunofluorescence was performed on constitutively expressing 2a cells. Cells were treated at 10 μM and 3 μM concentrations of cerulenin. To confirm whether NS5A was present on ER or on lipid droplets, 2a cells were probed with antibodies to NS5A and calnexin, an ER marker or NS5A and ADRP, a lipid droplet marker (Figure 4.8).

Figure 4.8. The effect of cerulenin treatment for 3 days on NS5A localisation in 2a cells using immunofluorescence. DMSO treated cells are shown in panels (a), (b), (e), (f), (i) and (j). Cerulenin treated cells are shown in panels (c), (d), (g), (h), (k) and (l). NS5A was detected using polyclonal NS5A sheep anti-serum (Macdonald et al., 2003). Mouse anti-calnexin was used to detect ER and rabbit anti-ADRP was used to detect lipid droplets. DAPI was used to stain the nucleus. Cells in panels (a), (c), (i) and (k) were probed with anti-ADRP and those in (b), (d), (j) and (l) were probed with anti-calnexin. Cells in panels (e - h) were probed with anti-NS5A. Panels (i), (j), (k) and (l) show the merged images. Areas of colocalisation were seen as yellow areas.

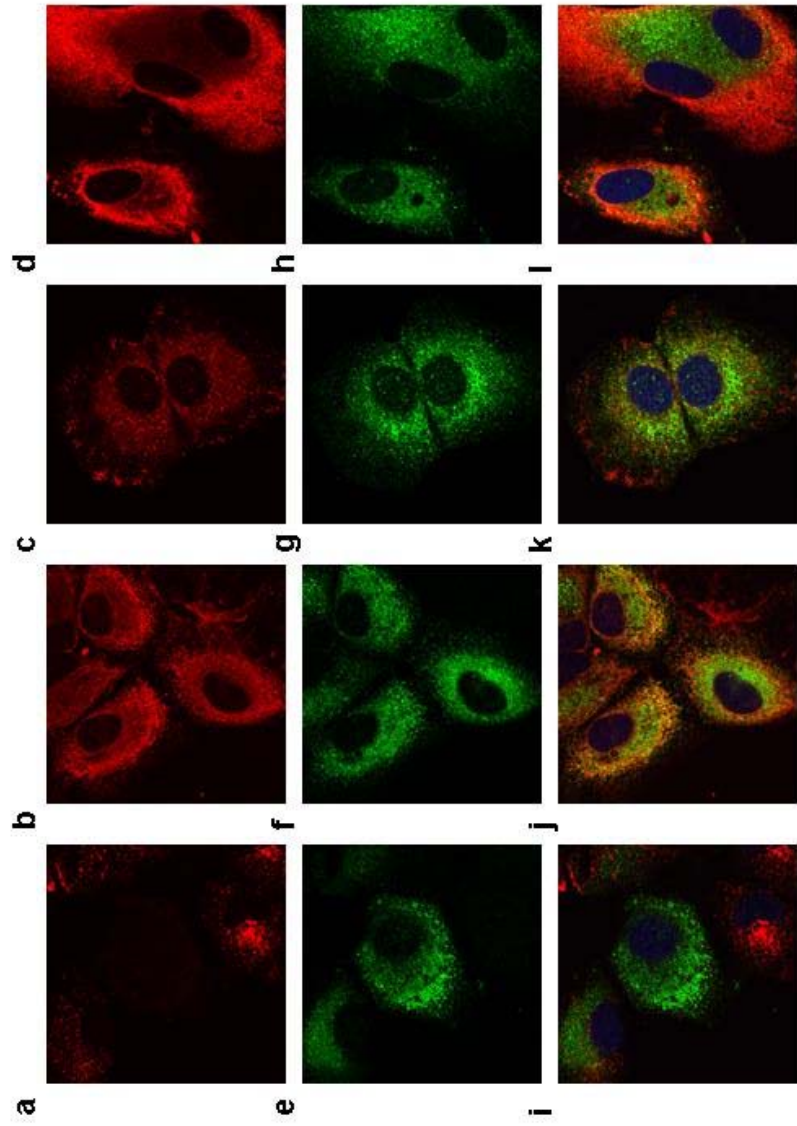


Figure 4.8 shows DMSO and cerulenin (10 μM) treated cells. NS5A maintained an ER pattern of staining in cells treated with DMSO alone or with DMSO and cerulenin. There was no movement of NS5A to lipid droplets or any noticeable morphological changes to the cells. Interestingly cells, which contained high expression of the replicon tended not to contain many lipid droplets. The reason for this could not be explained but was found consistently in other experiments. Treatment of replicon cells with cerulenin led to a more diffuse staining of ADRP rather than its normal discrete lipid droplet punctuate staining. DMSO-treated replicon cells displayed an ER staining with some colocalisation with calnexin. There were no obvious differences between replicon cells treated with DMSO or cerulenin.

4.6 Discussion

Initially experiments were performed to try and establish a correlation between the inhibition of FAS by cerulenin and the reduction in HCV replicon RNA levels. In other studies cerulenin treatment of replicon cell lines had an inhibitory effect on replicon RNA levels (Su et al., 2002). In the study by Su et al. (2002) replicon cells were treated at an upper concentration of 44.8 μM cerulenin. In my experiment dose response (Figure 4.1b) curve of cerulenin's toxicity showed this concentration resulted in a cell viability of only 20 % of that of the DMSO control. This was possibly because the medium was changed daily to minimise compound degradation in our study. Also, in the former study, data was shown only at the 8 hrs period for 44.8 μM cerulenin. There was no result displayed at their second time point of 18 hrs. The reason for this was never explained.

In our study results showed a similar inhibitory effect of cerulenin on HCV RNA levels compared to the study by Su et al. (2002). These inhibitory effects are comparable to those seen in the original study where HCV RNA was 52 % and 69 % of that of the DMSO control at 22.4 μM and 4.5 μM respectively. However, fatty acid biosynthesis was not effectively inhibited by cerulenin. The results had indicated that the effect on fatty acid biosynthesis may have been due to its toxic effects. Why these cell lines were resistant was unclear.

The luciferase results showed a dose dependent decrease in HCV RNA levels at all concentrations of cerulenin. Also these results showed the gradual decrease

in HCV RNA levels over the 3 days at all concentration of cerulenin. At the lowest concentration of 1 μM , fatty acid biosynthesis is inhibited minimally however there is a progressive decline in the levels of HCV RNA over 72 hrs. Therefore, extending the length of treatment of cell expressing the constitutive replicon to a week period or more may improve cerulenin's inhibitory effects.

Assessing the contribution of toxicity to effects seen on the replicon is difficult. Ideally a therapeutic index should be calculated as the ratio between toxicity and the effect seen. To calculate this, a TD_{50} (concentration at which 50 % growth inhibition occurs) value would be compared to the effective concentration or EC_{50} (concentration at which 50 % effect occurs). For particularly toxic compounds, the ratio would be low. In our study although we were able to estimate EC_{50} the accuracy was reduced because we only had a small number of points on our graph in which to extrapolate a curve. Ideally to draw dose response curves it is better to have a range of concentrations as this allows fewer margins for error when drawing the curve. In our study there were two separate therapeutic indices that we were looking at. These were: the therapeutic index for the effect of cerulenin on HCV RNA levels and the therapeutic index for the effect of cerulenin on fatty acid biosynthesis. The therapeutic indices obtained for 1b and 1b-C cells treated with cerulenin obtained from Sigma was low for both effects on fatty acid biosynthesis and HCV replication. This indicated that the toxic effects of the drug may contribute to a large proportion of the effects observed. 1b and 1b-C cells treated with cerulenin obtained from Axxora Ltd still had low therapeutic ratios but were slightly greater than those obtained for cerulenin from Sigma. The therapeutic indices for effects on HCV replication for the constitutive and transient 2a replicons were approximately 3:1 and 7:1 respectively. These were better than those seen with the 1b and 1b-C cells. However the effects on fatty acid biosynthesis again produced low ratios. This might indicate that fatty acid biosynthesis could not be inhibited with cerulenin without a consequence on cell viability. Effects on replicon RNA seen at concentrations that were toxic were not considered as reliable indicators that the drug was acting on HCV RNA levels by a non-toxic mechanism. Therefore, I conclude that in 1b and 1b-C expressing cells, cerulenin was unable to inhibit fatty acid biosynthesis effectively without an effect on cell viability.

Inhibition of the replicon might have been caused by an action of cerulenin other than its effect on fatty acid biosynthesis. A number of non-specific effects have also been attributed to cerulenin. Cerulenin has been shown to prevent acylation of vesicular stomatitis virus glycoproteins proteins (Schlesinger et al., 1982). Furthermore, cerulenin has been shown to bind β -keto-acyl-ACP synthase thereby directly inhibiting the enzyme involved in acylation. Whether cerulenin's inhibitory effects on HCV RNA levels were due to this other function of cerulenin was not clear. Previous studies would indicate that inhibition of fatty acid biosynthesis was an important factor in reducing HCV replication. This particularly was highlighted by the use of another inhibitor, TOFA, which inhibits Acetyl CoA Carboxylase (Figure 4.9). TOFA also led to a decrease in HCV RNA levels in these studies (Kapadia et al., 2005). Furthermore we had also performed preliminary studies on 1b and 1b-C cells using another FAS inhibitor, C75, which gave similar results to those obtained with cerulenin (data not shown). C75 is structurally very similar to cerulenin but is reported to be more specific. These preliminary studies showed that C75 was able to inhibit HCV RNA and fatty acid biosynthesis however toxicity of the drug is also a problem. These findings indicated that in 1b and 1b-C cells, inhibition of fatty acid biosynthesis was not an absolute requirement for inhibition of HCV replicon replication by cerulenin and some other inhibitory mechanism was acting on HCV replicon RNA levels.

Cerulenin treatment of tumour cell lines can induce apoptosis (Kuhajda F, 2006). Many studies in cancer research have highlighted the high expression of FAS to be associated with aggressive cancers and in some cases a possible target for therapies. FAS has been attributed as being important in cancers such as breast cancers (Kuhajda F, 2006) and prostate cancers (Bandyopadhyay et al., 2005). Treatment with FAS inhibitors (Kuhajda et al., 1994) and FAS RNAi's (Bandyopadhyay et al., 2005) can induce apoptosis in tumour cells. Previous studies had indicated that, rather than apoptosis being the result of fatty acid starvation, it was caused by the build up of malonyl CoA (Pizer et al., 2000). In our study, to investigate whether the reduction in cell viability, fatty acid biosynthesis and HCV RNA levels was due apoptotic effects of cerulenin,

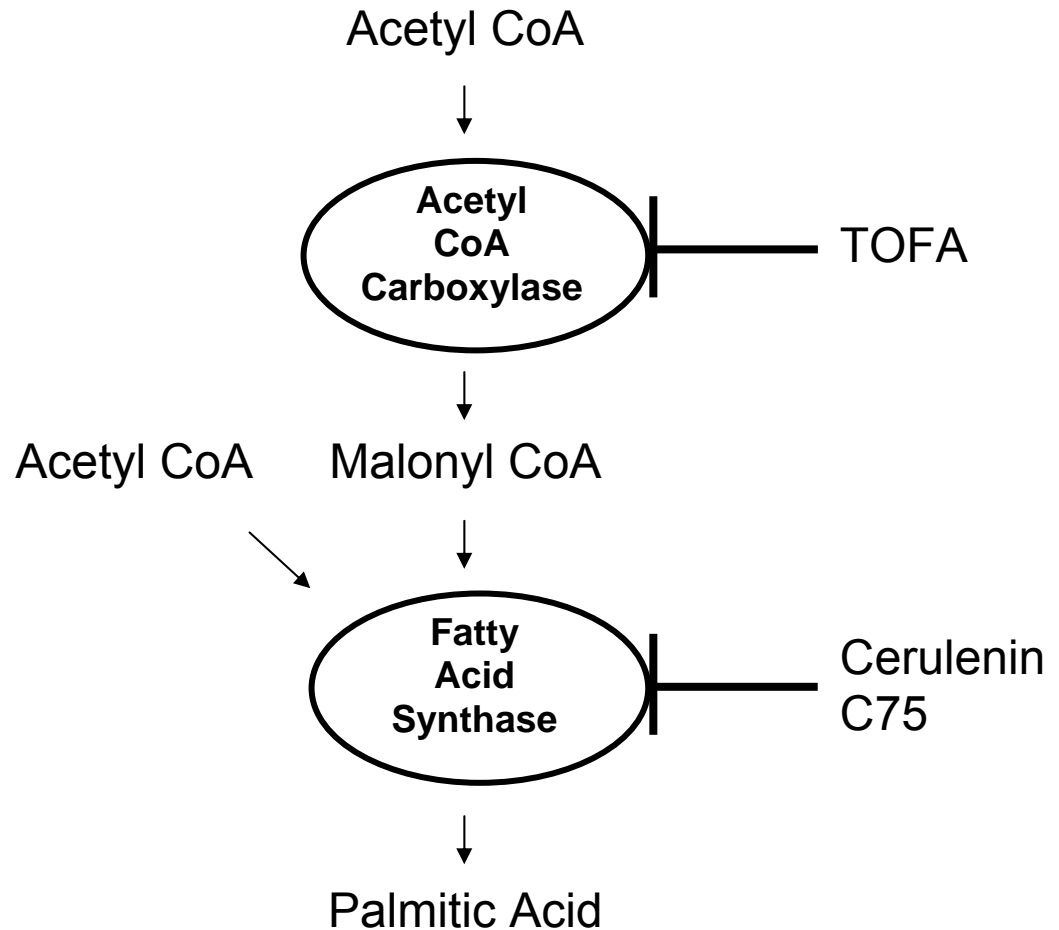


Figure 4.9. A diagrammatic representation of the fatty acid biosynthesis pathway. Initially acetyl CoA is converted to malonyl CoA by the rate limiting enzyme Acetyl CoA Carboxylase. Acetyl CoA is used to prime the fatty acid chain where sequentially elongated using malonyl CoA as a substrate is performed by the enzyme, fatty acid synthase. The end product is a 16 carbon fatty acid, palmitic acid, which can be elongated and desaturated to form other fatty acids. Inhibitors of the enzymes are shown to the right and the diagram.

experiments could be repeated with TOFA (Figure 4.9). As mentioned, TOFA inhibits Acetyl CoA Carboxylase the enzyme prior to FAS which prevents malonyl CoA accumulation and therefore does not induce the same toxic effect that cerulenin does.

The study highlighted the slight differences in the reaction of cells to cerulenin obtained from different suppliers. There appeared no differences in chemical properties between cerulenin obtained from different suppliers apart from the purity promised which were $\geq 98\%$ purity and $\geq 95\%$ purity from Axxora Ltd and Sigma-Aldrich respectively. It was possible that a small amount of impurity in the stock was able to subtly alter cells reactions to the drug. However, the exact reason for the differences in response to cerulenin obtained from different suppliers was unclear.

Cells with different passage history from the same original identified cell line may act distinctly differently to one another. Here, differences were found with HuH-7 cells, which had come from different laboratories. University of Lille HuH-7 cells behaved differently in their response to cerulenin than HuH-7 cells that had originated from a stock in Germany (Lohmann et al., 1999). Whether the variations between these two HuH-7 cell lines was due to differences in HuH-7 cells between laboratories or due to a change after transport to our laboratory is not clear. It was possible that differences had occurred because the 1b and 1b-C cells were of a high passage number when experiments had been performed. Originally establishment of replicon cell lines had found passage number to be critical for successful transfection (Lohmann et al., 1999). A passage number of 128 increased the permissiveness of the HuH-7 cells to HCV replicon replication compared to cells of different passage numbers. HuH-7 cells contain a constantly changing cellular environment, which can be heterogeneous between cells from different passage numbers or histories. Also the enrichment process for highly expressing cells might have caused a selective pressure on a cell clone, which had resulted in resistance to cerulenin's effects. HuH-7 cells obtained from different sources will also have been grown in different culture conditions. Small variations in suppliers medium, serum and additives could have an effect on cell growth and heterogeneity. To answer these questions experiments should be repeated including HuH-7 cells obtained from the 1b and

1b-C cells original source in Heidelberg and also the original 5-15 cells that had been received before enrichment for high expression.

Although in our study it was difficult to show a direct association between the reduction of HCV RNA and the inhibition of fatty acid biosynthesis, the study by Su et al (2002) had suggested fatty acid biosynthesis to be important for HCV replication. Had only 2a and 2a-C cells been treated, then an association might have appeared more likely. However, the work with the 1b and 1b-C cells indicated that cerulenin inhibited by mechanisms other than that of inhibition of fatty acid biosynthesis. It may have been that this was a cell type specific difference and the mechanisms of cerulenin mediated HCV inhibition were different between the two HuH-7 stocks. However, this does highlight the importance of confirming the action of a drug that is being tested. It would be possible to assess the importance of fatty acid biosynthesis in both these systems by supplementing cells with exogenous palmitic acid. Palmitic acid is the final product of FAS, which is then modified for incorporation into complex lipids (Figure 4.9). By supplying cells with palmitic acid it would be possible to rescue cells from the cerulenin induced fatty acid blockade. If the end product of FAS is an important factor for HCV replication, the addition of exogenous palmitic acid should rescue HCV inhibition. TOFA also could be used as an alternate method of assessing the importance of fatty acid biosynthesis for HCV replication. Unlike cerulenin and C75, TOFA is not reported to have any non-specific effects and does not induce the same cytotoxicity, so may prove as a more reliable compound to use.

In conclusion, the 1b and 1b-C cell line were resistant to the inhibitory effects of cerulenin on fatty acid biosynthesis. The contribution to the reduction of HCV RNA levels by the inhibition of fatty acid biosynthesis could not be correlated directly. Although work with University of Lille HuH-7 derived cell lines indicated that there may be some association, further work is necessary in order to confirm this. However, our study highlights the potential for different responses to drugs by clonal cell lines with different histories. Here, all cell lines were derived from HuH-7 cells but their passage history and source have been different. If this phenomenon had not been identified, differences in behaviour of replicons might erroneously have been attributed to genotype differences.

Chapter 5

5 The effect of fatty acids on the replication of the JFH1 HCV replicon

5.1 Introduction

The role of fatty acids in the control of HCV replication was recently demonstrated using an HCV subgenomic replicon (Kapadia et al., 2005; Leu et al., 2004). It was found that different fatty acids influenced HCV replication differently dependent on their degree of saturation (Leu et al., 2004). Treatment of replicon-expressing cells with monounsaturated and saturated fatty acids caused a small increase in HCV replicon RNA levels. In contrast, polyunsaturated fatty acids (PUFAs) reduced HCV replication. However, the less unsaturated a fatty acid was, the smaller the inhibitory effect on HCV RNA levels. Leu et al (2004) went further and showed that the PUFA, arachidonic acid (AA), acted synergistically with IFN- α in reducing HCV RNA replication. The combined effects of AA and IFN- α were greater than the sum of their individual effects. Both these studies failed to identify a mechanism for the inhibition by PUFAs of HCV replication (Kapadia et al, 2005; Leu et al., 2004).

Polyunsaturated fatty acids have long been appreciated as being able to regulate lipid metabolism. They activate long chain fatty acid β -oxidation by acting as ligands for the PPAR family of transcription factors, which control enzymes involved in fatty acid oxidation and storage (Smith S, 2002). They can also down-regulate fatty acid biosynthesis by antagonising liver X receptor (LXR). LXR is a transcription factor, which dimerises with sterol regulatory element binding

protein (SREBP) and together they transactivate lipogenic gene expression (Horton J, 2002). Interestingly, the same PUFAs, which had been shown to act as anti-lipogenic agents, were able to inhibit HCV replication as discussed above. The differing effects of fatty acids on HCV replication, depending on their saturation was also shown in a study by Kapadia et al. (2005). The only differences between the studies of Leu et al and Kapadia et al was that the latter did not investigate the effects of the unsaturated fatty acids γ -linolenic and linoleic acid or the saturated fatty acid, stearic acid on HCV replicon replication and different concentrations of fatty acids were used. Both studies came to similar conclusions that PUFAs acted as inhibitors of HCV replication and that saturated fatty acids induced replication. Previously, cerulenin and TOFA (an inhibitor of acetyl CoA carboxylase), inhibitors of fatty acid biosynthesis, had been used to reduce HCV replicon RNA levels in a dose dependent manner (Kapadia et al., 2005; Su et al., 2002). It had also been shown that treatment of replicon-expressing cells with nystatin, an inducer of fatty acid biosynthesis, led to an increase in replicon RNA levels (Su et al., 2002). It was therefore possible that the mechanism behind control of HCV replication by exogenously supplied fatty acid was mediated by their ability to downregulate fatty acid biosynthesis. However, inhibition of HCV replication by PUFAs was shown to act by a mechanism that was independent of the LXR-SREBP-1c pathway (Kapadia et al., 2005). Replicon-expressing cells were treated in combination with an agonist of LXR and 3 different PUFAs (Arachidonic acid, EPA and DHA). RNA levels were measured using RT-PCR for HCV replicon, SREBP-1c and fatty acid synthase (FAS). LXR induction by the agonist caused an upregulation of mRNA expression for the fatty acid biosynthetic genes, SREBP-1c and FAS. There was also a slight increase in HCV RNA levels. However, PUFA treatment resulted in a reduction in HCV RNA, SREBP-1c and FAS mRNA levels. Combination treatment, with both agonist and PUFA, rescued cells from inhibition of fatty acid biosynthesis however HCV RNA levels did not recover. This suggested that the mechanism of HCV inhibition by PUFAs was independent of their inhibitory effect on the fatty acid biosynthetic pathway.

PUFAs have other functions in the cell whereby they are incorporated into phospholipids and alter membrane composition. Membranes of the cell are thought to contain lipid microdomains, e.g. detergent-resistant membranes (Ma et al., 2004; Stulnig et al., 2001). Cholesterol and saturated fatty acids act as

stabilising influences on these microdomains and allow the recruitment of cellular membrane bound proteins e.g. the intracellular Src family of protein-tyrosine kinases which are involved in T-cell signalling. Incorporation of PUFAs into membranes causes a disruption of these microdomains and a loss of membrane-bound proteins which can affect cell signalling (Stulnig et al., 2001). The loss of membrane-bound proteins may occur also by PUFA inhibition of the palmitylation of proteins and therefore their association with the membrane.

HCV replication complexes containing newly synthesised HCV RNA have been isolated from detergent resistant membrane fractions of cell extracts in replicon harbouring cells lines (Aizaki et al., 2004; Shi et al., 2003). In these studies, replication complexes containing all the non-structural (NS) proteins co-fractionated with the lipid raft associated intracellular membrane protein, caveolin-2 (Shi et al., 2003). Furthermore, these replication complexes supported active viral replication. It was also shown that in detergent-resistant membranes which contained replication complexes HCV RNA and protein were protected from RNase and protease degradation (Aizaki et al., 2004). These observations are consistent with HCV forming sites in lipid microdomains which form a platform for its replication. A possible mechanism for PUFA inhibition of HCV RNA replication may be their ability to disrupt lipid microdomains by changing the constituents of the lipid bilayer. By destabilising lipid microdomains in the ER membrane, replication complex formation may be prevented.

The ability of PUFAs to reduce tumour cell viability is well recognised. This has been shown in breast cancer cells, pancreatic cancer cells and hepatic cells (Foretz et al., 1999 ; Schley et al, 2005; Tetsuya et al., 2005). The mechanism behind this reduction in cell viability is not known but it may be a combination of induction of apoptotic pathways and reduction in cell proliferation (Schley et al., 2005). Since HCV replicon cell lines are all derived from tumours, it was important to measure cell viability when performing experiments involving treatment with PUFAs.

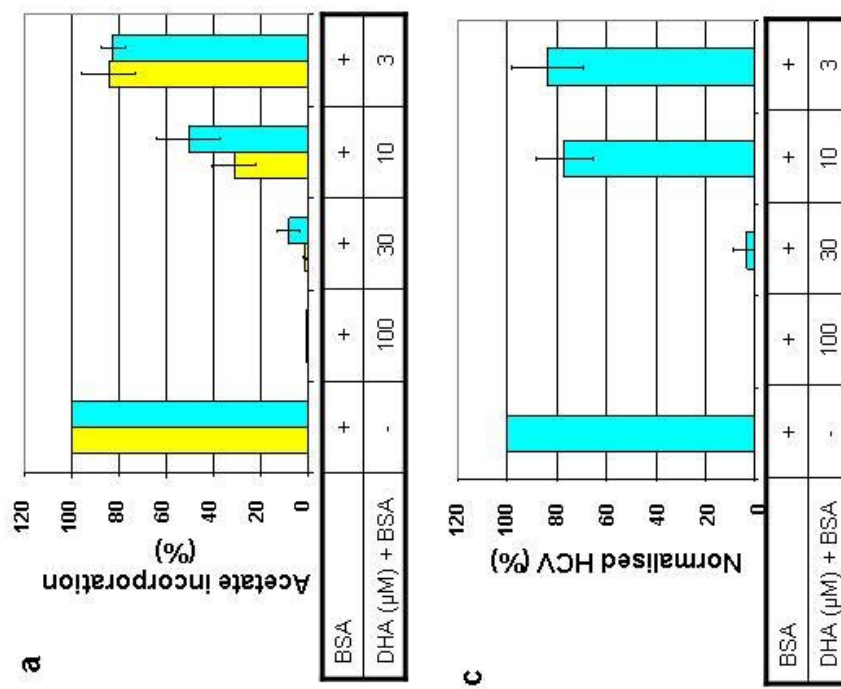
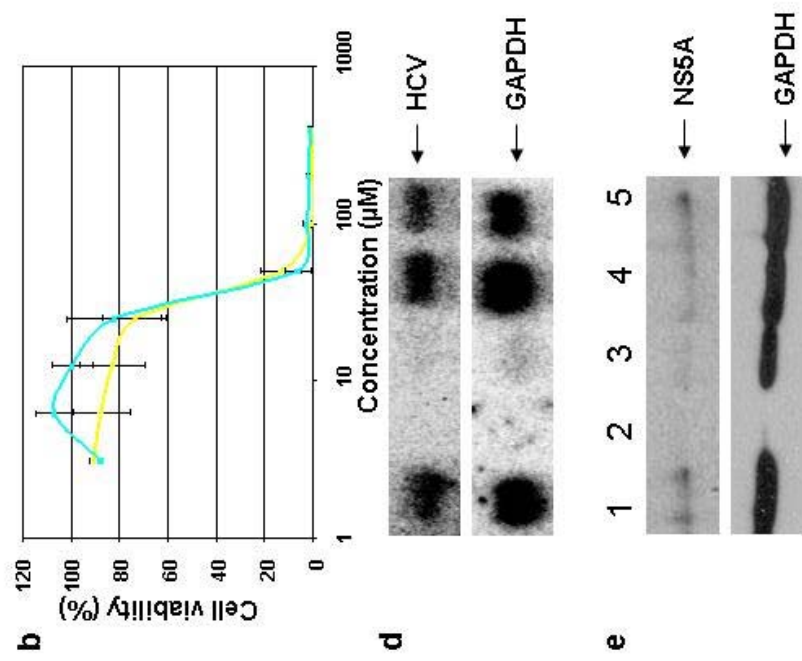
5.2 Docosahexaenoic Acid (DHA) treatment cells expressing genotype 2a replicons

5.2.1 DHA treatment of cells constitutively expressing HCV 2a replicon

DHA is a 22 carbon fatty acid, which contains 6 double bonds between carbon atoms. As previously described, PUFA treatment of replicon-harbouring cell lines led to a reduction in HCV RNA levels. However, previous studies had indicated that the mechanism behind PUFA inhibition was independent of the ability to downregulate fatty acid biosynthetic pathways. Measuring SREBP-1c mRNA is not an adequate method of measuring SREBP-1c activity as SREBP-1c protein expression is controlled pre- and post-transcriptionally (Horton et al., 2002). A more accurate method of ascertaining the effect of PUFAs on fatty acid biosynthesis would be to measure fatty acid production. Our studies extended the original work by measuring fatty acid production and PUFA induced cytotoxic effects. All studies were performed on a JFH1 genotype 2a expressing cell line (2a) and its IFN- α cured derivative (2a-C) as described in section 4.2.1. Cells were grown in medium, which contained 5 % rather than 10 % foetal calf serum (FCS), to minimise the effects of serum fatty acids on experiments. Completely serum free medium could not be used as cells died under these conditions. PUFAs were delivered to the cell lines at four concentrations (100 μ M, 30 μ M, 10 μ M and 3 μ M) conjugated to fatty acid free BSA. PUFAs were conjugated to BSA to minimise the effect of their acidic properties on cells. Fatty acids are transported in blood conjugated to BSA, so this represents a physiological method of delivery to cells. BSA was kept at a constant concentration of 20 μ l/ml in test wells. A "BSA only" control was included. 2a and 2a-C cells were grown for 72 hrs under these experimental conditions. Medium was changed daily to minimise the oxidation of the PUFAs. Assays and extractions were performed at 72 hrs. The results shown are from three experiments.

Figure 5.1a shows that DHA efficiently inhibited fatty acid biosynthesis in a dose-dependent manner. Replicon and cured cells responded similarly. However, at 30 μ M and 10 μ M, fatty acid biosynthesis in replicon cells was slightly less inhibited than that seen in cured cells. In fact, at 10 μ M there was a 20 %

Figure 5.1. Treatment of 2a (light blue) and 2a-C (yellow) expressing cell lines with Docosahexaenoic Acid (DHA); BSA conjugates. Assays were performed to measure cellular fatty acid biosynthesis (a) and cellular toxicity (b). RNA was resolved in a 1 % formaldehyde gel (d). HCV RNA replication was quantified after northern blot analysis (d) and is represented as a percentage of that of the BSA control (c). HCV NS5A protein expression was measured by Western blot analysis (e) where samples were separated on a 10 % polyacrylamide gel. NS5A was detected using the polyclonal NS5A sheep anti-serum (Macdonald et al., 2003). RNA and protein extracts were obtained from experiments with 2a cells that were treated with BSA only (lane 1) or with DHA with 100 μ M, 30 μ M, 10 μ M and 3 μ M (lanes 2, 3, 4 and 5 respectively). BSA was kept constant at 20 μ l/ml.



difference between inhibition of fatty acid biosynthesis in cured and replicon cells. This result was consistent but the reasons for this observation were not known. Nevertheless, at 100 μM and 3 μM , replicon and cured cells behaved similarly in their response to DHA such that fatty acid biosynthesis was approximately 0.8 % and 82 % of that of the BSA control respectively.

The MTT assay (Figure 5.1b) revealed that replicon and cured cell lines behaved in a similar manner in response to treatment with DHA. There was 100 % cell death at the highest concentration of 100 μM and 50 % cell viability (toxic dose 50/ TD_{50}) at approximately 35 μM . This indicated that the effects on fatty acid biosynthesis that were seen at 100 μM were due to cell death. At 50 μM DHA 100 % cell mortality was almost achieved.

HCV replication was inhibited by all concentrations of DHA (Figure 5.1c & d). As previously discussed, effects seen at the upper concentration of 100 μM were caused by cell death which resulted in the complete inhibition of HCV replication. At 30 μM HCV RNA levels were approximately 5 % of that of the BSA control. However, DHA was toxic at this concentration. At the non-toxic concentrations of 10 μM and 3 μM , there was still slight inhibition of HCV replicon replication, approximately 77 % and 84 % of that of the BSA control respectively. At these concentrations there was also inhibition of fatty acid biosynthesis at approximately 40 % and 82 % respectively.

Figure 5.1e shows NS5A expression appears reduced at all concentrations of DHA. However GAPDH levels are virtually undetectable at 100 μM .

5.2.2 DHA treatment of cells transiently expressing HCV 2a replicon

Cells transiently expressing the JFH1 genotype 2a replicon, as previously described in the section 4.2.2., were then treated with DHA. The experiments were repeated, as in section 5.2.1, at four concentrations of DHA and replication was assayed every 24 hrs over 72 hrs. The experiment was repeated 3 times. RNA was extracted and fatty acid biosynthesis assayed for one of the three experiments.

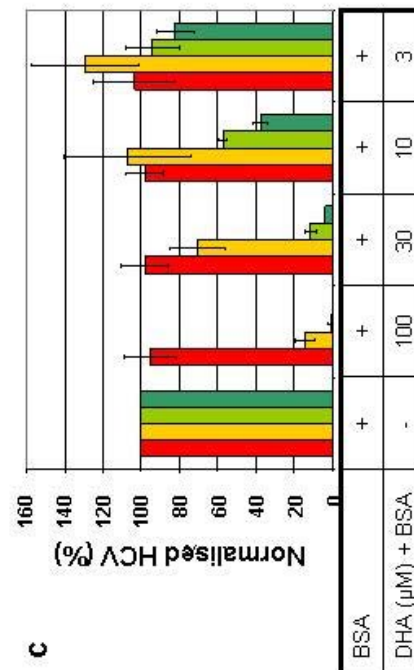
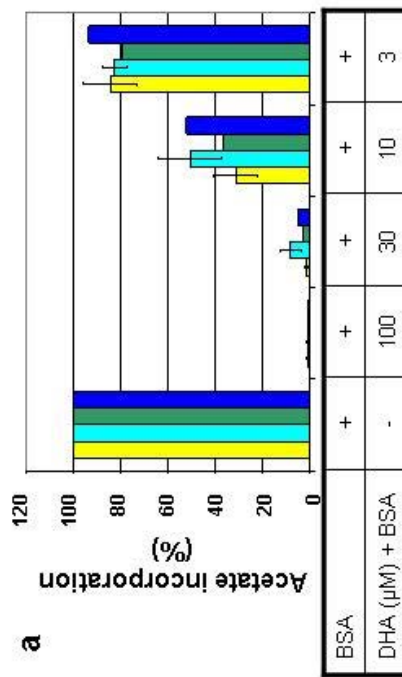
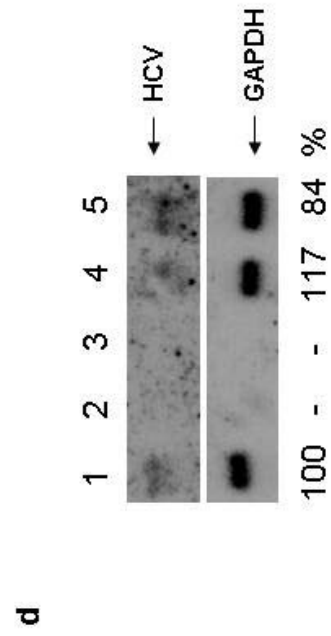
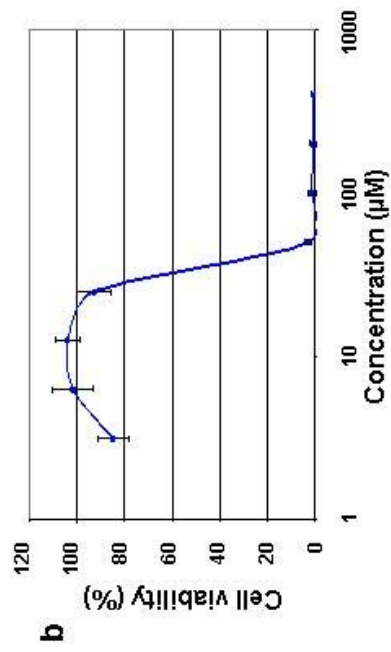
Figure 5.2a shows a comparison of the effects of DHA treatment on fatty acid biosynthesis in cells constitutively or transiently expressing the 2a replicon. Both groups of cells behaved in a similar manner on DHA treatment whether they contained a transient or constitutive replicon. Also the JFH1 transiently expressing replicon cells behaved in a similar fashion to the JFH1 GND, polymerase knock-out replicon. Fatty acid biosynthesis was reduced in a dose-dependent manner at all concentrations.

Viability of cells transiently and constitutively expressing replicon were similar on DHA treatment. DHA was again highly toxic at 100 μM in HuH-7 cells transiently expressing JFH1 replicon (Figure 5.2b). Similarly to the cells constitutively expressing 2a replicon, DHA was almost completely lethal at 50 μM and had a TD_{50} at approximately 35 μM .

Figure 5.2c shows DHA treatment reduced HCV replication at all concentrations in a dose dependant manner. At 72 hrs, replication was 0 %, 4 %, 37 % and 82 % of that of the BSA control at 100 μM , 30 μM , 10 μM and 3 μM respectively. These results were similar to those that were found with the cells expressing the constitutive 2a replicon. However, there was relatively greater inhibition of replication with cells expressing the transient replicon at 10 μM when comparing the two systems. Even so, DHA again reduced HCV replication and this occurred progressively over the 3 days. As previously discussed suppression of HCV RNA replication at 100 μM DHA was attributed to cell death.

Figure 5.2d shows that, as already indicated with the luciferase results, HCV RNA replication measured by northern blot analysis was reduced at 3 μM concentrations used. However, the lack of RNA detected at two top concentrations of DHA was the result of insufficient numbers of cells surviving and at 10 μM there was an increase in replication.

Figure 5.2. The effect of treatment with DHA:BSA conjugates on transient JFH1 and JFH1 "GND" replicons. Assays were performed to measure cellular fatty acid biosynthesis (a) and cellular toxicity (b). The fatty acid biosynthesis assay (a) performed at 72 hrs shows transient JFH1 (dark blue) and JFH1 GND (green) replicons along with constitutive 2a (light blue) and 2a-C (yellow) results for comparison. Cellular toxicity was measured at 72 hrs. HCV RNA replication was assayed using luciferase activity (c) and Northern blot analysis (d) where RNA was obtained at 72 hrs. Luciferase activity (c) of transient replicons was assayed for untreated, BSA treated and 4 concentrations of DHA, 100 μM , 30 μM , 10 μM and 3 μM . BSA was kept constant at 20 $\mu\text{l/ml}$. Luciferase assays were performed at; 4 hrs (orange), 24 hrs (yellow), 48 hrs (light green) and 72 hrs (dark green). RNA extracts were obtained that were treated with BSA only (lane 1) or with DHA with 100 μM , 30 μM , 10 μM and 3 μM (lanes 2, 3, 4 and 5 respectively) was resolved in a 1 % formaldehyde gel.



5.3 Eicosapentaenoic Acid (EPA) treatment of cells expressing genotype 2a replicons

5.3.1 EPA treatment of cells constitutively expressing HCV 2a replicon

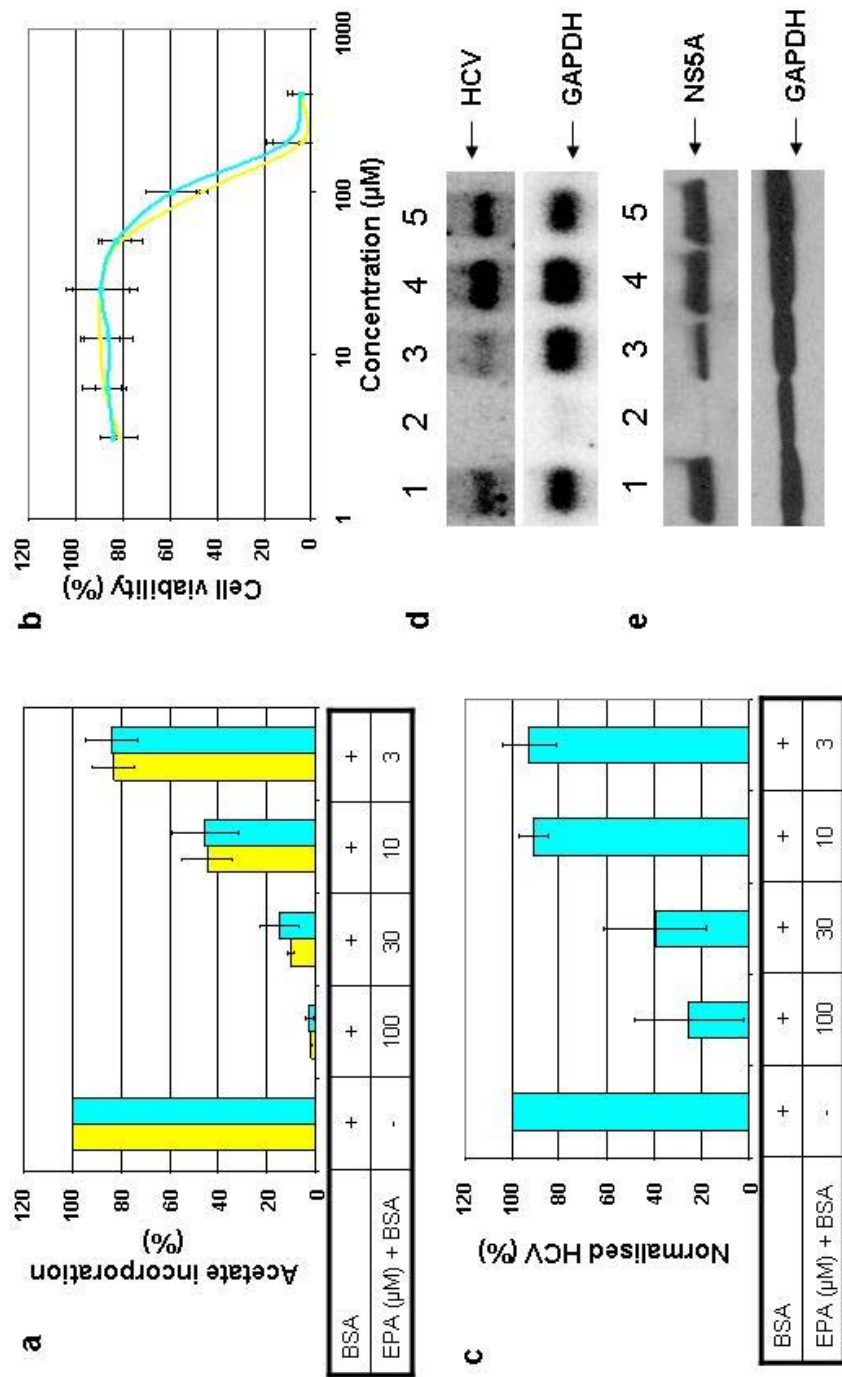
To ascertain whether the effects seen with DHA were unique to DHA or a general effect of PUFAs, experiments were repeated using EPA. Structurally EPA is very similar to DHA. Both are omega 3 PUFAs, which means that they contain their first double bond on the 3rd carbon from the methyl end of the fatty acid. EPA is a 20 carbon fatty acid that contains 5 double bonds. Experiments were performed as in section 5.1.1 in which cells expressing the constitutive HCV genotype 2a replicon were treated at four concentrations of EPA conjugated to BSA. At 72 hrs, RNA and protein were extracted and fatty acid biosynthesis assays and an MTT assay were carried out. Results are shown as an average of three experiments with their corresponding standard deviations.

Figure 5.3a shows that fatty acid biosynthesis was inhibited by EPA treatment in a dose dependent manner. Replicon and cured cells behaved similarly in their response to EPA treatment. Fatty acid biosynthesis was reduced to approximately 2 %, 12 %, 45 % and 85 % of that of the BSA control at 100 μ M, 30 μ M, 10 μ M and 3 μ M. Therefore EPA inhibited fatty acid biosynthesis in a similar manner to DHA.

However EPA was less toxic than DHA (Figure 5.3b). The toxicity assay showed that at the highest concentration of 100 μ M EPA cell viability was reduced to only 50 % of that of the BSA control. Again both replicon and cured cells behaved in a similar manner. Cell viability in response to lower concentrations of EPA of 30 μ M, 10 μ M and 3 μ M was the same as the BSA control. This meant that although toxic effects might account for inhibitory effects at 100 μ M, effects at lower concentrations were likely to be specific to EPA and not due to toxic effects.

Reduction of HCV RNA was found at all concentrations of EPA used (Figure 5.3c & d). EPA treatment reduced HCV RNA levels to approximately 25 %, 35 %, 90 % and 92 % of that of the BSA control at 100 μ M, 30 μ M, 10 μ M and 3 μ M.

Figure 5.3. Treatment of 2a (light blue) and 2a-C (yellow) expressing cell lines with Eicosapentaenoic Acid (EPA): BSA conjugates. Assays were performed to measure cellular fatty acid biosynthesis (a) and cellular toxicity (b). RNA was resolved in a 1 % formaldehyde gel (d). HCV RNA replication was quantified after northern blot analysis (d) and is represented as a percentage of that of the BSA control (c). HCV NS5A protein expression was measured by Western blot analysis (e) where samples were separated on a 10 % polyacrylamide gel. NS5A was detected using the polyclonal NS5A sheep anti-serum (Macdonald et al., 2003). RNA and protein extracts were obtained from experiments with 2a cells that were treated with BSA only (lane 1) or with EPA with 100 μM , 30 μM , 10 μM and 3 μM (lanes 2, 3, 4 and 5 respectively). BSA was kept constant at 20 $\mu\text{l/ml}$.



However, there was variation between the experiments, which led to an increased standard deviation at 100 μM and 30 μM .

Figure 5.3e shows NS5A expression appears reduced at 100 μM , 30 μM and 10 μM concentrations of EPA, however this is difficult to assess without quantifying. Again GAPDH levels are reduced at 100 μM however the effect is less than that seen with DHA.

In conclusion, EPA treatment inhibited both HCV replication and fatty acid biosynthesis in a dose dependent fashion. EPA was less toxic to cells than DHA and therefore effects on replicon RNA levels were more likely to represent the inhibitory effects of the PUFA.

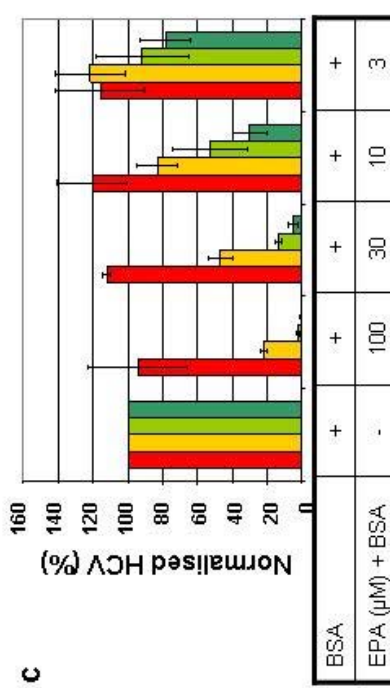
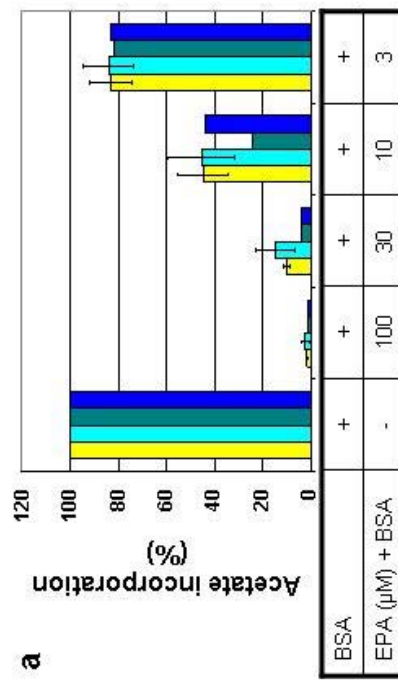
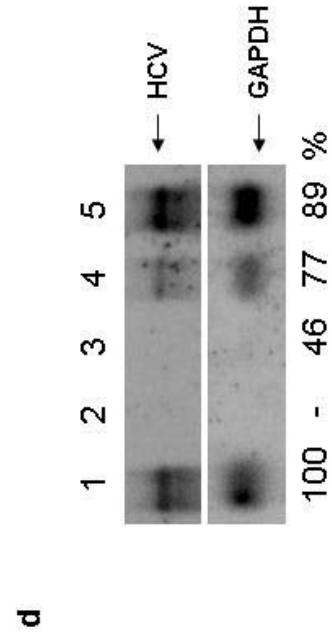
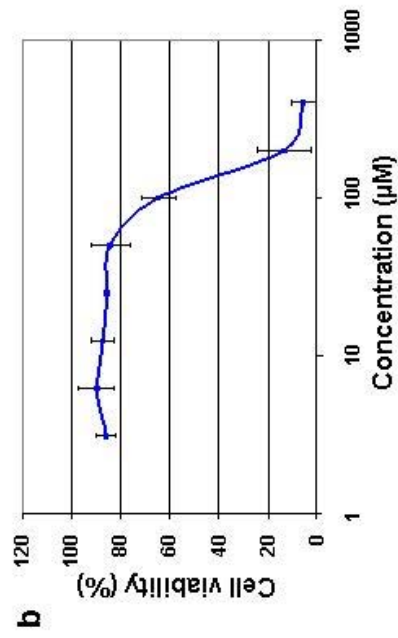
5.3.2 EPA treatment of cells transiently expressing HCV 2a replicon

Experiments were repeated for EPA treatment of cells expressing the transient replicon as in section 5.1.2. Luciferase activity was measured daily. RNA was extracted and fatty acid biosynthesis assayed for one of the three repeat experiments.

Figure 5.4a shows a comparison of fatty acid biosynthesis assays performed for the constitutive and transient replicons. Cells expressing the transient replicon behaved broadly in a similar manner to cells expressing the constitutive replicon. There were, however, some slight differences. At 30 μM , fatty acid biosynthesis in cells expressing the transient replicon was reduced to approximately 4 % of that of the BSA control, compared to approximately 12 % in cells expressing the constitutive replicon. The reason for this was unknown. However although the effect in cells expressing the transient replicon was more pronounced, it followed a similar trend to cells expressing the constitutive replicon. Also there was a difference at 10 μM EPA, where fatty acid biosynthesis in cells expressing the transient JFH1 replicon was reduced more than that seen in cells expressing the constitutive replicon.

Figure 5.4b shows an MTT assay for EPA which shows that the dose response curve to EPA was similar in cells expressing the transient replicon and those expressing the constitutive replicon. EPA was slightly less toxic to cells

Figure 5.4. The effect of treatment with EPA:BSA conjugates on transient JFH1 and JFH1 "GND" replicons. Assays were performed to measure cellular fatty acid biosynthesis (a) and cellular toxicity (b). The fatty acid biosynthesis assay (a) performed at 72 hrs shows JFH1 (dark blue) and JFH1 GND (green) along with 2a (light blue) and 2a-C (yellow) results for comparison. Cellular toxicity was measured at 72 hrs. HCV RNA replication was measured by luciferase activity (c) and Northern blot analysis (d) where RNA was obtained at 72 hrs. Luciferase activity (c) of transient replicons was assayed for untreated, BSA treated and 4 concentrations of EPA, 100 μ M, 30 μ M, 10 μ M and 3 μ M. BSA was kept constant at a 20 μ l/ml. Luciferase assays were performed at; 4 hrs (orange), 24 hrs (yellow), 48 hrs (light green) and 72 hrs (dark green). RNA extracts were obtained that were treated with BSA only (lane 1) or with EPA with 100 μ M, 30 μ M, 10 μ M and 3 μ M (lanes 2, 3, 4 and 5 respectively) was resolved in a 1 % formaldehyde gel.



expressing the transient replicon with a TD_{50} of at $125 \mu\text{M}$. This compares to a TD_{50} of $100 \mu\text{M}$ in the constitutive system. The reason for this was unclear. At $100 \mu\text{M}$, cells expressing the transient replicon had a cell viability of 64 % of that of the BSA control. The toxicity assay showed EPA to be less toxic than DHA where EPA concentrations $30 \mu\text{M}$, $10 \mu\text{M}$ and $3 \mu\text{M}$ were all within a non-toxic range.

EPA also inhibited HCV replication in the transient system (Figure 5.4c). EPA reduced replication in a dose dependent fashion at all concentrations used. At 72 hrs, HCV replication was reduced to 1 %, 5 %, 30 % and 78 % of that of the BSA control at $100 \mu\text{M}$, $30 \mu\text{M}$, $10 \mu\text{M}$ and $3 \mu\text{M}$. Although toxicity may contribute to some of the inhibition seen at $100 \mu\text{M}$, other reductions in HCV replication occurred in the non-toxic range. As already mentioned the constitutive replicon RNA levels were 25 %, 35 %, 90 % and 92 % at $100 \mu\text{M}$, $30 \mu\text{M}$, $10 \mu\text{M}$ and $3 \mu\text{M}$ EPA, respectively. There were distinct differences in the response between cells expressing the transient replicon and cells expressing the constitutive replicon. However the results obtained from cells expressing the transient replicon were more consistent.

A Northern blot of luciferase RNA (Figure 5.4d) showed that at $100 \mu\text{M}$ and $30 \mu\text{M}$ no RNA was detected and at $10 \mu\text{M}$ and $3 \mu\text{M}$ HCV RNA was 77 % and 89 % of that of the BSA control. These values were greater than the equivalent luciferase values obtained at 72 hrs at these concentrations. The reason for this was unclear.

5.4 Oleic Acid (OLA) treatment of cells expressing genotype 2a replicons

5.4.1 OLA treatment of cells constitutively expressing HCV 2a replicon

Our previous work with PUFAs had shown that they were able to reduce HCV replication in cells expressing both the transient and constitutive replicons. In order to confirm that this was a unique property of PUFAs and not a general property of all fatty acids, experiments were repeated using a monounsaturated fatty acid oleic acid (OLA). OLA is an 18-carbon fatty acid with one double

bond. As previously, experiments were performed on cells expressing the constitutive and transient JFH1 genotype 2a replicon containing cells. Cells were treated at four concentrations; 100 μM , 30 μM , 10 μM and 3 μM OLA conjugated to BSA. BSA was kept constant (20 $\mu\text{l/ml}$) in all test wells. Cells were treated for 72 hrs. Medium was changed daily and on the third day, RNA and protein were extracted and fatty acid biosynthesis and toxicity assayed. Results are shown as the average of only 2 experiments.

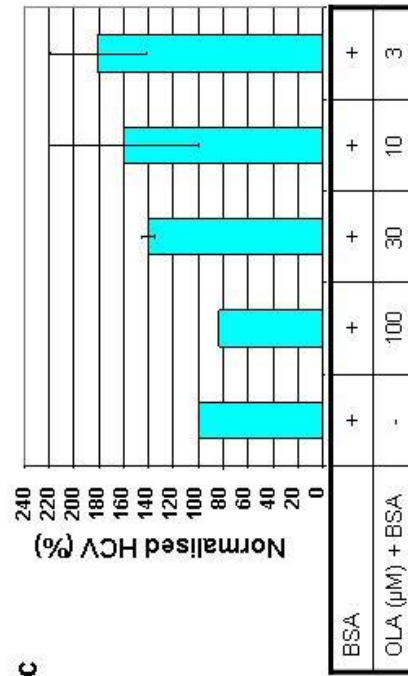
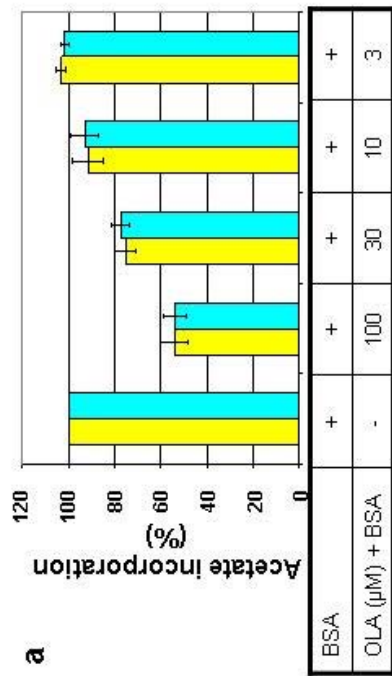
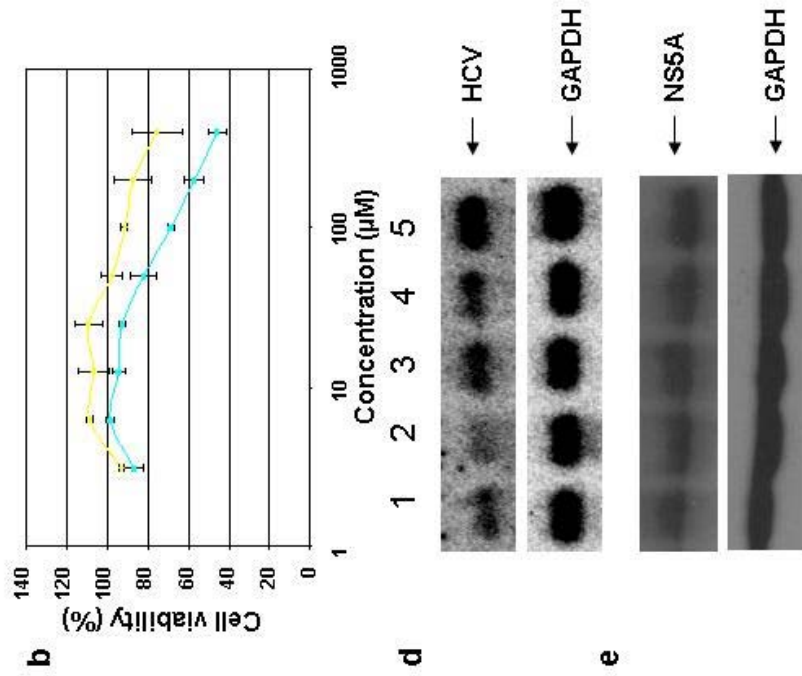
Figure 5.5a shows OLA inhibited fatty acid biosynthesis in cells constitutively expressing replicon and in cured cells in a similar fashion. Fatty acid biosynthesis was 54 %, 76 %, 92 % and 102 % of that of the BSA control at 100 μM , 30 μM , 10 μM and 3 μM . Unexpectedly OLA reduced fatty acid biosynthesis in cured and replicon expressing cells. At the 100 μM , there was only 50 % of acetate incorporation compared to that of the BSA control. This inhibition was less than that seen with PUFAs.

Interestingly, the viability of OLA treated cured and replicon-expressing cells was different from PUFA treated cells (Figure 5.5b). Also, replicon and cured cells behaved differently in their response to OLA. Their dose response curves were similar but OLA appeared to be more toxic to replicon cells. A TD_{50} was obtained at approximately 310 μM for replicon cells. It was impossible to estimate TD_{50} for the cured cells. At 100 μM , cured and replicon cells had cell viabilities of 91 % and 69 % of that of the BSA control respectively.

Figure 5.5c and d shows HCV replication was not reduced in OLA treated replicon cells as had previously been seen with PUFA treatment. A slight reduction of HCV RNA level was seen at 100 μM to 83 % of that of the BSA control. However we have had to disregard results of RNA replication at 100 μM because there was only one experiment available as the RNA from another experiment at 100 μM concentration had degraded. Treatment with the lower concentrations of OLA resulted in increases in HCV RNA levels. At 30 μM , 10 μM and 3 μM HCV RNA was 140 %, 160 % and 189 % of that of the BSA control. A large amount of variation between experiments was seen especially at 10 μM and 3 μM .

Figure 5.5e shows NS5A expression expressed at a similar level at 100 μM , 30 μM , 10 μM and 3 μM concentrations of OLA.

Figure 5.5. Treatment of 2a (light blue) and 2a-C (yellow) expressing cell lines with Oleic Acid (OLA): BSA conjugates. Assays were performed to measure cellular fatty acid biosynthesis (a) and cellular toxicity (b). RNA was resolved in a 1 % formaldehyde gel (d). HCV RNA replication was quantified after northern blot analysis (d) and is represented as a percentage of that of the BSA control (c). HCV NS5A protein expression was measured by Western blot analysis (e) where samples were separated on a 10 % polyacrylamide gel. NS5A was detected using the polyclonal NS5A sheep anti-serum (Macdonald et al., 2003). RNA and protein extracts were obtained from experiments with 2a cells that were treated with BSA only (lane 1) or with OLA with 100 μ M, 30 μ M, 10 μ M and 3 μ M (lanes 2, 3, 4 and 5 respectively). BSA was kept constant at 20 μ l/ml.



In conclusion OLA was shown to inhibit fatty acid biosynthesis in cured and replicon expressing cells however the effect was not as pronounced as that seen with PUFA treatment of cells. OLA was less toxic than PUFAs, failing to induce 100 % cell death even at 400 μM . Although it was difficult to ascertain whether OLA genuinely increased HCV replication (because of the variation between experiments), was not reduced as seen with PUFA treatment of cells.

5.4.2 OLA treatment of cells transiently expressing HCV 2a replicon

In order to confirm the effects seen with OLA treatment of cells constitutively expressing the genotype 2a replicon, experiments were repeated using cells transiently expressing the genotype 2a replicon. Experiments were performed as in sections 5.2.2 and 5.3.2 except using OLA.

Figure 5.6a shows that the response of cells transiently expressing the JFH1 replicon and JFH1 GND replicon was similar to that obtained from cells constitutively expressing replicon. However there were some differences between the two systems. Notably, cells transiently expressing the JFH1 replicon had higher rates of fatty acid biosynthesis at 10 μM and 3 μM of OLA compared to the equivalent of cells transiently expressing the JFH1 GND replicon. Also, at OLA concentrations of 10 μM and 3 μM there were approximately 42 % and 55 % increases in fatty acid biosynthesis respectively compared to cells expressing the JFH1 GND transient replicon. This was unexpected as all other results had followed a similar trend to cells expressing the constitutive replicon. However this experiment had only been performed once and would need to be repeated.

The viability of cells transiently expressing replicon showed OLA to be less toxic than that seen with cells constitutively expressing replicon. At 100 μM , cell viability was 94 % of that of the BSA control. Cell viability did not drop below 50 % even at 400 μM . This again showed that OLA did not induce the reduction in cell viability that was seen with PUFAs. The dose response was similar to that of cured cells in Figure 5.5b. All concentrations tested were considered to be within a non-toxic range.

Figure 5.6. The effect of treatment with OLA:BSA conjugates on transient JFH1 and JFH1 "GND" replicons. Assays were performed to measure cellular fatty acid biosynthesis (a) and cellular toxicity (b). The fatty acid biosynthesis assay (a) performed at 72 hrs shows JFH1 (dark blue) and JFH1 GND (green) along with 2a (light blue) and 2a-C (yellow) results for comparison. Cellular toxicity was measured at 72 hrs. HCV RNA replication was measured by luciferase activity (c) and Northern blot analysis (d) where RNA was obtained at 72 hrs. Luciferase activity (c) of transient replicons was assayed for untreated, BSA treated and 4 concentrations of OLA, 100 μ M, 30 μ M, 10 μ M and 3 μ M. BSA was kept constant at 20 μ l/ml. Luciferase assays were performed at: 4 hrs (orange), 24 hrs (yellow), 48 hrs (light green) and 72 hrs (dark green). RNA extracts were obtained that were treated with BSA only (lane 1) or with DHA with 100 μ M, 30 μ M, 10 μ M and 3 μ M (lanes 2, 3, 4 and 5 respectively) was resolved in a 1 % formaldehyde gel.

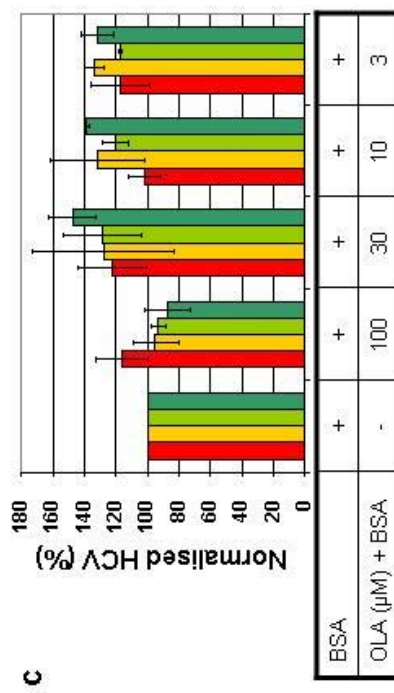
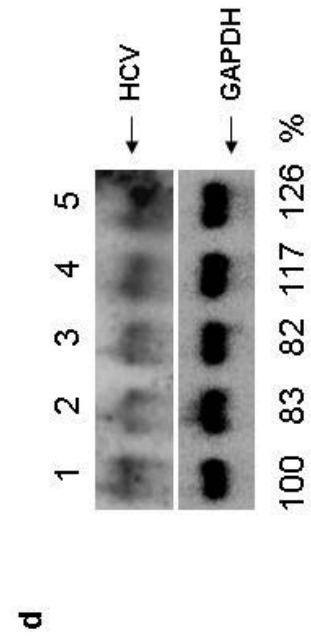
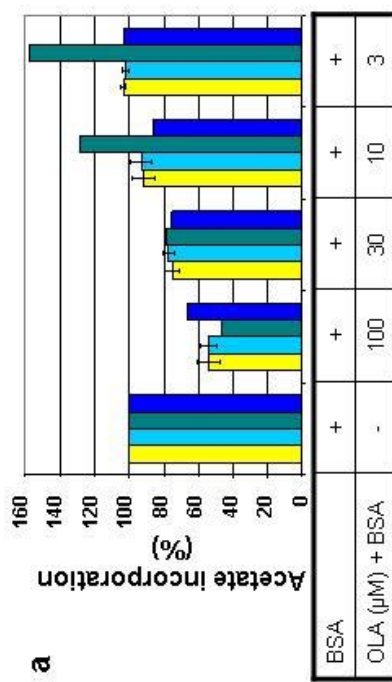
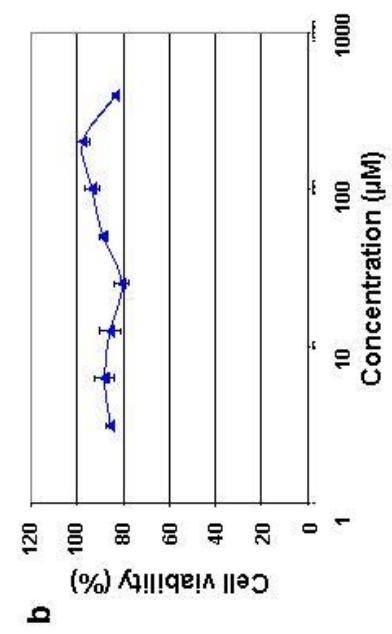


Figure 5.6c showed that, as seen with cells constitutively expressing replicon, at 100 μM there was a slight reduction in HCV replication to approximately 86 % of that of the BSA control. However at 30 μM , 10 μM and 3 μM , replication was 147 %, 138 % and 131 % of that of the BSA control. These results were more definitive than results obtained from cells constitutively expressing replicon, as there was less variation within the standard deviation. OLA treatment of cells transiently expressing replicon led to an induction of HCV replication at lower concentrations. Conversely, at 100 μM it led to a slight inhibition. These results were then confirmed using Northern blot (Figure 5.6d) although there was still a lack of sensitivity compared to the luciferase values and at 30 μM , HCV RNA was 83 % of that of the BSA control.

5.5 NS5A localisation in fatty acid treated cells

5.5.1 PUFA treatment of cell constitutively expressing genotype 2a replicon

Previous experiments were designed to show if there was any correlation between the effect of PUFAs on fatty acid biosynthesis and their effect on HCV replication. Although reduced levels of HCV replication were found when fatty acid biosynthesis was inhibited, this inhibition could not have been the only factor causing this reduction. OLA reduced fatty acid biosynthesis at 30 μM and 10 μM (Section 5.3) but there was no reduction in HCV RNA levels. This meant that PUFAs may inhibit HCV replication by a mechanism other than their effect on fatty acid biosynthesis. One possible explanation was that PUFAs were causing changes in the ER membrane thereby disrupting replication complex formation. The irregular structure of PUFAs created by the extensive double bonding leads to changes in membrane fluidity. This results in disruption of lipid-raft like structures. Our hypothesis was that PUFAs were disrupting replication complex formation and stability and thereby reducing HCV replication. In order to investigate this further, cells were treated with non-toxic concentrations of DHA and EPA at 10 μM for 72 hrs and on the 3rd day, HCV proteins were visualised using NS5A as an indicator of replication complex formation. Cells were also stained for the ER marker, calnexin, and the lipid droplet marker, ADRP.

Figure 5.7 shows the effect of DHA treatment on replicon expressing cells compared to BSA-treated replicon cells. BSA-treated replicon cells displayed diffuse staining of NS5A with the appearance of several more concentrated foci. NS5A showed some colocalisation with the calnexin ER marker. There was no colocalisation of NS5A with lipid droplets. At 10 μM DHA, NS5A expression appeared reduced compared to that of the control, although this was difficult to quantify. Nevertheless, NS5A seemed to have a less diffuse staining pattern and was now found mostly in the foci. There was an increase in the number of lipid droplets that were present compared to the BSA control and some areas of possible co localisation. However this was unclear.

Figure 5.8 shows that EPA treatment, like DHA treatment, caused an altered NS5A expression pattern. EPA treatment of replicon cells changed its expression pattern from having a diffuse ER appearance to being mainly associated with foci. EPA treated replicon cells contained more lipid droplets than BSA treated replicon cells. Also there appeared some co localisation between lipid droplets and NS5A. However, due to the large number of lipid droplets present, it was difficult to ascertain whether this was true co-localisation.

The results of PUFA treatment of cells failed to give a clear idea of what was happening to cause a downregulation of HCV replicon replication. It had been hoped that PUFA treatment of cells might lead to abolition of NS5A foci and therefore replication complexes but this was not seen. In fact the opposite occurred in that the diffuse staining found in the BSA control was lost and NS5A was mainly found in foci.

5.5.2 OLA treatment of cell constitutively expressing genotype 2a replicon

For comparison, cells were also treated with OLA to see the effects of a monounsaturated fatty acid on NS5A localisation. The previous results suggested that OLA treatment resulted in an increase in replication at 30 μM . Cells constitutively expressing the genotype 2a replicon were incubated for 3 days in 30 μM OLA conjugated to BSA. Media were changed daily and the experiments were performed in parallel with the PUFA experiments.

Figure 5.7. The effect of DHA treatment for 3 days on NS5A localisation in 2a cells using immunofluorescence. BSA treated replicon expressing cells (a, b, e, f, i & j) and DHA treated replicon expressing cells (c, d, g, h, k & l) were stained with combinations of antibodies. NS5A (e-l) was detected using polyclonal NS5A sheep anti-serum (Macdonald et al., 2003). Mouse anti-calnexin (b, d, j & l) was used to detect ER and rabbit anti-ADRP (a, c, i & k) was used to detect lipid droplets. DAPI (i-l) was used to stain the nucleus. Merged images are shown in panel i-l. Areas of co localisation were seen as yellow areas.

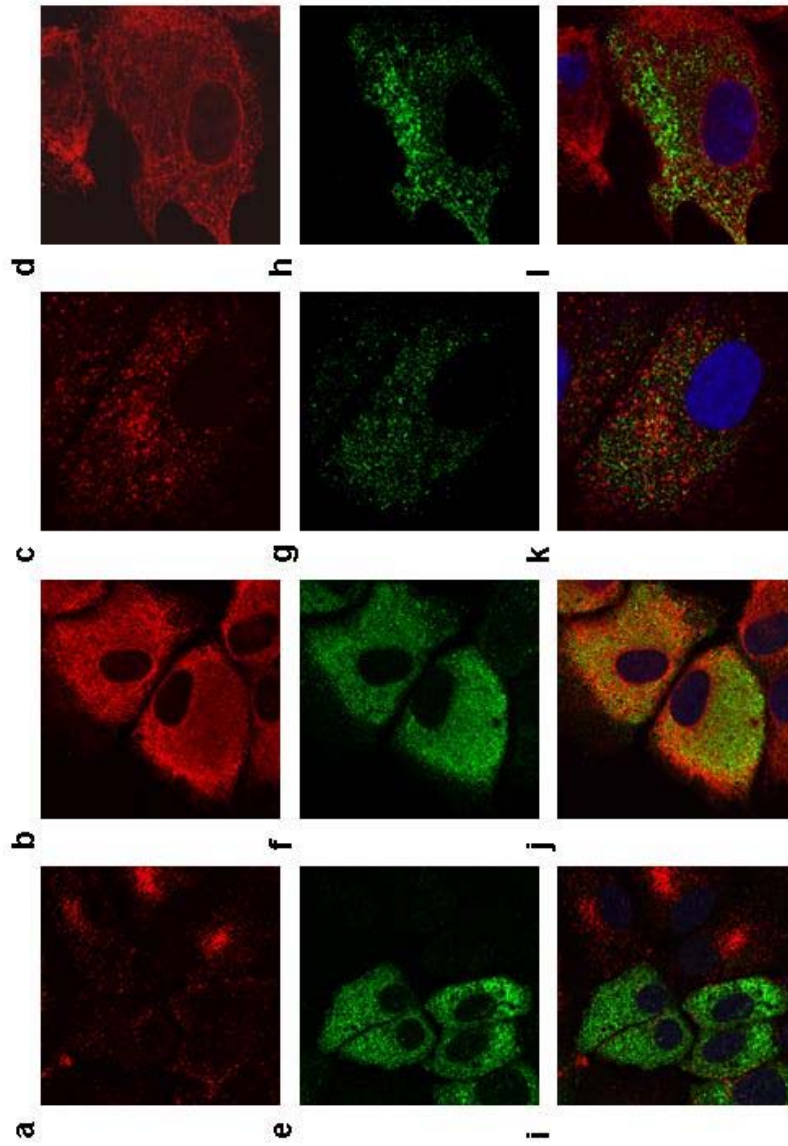


Figure 5.8. The effect of EPA treatment for 3 days on NS5A localisation in 2a cells using immunofluorescence. BSA treated replicon expressing cells (a, b, e, f, i & j) and EPA treated replicon expressing cells (c, d, g, h, k & l) were stained with combinations of antibodies. NS5A (e-l) was detected using polyclonal NS5A sheep anti-serum (Macdonald et al., 2003). Mouse anti-calnexin (b, d, j & l) was used to detect ER and rabbit anti-ADRP (a, c, i & k) was used to detect lipid droplets. DAPI (i-l) was used to stain the nucleus. Merged images are shown in panel i-l. Areas of co localisation were seen as yellow areas.

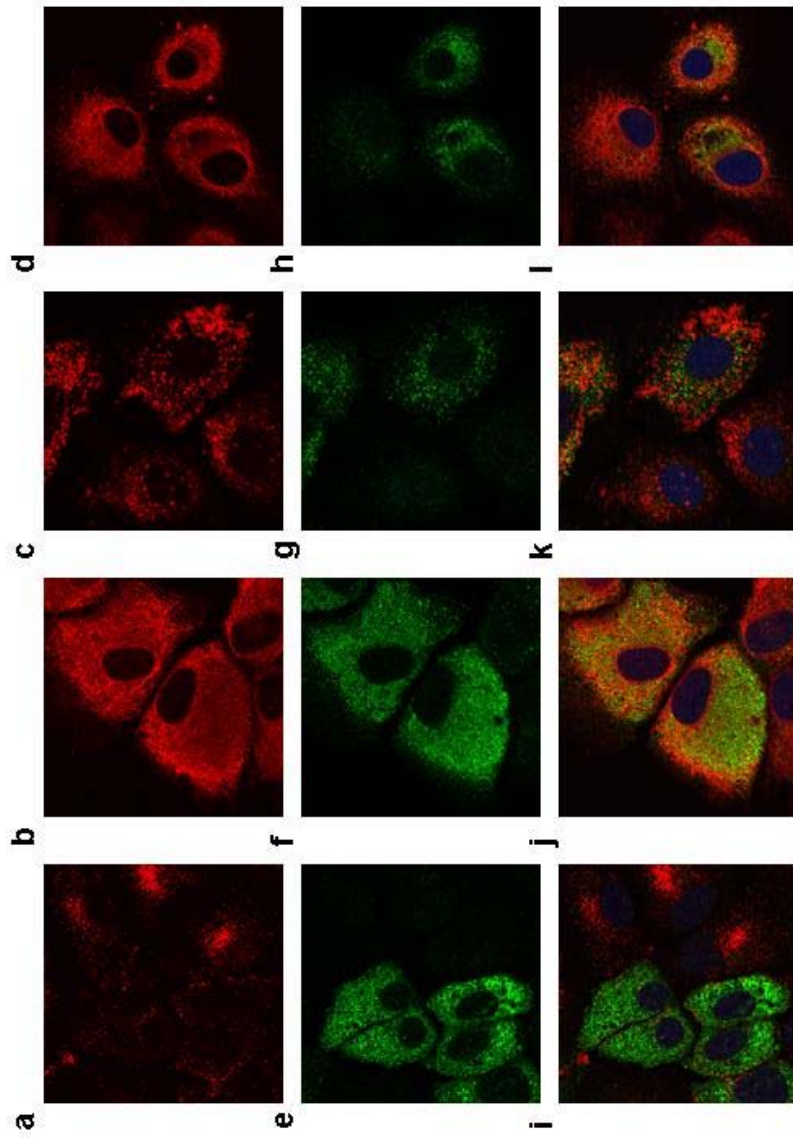


Figure 5.9 shows that, unlike in PUFA-treated cells, NS5A had a distinctly different expression pattern after OLA treatment of replicon cells. OLA treatment, as with PUFA, treatment led to an increase in the number and size of lipid droplets. Again, rather than a diffuse staining pattern, NS5A was found mainly in foci but the foci in these cells were larger and more intense than in either control or PUFA-treated cells.

5.6 The effect of fatty acid treatment on ER membrane fluidity

Our hypothesis for PUFA-induced reduction of HCV RNA levels had been that PUFAs were disrupting the ER membrane and interfering with membrane bound protein association, which was affecting replication complex formation. Although IF studies had been inconclusive, there did appear to be either a relocalisation or reduction of NS5A in PUFA-treated cells. PUFAs have the ability to increase membrane fluidity due to their irregular structure. In order to ascertain if the incorporation of PUFAs into the ER membrane was changing the dynamics of membrane-bound proteins, fluorescence recovery after photobleaching (FRAP) was performed on an ER membrane bound protein called DNase X. Plasmid constructs expressing GFP-DNase X fusion protein were transfected into HuH-7 cells which were incubated overnight in the presence or absence of fatty acid conjugated to BSA. Cells were treated at 10 μM EPA and 10 μM DHA and 30 μM OLA. Figure 5.10 shows data from one preliminary experiment investigating the effect of fatty acid on the mobility of the ER membrane protein GFP-DNase X.

Figure 5.10 shows that fatty acid treatment of cells had no significant effect on the recovery of GFP-DNase X into the bleached area of the ER membrane. DHA, and OLA-treated cells behaved similarly to the BSA-treated cells. EPA-treatment of cells appeared to lead to a slight decrease in membrane protein mobility compared to the BSA control. The experiment indicated that fatty acid treatment of cells expressing the GFP-DNase X protein did not affect its mobility as expected. However, these results were obtained from one experiment and need to be repeated.

Figure 5.9. The effect of OLA treatment for 3 days on NS5A localisation in 2a cells using immunofluorescence. BSA treated replicon expressing cells (a, b, e, f, i & j) and OLA treated replicon expressing cells (c, d, g, h, k & l) were stained with combinations of antibodies. NS5A (e-l) was detected using polyclonal NS5A sheep anti-serum (Macdonald et al., 2003). Mouse anti-calnexin (b, d, j & l) was used to detect ER and rabbit anti-ADRP (a, c, i & k) was used to detect lipid droplets. DAPI (i-l) was used to stain the nucleus. Merged images are shown in panel i-l. Areas of co localisation were seen as yellow areas.

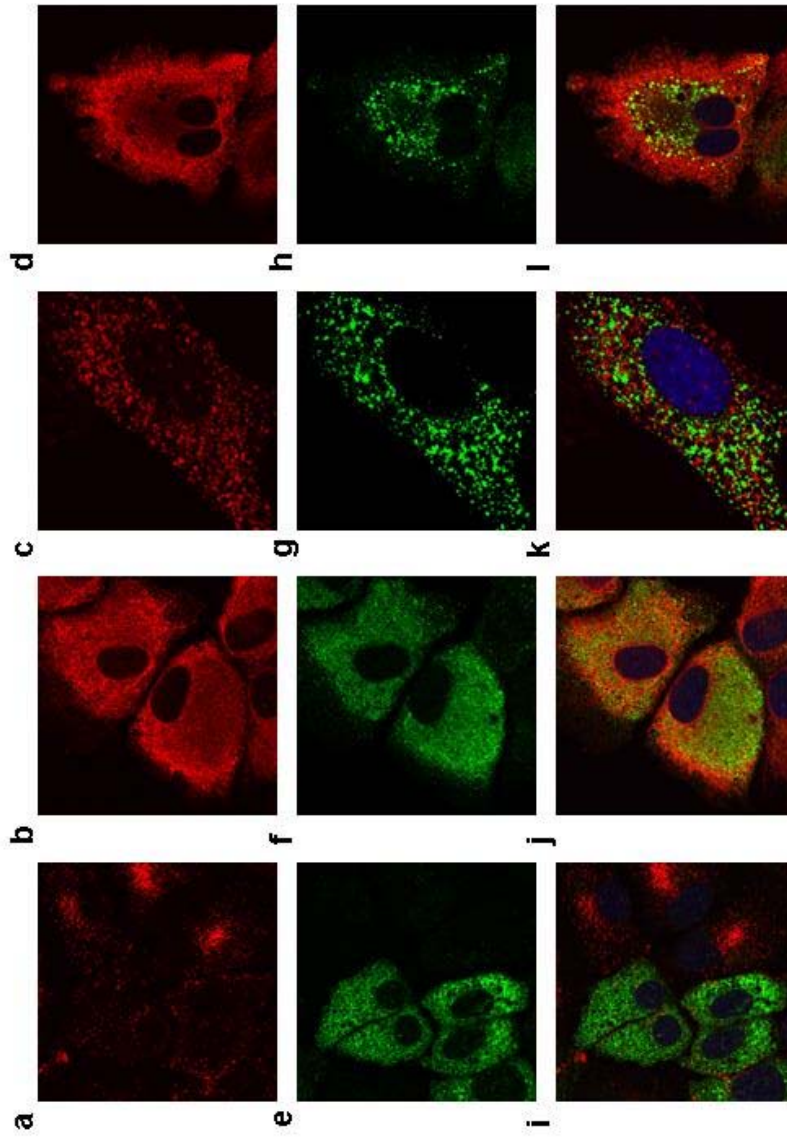
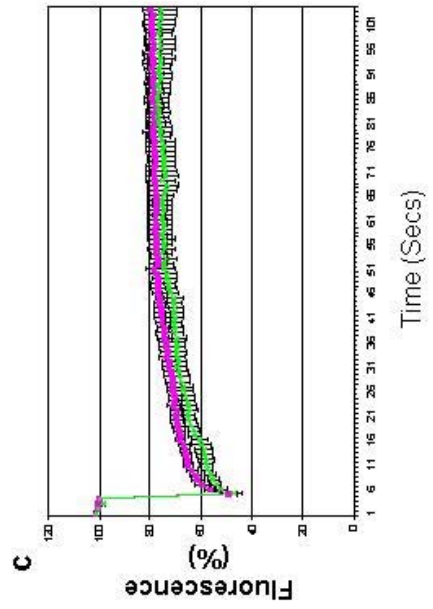
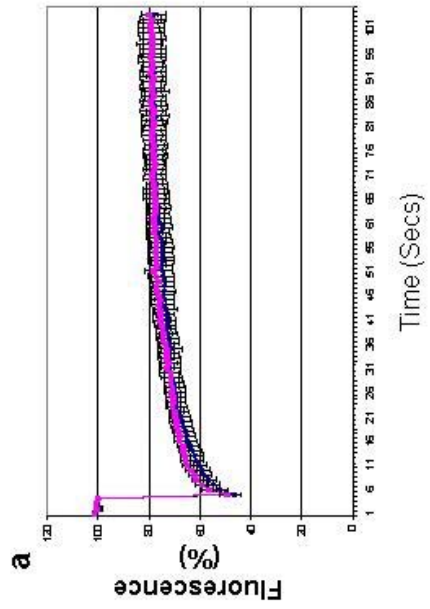
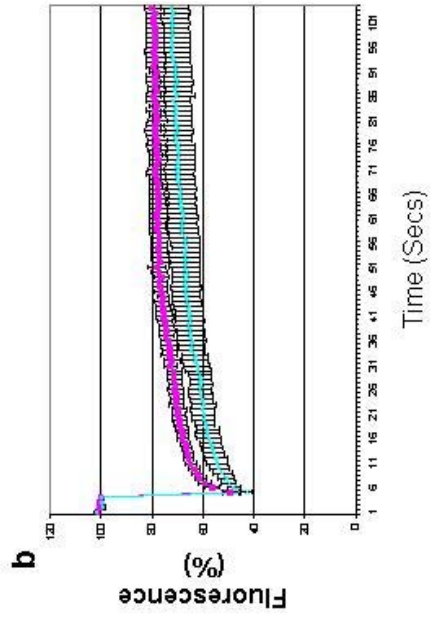


Figure 5.10. Fluorescence recovery after photobleaching (FRAP) analysis on the effect of fatty acids on ER membrane mobility of GFP-DNase X in Huh-7 cells. Data is represented as percentage values for the recovery of fluorescence to the bleached area which was calculated using the equation in section 2.12. FRAP was performed to measure the difference in recovery after bleaching in Huh-7 cells treated with a) DHA (blue)(10 μ M), b) EPA (light blue)(10 μ M) and c) OLA (green)(30 μ M) for 72 hrs. BSA treated cells (pink a-c) were used as a comparison for effects of fatty acid on membrane fluidity.



5.7 Discussion

Results had showed that PUFA treatment of replicon-expressing cells led to a reduction in HCV replication and fatty acid biosynthesis. However there was an associated toxicity at higher concentrations, which reduced cell viability. There were some differences between results presented here on the effect of PUFAs on replicon replication and previous studies (Kapadia et al., 2005; Leu et al., 2004) notably the concentration at which the PUFAs were added to cells. Although PUFAs had been extensively reported in the literature to reduce viability of cancer cells neither of the previous studies on the effects of PUFAs on HCV replication mentions this property as being a problem. In Leu et al (2004), a maximum concentration of 100 μM fatty acid was used. At this concentration, DHA was cytotoxic resulting in high levels of the cell death. Nevertheless in their study they found another PUFA, arachidonic acid to have 50 % cell viability between 300-400 μM at 72 hrs. These concentrations were far higher than any used in our study. The study by Kapadia et al (2005) had used fatty acids at 50 μM concentrations. However, there was no mention of fatty acid toxicity. It was clear from our own study that PUFAs do reduce cell viability and this differs from the effects of the monounsaturated fatty acid, OLA. In our study, media were changed daily but there is no mention of this in the previous two studies. Changing the media allowed for a continual fresh supply of PUFA to be delivered, minimising degradation. Also in our study, PUFAs were conjugated to BSA prior to being applied to culture, which had only previously been mentioned by Kapadia et al. (2005). Conjugating to BSA more represents more physiological conditions and minimises the acidity of free fatty acids.

Another important factor that became clear during the course of our study was that different batches of PUFA can vary in their ability to induce toxic effects on cells. This was most notable with one batch of DHA, which was less lethal. All experiments performed with that batch were equivalent to each other in their response but differed from other batches used. To minimise variation caused by batch variation, all experiments were performed with the same batch of fatty acid. The reason for variation between batches of fatty acid was not clear as the manufacturer guaranteed stability of the compound for up to a year after purchase.

It was important to note that our experiments used a genotype 2a replicon whereas previous studies had used genotype 1 replicons. This also may have contributed to differences between studies. However, experiments would need to be repeated using genotype 1b expressing cell lines in order to confirm this. The trend that PUFAs have an inhibitory role on replication whereas OLA does not was found consistently between studies. One main difference with regard to the use of OLA was that in our study at 100 μM it had inhibitory effects but in Leu et al. (2002) this concentration had induced replication to 162.73 % of that of the control. This might be explained by differences in cell lines used or possibly the BSA delivery method.

Ideally, as with cerulenin, it would be useful to calculate a therapeutic index for fatty acid treatment of cells. Again, there are two factors to consider: the ratio of effect on fatty acid biosynthesis to cell toxicity and the ratio of effect on HCV RNA levels to cell toxicity. A therapeutic index of approximately 3:1 was obtained for the effects of DHA on fatty acid biosynthesis for cells both constitutively and transiently expressing the HCV replicon. The two methods used to assess HCV replication, Northern blots and luciferase assays, gave some inconsistent results. The results with the constitutive replicon showed a therapeutic ratio that was lower than 3:1 and the transient replicon had a ratio that was higher than this. This would indicate that DHA is more efficient at reducing HCV replication in the transient replicon than the constitutive replicon.

EPA treatment inhibited fatty acid biosynthesis with a therapeutic ratio of approximately 4:1. EPA was slightly more effective at reducing fatty acid biosynthesis in a non-toxic manner than DHA. However, the real difference between EPA and DHA was seen when considering the effect of EPA on HCV replication. Again, as with DHA, the transient replicon responded with a greater reduction in HCV replication upon EPA treatment. Treatment of the transient replicon with EPA gave a therapeutic index of approximately 25:1 compared to 10:1 with the constitutive replicon. Both these ratios were far higher than those seen with DHA treatment of cells. EPA treatment reduced HCV replication at more non-toxic concentrations than DHA. This is interesting because their therapeutic ratios for reduction of fatty acid biosynthesis were similar. The inhibition of HCV replication by EPA might be the result of a combination of different mechanisms apart from its inhibitory effects on fatty acid biosynthesis.

Therefore, inhibition of HCV RNA levels could not be attributed solely to inhibition of fatty acid biosynthesis.

The relatively low therapeutic indices for the effect of EPA on fatty acid biosynthesis compared to effects on HCV RNA levels may be a result of using cancer cell lines. It is possible that, in cancer cells, fatty acid biosynthesis is a requirement for successful cell growth. As mentioned in chapter 4, up-regulation of fatty acid synthase has been reported in several cancer types. In particular, FAS upregulation occurs in an aggressive subtype of breast tumours (Menendez et al., 2004). This might mean that it is impossible to completely inhibit fatty acid biosynthesis in tumour cell lines without a corresponding drop in cell viability.

The results showed inconsistencies in HCV replication response between Northern blots and luciferase assay data. Although the general trend between experiments was the same, luciferase expression with the transient replicon was more sensitive in its response to fatty acid treatment than that seen by replicon RNA levels with the constitutive replicon. This highlighted the difficulties in using Northern blots. If the variation had occurred at the experimental level due to instability of the PUFA or perhaps some adverse condition that made the cells grow slower then there should also be some variation in the figures obtained for the fatty acid biosynthesis assay. However, this was not the case. Therefore, this variation must have been introduced when processing the Northern blot possibly due to poor transfer of RNA or degradation of probe. RNA degradation was normally identified early in the procedure because ribosomal bands were visualised by ethidium bromide staining. More consistent results obtained with luciferase assays compared to inconsistent Northern results provided a more reliable system for measuring replication levels. However, a study by Su et al. (1999) had seen similar inconsistencies in Northern results after treatment of cells with fatty acid inhibitors and inducers. They noted that constitutive and transient replicons could differ in their extent of response. Nystatin, an inducer of lipid metabolism, increased replicon RNA levels in the constitutive system to 250 % of that of the control whereas the equivalent figure was 150 % in the luciferase system. Although both systems give an indication of replication, neither directly looks at replication itself. The luciferase replicon measures replication indirectly through luciferase activity. Although an increase

in luciferase signal requires replication to occur, the assay itself measures the translation and enzymatic activity of luciferase. However, this method gives a better idea of the kinetics of replication as it starts from zero replication. Effects of fatty acids on the constitutive replicon were measured by quantifying HCV RNA at the end of the 72 hour period and therefore might seem a better system for looking at replication. However, this system looks at the “turn over” of RNA rather than directly at replication. Northern blots were performed on the luciferase replicon RNA to determine whether the effect seen was due to effects on replicon replication or effects on luciferase translation and enzymatic activity. Preferably Northern blots should be repeated for the RNA extracted from cells expressing the transient replicon as technical difficulties with high backgrounds may have given false quantitative estimate which led to inconsistencies between the luciferase values and the values obtained by Northern blot from the transient system.

The extent of the inhibitory effects of PUFAs on replicon replication was not found with OLA. Both PUFAs had an inhibitory effect on HCV replication at all concentrations. OLA treatment gave a reduction in HCV levels at the highest concentration of 100 μM but led to increases in replication at other concentrations. OLA also reduced fatty acid biosynthesis in a dose-dependent manner. However, the effect was not as pronounced as that seen with PUFA inhibition. As previously reported, the inhibition of fatty acid biosynthesis by PUFAs occurs by antagonising LXR (Kapadia et al., 2005). It has also been reported that OLA can antagonise LXR but the effects are less dramatic than those found with PUFAs. This antagonism of LXR is not seen with saturated fatty acids (Jump D, 2004), which could explain the reduction in fatty acid biosynthesis. Results indicated that a reduction in fatty acid biosynthesis was not a prerequisite for reduction of HCV RNA levels. Had it been a prerequisite, then OLA might have inhibited HCV replication at 30 μM and 10 μM . However in our hands OLA had two different effects. At 100 μM , HCV replication was reduced and at lower concentrations replication was induced. These seemingly contradictory roles of OLA may indicate that it had a dual effect. Our hypothesis is that inhibition of fatty acid biosynthesis led to a reduction in HCV replication at certain concentrations. At lower concentrations OLA did not reduce fatty acid biosynthesis to an extent that would lead to a reduction of HCV RNA levels and its inductive effects on HCV RNA levels countered its

inhibitory effects. It was also important to appreciate that de novo produced fatty acids (new fats) can have distinctly different abilities in altering metabolic pathways compared to exogenously produced fatty acids (old fats)(Gibbons, 2005). It may be useful to ascertain where OLA was being incorporated in to the cell using thin layer chromatography. This would answer whether OLA was being stored as triacylglycerols in lipid droplets, as our IF experiments suggested, whether it was being incorporated into phospholipid components of the cells or if it was present mainly as free fatty acid.

Some of the OLA data that we obtained were contradictory to the data obtained by Leu et al. (2004) where they had found an increase in HCV RNA at 100 μ M. However they measured expression of a genotype 1b HCV replicon at 24 hrs. In our study, replication of the transient replicon at 24 hrs was slightly increased compared to the control but not to the same extent seen in Leu et al. (2004). Nevertheless cells expressing both transient and constitutive replicons gave the same results in our studies although there had only been one experiment performed with the constitutive replicon.

The OLA experiments had indicated that reduction of fatty acid biosynthesis was not a prerequisite for inhibition of HCV replication. In fact, an induction of HCV replication was possible when fatty acid biosynthesis was being reduced. This would counter the argument that inhibition of fatty acid biosynthesis was necessary for reduction of HCV replication. However, it was difficult to determine exactly whether this was true, as OLA appeared to have different functions at different concentrations. The ability of OLA to inhibit fatty acid biosynthesis without reducing HCV RNA levels and the difficulty in correlating PUFA inhibition of fatty acid biosynthesis to a reduction in HCV RNA levels might mean that PUFA mediated inhibition of HCV occurred by a mechanism other than effects on fatty acid biosynthesis. This had been previously suggested by Kapadia et al. (2005) where they had been able to rescue PUFA mediated fatty acid inhibition by treating cells in combination with an LXR agonist. Although fatty acid biosynthesis was induced by LXR agonist treatment, HCV replication was still inhibited. Therefore, it would be interesting to ascertain whether LXR agonist treatment in our system could restore fatty acid biosynthesis while maintaining HCV replication inhibition. This could answer not only whether HCV replication inhibition is as a consequence of a reduction in fatty acid

biosynthesis but also whether toxicity induced by PUFA treatment is due to fatty acid biosynthesis being reduced. It may be that the reduction of fatty acid biosynthesis was purely coincidental and that PUFAs act on HCV replication by another mechanism. Also it would be useful to measure the expression of FAS and SREBP-1c in our cell extracts for comparison with the results obtained from Kapadia et al. (2005).

We had hoped that IF and membrane fluidity studies might help answer how PUFAs inhibit HCV RNA replication. However, IF results did not give any conclusive indication of mechanism as there appeared to be a general downregulation of NS5A expression. When comparing control cells to PUFA treated cells, the diffuse ER staining seen in control cells was not present and NS5A was mainly found in foci. Other studies have shown that only a small percentage of replication complexes are actively involved in HCV replication at any one time. Therefore in these cells although HCV replication is down-regulated the few replication complexes remaining could be sufficient to sustain replicon RNA (Quinkert et al., 2005). OLA treatment of replicon led to noticeable differences in NS5A foci compared to BSA control cells. The foci appeared larger and more concentrated with NS5A protein. It was not known whether these were merely aggregates of NS5A or large replication complex foci. If the latter, it was conceivable that large replication complexes were forming which led to the increases in replication seen in the previous OLA experiments. It may be that OLA was able to provide a more beneficial environment for replication complex formation, which led to these oversized complexes. It would be interesting to repeat the IF studies comparing 100 μM and 30 μM concentrations of OLA to see whether the large foci were present at 100 μM .

Preliminary membrane fluidity studies based on movement of a membrane-bound protein indicated that DHA did not noticeably affect the mobility of the ER marker DNase X. Although EPA appeared to slightly reduce membrane fluidity, which was contrary to our hypothesis, this was obtained from just one experiment and would need to be repeated. More importantly, it may be more useful to observe the effect of PUFAs on the mobility of HCV proteins, rather than DNase X. For example, it would be interesting to investigate the effects

of PUFAs on the mobility of NS4B protein. This has been suggested as being a platform protein for replication complex assembly (Yu et al., 2006).

Further experiments investigating where supplied fatty acids are being incorporated in the cell may help to identify why they affect HCV replication. Immunofluorescence suggested that there is an increase in lipid droplets so, some fatty acids must be being stored as triacylglycerols. Radiolabelled fatty acids would allow fatty acids to be traced to the lipid group using thin layer chromatography. Also previous cell fractionation experiments indicated that HCV RNA was found in fractions containing lipid rafts. High-pressure liquid chromatography (HPLC) could be used to identify different fatty acid types and determine whether there is an increase in the ratio of PUFAs in fractions, which contain HCV replication complexes.

It was also possible that PUFAs were affecting cholesterol biosynthesis as they affect the global transcription of lipid metabolism genes and can also directly inhibit farnesyl diphosphate, a key enzyme in the cholesterol pathway (Le Jossic-Corcus et al., 2005). PUFA inhibition of HCV RNA replication may be caused by inhibition of the same cholesterol pathway that was altered by the use of geranylgeranylation inhibitors (Kapadia et al., 2005). If so, supplying geranylgeranoil would restore HCV RNA levels from PUFA mediated inhibition.

EPA and DHA treatment of cells transiently expressing replicon showed the level of reduction in replication increased over 72 hrs. PUFAs at 3 μM concentration were non toxic and therefore it would be interesting to extend for the longer periods the PUFA treatment of cells constitutively expressing replicon. Treatment of cells constitutively expressing replicon with IFN allows removal of replicon RNA to produce an HCV RNA negative population of cells. Prolonged treatment of replicon cells with PUFA may similarly cure them of replicon RNA.

With the advent of the JFH1 infectious system, it would be useful to extend our study to investigate the effect on the infectious system. It might be possible to reduce replication and expression without a consequent effect on HCV infection. This depends on which part of the HCV lifecycle is the rate-limiting step for successful infection. Is it entry of the virus, replication and expression of viral RNA and protein or assembly and release of new virus particles? These

experiments would be crucial in identifying the possible role of PUFAs HCV therapy.

There is interest in PUFAs not only because of their ability to reduce HCV replication but also their inherent health benefits. If PUFAs were able to reduce HCV infection, then their use in combination with existing therapies could be valuable. Already, their beneficial use in combination with IFN treatment had been hinted at in the study by Leu et al. (2004). A combination of arachidonic acid and IFN treatment showed that it was possible to obtain a synergistic inhibitory effect on HCV replicon replication. Already considered beneficial, essential fatty acids, which are required in the diet, could be used in combination with IFN treatment to treat HCV-infected patients. Although it is difficult to determine their effect on HCV infection, an improvement of liver disease might be expected. A clinical study to investigate the effects of PUFA treatment on HCV infected patients would now be justified.

Chapter 6

6 Making a genotype three expressing replicon HuH-7 cell line

6.1 Introduction

The pathogenesis of liver disease as a result of HCV infection is still not fully understood. Whether liver damage is a consequence of viral infection or due to an immune mediated response is not known. Immune-mediated pathways leading to liver damage are more likely since it has been shown there is no correlation between viral RNA titres and liver damage (Wejstal R, 1995).

One of the most common pathologies in chronic infection is steatosis, which is found in 50 % patients. Steatosis is the accumulation of intracytoplasmic lipid droplets within hepatocytes (Zhu A, 2003). The metabolic cause of steatosis is still not understood although there are many predisposing factors. These include increasing age, increased body mass index (BMI), alcohol abuse, intolerance of insulin, drugs and concomitant infections. It is still not clear whether steatosis is a direct effect of viral infection or is a secondary consequence. Steatosis may create a beneficial environment for viral replication (Adinolfi et al., 2001).

Several studies have identified HCV genotype 3 as being strongly associated with the presence of steatosis and suggested that HCV genotype 3 may cause steatosis as a cytopathic effect (Adinolfi et al., 2001; Quadri et al., 2001; Rubbia-Brandt et al., 2001). Steatosis has been shown to accelerate fibrosis over time in patients with genotype 3 (Westin et al., 2002). Kumar et al. (2002) reported changes in the degree of steatosis after a sustained viral response (SVR). Patients with genotype 3 who achieved a SVR to therapy almost invariably showed a complete reversal of steatosis. This was not observed in patients infected with genotype 1 strain who displayed steatosis.

The lack of a cell-based system has limited research with genotype 3. Until recently HCV researchers had no method of investigating viral replication, expression and particle assembly. This was changed by the development of a modified autonomously replicating HCV genotype 1b genome (Lohmann et al., 1999). The genome required specific modifications and cell passage number was important for successful cell line establishment. This system was further extended to HCV genotype 1a strain where again the genome was modified and the cell line used was important for successful replication (Blight et al., 2003). However both of these systems investigated only viral replication and expression. In most cases HCV structural genes were omitted. However, even when structural genes were included particle formation was not observed. The production of infectious particles was achieved only after the isolation of a HCV genotype 2a isolate from a patient with fulminant hepatitis (Wakita et al., 2005). Therefore, present replicon systems are available for only genotypes 1b, 1a and 2a. Due to HCV genotype 3 being implicated in having a possible viral cytopathic effect creation of a replicon expressing cell line was desirable. Apart from this, possession of a full-length genotype three sequence was also desirable as there are few full-length genotype 3 sequences available.

The aim of this study was to assemble a full-length genotype 3 genome, which could be used to make a replicon expressing cell line.

6.2 Selection of a patient serum

The criteria for selection of patient serum were;

- an isolate obtained from a patient infected with HCV genotype 3
- availability of several aliquots of stored serum and a stored liver biopsy

The isolate used in our study was derived from serum from a 37 year old Glasgow male (GM) patient infected with HCV genotype 3a. The genotype had been determined by restriction fragment length polymorphism (RFLP) and direct sequencing of NS5A gene (performed by Carol-Anne Smith). West Glasgow Ethical Committee had authorised the study and informed patient consent was obtained on collection of serum and biopsy samples. The patient was

subsequently treated with pegylated interferon- α and ribavirin and displayed a sustained viral response. Liver biopsies and serum samples were taken before, during and post anti-viral therapy. Liver biopsies were classified according to the Ishak score. A liver biopsy taken after treatment showed an Ishak score of fibrosis stage 0/6 and inflammation 3/18 (one each for portal, interface and parenchyma). The biopsy showed minimal steatosis which had slightly improved compared to the previous biopsy which was obtained before IFN- α treatment. The liver biopsy prior to therapy displayed moderate to minimal steatosis.

The patient had no history of intravenous drug use and did not drink to excess. GM patient was 1.74 m tall and weighed 73.1 kg. This made his body mass index 24.14, which is between the range 18.5 and 24.9 and was classed as normal.

6.3 Assembling a majority sequence

6.3.1 Amplification of the genome

It was first necessary to determine the complete sequence of the GM isolate. Using a similar principle that had been used to assemble a genotype 1b replicon, a majority sequence was deduced (Lohmann et al., 1999). This comprised an HCV sequence, which corresponded to the most frequent base at any given locus and was achieved using RT-PCR and direct sequencing of PCR products. Primers were designed in regions of homology shared between 4 HCV genotype 3 genomes; NZL1 (Sakamoto et al., 1994), Ka3503a (Yamada et al., 1994), TR3b (Chayama et al., 1994) and 3aCB (Shukla et al., 1998). In total, 37 primers both sense and anti-sense were used for RT, PCR and sequencing of the genome. In most cases primers were designed to fit the following criteria:

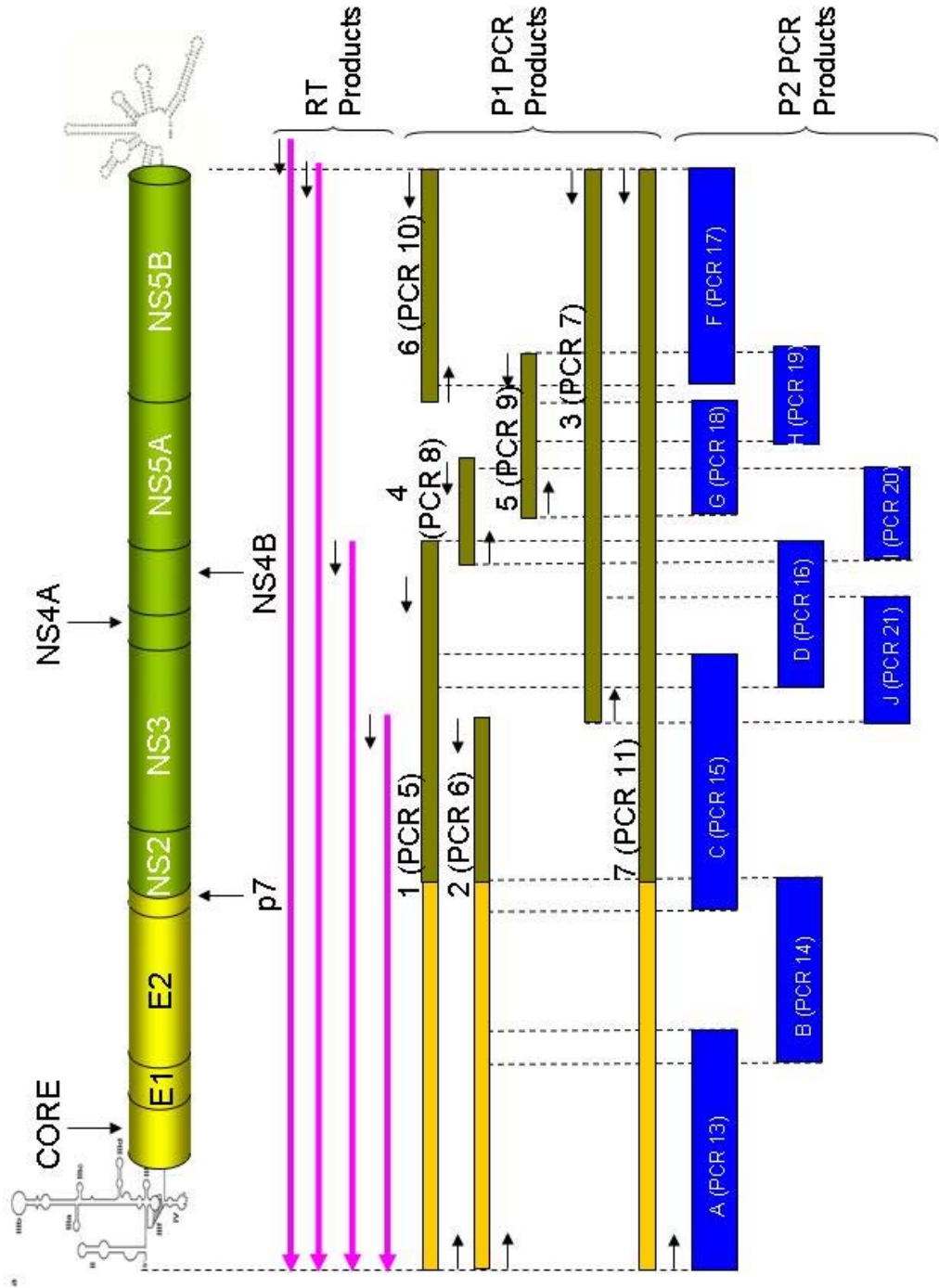
- a length of approximately 20 nucleotides
- a T_m between 50-70°C
- a GC content of between 40-60 %

All primers are listed in section 2.1.11 in Chapter 2 where primer sequence, name and use are indicated.

Initially RNA was extracted from serum or biopsy and reverse transcribed using an Omiscript reverse transcription kit. RT primers were used, which annealed to the 3' periphery of the genome on the X-tail (PM 3AS), at the stop codon (a9425gt3) and within NS4B (a6120gt3) and NS3 (a4935gt3). A diagrammatic representation of all RT reactions and PCRs is found in figure 6.1. Synthesis of a cDNA template from RNA was confirmed using real time PCR of the 5'UTR (data not shown). The presence of template in a reaction indicated successful RT, generating transcripts from the RT primer point of origin to the 5'UTR. The cDNA could then be used as a template for PCR amplification.

Nested and semi-nested PCR was used to amplify areas of the genome. This principle requires two rounds of PCR. The first round (P1) of PCR amplifies a region of interest and the second round (P2) amplifies a region that is internal or partially internal to the P1 PCR primers. This allows for specific high yield amplification from templates with low copy number. Initially diagnostic nested PCR was used to confirm the presence of template using *Taq* Polymerase. This was performed to confirm the real-time PCR result before using the more expensive BD Advantage 2 Polymerase kit and *Pfu* polymerase. Two regions were used for this process: one of which was in the 5'UTR region (P1-PCR 1 and P2-PCR 2) and the other, which was in NS5A (P1-PCR 3 and P2-PCR 4). After this P1 PCR products 1 (PCR 5), 2 (PCR 6), 3 (PCR 7) and 7 (PCR 11) were amplified (Figure 6.1). Technical problems were encountered when attempting to amplify the 3' end of the genome. The reasons underlying the difficulties will be discussed in more detail in section 6.2. After the P1 PCR, P2 PCR products, a (PCR 13), b (PCR 14), c (PCR 15), d (PCR 16), f (PCR 17), g (PCR 18), h (PCR 19), i (PCR 20) and j (PCR 21) (Figure 6.1) were amplified as described in section 2.2.5, an aliquot of the P2 PCR products was resolved by agarose gel electrophoresis to confirm the PCR had been successful and a product of the correct size generated. Once the correct P2 PCR product had been confirmed, the whole sample was electrophoresed through an agarose gel and the PCR product excised and purified. The concentration of the purified PCR product was estimated by running an aliquot of PCR product on a DNA Mass ladder. PCR products covering the entire genome up to base 9320 were then sent for direct sequencing. Initially the sequence of the very 3' end of the genome could not be obtained.

Figure 6.1. Diagrammatic representation of RTs, and PCRs performed on GM genotype 3 genome. RTs (pink) were performed from various places in the genome using Omniscript RT kit. First round or P1 PCR products (gold and green) were performed from cDNAs obtained from RT reactions. P1 PCR products 1, 2, 3 and 7 were amplified with BD Advantage 2 polymerase kit. P1 PCR products 4, 5 and 6 were amplified using *Pfu* polymerase. Second round or P2 PCR products (blue) were all amplified using *Pfu* polymerase



Optimisation of PCRs generated for sequencing purposes

As described above, nested PCR was used to amplify the genome. Diagnostic PCR identified whether RTs were successful so that P2 amplifications could be performed. Figure 6.2 shows, in lanes 2, 4 and 6, 270 base pair products from a diagnostic PCR used to amplify a region in the 5'UTR. The yield of PCR in lane 2 appears less than that in lanes 4 and 6. Also, there appears to be some non-specific product of less than 100 bp, which is also present in the negative control. This is unlikely to be a dimer of the primers given its close migration to the 100 bp marker. Such first round PCR templates as in lane 2 were not used for further amplifications.

Once the presence of a diagnostic PCR product had been confirmed, PCR fragments from other regions of the cDNA template were amplified for sequencing. Figure 6.3 shows agarose gel electrophoresis for optimisation of PCR conditions for amplification of fragment c (**PCR 15**). The PCR, which produced the best yield of product occurred at an annealing temperature of 60°C.

6.3.2 Assembling majority sequence

A consensus sequence was made by aligning sequences obtained from direct sequence reactions. As the PCR fragments overlapped, it was possible to assemble a contiguous sequence of DNA (contig). This comprised a series of overlapping fragments that encompassed the entire length of the genome. A UNIX based contig mapping program called GELSTART (Generic Computer Group programs) was used to assemble the contig and calculate a consensus. Before sequences were input into GELSTART, the original electropherogram was examined to ensure that the sequence was of good quality. Sequences, which were inserted into GELSTART, were assembled under the following conditions:

- word size - 0.5
- fraction of words in overlap - 6
- minimum overlap - default

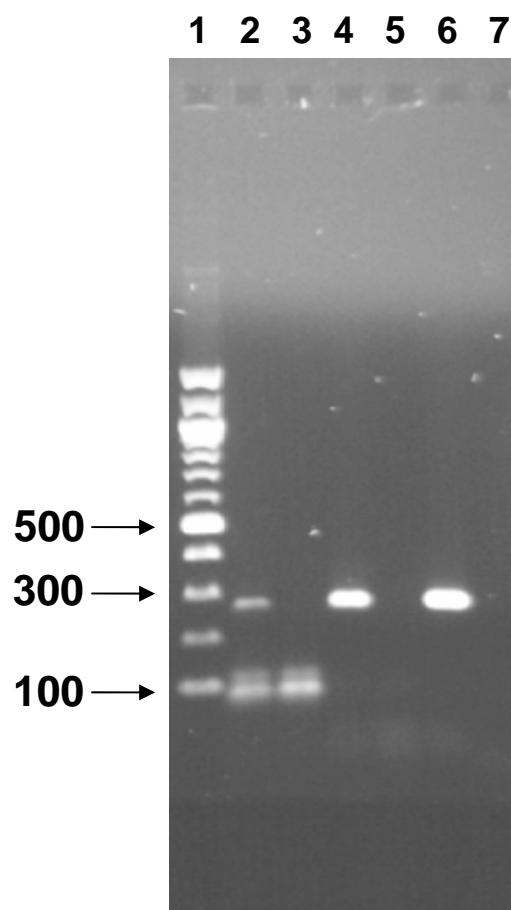


Figure 6.2. Agarose gel electrophoresis of second round PCR products used to ascertain if HCV cDNA was present. PCR products are in lanes 2, 4 and 6. Negative controls are in lanes 3, 5 and 7. Lane 1 contains NEB 100 bp ladder.

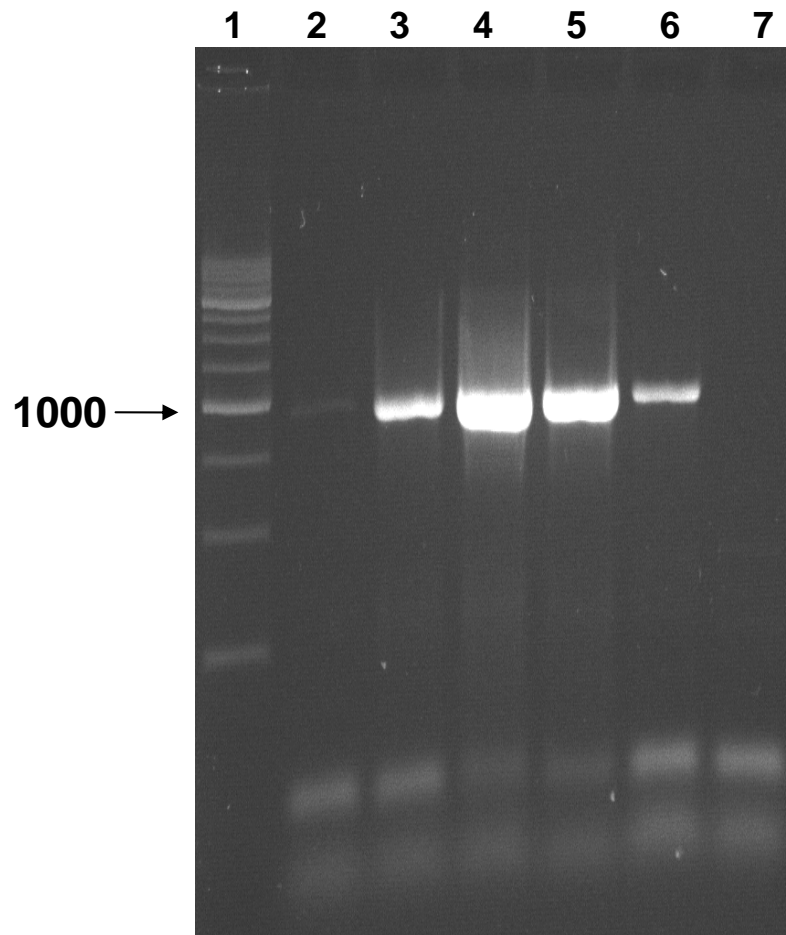


Figure 6.3. Agarose gel electrophoresis of optimisation of PCR amplification for fragment C. Lane 2 - 7 contain PCR amplification fragments generated at varying temperatures starting in lane 2 at 50°C and ending in lane 6 at 70°C, increasing in increments of 5°C. Lanes 1 and lane 7 contain molecular weight marker XVI (Roche) and the negative control for the 60°C PCR, respectively.

After the contig had been assembled, it was necessary to perform manual alignments to assign nucleotide type at regions where the consensus was unclear. This required closer scrutiny of the electropherogram to ascertain whether the nucleotide at that position had been assigned correctly.

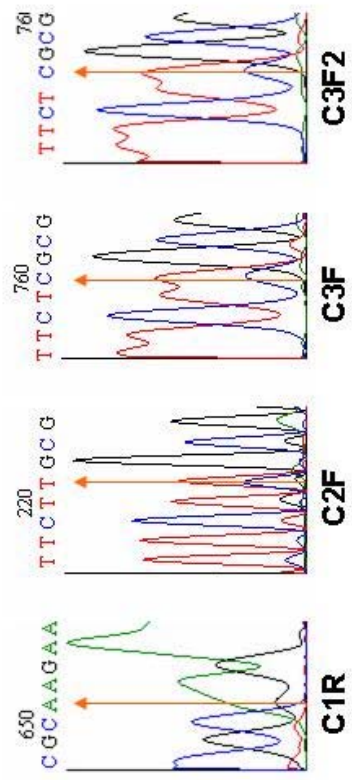
By way of example, figure 6.4 shows how an ambiguity in a sequence alignment from sequences produced from fragment c was resolved. The multiple sequence alignment had been unable to decide between assigning a T nucleotide or a C nucleotide. There were four sequences used in the alignment C1R, C2F, C3F and C3F2. These primers produced sequence between 3471 bases and 4098 bases long. The output sequence for CF3 and CF32 had been assigned to a C. However, checking the electropherogram showed that although the output sequence had assigned a C, the electropherograms indicated a T residue at this position. Although the sequence for C1R was difficult to ascertain whether the position was a C or T, other sequences showed a T peak at this point. A C peak was present at this region but was less pronounced. This might have suggested that a C variant of the majority sequence at this position in the genome was present within the viral quasispecies.

Once the majority sequence had been assembled (Appendix 1), it was possible to compare the sequence with other genotype 3 sequences. A comparison between the nucleotide sequence of GM isolate and the genotype 3a isolate sequence, 3aCB (Shukla et al., 1998) found 93 % identity between sequences. Sequence identity with genotype 3b isolate nucleotide sequence TR3b was lower at 78.5 % (Chayama et al., 1994). A comparison between the nucleotide sequence of isolate GM and the genotype 1b Con1 sequence found 68.1 % identity (Lohmann et al., 1999). Multiple alignments of the GM isolate protein sequence with 3aCB, TR3b and Con1 found an amino acid deletion at valine 1756. This valine occurred in the linker sequence between two amphipatic helices in NS4B. A protein sequence alignment performed with GM and JFH1 genotype 2a sequences showed that although the valine was not present in JFH1 an amino acid deletion of a methionine still occurred at this position (Kato et al., 2001). Valine and methionine are both neutral non-polar residues. The significance of the deleted amino acid in isolate GM was unknown.

Figure 6.4. Multiple sequence alignment (a) and electropherograms of sequencing products produced from sequencing primers C1R, C2F, and C3F. C3F was performed on two different occasions and the second of which is called CF32. In panel (a) areas of homology are shown in red and regions of mismatch are shown in blue. A consensus is shown below the 4 sequences. Panel (b) shows electropherograms for the area where the ambiguity occurs. An arrow on the sequence indicates which electropherogram peaks are concerned. Note that C1R was produced from a antisense sequencing primer and displays the reverse complement

a

C1R TACGGTAAGTTTCTTGGGACGGGGGTGTT
 C2F TACGGTAAGTTTCTTGGGACGGGGGTGTT
 C3F TACGGTAAGTTTCTCCTGGACGGGGGTGTT
 C3F2 TACGGTAAGTTTCTCCTGGACGGGGGTGTT
 Consensus TACGGTAAGTTTCTTGGGACGGGGGTGTT

b

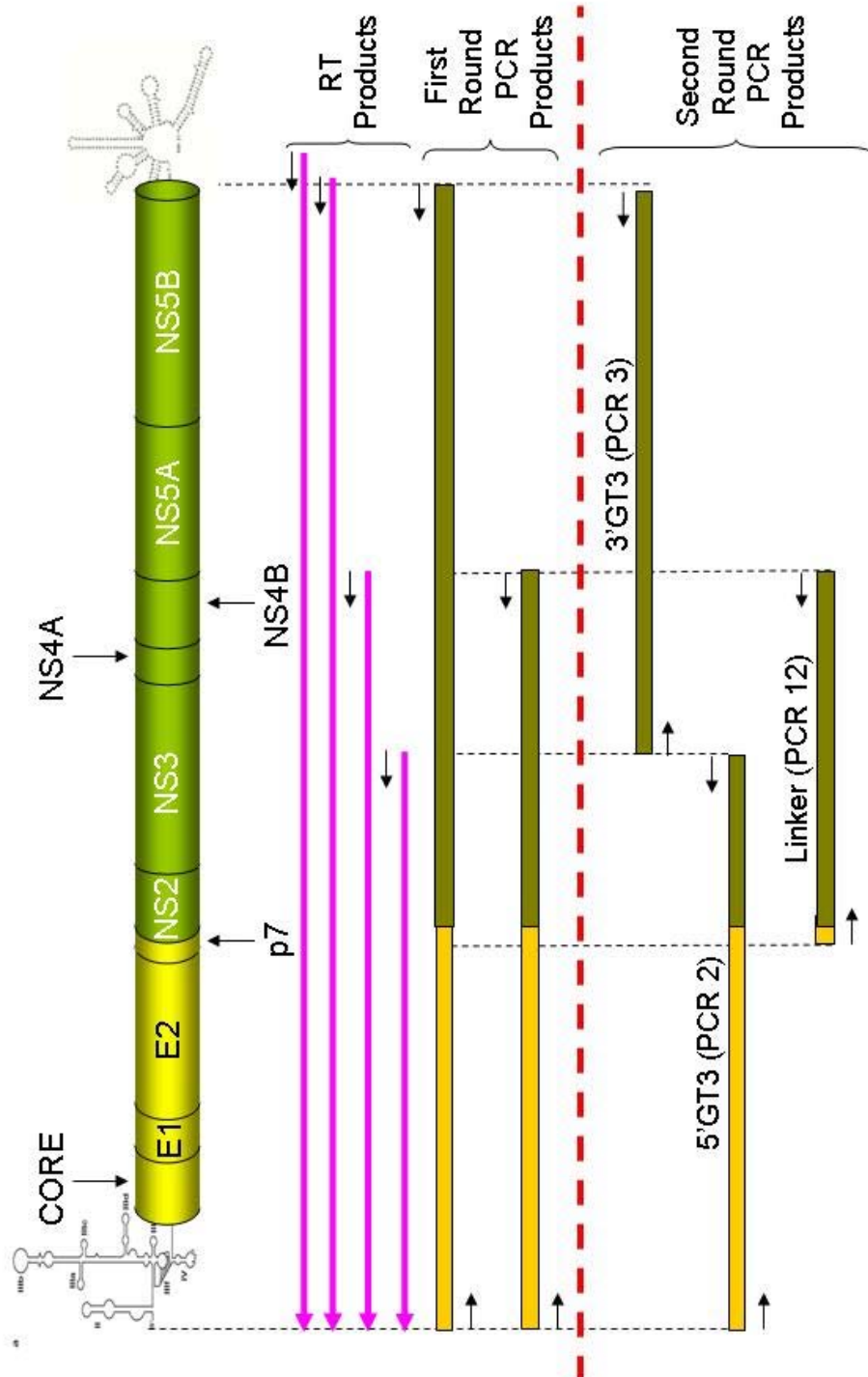
6.4 Assembling a genotype 3 replicon that would express constitutively in cells

6.4.1 Cloning the genome

In order to assemble a genotype 3 replicon it was first necessary to clone the genome into vectors so that sequences could be modified and propagated as required. As already explained in section 6.2.1 cDNAs had been made from RNA templates extracted from serum samples. Using these cDNAs as templates, first round PCRs amplified regions to produce 2 products (Figure 6.5). One product contained the full-length genome amplification and one contained sequences from the 5'UTR to NS4B. These were then used to as templates to perform second round PCR. The genome was ligated into pCR2.1 Topo and pGEM T-Easy plasmids in three sections using the T/A cloning method (Figure 6.6). This required a single A nucleotide overhang at the 3' end of a PCR product which was achieved by incubating PCR products with *Taq* polymerase and dATP. All subsequent ligations which directly cloned a PCR product into pGEM T-Easy were performed using this method (Figure 6.6). pCR2.1(5'GT3) contained sequences from the 5'UTR to NS3 (at base 4935). The pGEM linker contained an internal amplification fragment from p7 (at base 2622) to NS4B (at base 6120) cloned into pGEM T-Easy. pCR2.1 (3'GT3) contained sequences from the NS3 (at base 4918) to the 3' end of the genome.

Amplification of the 3' end of the genome consistently produced products, which were smaller in size than expected. Figure 6.7 shows that the yield of the PCR product obtained for amplification of the 3' end of the genome (PCR 7) was less than that obtained for amplification of the 5' end of the genome (PCR 6). The expected size of the 3'(GT3) fragment was approximately 4490 bases but products were smaller than the 4361 marker. A comparison of the majority sequence with other genotype 3 isolates had indicated that the viral genome contained a full sequence therefore this suggested one of the PCR primers was mis-priming. The PCR product amplified was cloned into pCR2.13'(GT3). The presence of the 3'(GT3) product was confirmed by restriction digest using *HpaI* and *EcoRV*. This confirmed the presence of the 3' end of the 3'(GT3) product. As expected a truncated PCR product had been produced where the anti-sense

Figure 6.5. Diagrammatic representation of cDNAs and PCRs performed on GM genotype 3 genome. cDNAs (pink) were obtained from various places in the genome using Omniscript RT kit. First Round PCR products (gold and green) were obtained from cDNAs obtained from RT reactions. First and Second Round PCRs were amplified with BD Advantage 2 polymerase kit. The linker P2 product was amplified using HF-2 Polymerase.



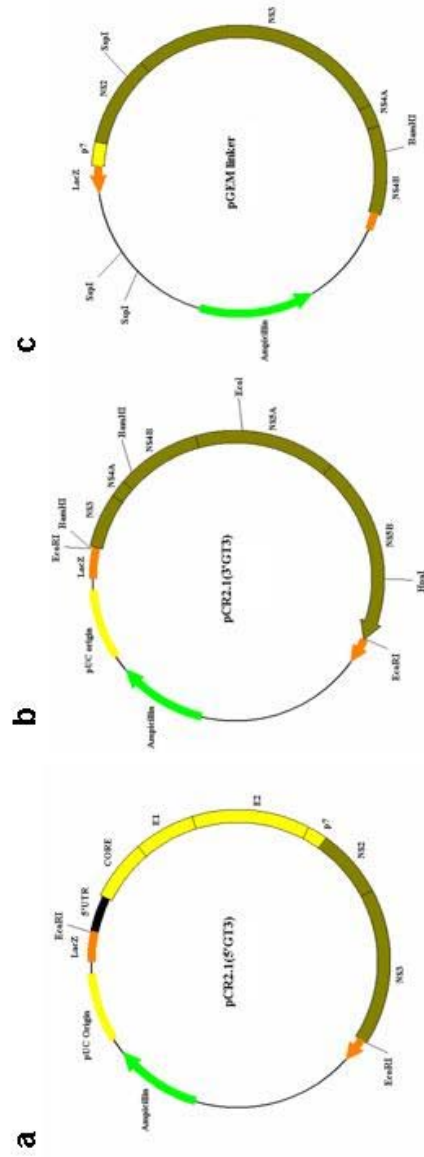


Figure 6. Diagrammatic representation of plasmid diagrams for pCR2.1(5'GT3), pCR2.1(3'GT3) and pGEW linker.

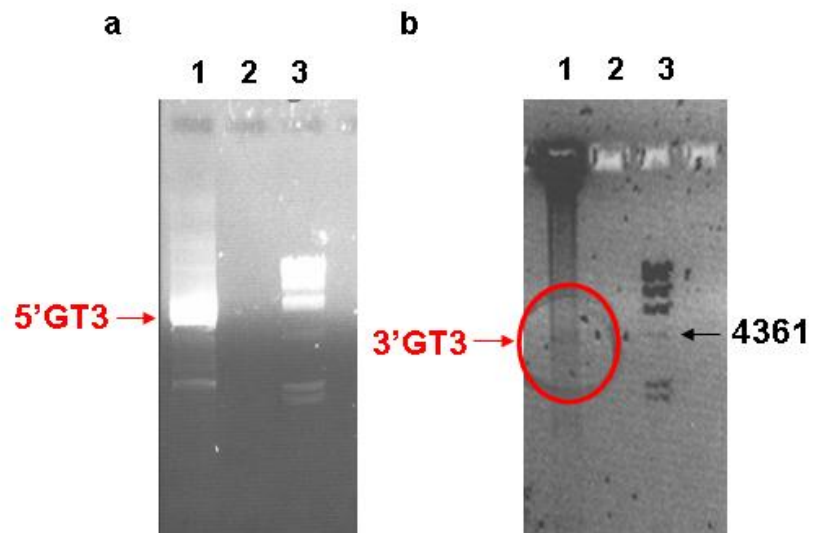


Figure 6.7. Agarose gel electrophoresis of second round PCR products of GM genotype 3 HCV 5' (a) and 3' (b) ends of the genome. a) shows amplification (PCR 2) of the 5'GT3 product from the end of the 5'UTR to base 4935 and b) shows amplification (PCR 3) of 3'GT3 product from base 4928 to base 9425 (circled). a) shows a positive image and b) shows a negative image to allow better product visualisation. PCR products (lane 1), negative control (lane 2) and molecular weight marker II (Roche)(lane 3).

PCR primer (Primer 77) had misprimed producing a PCR product approximately 200-300 bases shorter at the 3' end of the product. Figure 6.8 shows an *HpaI* and *EcoRV* digest of the pCR2.1(3'GT3) with the insert in 3'-5' orientation. If full-length product had been present digested DNA fragments of 4701 bp and 3618 bp would be produced. The digest showed that the larger fragment of 4701, which was derived from the very 3' terminal of the genome, was truncated. This supported the hypothesis that the anti-sense PCR primer had mis-primed. Diagnostic PCR was also performed on the pCR2.1(3'GT3) clones to determine whether it was possible to amplify fragments D, G H and F (Figure 6.1). It was possible to amplify fragments D, G and H but fragment F failed to amplify.

6.4.1.1 Cloning the 3' end of the genome

Previous PCRs had been unable to amplify the region of the genome, which contained the stop codon and 3' UTR. The majority sequence had been made as far as base 9319 but attempts to amplify to the end of the coding sequence using proofreading enzymes had been unsuccessful. Despite varying annealing temperatures, different concentrations of reaction buffer and magnesium salts, all attempts to amplify the 3' UTR were unsuccessful. Changing the polymerase to *Taq* polymerase allowed amplification of the last 100 bases of the genome. Furthermore, by lowering the annealing temperature to 46°C a PCR product was produced which was the correct size to be the 3' UTR.

Although initial attempts to amplify the 3'UTR failed it was eventually obtained from a PCR made by a previous laboratory member, Dr Petra Preikschat. She had made PCR products containing the full length 3' UTR derived from the same GM isolate used in my studies after using Superscript RT and *Taq* polymerase PCR. The original superscript RT was performed as described in section 2.2.3.2. and PCRs were performed as with previous 3'UTR amplifications (PCR 23) using primer 80 instead of primer 39. Semi-nested PCR was performed on these products using *Taq* polymerase to produce a high yield product containing the complete 3'UTR. As the last 98 bases of the HCV genome are highly conserved an antisense primer was designed based on other HCV sequences. Due to the last 3 nucleotides of the genome being "AGT" the addition of ACT 3' to this created a *ScaI* restriction enzyme.

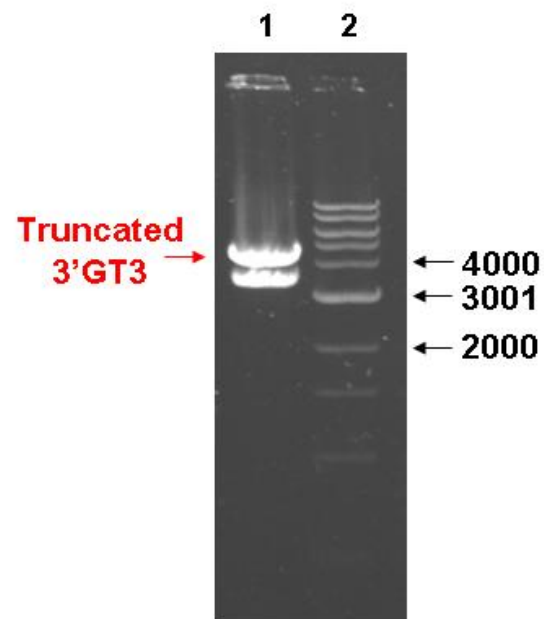


Figure 6.8. Agarose gel electrophoresis of an *HpaI* and *EcoRV* restriction enzyme digest of pCR2.1(3'GT3). The panel shows an *HpaI/EcoRV* restriction enzyme digest of a pCR2.1(3'GT3) where the insert is in the 3'-5' direction. The truncated 3'GT3 restriction digested product is indicated. Lane 1 shows digest of plasmid DNA. Lane 2 contains a 1 Kb ladder (NEB). DNA ladder sizes are indicated beside the panel.

site. Digestion of clones containing the *ScaI* restriction site produced blunt ended DNA fragments, which allowed “run off” transcripts to be made, which contained only HCV sequence. Resultant PCR products were then cloned into pGEM T-Easy vectors to create the pGEM 3’UTR plasmid. Plasmids were analysed by restriction enzyme digest and sequencing. Figure 6.9 shows that the 3’ UTR sequence of isolate GM is similar to other genotype 3 3’ UTR sequences. The alignment uses four genotype 3 sequences TR3b (Chayama et al., 1994), 3aCB (Shukla et al., 1998), Ka3503a (Yamada et al., 1994) and NZL1 (Sakamoto et al., 1994) and the 5-15 1b replicon sequence, derived from the Con1 isolate (Lohmann et al., 1999). For comparison the 1b sequence showed that the extra sequence within the variable region of the 1b isolate was not present. The cloning of the GM 3’ UTR completed the cloning of the GM genome which could now be modified for assembly of a genotype 3 replicon.

6.4.2 Modification of the isolate GM genome

6.4.2.1 Incorporation of a T7 promoter flanking the 5’UTR

In order to produce “run off” replicon RNA transcripts it was necessary to engineer a T7 promoter to flank the 5’ UTR. This was achieved using PCR and cloning. The T7-5’UTR-GT3 primer which contained a truncated T7 promoter flanking a small portion of the 5’ UTR was used together with a 3550-gt3*SpeI* primer in a PCR described in section 2.2.5 (PCR 24). pCR2.1(5’GT3) was used as a template for amplification of this region. The resultant PCR product produced a 3550 bp fragment which was cloned into pGEM T-Easy. Clones were initially analysed by restriction enzyme digest to determine if they contained an insert of appropriate size. To determine whether the T7 promoter had been appropriately incorporated onto the 5’ end of the genome, sequence analysis was performed. Figure 6.10 shows successful incorporation of the T7 promoter. The minimal T7 promoter sequence was used as it had been successfully employed with the genotype 1b replicon.

6.4.2.2 Cloning the EMCV IRES and neomycin gene to the 5’UTR

The original 1b genome had been modified to create a bicistronic replicon in which the first cistron was under the control of the HCV internal ribosome entry site (IRES) resulting in translation of the neomycin phosphotransferase gene and

Figure 6.9. Multiple sequence alignment of 4 genotype 3'UTR sequences, the GM isolate 3'UTR and the 1b 3'UTR sequence. Areas of homology are coloured in red. A consensus is shown below the alignment where capital letters indicate that sequences are completely homologous and lower case letters indicate that there is some differences between sequences. The stop codon is highlighted in yellow.

Stop
Codon

```

NZL1      1 TTGGCTACTCCTACTAACAGTAGGGGTAGGCATCTTTCTCTTGCCAGCTCGATGAGCTGG
3 aCB     1 TTGGCTACTCCTACTAACGGTAGGGGTAGGCATCTTTCTCTTGCCAGCTCGGTGAGCTGG
Tr3b     1 TTGGCTACTCCTACTAACCGTAGGGGTAGGCATTTCTCTTGCCAGCTCGGTGAGCTGG
Ka350    1 TTGGCTACTCCTACTAACAGTAGGGGTAGGCATCTTTCTCTTGCCAGCTCGGTGAGCTGG
GM       1 TTGGCTACTCCTACTAACGGTAGGGGTAGGCATCTTTCTCTTGCCAGCTCGGTGAGCTGG
5-151b   1 GTGGCTACTCCTACTTCTGTAGGGGTAGGCATCTATCTATCTCCCAACCGATGAAACGGG
consensus 1 ttgacctactcctactaacagtaggggtaggcatactttctcttggcagctcgaatgagctgg

```

```

NZL1      61 TAAGATAACA CTCCATTTCTTTTTGTTTTTTTTTTTTTTTTTTTTTTTTTTTTTTTTTTT
3 aCB     61 TAAGATAACA CTCCA-----
Tr3b     61 TAGGTAAACA CCCCACCCCTGTCTTTTTT-----
Ka350    61 TAGGATAACA CTCCATTTCTTTTTGTTTTTTTTTTTTTTTTTTTTTTTTTTTTTTTTTTT
GM       61 TAAGATAACA CTCCCTTTCTTTTTGTTTTTTTTTTTTTTTTTTTTTTTTTTTTTTTTTTT
5-151b   53 GAGCTAAACA CTCCAGGCCAATAGGCCAACCCTGTTTTTTCCCTTTTTTTTTTTTTTTTTTTT
consensus 61 tAagataACA CtCCattctcttttttgtttt tttttttttttt

```



Additional sequence only found in 1b replicon but not in GM isolate 3'UTR sequence

the second cistron was controlled by the encephalomyocarditis virus (EMCV) IRES resulting in translation of the non-structural genes. In designing the genotype 3 replicon, a similar arrangement was envisaged. Therefore, it was necessary to clone the neomycin phosphotransferase gene and the EMCV IRES. This was achieved by amplifying this region from a plasmid containing the 1b replicon. Amplification (described in section 2.2.5, PCR 25) used an antisense primer, which bound the 3' of the EMCV IRES and incorporated a *Bgl*II site into the sequence to allow subsequent cloning. However this *Bgl*II was removed in the final construct by site directed mutagenesis to return the EMCV IRES to its original sequence. The resultant PCR product was cloned into pGEM T-Easy and analysed by restriction enzyme digest to confirm the presence of insert.

Once a clone containing the neomycin and EMCV IRES was obtained it was used as a vector to clone in a 5'UTR flanked by a T7 promoter (Figure 6.11). This was done by digesting pGEMT7(5'GT3) and pGEMneo-emcv with *Spe*I and *Stu*I and ligating the neo-emcv fragment produced into the pGEMT7(5'GT3) recipient vector. Successful ligations were analysed by restriction enzyme digest to determine if insert was present. The resultant plasmid was called pGEMT7-emcv.

6.4.2.3 Cloning NS3, 4A and 4B into pGEM T7 emcv

In order to clone the non structural genes to be under control of the EMCV IRES, it was first necessary to modify NS3 by incorporating a start codon before its coding sequence. This was done by amplifying a product from pGEM linker plasmid by the PCR described in section 2.2.5 (PCR 26). The *Bgl*II restriction site that was placed at the end of the EMCV sequence was also placed in the sense primer before the start codon. A *Spe*I restriction site was also incorporated into the a6120-gt3 primer to allow subsequent cloning of the PCR product. Successful amplifications were then cloned into pGEM T-Easy and analysed for the presence of insert by restriction enzyme digest. The resultant plasmid was called pGEMNS3-GT3.

A 2701 base fragment from pGEMNS3-GT3 containing NS3, 4A and 4B was cloned into pGEMT7-emcv by digesting pGEMNS3-GT3 and pGEMT7-emcv with *Bgl*II and *Spe*I (Figure 6.12). The resultant plasmid contained the 5'UTR flanked by a T7 promoter, a neomycin phosphotransferase gene, the EMCV IRES and NS3-4B.

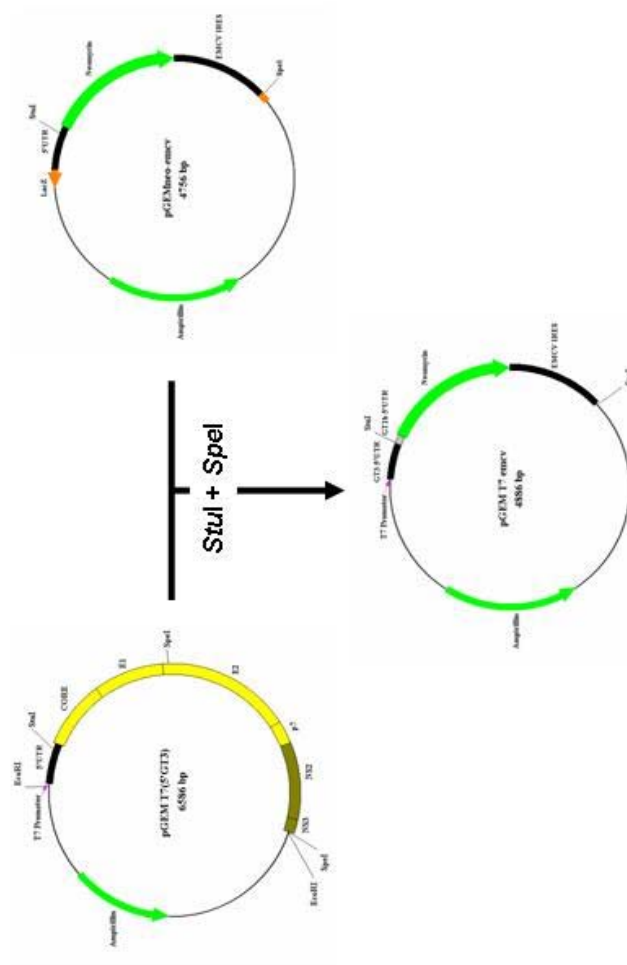


Figure 6.11. Diagrammatic representation of the cloning of pGEMT7-ermcv with *SpeI* and *StuI* restriction enzyme digest of pGEMT7(5'GT3) and pGEMneo-ermcv. The *SpeI*/*StuI* digested neo-ermcv fragment was ligated into the *SpeI*/*StuI* pGEMT7(5'GT3) plasmid. This produced pGEMT7-ermcv.

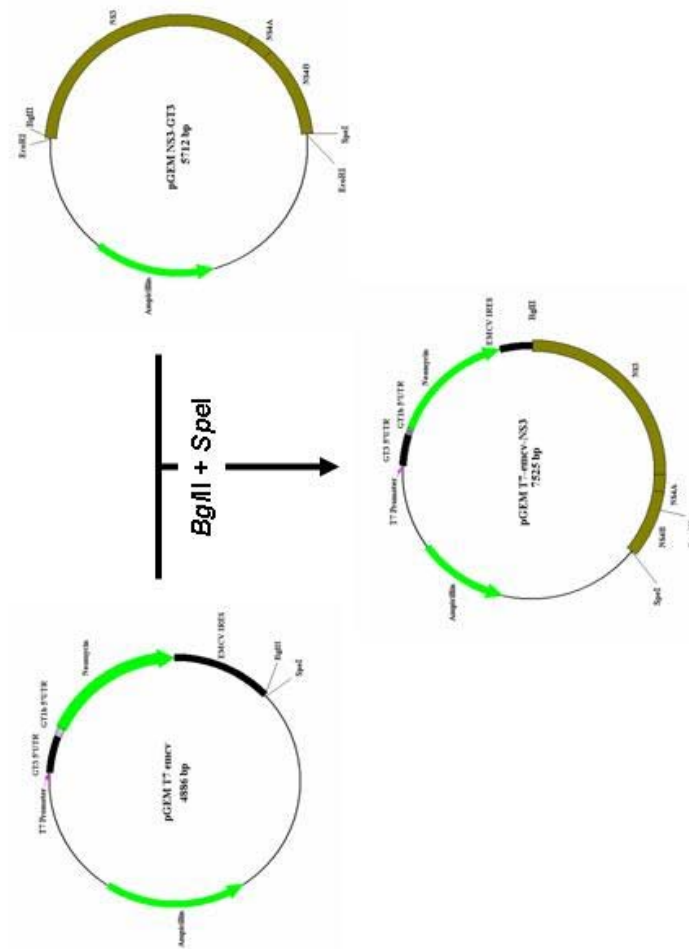


Figure 6.12. Diagrammatic representation of the cloning of pGEM11-emuV-NS3 with *Bgl*II and *Spe*I restriction enzyme digest of pGEM11-emuV and pGEMNS3-GT3. The *Bgl*II/*Spe*I digested NS3-NS4B fragment was ligated into the *Bgl*II/*Spe*I digested pGEM11-emuV plasmid. This produced pGEM11-emuV-NS3.

Restriction enzyme digest was used to confirm successful cloning. The resultant plasmid was called pGEM7-emcv-NS3 and was 7525 bases in length.

6.4.2.4 Cloning the 3'UTR onto pCR2.1(3'GT3)

As already discussed, pCR2.1(3'GT3) was truncated at the very 3' border of the insert missing part of NS5B coding sequence and also the 3'UTR. Using the insert from pGEM3'UTR, it was possible to reassemble the clone so that the full 3' sequence was present (Figure 6.13). This was performed by digesting pGEM3'UTR with *HpaI* and *SpeI* to release a 850 base fragment which could then be cloned into pCR2.1(3'GT3). Presence of the insert was confirmed by restriction enzyme digest. The resultant plasmid was called pGEM(GT3)-X and was 8386 bases in length.

6.4.2.5 Transferring the 5' and 3' of the replicon into pUC18 and removal of the *BglII* restriction enzyme site

In order to transcribe the RNA replicon, a truncated T7 promoter had been fused to the 5'UTR of the HCV sequence. However the pGEM T-Easy plasmid already has an endogenous T7 promoter within its sequence. Therefore it was necessary to clone into another plasmid vector, which did not have a T7 promoter. The plasmid pUC18 was used for this where *EcoRI* and *BamHI* digests of pGEM7-emcv-NS3 produced a 4066 base fragment, which was cloned into a digested pUC18 vector. Successful transformants were confirmed for presence the new plasmid construct by restriction enzyme digest. The plasmid was called pUC18T7-NS3 (Figure 6.14).

Previously a *BglII* restriction enzyme site had been incorporated into the 3' end of the EMCV IRES to allow cloning of the HCV genome. However it was thought that this may affect the efficiency of the EMCV IRES so it was necessary to remove the *BglII* restriction enzyme site. This was achieved by using site directed mutagenesis where primers were designed to mutate the sequence back to the EMCV IRES consensus. Successful revertant mutants were analysed by restriction enzyme digest and sequencing. Mutants lacking the *BglII* site were used for future cloning.

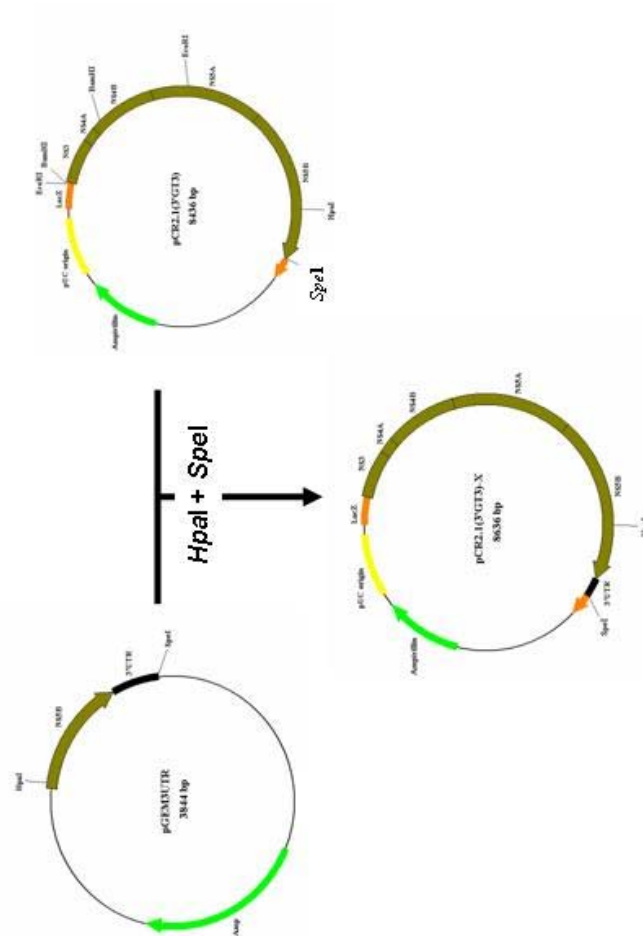


Figure 6.13. Diagrammatic representation of the cloning of pGEM(3'GT3)-X with *HpaI* and *SpeI* restriction enzyme digest of pCR2.1(3'GT3) and pGEM3'UTR. The *HpaI*/*SpeI* digested 3'UTR fragment was ligated into the *HpaI*/*SpeI* pCR2.1(3'GT3). This produced pCR2.1(3'GT3)-X.

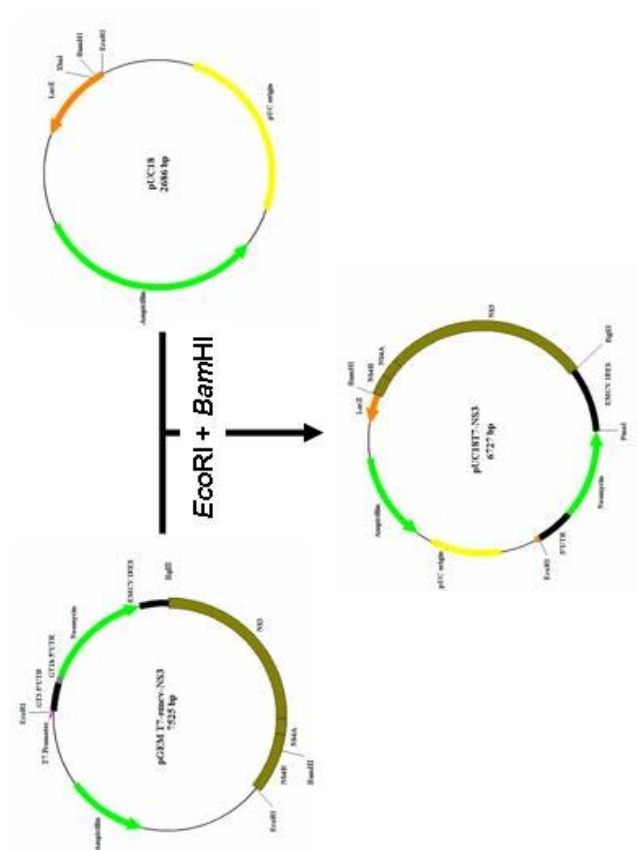


Figure 6.14. Diagrammatic representation of the cloning of pUC18T7-NS3 with *EcoRI* and *BamHI* restriction enzyme digest of pGEMT7-emcv-NS3 and pUC18. The *EcoRI/BamHI* digested T7-emcv-NS3 fragment was ligated into the *EcoRI/BamHI* pUC18. This produced pUC18T7-NS3.

The 3' end of the genome was also cloned into pUC18. This was done by digesting pCR2.1(3'GT3)-X with *Bam*HI and *Spe*I to release a fragment of 3980 bases which was cloned into *Bam*HI and *Xba*I digested pUC18 (Figure 6.15). *Xba*I was used as oppose to *Spe*I because there was no *Spe*I site in pUC18. However *Xba*I produced a sticky overhang after being cut, which could religate with *Spe*I. Successful plasmid constructs were analysed by restriction enzyme digest for the presence of the ligated fragment. The resultant plasmid was called pUC18(3'GT3).

6.4.3 Sequencing plasmid constructs and site directed mutagenesis

In section 6.2.3 it was described how the majority sequence for isolate GM was assembled. It was therefore necessary to mutate the sequence of the cloned parts of the genome to the majority sequence. Sequencing was performed on pUC18T7-NS3 and pUC18(3'GT3) using primers previously used for assembly of the majority sequence described in section 2.1.11. Two internal primers in the EMCV IRES were also used to obtain sequence that covered this area of the construct. Sequence contigs were aligned using the "Gel Start" program (Generic Computer Group programs) and a consensus obtained. The plasmid consensus sequence was then aligned with the majority sequence to deduce where they differed from each other. A sequence alignment of pUC18T7-NS3 sequences with majority sequence showed one difference in the 5'UTR and one non-synonymous difference in the non-structural protein region in NS3. Sequence alignment was also performed between the neomycin-EMCV IRES sequence from the 1b replicon. It was found that 1 synonymous difference occurred in neomycin phosphotransferase gene and 2 deletions in the EMCV IRES. The reason for this may have been that error prone *Taq* polymerase had been used after problems with the use of proof reading enzymes. One of the deletions had occurred over a Poly-C tract of 10 cystine nucleotides. This repetitive sequence may have been difficult to amplify. A sequence alignment with pUC18(3'GT3) found 5 non-synonymous mutations and 17 synonymous mutations. All non-synonymous mutations in pUC18T7-NS3 and pUC18(3'GT3) are described in table 6.1.

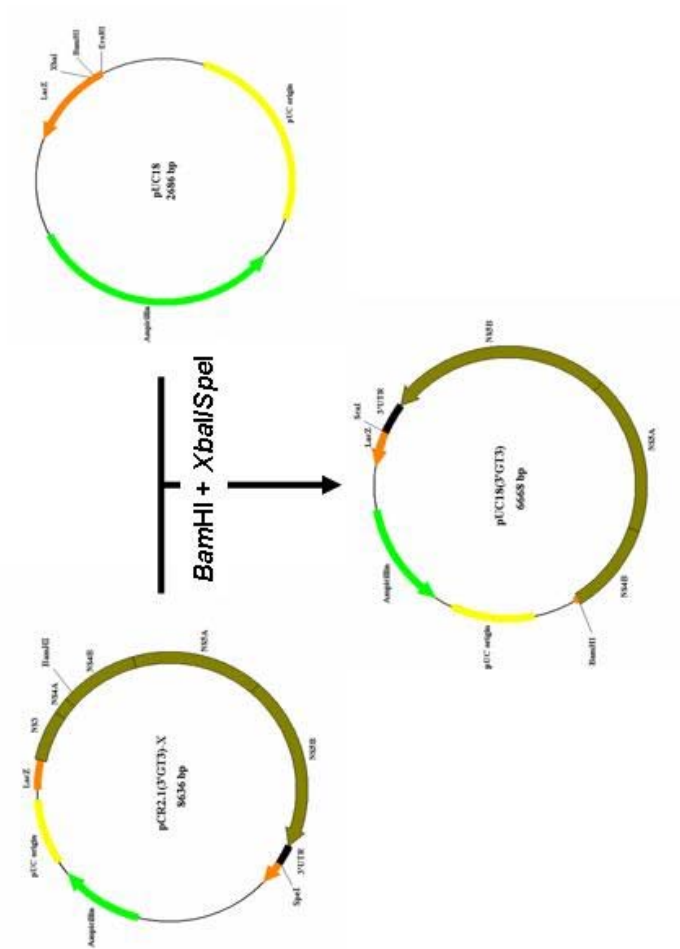


Figure 6.15. Diagrammatic representation of the cloning of pUC18(3'GT3) with *Bam*HI and *Xba*I/*Spe*I restriction enzyme digest of PCR2.1(3'GT3)-X and pUC18. The *Bam*HI/*Spe*I digested (3'GT3)-X fragment was ligated into the *Hpa*I/*Xba*I pUC18. This produced pUC18(3'GT3).

Mutation Name	Location in genome (nucleotide)	Codon difference	Nucleotide/Amino acid change (from → to)
Mutation 1	228	G → T	Deletion → Adenine
Mutation 2	4824	GCC → ACC	Alanine → Threonine
Mutation 3	6303	GAC → GAA	Aspartic acid → Glutamic acid
Mutation 4	7805	GCG → GTG	Alanine → Valine
Mutation 5	8315	ATT → ACT	Isoleucine → Threonine
Mutation 6	8979	GCT → ACT	Threonine → Alanine
Mutation 7	9111	GCCC → GCC	Insertion → Alanine

Table 6.1. A table indicating the position of non-synonymous mutations and their location in the genome. Where applicable amino acid codon and amino acid conversion is shown.

Site-directed mutagenesis was used to mutate non-synonymous bases in pUC18T7-NS3 and pUC18(3'GT3) to the majority sequence. In total there were 7 differences to be corrected in the plasmid constructs. Primers were designed as follows as described by the stratagene site-directed PCR protocol (section 2.2.15, PCR 27).

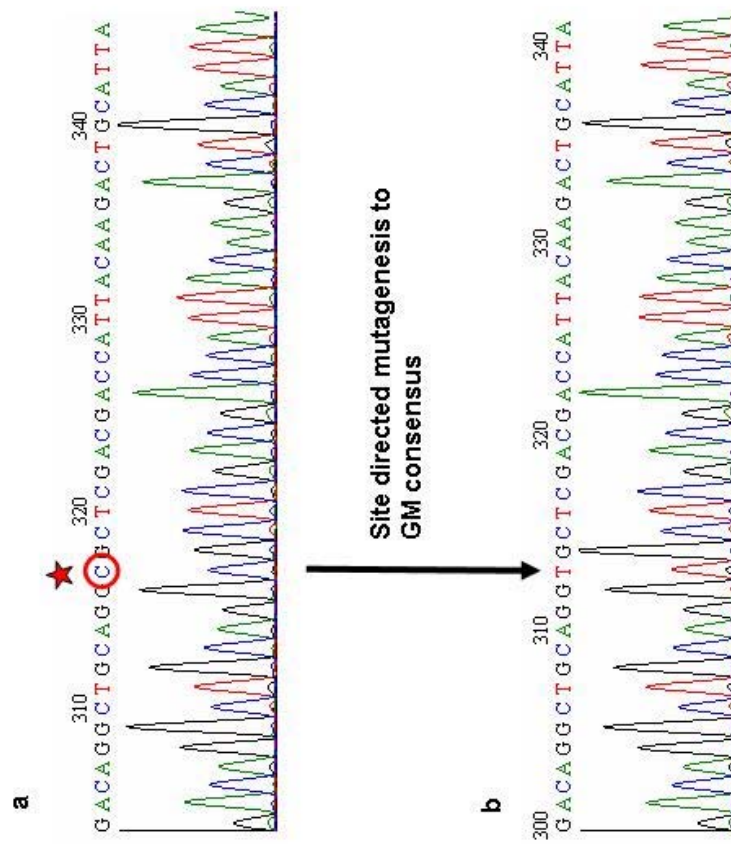
Site directed mutagenesis PCRs were performed using the BD Advantage 2 polymerase mix. Clones were selected and analysed by sequencing. Figure 6.16 shows electropherograms before and after site directed mutagenesis for mutation 4. The GCG was changed back to the majority GTG (A>V).

To minimise the amount of time it took to mutate plasmids, rather than perform one mutation then the next till all were done in a sequential manner, site-directed mutageneses was performed in parallel. For instance, to obtain the pUC18NS3-Mut1,2 plasmid, both site directed mutagenesis PCRs were performed at the same time in separate reactions. Resultant plasmids, which had successfully taken the reverted mutations, then were cloned together by digesting plasmids with *Bmg*BI and *Eco*RI (Figure 6.17). Here, only two mutations were involved. However in pUC18(3'GT3) there were 5 sites to be mutated. An initial round of mutagenesis was used to produce pUC18 (3'GT3) Mut3, pUC18 (3'GT3) Mut4 and pUC18 (3'GT3) Mut7. These were then confirmed by direct sequencing and used as templates for a second round of mutagenesis. PCR was used to generate mutation 5 in pUC18(3'GT3)Mut4 and also mutation 6 in pUC18(3'GT3)Mut7. Once all the mutagenesis was completed and successful mutations had been confirmed by sequencing, fragments were joined together into one plasmid (Figure 6.18). This was performed by digesting pUC18(3'GT3)Mut3 with *Bam*HI and *Eco*RI to produce a 1140 base DNA fragment, pUC18(3'GT3)Mut4,5 with *Eco*RI and *Hpa*I to produce a 2030 base DNA fragment and pUC18(3'GT3)Mut6,7 with *Bam*HI and *Hpa*I to produce a 3490 base DNA fragment. The resultant plasmid pUC18(3'GT3)Mut3-7 was analysed by restriction enzyme digest to confirm the presence of the complete 3'GT3 fragment.

6.4.3.1 Cloning the EMCV IRES

Nucleotide sequencing had indicated that the EMCV IRES had two mutations, which might affect its activity. Because one was a deletion it was decided it

Figure 6.16. Electropherograms of sequence obtained from pUC18(3'GT3) before (a) and after (b) site-directed mutagenesis of mutation 4. The base to be mutated is circled and is starred.



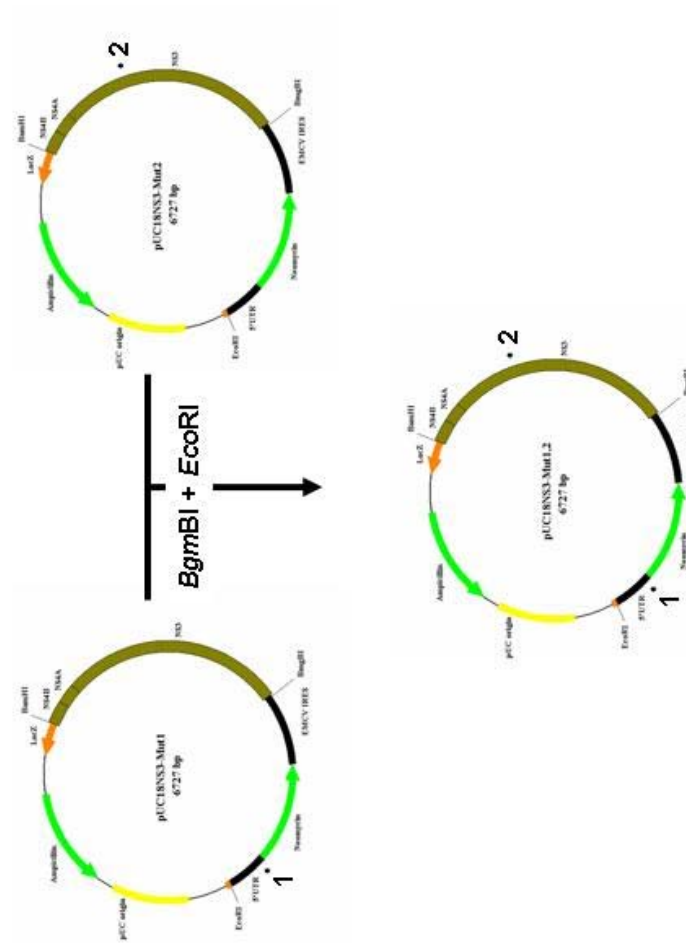
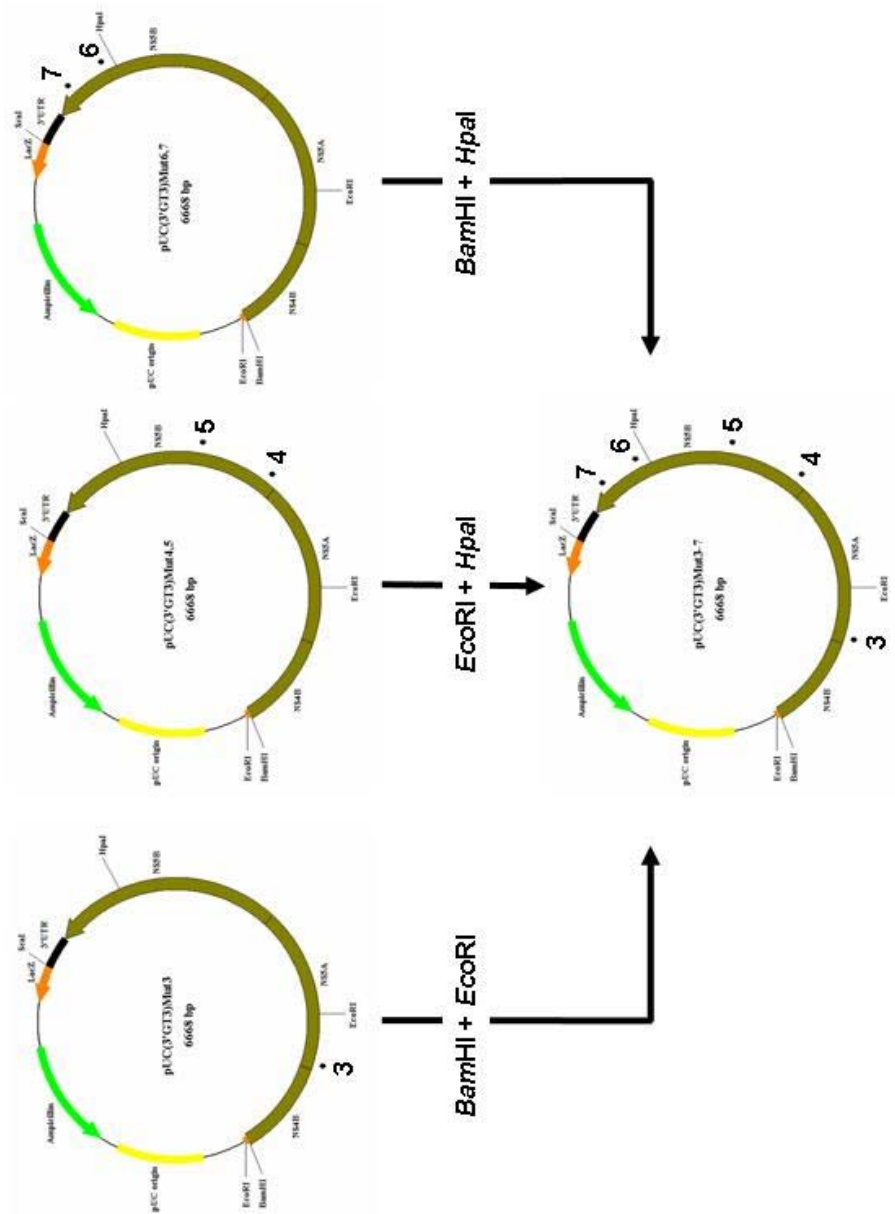


Figure 6.17. Diagrammatic representation of the cloning of pUC18T7-NS3 Mut1-2. *BgmBI* and *EcoRI* restriction enzyme digest of pUC18T7-NS3 Mut1 and pUC18T7-NS3 Mut2. The *BgmBI/EcoRI* digested NS3-NS4B-Mut2 fragment was ligated into the *BgmBI/EcoRI* pUC18 NS3-Mut1. This produced pUC18 NS3-Mut1,2. Mutations are indicated as a dot and their mutation name.

Figure 6.18. Diagrammatic representation of the cloning of pUC18(3'GT3)Mut3-7. Initially site-directed mutagenesis was performed in parallel to produce pUC18(3'GT3)Mut3, pUC18(3'GT3)Mut4,5 and pUC18(3'GT3)Mut6,7. A triple ligation was performed with three insert fragments of DNA. pUC18(3'GT3)Mut6,7 was digested with *Bam*HI and *Hpa*I and used as a vector to mutagenized fragments of DNA from pUC18(3'GT3)Mut3 digested with *Bam*HI and *Eco*RI and pUC18(3'GT3)Mut4,5 digested with *Eco*RI and *Hpa*I. Mutations are indicated as a dot and their mutation name.



would be quicker and easier to clone the EMCV IRES again using the high fidelity BD Advantage 2 polymerase mix for its amplification. The PCR was performed as before and the product was insert into pGEM T-Easy to produce pGEM5'emcv. This was cloned into pUC18NS3-Mut1,2 by digesting both plasmids with *Ascl* and *BmgBI* to release a 1300 base fragment from pGEM5'emcv which could be cloned into pUC18NS3-Mut1,2. The resultant plasmid pUC18emcvMut1,2 was analysed by sequencing to confirm the presence of an intact EMCV IRES.

6.4.4 Cloning the genome into pSP64 Poly-A Vector

Initially, I attempted to join the mutated genome in pUC18 by cloning the 3'GT3 mutated sequence into pUC18emcvMut1-2 using restriction enzyme sites *BamHI* and *Sspl*. *BamHI* cut the genome at a unique site and *Sspl* cut in the vector sequence after the Ampicillin resistance gene. However, all attempts to clone the entire genome in pUC18 were unsuccessful. Therefore an alternate approach was adopted using another vector for holding the genome.

pSP64PolyA cloning plasmid, which does not contain a T7 promoter, was selected as a suitable vector for carrying the genotype 3 replicon. Initially the 5' end of the genome was excised from pUC18emcvMut1,2 using *EcoRI* and *BamHI* restriction enzymes. The 4062 base fragment was then cloned into a pSP64PolyA vector which had been digested with *EcoRI* and *BamHI* restriction enzymes. The resultant plasmid pSP64 GM-NS3 was 7003 bases in size (Figure 6.19).

To assemble the complete replicon, pSP64GM-NS3 plasmid was digested with *BamHI* and *Sspl* to produce a 6107 base fragment. The 3' of the genome was then cloned onto this by digesting pUC18(3'GT3)Mut3-7 with *BamHI* and *Sspl* to produce a 4594 base fragment. The resultant plasmid pSP64 GM was 10701 bases in length and contained a complete genotype 3 replicon (Figure 6.20).

6.4.5 Incorporation of the NS5A adaptive mutation and NS5B null mutation

Previous genotype 1 replicons had been found to accumulate adaptive mutations for high expression in cell culture. One highly adaptive mutation had been described in NS5A at amino acid position 2204 (Serine>Isoleucine). It was

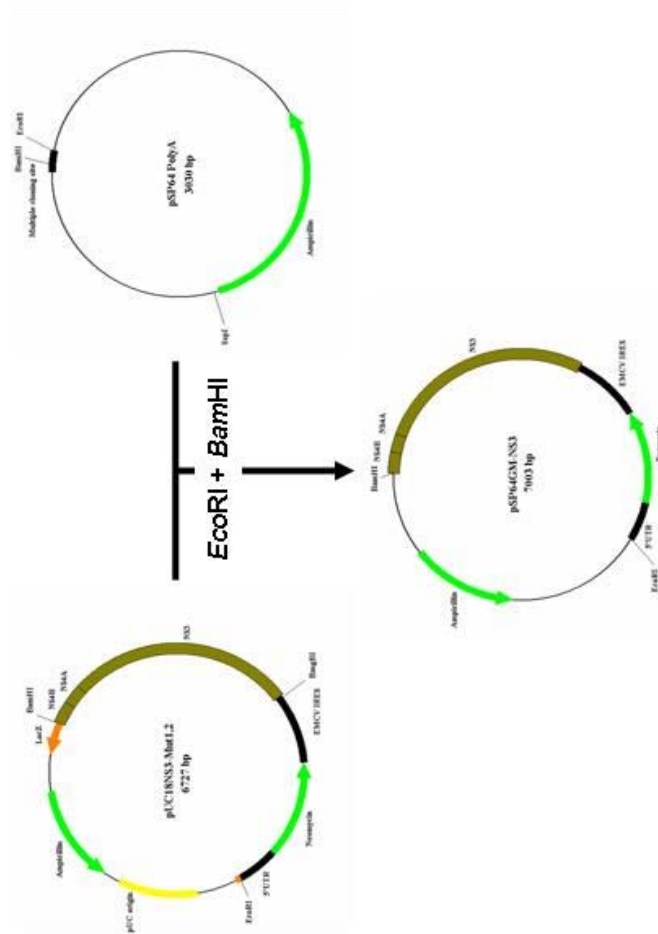


Figure 6.19. Diagrammatic representation of the cloning of pSP64GM-NS3 with *EcoRI* and *BamHI* restriction enzyme digest of pUC18NS3-Mut1,2 and pSP64 Poly A. The *EcoRI/BamHI* digested NS3-Mut1,2 fragment was ligated into the *EcoRI/BamHI* pSP64PolyA. This produced pSP64GM-NS3

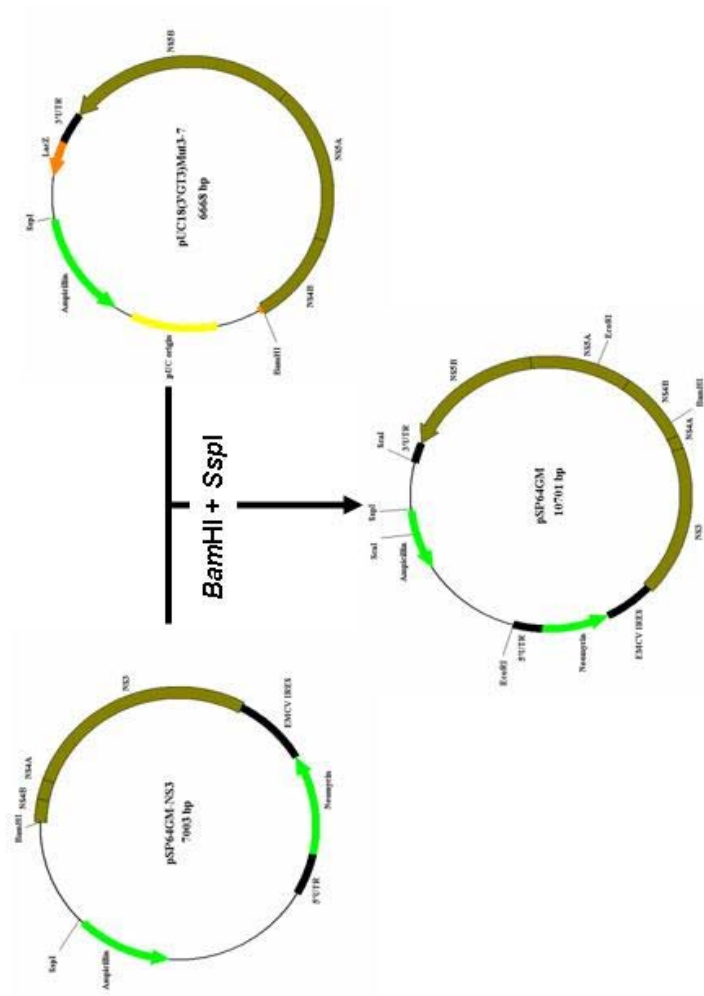


Figure 6.20. Diagrammatic representation of the cloning of pSP64GM with *Bam*HI and *Ssp*I restriction enzyme digest of pSP64GM-NS3 and pUC18(3'GT3)Mut3-7. The *Bam*HI/*Ssp*I digested (3'GT3)Mut3-7 fragment was ligated into the *Bam*HI/*Ssp*I pSP64GM-NS3. This produced pSP64GM.

decided to incorporate this mutation into our genotype 3 replicon as it might aid establishing replication. The mutation was incorporated by performing site-directed mutagenesis. Primers were designed to incorporate the mutation into NS5A (Section 2.1.11) as PCR protocol described in section 2.2.15. Successful mutants were confirmed by direct sequencing of plasmid DNA and resultant plasmids called pSP64GM*.

It was also necessary to produce a negative control replicon. The negative control replicon was exactly the same as pSP64GM except it contained a null mutation in the GDD motif found of the NS5B gene (GDD>GND). Site directed mutagenesis was used to mutate the sequence of pSP64GM. The resultant plasmid pSP64GMGND was confirmed for mutated sequence by direct sequencing of plasmid DNA. The three replicons used to establish a HuH-7 cell lines expressing the genotype 3 replicon are diagrammatically represented in Figure 6.21.

6.5 In-vitro transcription of constitutive replicons and electroporation into cells

Once replicons were assembled, RNA was transcribed from *ScaI* linearised plasmid. The digestion of the *ScaI* restriction enzyme site, which had previously been engineered to flank the 3' of the genome, enabled run off transcripts to be synthesised, which contained only HCV sequence. In order to minimise the amount of uncut plasmid, as this would interfere with the in-vitro transcription, cut DNA was agarose gel electrophoresed and gel extracted. Purified DNA was quantified by spectrophotometry and used for in-vitro transcriptions.

Figure 6.22 shows that the truncated T7 promoter flanking the 5' of the genome was able to synthesis a comparable amount of RNA compared to the equivalent 1b replicon. This indicated that the T7 promoter was functional. RNA obtained from these in-vitro transcriptions was DNase I treated with "Ambion DNase turbo" and purified by phenol chloroform extraction and ethanol precipitation (Section 2.2.13.4 and 5) to ensure that the DNA template was removed.

Figure 6.23 shows strains of HuH-7 (HuH-7, 2a-C and 1b-C) cells electroporated with purified RNA from 1b, GM, GM* and GMGND replicons. The results showed

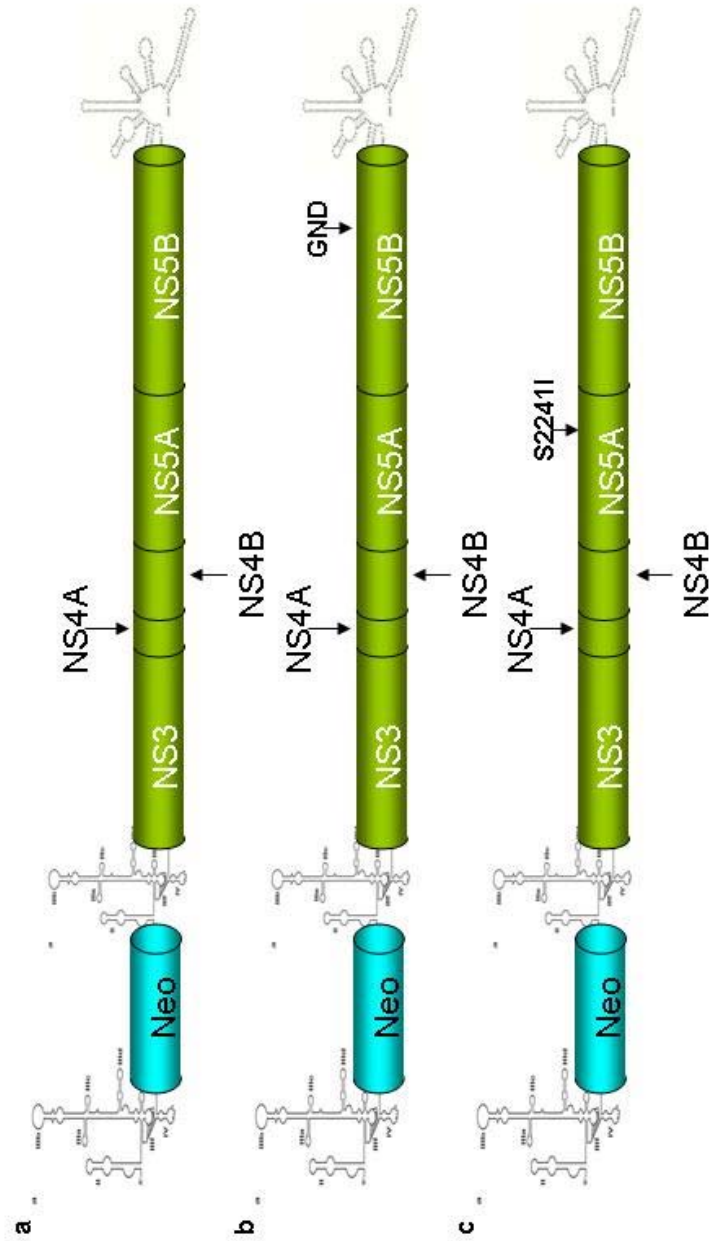


Figure 6.21. Diagrammatic representation of the RNA of genotype 3 replicons (GM, GM* and GM GND) produced after in-vitro transcriptions from *ScaI* digested pSP64 GM (a), pSP64 GM GND (b) and pSP64 GM* (c) plasmids.

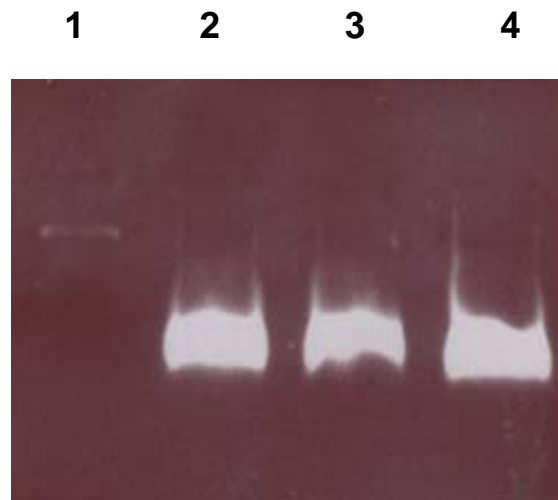
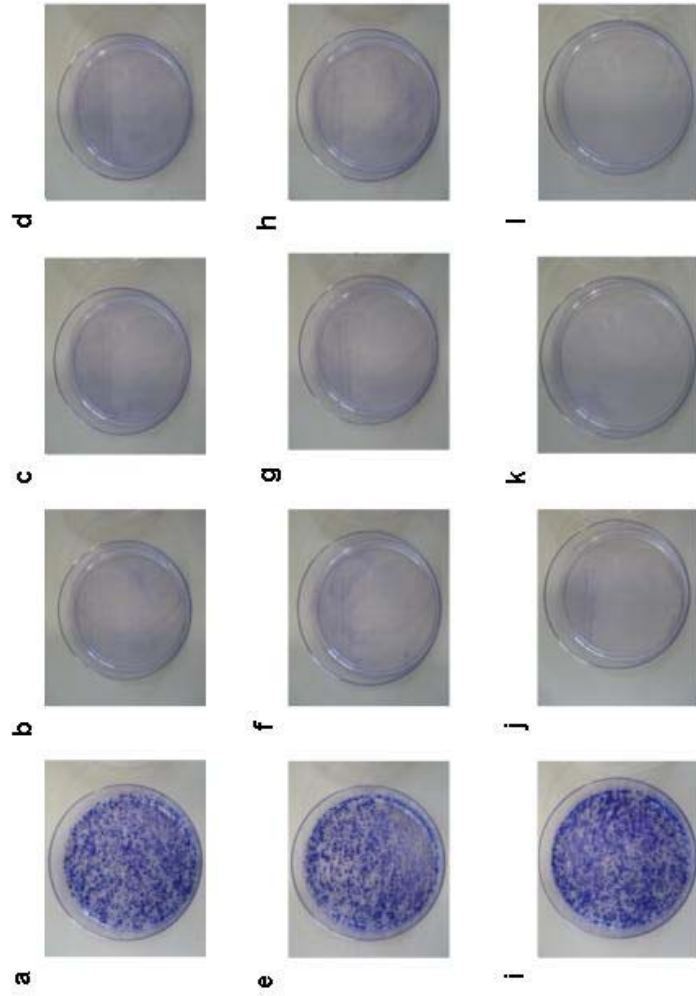


Figure 6.22. Agarose gel electrophoresis of in-vitro transcribed RNA synthesised from linearised plasmid vector using the Ambion Megascript in-vitro transcription kit. Lane 1 contains a negative control. Lane 2 contains *Xba*I digested, mung bean treated pK389neoNS3-3'/5.1 containing the genotype 1b replicon. Lanes 2 and 3 contain *Sca*I restriction enzyme digested pSP64GM* and pSP64GMGND respectively.

Figure 6.23. Colony formation assay for HUH7 (a-d), 2a-C (e-h) and 1b-C (i-l) cells (2×10^6 cells/electroporation) electroporated with 20 μg of RNA from genotypes 1 and 3 replicons. Cells were grown for 48 hrs in culture medium after which G418 was added (10mg/ml). 2×10^6 cells were seeded per 90mm dish. Cells were grown for 4 weeks and medium was changed twice weekly. Panels a, e & i shows cells electroporated with RNA from a 1b replicon. Panels b, f & j shows cells electroporated with RNA from a GM* replicon. Panels c, g & k shows cells electroporated with RNA from a GM* replicon. Panels d, h & l shows cells electroporated with RNA from a GMGND replicon



1b replicon RNA was able to produce colonies, which were resistant to G418 selection and therefore contain actively replicating 1b replicon RNA. There appeared no difference between the ability of 1b replicons to replicate in naïve HuH-7 cells compared to 2a-C cells or 1b-C cells. All GM replicons failed to produce colonies in all cell types. This experiment was repeated twice.

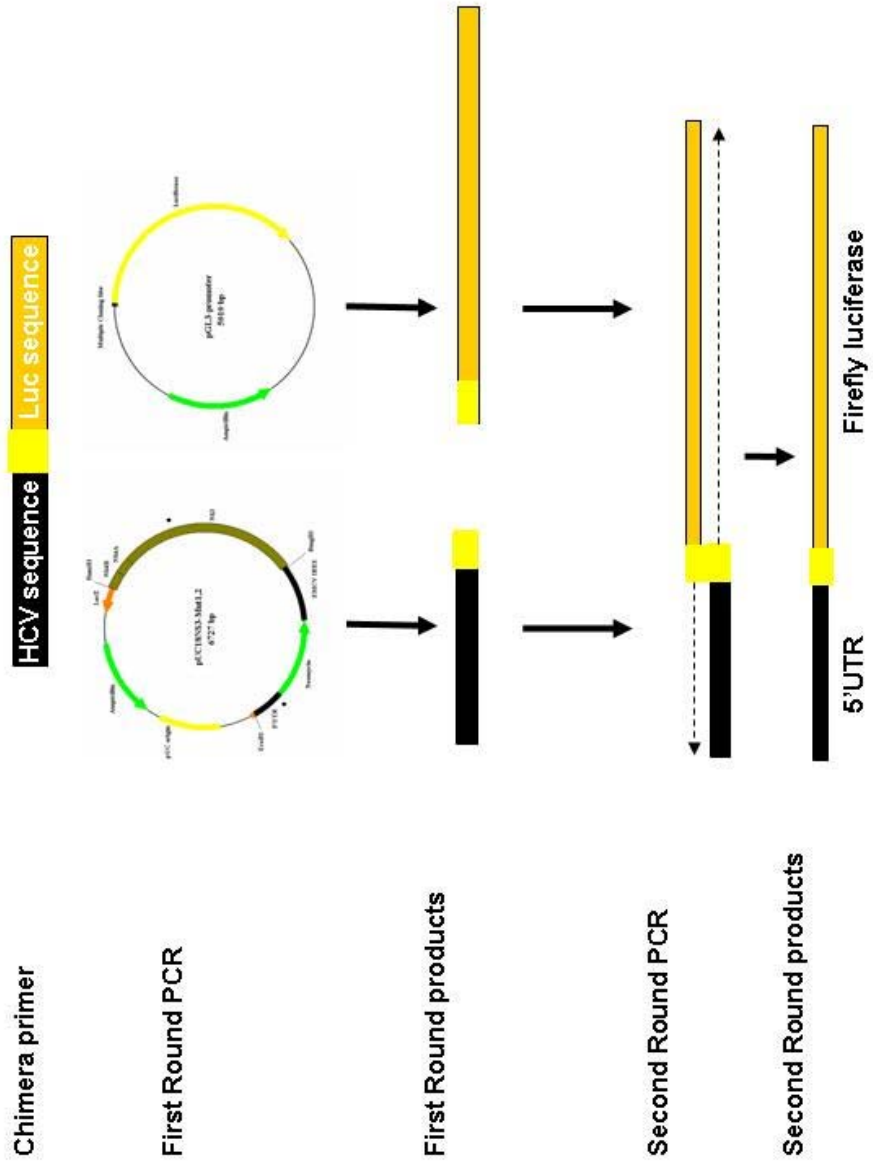
6.6 Assembling a genotype 3 replicon that would transiently express in cells

6.6.1 Fusion of the 5'UTR to firefly luciferase

In parallel to the formation of cells constitutively expressing GM replicons, replicons that could transiently express in cells were also made. This used the same principle employed as when the transient genotype 2a replicon was made (Targett-Adams et al., 2005). A firefly luciferase gene was placed under control of the HCV 5'UTR in place of the neomycin phosphotransferase gene. Figure 6.24 shows the strategy that was used to fuse the HCV 5'UTR to the luciferase gene. Two primers, aluc-GT3(2) and sluc-Not1(2), were designed which contained regions of homology to each other. These were used to amplify the HCV 5'UTR (PCR 29) and the firefly luciferase gene (PCR 28). These products were used in a self priming PCR to produce a 5'UTR fused to the luciferase gene (PCR 30). The antisense primer in the luciferase PCR contained a *PmeI* restriction enzyme site at the end of the gene to allow cloning adjacent to the EMCV IRES. The final fused product was cloned into pGEM T-Easy and clones were analysed for the presence of the fusion product by restriction enzyme digest and direct sequencing. The resultant plasmid was called pGEMluc.

To place the luciferase gene under control of a T7 promoter, pGEMluc was digested with *AgeI* and *PmeI* to produce a 1900 base fragment that could be cloned in pGEMT7-emcv after digestion with *AgeI* and *PmeI* (Figure 6.25). The resultant plasmid, pGEMT7-luc-emcv, was analysed by restriction enzyme digest to confirm the presence of the firefly luciferase gene.

Figure 6.24. Diagrammatic representation of PCRs used to fuse the coding sequence of isolate GM to the firefly luciferase gene. PCR was used to produce two products from pUC18T7-NS3 and pGL3promoter which had a short region of homology to each other. These products were then used to self prime in a first round *Pfx* Platinum Polymerase PCR over 8 cycles with an annealing temperature of 60°C. Sense primers to the GM isolate sequence and antisense primers for luciferase gene were used amplify the second round product over 25 cycles at annealing temperature of 60°C



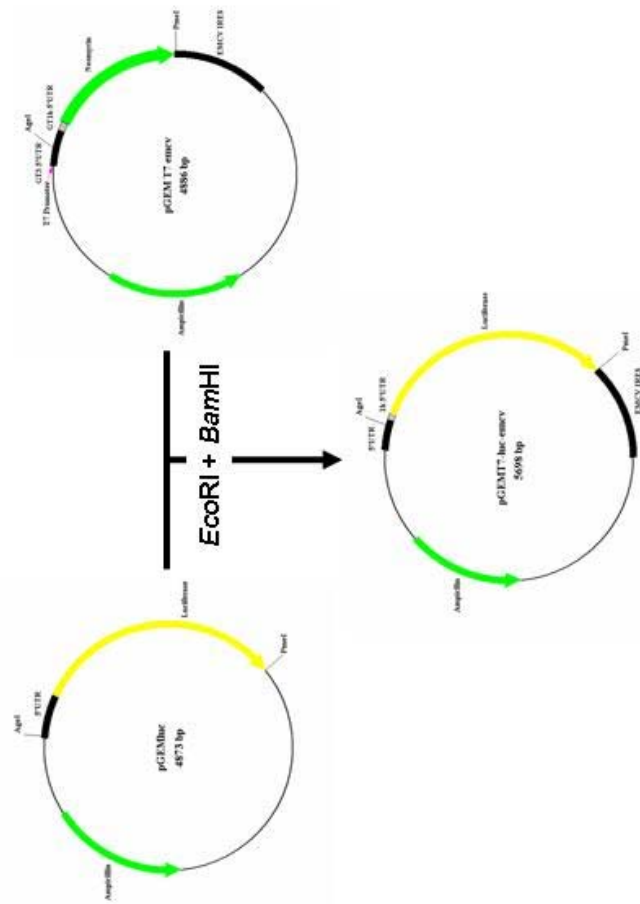


Figure 6.25. Diagrammatic representation of the cloning of pGEM17-luc-emyv with AgeI and PmeI restriction enzyme digest of pGEM1uc and pGEM17-emyv. The AgeI/PmeI digested luciferase fragment was ligated into the AgeI/PmeI pGEM17-emyv. This produced pGEM17-luc-emyv.

6.6.2 Removal of an internal *ScaI* restriction enzyme site in the luciferase gene

In order to synthesise run off transcripts, the previous replicon had incorporated a *ScaI* restriction enzyme site at the 3' end of the genome. However it was found that the coding sequence of the luciferase gene already contained a *ScaI* restriction enzyme site (Figure 6.26a). This problem was overcome by changing the wobble bases in the glutamic acid codon so that the nucleotide sequence was changed but the amino acid sequence remained the same. Site-directed mutagenesis was used to change the G base of the GAG codon to an A. The plasmid produced from this mutagenesis was called pGEMT7-luc Δ *ScaI*. Successful mutants were confirmed by restriction enzyme digest (Figure 6.26b) in which, if mutagenesis had been successful, the plasmid would be linearised as seen in lane 1.

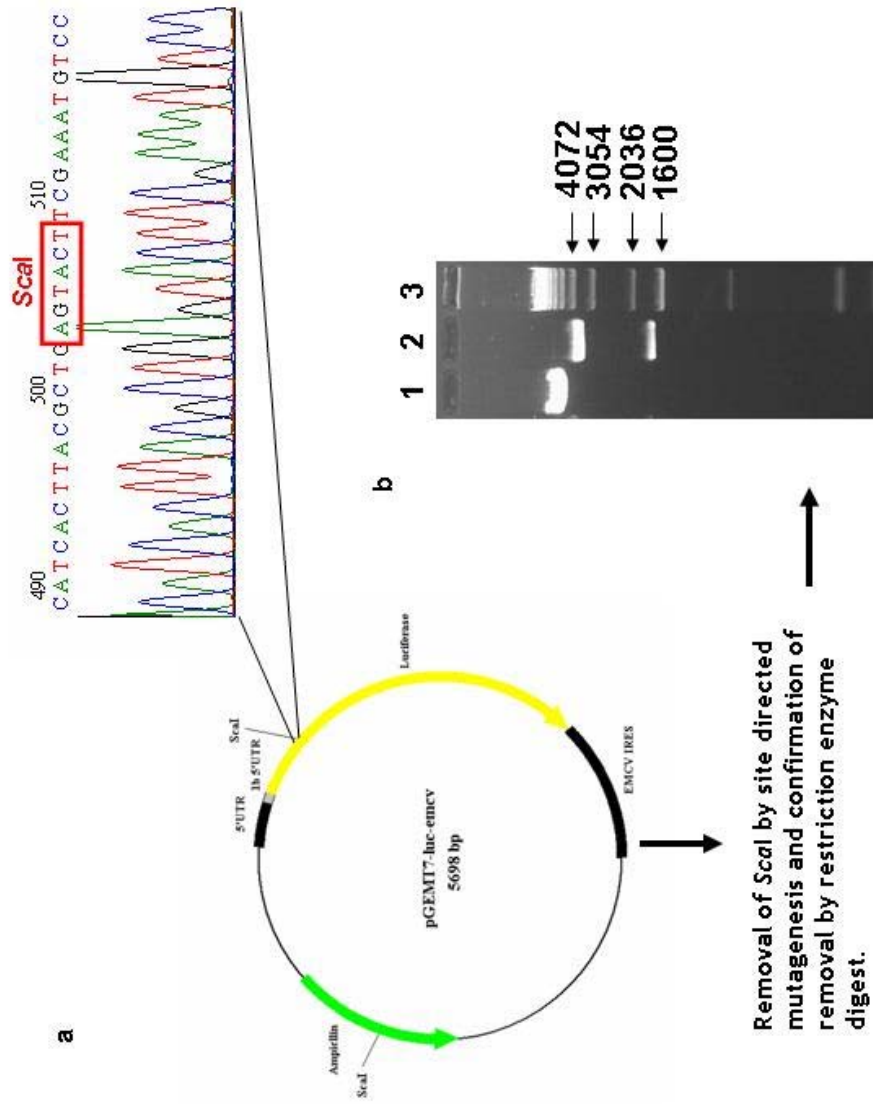
6.6.3 Assembly of the transient replicon

The transient replicon was also assembled in pSP64PolyA vector because this vector lacks an endogenous T7 promoter. Initially the luciferase was excised, using *EcoRI* and *PmeI*, from pGEMT7-luc Δ *ScaI* to release a 2083 base fragment. This was cloned into pSP64GM-NS3 where the neomycin phosphotransferase gene had been removed by digestion with *EcoRI* and *PmeI* (Figure 6.27). The resultant plasmid pSP64lucNS3 was 7893 bases in length and presence of the luciferase gene was confirmed by restriction enzyme digest.

The complete sequence of the replicon was assembled by excising the 3' of the genome from pUC18(3'GT3)Mut3-7 with *BamHI* and *SspI*. This produced a 6107 base fragment, which was cloned into pSP64lucNS3 digested with *BamHI* and *SspI* (Figure 6.28). The resultant plasmid, pSP64luc-GM, was 11561 bases in length and was analysed by restriction enzyme digestion.

Replicons were assembled for the GM majority sequence, a GM majority sequence with the adaptive mutation (GM*) and a GM majority sequence with a null GND mutation. These 2 variations on the replicon were made by digesting pSP64GM* and pSP64GMGND with *BamHI* and *SspI* and cloning as previously described.

Figure 6.26. Diagrammatic of representation of the removal of the *ScaI* restriction enzyme site in the firefly luciferase gene (a). Sequencing of the luciferase showed a *ScaI* restriction enzyme site within the luciferase sequence. Site directed mutagenesis of pGEMT7-luc-*emcv* was used to remove the *ScaI* restriction site to produce pGEMT7-luc Δ *ScaI*. The loss of the *ScaI* restriction site was confirmed by restriction enzyme digest (b). Lanes 1 and 2 contain plasmid DNA which has been digested with *ScaI*. Lane 3 contains molecular weight marker (Invitrogen 1 Kb ladder)



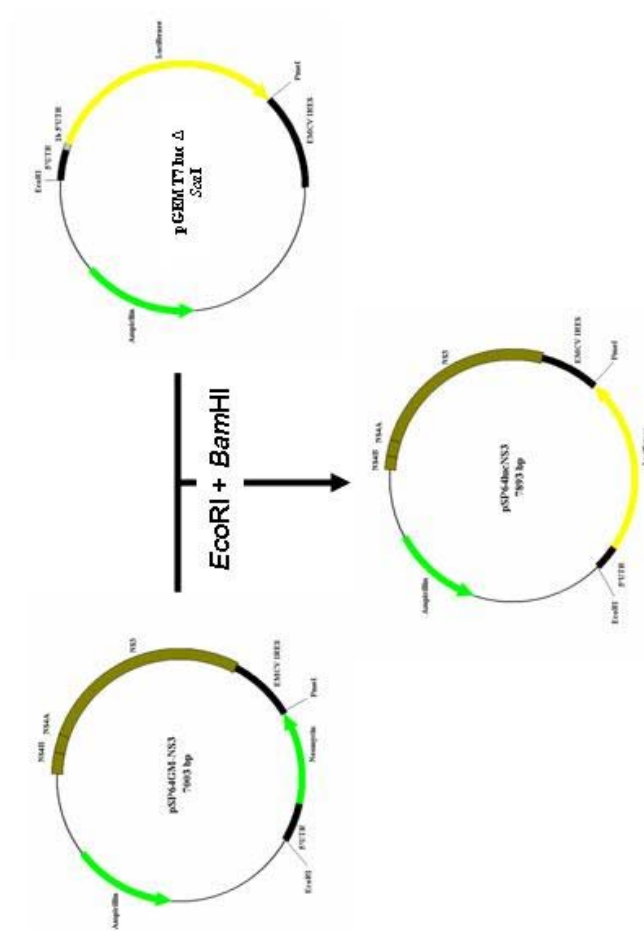


Figure 6.27. Diagrammatic representation of the cloning of pSP64lucNS3 with *EcoRI* and *PmeI* restriction enzyme digest of pGEMT7-luc Δ ScaI and pSP64 GM NS3. The *EcoRI*/*PmeI* digested luciferase fragment was ligated into *EcoRI*/*PmeI* pGEMGM-NS3. This produced pSP64lucNS3.

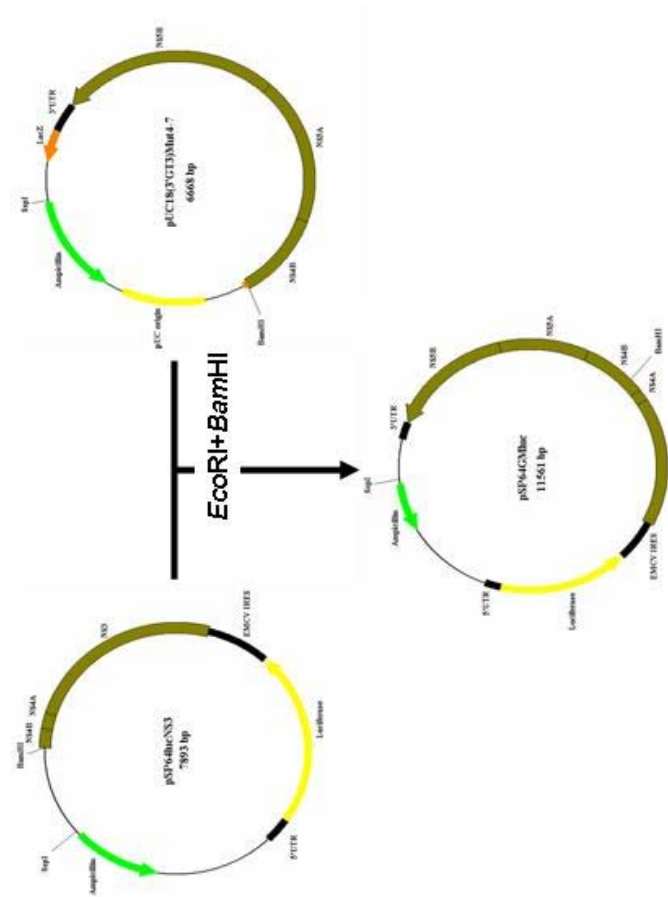


Figure 6.28. Diagrammatic representation of the cloning of pSP64GW-luc with *Bam*HI and *Ssp*I restriction enzyme digest of pSP64lucNS3 and pUC18(3'GT3)Mut3-7. The *Bam*HI/*Ssp*I digested (3'GT3)Mut3-7 fragment was ligated into *Bam*HI/*Ssp*I pGEMlucNS3. This produced pSP64GW-luc.

6.7 In-vitro transcription of transient replicons and electroporation into cells

Plasmids containing the GM luciferase replicons were linearised with *ScaI* so that synthesis of RNA replicons could be performed using in-vitro transcription. Linearised pSP64GM-luc, pSP64GM*-luc and pSP64GMGND-luc plasmids were used

to produce RNA replicons for GM-luc, GM*-luc and GMGND-luc respectively (Figure 6.29). Linearised plasmid was purified after agarose gel electrophoresis and used in in-vitro transcriptions.

Figure 6.30 shows that none of the GM luciferase replicons were able to replicate in any of the 3 HuH-7 cell types. However the JFH1 positive control was able effectively to replicate over the 72 hrs in all 3 cell types. This was compared to the JFH1 GND replicon, which does not actively replicate in any of the cells. This replicon showed an initial luciferase value, which represents translation of the input RNA, but because the replicon was replication deficient there was no replication and luciferase values decrease over the 72 hrs. All the GM luciferase replicons showed a luciferase values comparable to background where there was no initial luciferase activity from the expression of input RNA. Their luciferase values obtained varied minimally over the 72 hrs. These data are preliminary data as the complete experiment has only been performed once. However an additional luciferase assay had been performed for the above RNAs in naïve HuH-7 cells prior to the above experiment and similar results were obtained (data not shown).

6.8 Discussion

The cloning and sequencing of the HCV genome was reliant on reverse transcription of the genome using reverse transcriptase enzymes and amplification using polymerase enzymes. The initial RT step producing the cDNA template for future amplification was critical. A few of RT enzymes were used for this process each varying in their ability to produce successful product. Some RT enzymes like MMLV and Omniscript RT enzymes have difficulty dealing with secondary structure in RNA. However, it was found that “Superscript II” was able to deal more effectively with RNA secondary structures. Any errors

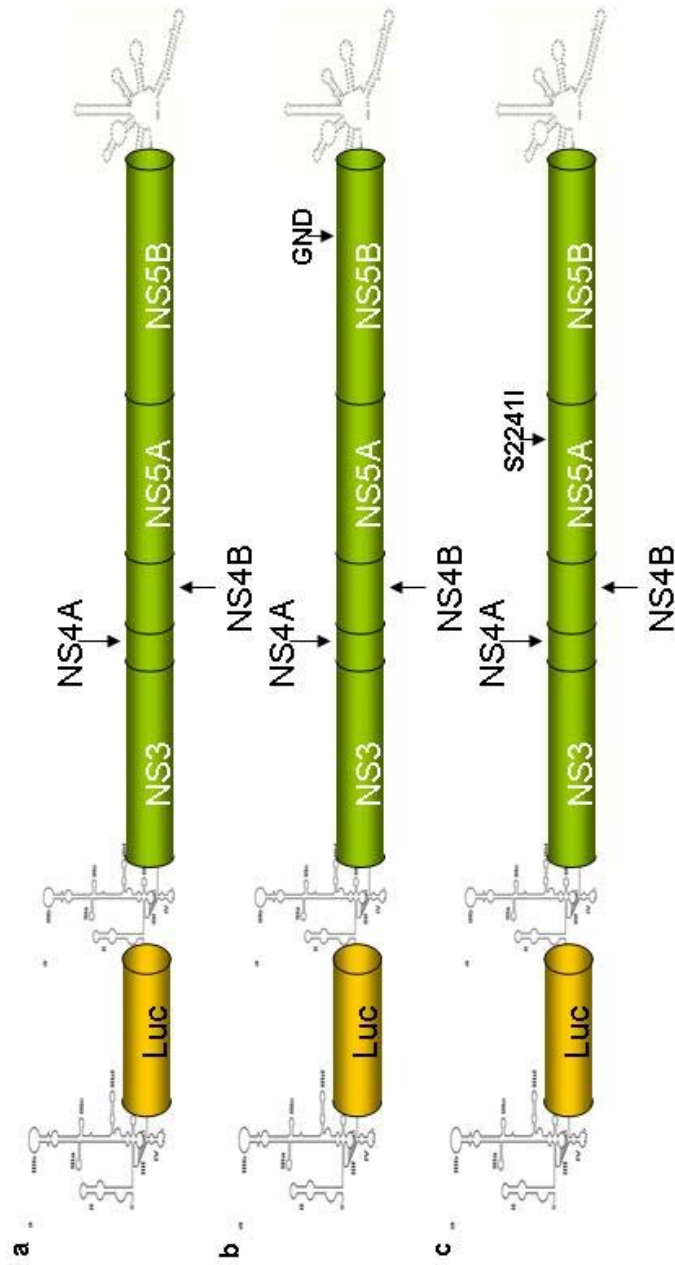
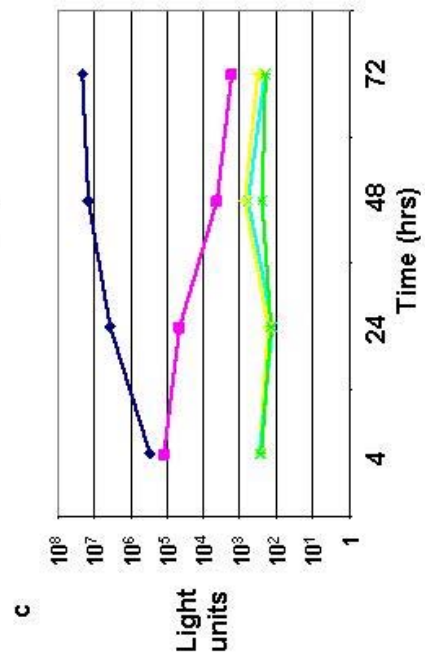
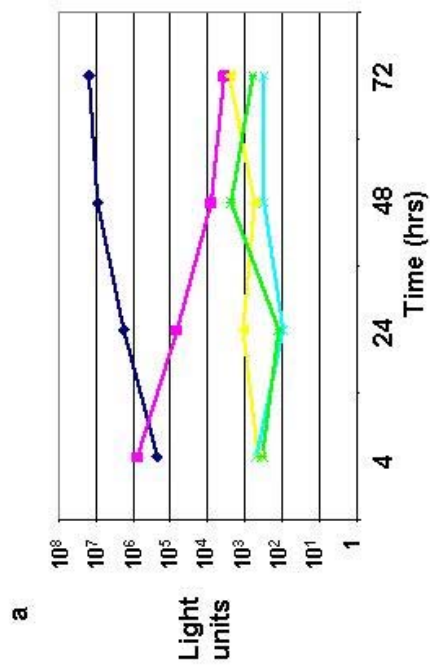
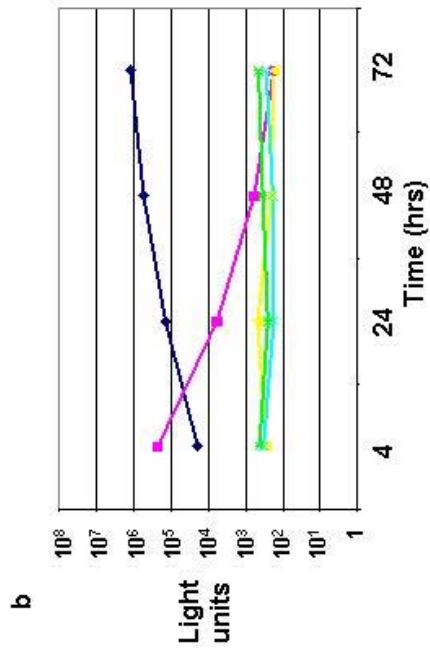


Figure 6.29. Diagrammatic representation of the RNA of genotype 3 transient replicons (GM, GM* and GM GND) produced after in-vitro transcriptions from *ScaI* digested pSP64 GM-luc (a), pSP64 GMGND-luc (b) and pSP64 GM*-luc (c) plasmids.

Figure 6.30. Graphs showing luciferase activity for electroporation performed in parallel for JFH1 and GM replicons into Huh7 (a), 2a-C (b) and 1b-C (c) cells (2×10^6 cells/electroporation). In-vitro transcribed RNA (5 μg) was electroporated into cells for JFH1 (dark blue), JFH1 GND (pink), GM (yellow), GM* (light blue) and GM GND (green) transient replicons. 35mm dishes were seeded with 2.5×10^5 cells. Cells were incubated for 3 days in culture medium and luciferase assays were performed at 4 hrs, 24 hrs, 48 hrs and 72 hrs.



produced by RT enzymes would be carried to the PCR level. Therefore keeping RT enzyme conditions at the required levels was critical. To minimise the errors in PCRs, proof reading enzymes were used. However, it should be recognised that although the frequency of mutation is less than that of non-proofreading enzymes, mutation may still occur. The error rate of *Taq* was described by Clontech Ltd as 2.75×10^{-5} errors/base pair/cycle. BD Advantage 2 polymerase mix and HF-2 polymerase were described as 3 x and 39 x more accurate than *Taq* respectively. *Pfu* polymerase was described as having an error rate of 1.3×10^{-6} errors/base/cycle. Invitrogen describes the fidelity of *Pfx* Platinum polymerase as 3.2×10^{-6} errors/base/cycle. This would place the polymerase enzymes in order of highest fidelity as follow: HF-2 polymerase > *Pfu* > *Pfx* > BD Advantage 2 polymerase mix > *Taq*. However it should be noted that a polymerase's actual error rate will be specific to the reaction itself as variations in reaction conditions can alter the error rate.

When assembling a majority sequence, polymerase errors were less important because errors only become important if the amount of starting material for amplification was very low and the mutation occurred in the first cycles of PCR. Most polymerase errors would be masked by the overwhelming consensus signal obtained during direct sequencing of PCR products. A majority allows for inherent errors caused by polymerase enzymes to occur, without these affecting the end consensus sequence.

The majority sequence is a theoretical sequence, which may not exist within a viral population. All it represented was the most common nucleotide frequency at any given position within the genome. It was shown with the genotype 1b replicon system that mutations might be incompatible for replication when combined in the same replicon (Lohmann et al., 2003). Although the replicon system is quite different from the "live" virus these studies highlighted an interesting point that strong adaptive mutations could be incompatible when combined. It therefore might be possible to have two populations of virus within the total viral population, one group with one mutation somewhere in the genome and the other with another mutation population in a different part of the genome. However both mutations were incompatible with each other so did not occur together. Therefore if these two groups occurred at similar frequencies this would result in the possibility of a majority sequence where the

mutations were combined. It is difficult to assess which is the best method for deciding the majority sequence as both sequencing several clones or sequencing PCR product may produce non-functional genomes. However we chose sequencing of PCR products as this would be looking at the average of millions of sequences rather than just several. The position would more than likely appear as a mixed base position in any majority produced. The hope was that deleterious mutations would be lost as they occurred at a low frequency.

Direct sequencing was reliant on bases being assigned by the “base caller” program used to translate electropherogram into raw sequence data. It was possible for a base to be assigned a type, which did not represent the highest electropherogram peak at that point. Analysis of electropherograms was necessary to combat this problem. The multiple alignments themselves highlighted these ambiguities, as in each case several sequences were examined in both forward and reverse directions. Most problems with sequencing that were encountered were due to too much or too little product or impurities in product and could be resolved by having further sequencing performed.

In some cases, analysis of ambiguities found nucleotide positions, which could either, be one nucleotide type or another which could not be resolved by additional sequencing. In these cases, both these bases may have been present within the viral population in similar frequencies. In most cases analysis of electropherogram data would show both bases present. However by using this and by analysing the consensus alignment of other genotype 3 sequences, a nucleotide could be assigned.

Amplification of the 3' end of the genome was initially difficult to achieve. Eventually it was possible to amplify to the stop codon by the use of *Taq* polymerase as opposed to a proof reading enzyme. The reason that the 3' end of the genome was more difficult to amplify than the rest of the genome was most likely due to structural elements found there. Amplification of the 3'UTR had also caused problems. The reason why it was so difficult to amplify the 3'UTR was most likely due to the secondary structure of the RNA. The critical step was again the reverse transcription. Several different RT enzymes had been tried. These had included an enzyme, which was thermophilic and could be used at increased temperatures, therefore not allowing renaturation of the RNA

template. However the 3'UTR was obtained by use of Dr Preikshat, a previous lab member's PCR samples. She had worked with isolate GM and successfully amplified the region. Although the same methodology had been used in my attempts to amplify the region they had all failed. This may have been because the RNA had degraded while in storage, as samples were several years old.

I found that successful amplification of the 3'UTR produced by Dr Preikshat was dependent on the polymerase used. Why most proofreading enzymes were unable to amplify the region was not known. Surprisingly *Taq* polymerase had been able to amplify the region. However the inclusion of DMSO was a prerequisite for this. The inclusion of this factor might indicate that the sequence has some secondary structure or G/C rich area, which under normal conditions causes polymerases to fall off the template. The most successful polymerase used was BD Advantage 2 polymerase mix, which was able to amplify most templates to a high yield.

Another problem with the 3'UTR apart from its secondary structure is that it contains a homopolymeric tract of A/T nucleotides approximately 100 nucleotides in length. Homopolymeric tracts cause problems as they cause slippage of the polymerase as it synthesises the new strand. This can lead to the incorporation of additional bases or alternatively the loss of the polymerase from the strand. This would lead to the failure of the PCR.

The site directed mutagenesis of cloned sequences to the majority was only performed at non-synonymous nucleotides. This should have resulted in a polyprotein, which was functional. However synonymous bases were not considered for mutation. It might have been better to mutate all bases as synonymous mutations may also have an effect on RNA secondary structure and cis-acting elements within the genome. As the importance of most of cis acting elements within the genome may not have been identified it is difficult to assess the effect of not mutating synonymous bases. Nevertheless it has been reported that some cis acting elements found in NS5B are essential for viral replication. Due to the nucleotide sequence being of importance rather than the codon sequence differences which occur in nucleotides other than the wobble base may be important for replication as well (Friebe et al., 2005). A non-synonymous difference between the majority sequence and the replicon was

found at nucleotide base 9003. This difference, within the replicon sequence, had been overlooked and not converted to the majority sequence. At this position a leucine residue is present however in the replicon a methionine residue was assigned. Whether this difference could prevent replication was not known. However, a change to the majority sequence would be needed to determine this.

Problems that had been encountered when cloning the full-length genome into pUC18 had suggested that some of the sequences were toxic to *E.coli*. The reason for this was unclear but was most likely due to the over expression of foreign membrane bound proteins. Similar occurrences have been found with other sequences from isolate GM. In a separate study, the structural genes of GM were found to mutate spontaneously in *E.coli* (Douglas et al., unpublished). Previous experience in the laboratory had led to full-length constructs of any HCV genotype to be grown at 30°C in order to minimise the chance of spontaneous mutation within the coding sequences. However in my study it was possible to circumvent this by subcloning into a different vector. A crucial point was to sequence all replicon clones to identify if any spontaneous deleterious mutation in *E.coli* had occurred which may affect expression and replication of input RNA.

The reason why isolate GM replicons failed to grow in cell culture was not understood. However, why genotype 1b, 1a and 2a are able to grow in cell culture is also not understood. It is thought that it may be a combination of viral and host cell factors, which contribute to successful replication. Now that the GM replicon has been made it would be interesting to perform more studies looking at effect of different passage numbers and different viral adaptive mutations. The ability of the genotype 2a replicon and not the 1b replicon to replicate in different cell types might indicate that its sequences are compatible for viral replication in a number of different cell types. Therefore chimera replicons between GM and genotype 2a could be made in order to establish a functional genotype 3 replicon. Initial work has been started to create several chimeras of GM and JFH1 luciferase replicons however these were not finished. The fact that there are currently replicons for only two of the genotypes highlights the difficulties associated with replication of replicons in cell culture. In fact, personal communication with Volker Lohmann revealed that this is not

just a problem that I encountered in my study but has also been found in his laboratory. Neither cells expressing the constitutive GM nor the transient GM replicon were able to replicate. The inclusion of the adaptive mutation in NS5A had no effect on successful replication. A single mutation may not be sufficient to support replication or may not be relevant in the context of genotype 3. Also, merely curing a cell line does not necessarily provide a more permissive environment for GM replicon replication. The permissiveness of the cells may change over passage history therefore testing cells at different passage number would also be of interest.

The failure of the transient replicon to give any signal might indicate that the initial expression of luciferase prior to replication at the 4 hrs period did not occur. This might indicate that translation from the HCV 5'UTR was not sufficient to be measured. It may be that the isolate GM has a sequence that is incompatible for replication in these HuH-7 cells. Therefore mutation on GM isolate would be required to establish a replicon expressing cell line.

Chapter seven

7 Final Discussion

7.1 Different cell responses to the fatty acid synthase inhibitor, cerulenin

The aim of our study was to find out whether there was an association between inhibition of fatty acid biosynthesis and levels of hepatitis C virus RNA. A microarray study by Su et al. (2000) had shown that some genes concerned with lipid metabolism were positively or negatively regulated in response to increase viremia and that HCV RNA levels fell on treatment with inhibitors of fatty acid biosynthesis.

Two separate approaches were used to reduce fatty acid biosynthesis in our study. These targeted enzymes within the pathway and the global transcription factor that controls lipogenic gene expression. Directly targeting fatty acid synthase (FAS) with the drug cerulenin reduced HCV RNA levels but inhibition of fatty acid biosynthesis could not be achieved in the initial genotype 1b expressing HuH-7 cell line. The reason for this was unclear but differences in clonal cell behaviour are not unrecognised. Both HCV genotype 1b and 1a replicons were successfully established in clonal cell lines which were highly permissive for HCV replication (Blight et al., 2003; Lohmann et al., 1999). As described by Lohmann et al. (2003), a progressive increase in permissiveness for HCV replication in naïve HuH-7 cells was found between passages 15 and 128. This suggested that the internal environment of cells was continually changing and at passage 128 the conditions were optimal for replication of the replicon. Blight et al. (2003) selected a HuH-7 cell line, which had increased permissiveness for replication. This was then “cured” by interferon treatment to produce the HuH-7.5 cell line. The ability of one clone to differ from others supports the idea that HuH-7 cells are extremely heterogeneous and are

continually changing. Two highly permissive HuH-7 cell lines from different laboratories, HuH-7.5 and HuH-7 lunet cells, were described as supporting similar levels of replicon replication. However, recent studies found Huh-7 lunet cells to be less permissive for JFH1 infection due to low expression of the CD81 cell surface molecule. Ectopic expression of CD81 on HuH-7 lunet cells increased their permissiveness to levels comparable to that of HuH-7.5 cells (Koutsoudakis et al., 2006). A highly permissive cell line derived from HuH-7.5 cells contained a defective RIG-I protein which was thought to increase their permissiveness to JFH1 viral infection (Zhong et al., 2005).

In our study we initially found that a HuH-7 genotype 1b expressing cell line, FAS was resistant to the effects of cerulenin. Interestingly, HCV RNA levels were reduced in these cells. However, whether this was due to toxic effects of cerulenin, which reduced cell viability, or non-specific effects of the drug where cell viability was not affected and neither was FAS, was unclear. Nevertheless, FAS activity in these HuH-7 cells behaved differently in their response to cerulenin compared to HuH-7 cells obtained from the University of Lille. Further work would be necessary to identify the reason for this. Had we not directly looked at fatty acid biosynthesis, reductions in HCV RNA levels might have been attributed to actions of the drug on fatty acid biosynthesis. Treatment of replicon harbouring HuH-7 cells derived from HuH-7 cells obtained from the University of Lille resulted in a reduction in HCV RNA levels when fatty acid biosynthesis was inhibited (Figure 4.5). Our study highlights the inherent problems of comparing data from different laboratories using cell lines with different passage histories.

7.2 Mechanisms by which PUFAs mediate inhibition of HCV replication

The effect of PUFAs on HCV replication was reduction in HCV RNA levels. HuH-7 cells expressing both transient and constitutive replicons responded similarly to PUFA treatment, although the effect was greater using the transient system. Similar inhibitory effects of PUFAs on HCV replication had previously been reported by Kapadia et al. (2005). Differences between studies might be accounted for by the different cell lines used and different drugs suppliers. The trend of PUFAs inhibiting and OLA increasing replication was consistent between

our study and other studies in the literature. It was difficult to correlate the effect on fatty acid biosynthesis with the effect on HCV replication. Although a reduction in fatty acid biosynthesis was accompanied by a reduction in HCV RNA levels, it was difficult to show that they correlated. In order to ascertain if the two are related additional concentrations of PUFA should be tested to allow a more accurate dose response curve to be produced. Recent data from Kapadia et al. (2005) might indicate that PUFA-mediated reduction of HCV RNA levels is not correlated with inhibition of fatty acid biosynthesis. They indicated that PUFA inhibition of HCV replication was accompanied by a reduction in SREBP-1c and FAS RNA levels. However, fatty acid biosynthesis could be rescued with an LXR agonist, which restored SREBP-1c and FAS RNA levels without an effect on HCV RNA levels. Although this study showed that SREBP-1c and FAS mRNA levels were induced, any increase in fatty acid production was not investigated. The increase in FAS mRNA would indicate that treatment with the LXR agonist resulted in a SREBP-1c induction of lipogenic gene expression. Certainly, SREBP-1c mRNA levels, in rat adipose tissue, do not correlate with changes in lipogenic gene expression (Bertile et al., 2004). Therefore, without measuring fatty acid biosynthesis the value of these data is unclear, as they provide no insight into the effect on intracellular fatty acid production.

Another proposed mechanism for PUFA-mediated inhibition of HCV replication was disruption of replication complex formation by altering the lipid composition of the ER membrane. Some indirect evidence of this is shown in the following studies. Chimeric mice with humanised livers were successfully infected with HCV genotypes 1a and 1b. It was then found that treatment of the mice with myriocin, an inhibitor of serine palmitoyl-transferase, caused a reduction in HCV replication. Myriocin treatment disrupts biosynthesis of sphingolipids. Sphingomyelin is a major component of lipid raft (see below) assembly and therefore indirectly affects lipid raft formation (Takuya et al., 2006). Membrane flotation assays had co-fractionated HCV RNA with the lipid raft protein, caveolin 2, in detergent resistant membrane fractions (Shi et al., 2003). By sequestering cholesterol from these fractions, HCV NS5A protein no longer co-fractionated with detergent-resistant membranes. This indicated that these regions were cholesterol rich regions required for raft integrity. Indeed, cholesterol biosynthesis was found to be important for HCV replication and

further studies showed that geranylgeranoil, a pre-cholesterol metabolite, was essential for HCV replication (Wang et al., 2005).

The role of PUFAs in disruption of lipid rafts is well established. Lipid rafts are detergent resistant areas of the membrane enriched with cholesterol and saturated and monounsaturated fatty acids. These act as a stable platform for the recruitment of cellular signalling proteins (Pitman et al., 2004). The presence of the more hydrophilic PUFAs disrupts these stable detergent resistant areas of the membrane by excluding hydrophobic cholesterol. This leads to the displacement of membrane bound proteins and can alter intracellular signalling (Stulnig et al., 2001).

It has been suggested that the prenylation of a host protein, FBL2, is essential for HCV replication (Wang et al., 2005). Lovastatin treatment of replicon expressing HuH-7 cells reduced the punctate staining of NS5A on the ER membrane (Ye et al., 2003). If PUFAs had been disrupting replication complex formation and its association with detergent resistant areas of the membrane, a similar effect might have been expected. However, my initial immunofluorescence studies had indicated that, although there was reduced expression of NS5A protein, punctate foci of NS5A were maintained. To study the effect of PUFA treatment on known lipid raft proteins may be useful when interpreting immunofluorescence and fluorescence recovery after photobleaching.

Nevertheless PUFA treatment reduces HCV RNA levels in replicon expressing cells. Health benefits from dietary PUFAs have been shown in which mortality in men who had had a myocardial infarction was reduced by 29 % if they ate two oily fish meals a week. Furthermore, omega 3 PUFAs can inhibit breast cancer growth but this is dependent on the background proportions of omega 6 PUFAs. PUFAs have been indicated as important beneficial constituents of the diet in other diseases such as rheumatoid arthritis, asthma, alcoholism and many others (Stillwell et al., 2003). It would be interesting to investigate if a reduction of viral RNA or an improvement in liver disease could be achieved by PUFA treatment of HCV-infected patients in combination with interferon therapy. Previous studies in transgenic mice had indicated that fibrosing steatohepatitis, which could result in more advanced liver disease, could be avoided by induction

of PPAR- α pathways reducing oxidative stress (Ip et al., 2003). PUFAs act as activating ligands for PPAR- α and could therefore reduce liver disease by a mechanism separate from reducing viral replication.

7.3 Variability between experiments

One of my main concerns was that in some cases there was marked variability between experiments reflected by increased standard deviations. This may have occurred due to instabilities with the compounds used. As described by the manufacturer, PUFAs readily oxidise in solution. It may be necessary to include anti-oxidants in the experiments to try to minimise this. However, this would introduce another variable. When PUFA results were compared to previous studies, variability was noted in these experiments too. In some cases there was up to 50 % variation between experiments in normalised values of HCV RNA levels (Kapadia et al., 2005). This may suggest that this is an inherent problem with these compounds. Variability between experiments was also found with cerulenin and TOFA treatment of cells (Kapadia et al., 2005; Su et al., 2002). In our studies, the main variation in experiments was in Northern blot analysis and in cell viability measurements. Northern blots were most likely to be affected due to incomplete removal of probe, which had bound non-specifically to membrane, incomplete binding of probe to target sequence or poor transfer of RNA to membrane. In most cases, because ribosomal bands were visualised integrity of RNA could be confirmed prior to Northern blotting. Quantitative real time PCR might also be used to assess HCV RNA levels. This would also allow more accurate estimation of RNA levels.

7.4 Assembling a genotype three replicon

The aim was to assemble a functioning replicon, which could be used to investigate the development of steatosis by HCV genotype 3. I was unable to create successful genotype 3 replicon expressing HuH-7 cell lines. However, the inherent difficulties with establishing the genotype 1b and 1a replicons in the HuH-7 cell line have been described (Blight et al., 2003; Lohmann et al., 1999). Both replicon adaptation and permissive cells lines were required. Why replicons are able to replicate successfully in some cell lines and not others is not understood. Furthermore, why the JFH1 genotype 2a replicon was more

successful at replicating is not known (Takanobu et al., 2003). The genotype 2a sequence, JFH1 was isolated from a patient with fulminant hepatitis. Fulminant hepatitis in HCV is rare so this might indicate the special nature of JFH1 (Takanobu et al., 2001). However, unpublished data by Wakita et al., (2006) presented at the 13th International Meeting of Hepatitis C Virus and Related Viruses suggested that the ability to replicate successfully in cell culture systems was specific to this genotype 2a isolate and not a feature of all isolates derived from patients with fulminant hepatitis. A genotype 1b sequence obtained from a patient with fulminant hepatitis was unable to replicate successfully and produce colonies. The fact that our genotype 3 replicon was unsuccessful was not surprising. Without knowing why replication is successful in replicons derived from some isolates and not others, creation of a replicon expressing cell line becomes difficult. Had there been more time, construction of chimera replicons between genotype 3 and genotype 2a could have been investigated for their replicative ability.

7.5 Future experiments

Experiments treating replicon-expressing cell lines had failed to show a direct association between the inhibitory effect of cerulenin on FAS and the inhibitory effect of cerulenin on HCV replicon RNA levels. In fact, non-specific effects of cerulenin may have accounted for the inhibition of HCV RNA levels independent of the effects on FAS. It may be useful to ascertain if cerulenin-treated cells could be rescued by supplying with the end product of the pathway, palmitic acid. If FAS inhibition was due to a cerulenin blockade of fatty acid biosynthesis a possible explanation may be that cerulenin treatment of cells is able to alter ER membrane function. In the bacteria *Staphylococcus Aureus*, exoprotein secretion can be blocked by cerulenin treatment resulting in interference of membrane function by fatty acid biosynthesis blockade (Adhikari et al., 2005). Indeed, a toxic effect of the related FAS inhibitor, C75, has been attributed to reduction in phospholipid production and membrane synthesis (Zhou et al., 2003). Stopping fatty acid biosynthesis may alter cellular signalling by altering ER membrane function and thereby alter HCV replication.

HCV NS4B protein has recently been described as being palmitoylated (Yu et al., 2006). The palmitoylation of proteins is important for interactions with

membranes and can anchor proteins to the membrane. It would be interesting to ascertain whether cerulenin could prevent NS4B from being palmitoylated and whether this has consequences in HCV replication since NS4B may act as a platform for replication complex assembly.

Cerulenin inhibition of HCV replicon and fatty acid biosynthesis was accompanied by loss in cell viability, which might partly be explained by the inhibitory effects on fatty acid biosynthesis. However, PUFAs were more effective at both inhibition of fatty acid biosynthesis and HCV replication. Further experiments are necessary in order to determine whether the inhibitory effect of PUFAs on HCV replication was as a consequence of their inhibitory effect on fatty acid biosynthesis. Our hypothesis had been that PUFAs were affecting membrane fluidity and replication complex formation by destabilising lipid raft structures. Initial IF and FRAP experiments had failed to determine whether this was the case. IF had indicated a general down-regulation of HCV expression but membrane associated foci (generated by NS4B) were still present and FRAP had not shown an increase in membrane fluidity. However, as discussed below, the ratio of saturated to unsaturated fatty acids within virally modified ER membrane is sufficient to disrupt viral replication. Therefore, it might be interesting to investigate inhibitors and inducers of the desaturase enzymes to determine the effect they have on viral replication. Additionally live cell analysis of GFP tagged NS4B, NS5A and known ER raft proteins may give more insight into the effect of PUFAs.

The reason for making a genotype 3 replicon was to investigate whether viral induced steatosis occurred. Although assembly of the genotype 3 replicon failed to produce a functional replicon, producing chimeric genotypes 3 and 2a replicons could be investigated. If a chimeric replicon was successful, this could add to our understanding of sequence requirements for replication in cell culture.

7.6 Lipid metabolism and other viruses

Lipid metabolism has been implicated in the life cycles of other viruses such as Epstein-Barr virus (EBV), human immunodeficiency virus (HIV), polio virus, vesicular stomatitis virus (VSV), and brome mosaic viruses (BMV).

EBV is a gammaherpesvirus, which can infect cells in either a lytic or latent fashion. Recently, it was found that EBV induces FAS expression in order to produce a lytic infection. Furthermore, ceruleinin and C75 prevented activation of lytic proteins attenuating the viral lifecycle (Li et al., 2004).

HIV, retrovirus, has been proposed to use lipid rafts not only in viral entry but also in the assembly and budding of the virus from the cell. Recently, a study found that functional HIV Nef protein could up-regulate cholesterol biosynthesis genes and the production of cholesterol. The up-regulation of cholesterol pathways had important consequences for the assembly of lipid rafts. This indicated that induction of cholesterol pathways may play a role in Nef mediated increased viral replication and virion infectivity (van 't Wout et al., 2005).

The importance of lipid metabolism was shown in a study with poliovirus, a positive sense single stranded RNA virus. Cerulenin inhibition of lipid metabolism caused a decrease in phospholipid production and membrane proliferation and inhibited poliovirus growth in HeLa cells. In normal infection, poliovirus induces phospholipid production and membrane biogenesis allowing the formation cytoplasmic vesicles. Cerulenin was able to decrease the cellular pool of fatty acids that could be used for phospholipid production and thereby inhibited viral replication (Carrasco L, 1990). Cerulenin mediated inhibition of RNA synthesis was also found with a negative sense ss RNA virus, VSV (Carrasco L, 1991).

BMV is a positive sense stranded RNA virus. It is a member of the alpha-like superfamily of human, animal and plant infecting viruses. Using traditional genetic methods, it was possible to identify host genes required for its life cycle in the yeast *Saccharomyces cerevisiae*. The *OLE1* yeast deletion mutant contains a mutation in the chromosomal yeast $\Delta 9$ fatty acid desaturase gene. This gene is responsible for the synthesis of unsaturated fatty acids. BMV was unable to replicate efficiently in *OLE1* and RNA replication was dependent on unsaturated fatty acids in the ER membrane. Membrane composition affecting fluidity was important for early stage viral replication (Lee et al., 2001). In addition, in wild-type yeast, BMV up-regulated membrane lipid synthesis inducing ER luminal spheres, which were the sites of viral replication. In BMV infected yeast *OLE1* mutants, luminal spheres were depleted of unsaturated fatty acids affecting the

ratio of saturated to unsaturated fatty acids. This in itself was sufficient to disrupt viral replication (Lee et al., 2001).

Membrane alteration induced by RNA viruses is well reported and the formation of stable ER membrane modification seems crucial to viral infection. As mentioned, in some cases it is possible to disrupt viral replication by targeting the cellular pathways that lead to the formation of lipids. The morphology of membrane modification varies between viruses. HCV induces the formation of a membranous web, consisting of small tightly associated vesicles embedded in a membranous matrix (Egger et al., 2002). Other flaviviruses, for instance Kunjin virus, have been described as producing convoluted membranes or small vesicle structures. Coronaviruses produce large double membrane vesicles, which are the site of active viral replication. Picornaviruses induce vast vesicular structures and the disintegration of internal structures causing the formation of vesicles between 70 - 500 nm in size. Between these RNA virus families the requirement for wrapping their replication complexes in membrane is a common feature. The reason why is unclear. It may be that these membrane modifications produce a stable environment for replication or alternatively concentrate viral proteins to increase efficiency. It also makes replication complexes less accessible to host cellular immune response proteins. Targeting cellular pathways, which are necessary for the production of membrane lipids has proved an efficient method of inhibiting viral growth and replication. With this knowledge the possibility that PUFAs, which are safe dietary supplements, have an inhibitory role, not just on HCV but possibly also on other viruses makes these fatty acids of important interest for research.

GTGCTACTCTCGGCGCTGGGATTTTGGCCCTCTTCGGCTTCTTTACCTTA
TCACCTTGGTATAAAGCATTGGATTAGCCGCCTCATGTGGTGGAAACCAGTA
CACCATATGTAGATGTGAGGCCGCCCTCCAAGTGTGGGTCCCCCCTTAC
TTGTACGAGGGAGTAGGGACGGTGCATCCTACTAGCAAGCCTGCTTCAT
CCATCTTTAATCTTTGACATCACTAAGCTGCTGATAGCAGTATTGGGCC
GTTATACTTAATACAGGCTGCCATCACTACCACCCCTACTTTGTGCGCG
CGCATGTAAGTCCGCCTTTGCATGTTCTGTCGCTCTGTGATGGGGGA
AAATACTTTAGATGATCATACTGAGCATTGGCAGATGGTTAAACACCTA
CCTATACGACCACCTAGCGCAATGCAACATTGGGCCGAGCCGGCCTCA
AAGACCTAGCAGTGGCCACTGAACCTGTAATATTTAGTCCCATGGAAATC
AAGGTCATCACCTGGGGCGCAGACACAGCGCTTGGCGAGATATTCTTTG
CGGGCTGCCGTTTCTGCGCGATTGGGCCGTGAGGTGTTGTTGGGACCTG
CTGATGACTATCGGGAGATGGGTTGGCGTCTGTTGGCTCCGATCACAGCA
TACGCCAGCAAACTAGGGCCCTTCTGGGACTATTGTGACTAGCTTGAC
TGGCAGGGATAAAAACGTGGTGACCGGTGAAGTGCAGGTGCTTTCCACGG
CTACCCAGACCTTCTAGGTACAACAATAGGAGGGGTTATGTGGACTGTC
TACCATGGTGCAGGCTCAAGGACACTTGGGGCGCTAAACATCCAGCGCT
CCAAATGTACACAAATGTAGATCAGGACCTCGTCGGGTGGCCAGCTCCTC
CAGGGACTAAGTCTTGAACCGTGGCGCTGGGGTCTGCAGACTTATAC
TTGGTTACCCCGCATGCTGATGTCATCCCTGCTAGGCGCAGGGGGGACTC
CACAGCGAGCTTGCTCAGTCTAGGCCTCTCGCTGTCTCAAGGGTTCCCT
CTGGAGTCCCTGTTATGTGCCCTTCGGGGCATGTTGCAGGGATCTTCAGG
GCTGCTGTGTGACCAGGGGTGTAGCAAAAAGCCCTACAGTTCATACCAGT
GGAAACCCTTAGCACACAGGCTAGGTCTCCATCTTTTTCTGACAATTCAA
CTCCTCTGCCGTCCACAGAGCTACCAAGTAGGGTACCTTCATGCCCG
ACCGGCAGTGGTAAGAGCACAAAGGTTCCGGCTGCTTATGTAGCGCAAGG
ATATAATGTTCTTGTGTTGAATCCATCGGTGGCGCCACACTAGGCTTCG
GCACCTTCATGTGCGGTGCCTATGGAATTGATCCCAACATCCGCACTGGG
AACCGCACCGTTACAACCTGGTGCTAAACTGACCTATCCACCTACGGTAA
GTTTCTTGGCGACGGGGGTTGTTCCGGGGGAGCATATGATGTGATTATCT
GTGATGAATGTCATGCCAAGACGCTACTAGCATATTGGGCATAGGCACG
GTCTTAGATCAAGCTGAGACGGCTGGGGTGAGGCTGACGGTTTTGGCGAC
AGCAACTCCCCCAGGCAGCATCACTGTGCCACACTTAACATCGAAGAAG
TGGCCTTGGGCTCTGACGGCGAGATCCCTTTCTACGGCAAGGCTATACCG
TTAGCCCAGCTTAAGGGGGGAGACACCTTATCTTTTGGCATTCCAAGAA
GAAATGTGATGAGATGGCATCCAAACTCAGAGGTATGGGGCTTAACGCTG
TAGCGTACTATAGGGTCTTGTGATGTGTCGTCATACCAACAGCAGGAGAC
GTCGTAGTTTGGCTACTGACGCCCTCATGACTGGATTACCCGGAGACTT
CGATTCTGTCATAGACTGCAACGTGGCTGTTGAACAGTACGTTGACTTCA
GCCTGGACCCTACCTTTTCCATTGAGACCCGCACTGCTCCCCAAGACGCG
GTTTCTCGCAGCCAACGTCGTGGCCGTACGGGCCGAGGTAGACTCGGTAC
GTATCGGTACGTCACCCCGGGTGGAGACCATCTGGAATGTTGACTCGG
TCGTCcTCTGTGAGTGCTATGACGCGGGCTGCTCGTGGTACGATCTGCAG
CCCCTGAGACCACAGTTAGACTGAGAGCTTACTTGTCCACACCCGGGTT
ACCCGTCTGCCAAGACCATTTAGACTTTTGGGAGAGTGTTTTTACTGGAC
TGACTCACATAGATGCCACTTTCTGTACAGACCAAGCAGCAGGGACTC
AATTTCTCGTACCTAACTGCCTACCAAGCCACTGTATGCGCTCGCGCGCA
GGCTCCTCCCCAAGTTGGGACGAGATGTGAAATGTCTCGTGGGCTCA
AGCCAACACTACATGGACCTACACCCCTTCTATATCGGTTGGGGCCTGTC
CAAAATGAAATCTGCTCGACACACCCGGTCACAAAATACATCATGGCATG
CATGTCAGCTGATCTGGAAGTAACCACCAGCACCTGGGTGTTGCTTGGAG
GGGTCTCGCGGCCCTAGCGGCCTACTGCTTGTGAGTGGCTGCGTTGTG
ATTGTGGGTATATCGAGCTGGGGGGCAAGCCAGCACTTGTACCAGACAA
AGAGGTGTTGTATCAACAATACGATGAGATGGAGGAGTGCTCACAAGCCG
CCCCATACATCGAACAAGCTCAGGTAATAGCCACCAGTTCAAGGAGAAA
GTTCTTGGGTTGTTGCAGCGGGCCACCCAACAACAAGCTGTCATTGAGCC
CATAGCTACCAACTGGCAAAAAGCTTGAGGTCTTCTGGCATAAGCATATGT
GGAATTTTGTGAGTGGGATCCAGTACCTAGCAGGCCTTTCCACCTTGCT
GGCAACCCTGCTGTGGCGTCTTATGGCGTTCAGTCTTCCAGTACCAG
TCCCCTGACGACCAACCAAACTATGTTTTTCAACATACTCGGGGGGTGGG
TTGCTACCCATTTGGCAGGGCCCCAGAGCTCTTCCGCATTCTGGTAAGC
GGTTTGGCCGGCCTGCCATAGGGGGTATAGGCCCTGGGTAGGGTCTTACT
TGACATCCTGGCAGGATACGGAGCTGGCGTCTCAGGCGCCTTGGTGGCTT
TTAAGATCATGGGAGGAGAACTCCCCACTGGTGAGGACGTGGTCAACCTG
TTACCCGCCATATTATCTCCAGGCGCCCTCGTCTCGGTGTGATATGCGC

TGCCATACTACGTCGACACGTAGGACCTGGAGAGGGGGCGGTGCAGTGGATGAACAGGCTCATCGCATTCCGATCCCGGGTAACCACGTCTCACCAGCGACTATGTCCCCGAGAGCGATGCTGCAGCGAAAGTCACTGCATTGCTGAGTTCTCTAACTGTCACAAGCCTGCTCCGGCGGCTGATCAATGAAGACTACC CAAGTCCCTTGACGCGGTGACTGGTTGCGTACCATCTGGGAaTGGGTTTGC ACTGCGTTGTCTGACTTCAAGACATGGCTCTCTGCTAAGATCATGCCAGC GCTCCCCGGGCTGCCCTTCATTTCTGTCAAAAGGGATAACAAGGGCGTGTGGCGGGGGACGGTGTGATGTCGACGCGCTGTCCTTGCGGGGCATCAATA ACCGGCCATGTGAAGAATGGGTCCATGCGGCTTGCAGGGCCGCGTACATGTGCTAACATGTGGTACGGTACATTCCCCATCAATGAGTACACCACTGGAC CCAGTACACCTTGCCACCACCAACTACACTCGCGCACTGTGGCGCGTG GCTGCCAACAGCTACGTTGAGGTGCGCCGGTGGGGGACTTCCACTACAT TACGGGGGCCACAGAAGATGAGCTCAAGTGTCCGTGCCAAGTGCCGGCTG CTGAGTTCTTTACTGAAGTGGACGGGGTGAAGCTTCCCGTTACGCCCCCT CCATGCAAGCCCCTGTTGAGAGATGAAATCACTTTCATGGTAGGGTTGAA TTCTACGCGATAGGATCTCAACTCCCCTGTGAGCCCGAACCGGATGTTT CCGTGCTGACCTCGATGTTGAGGGACCCTTCCCATATCACCGCCGAGACG GCAGCGCGCCGCTTGCAGCGGGTCCCCTCCATCAGAAGCTAGCTCATC CGCCAGTCAACTATCGGCTCCGTGCTGAAGGCCACTTGCCAGACGCATA GGCCTCATCCAGACGCTGAGCTAGTGGACGCCAATTGCTATGGCGGCAA GAGATGGGCAGCAACATTACACGGGTGGAGTCTGAAACAAAGGTTGTGAT TCTTGATTCATTGAGCCTCTGAGAGCCGAAACTGACGACGCCGAGCTCT CCGTGGCTGCGGAGTGTTCAGAAAACCTCCCAAGTATCCTCCAGCCCCT CCCATCTGGGCTAGGCCAGACTACAATCCTCCACTGTTGGACCGCTGGAA AGCACCGGATTATATACCACCAACTGTCCATGGATGCGCCTTACCACCGC GGGACGCTCCACCGGTGCCTCCCCCTCGAGGAAAAGAACAATTCAGCTG GATGGCTCCAATGTGTCGCGGGCGCTAGCTGCGTTGGCGAAAAGTCATT CCCGCCTCCGAAACCGCAGGAAGAAAATAGCTCATCCTCAGGGGTGACA CACAGTCCAGCACTACTTCCAAGGTGCCCCCTTCTCAGGGAGAGGAGTCC GACTCAGAGTCATGCTCGTCCATGCCTCCTCTCGAGGGAGAACC GGCGA TCCGGACTTGAGTTGCGACTCTTGGTCCACTGTTAGTGACAGCGAGGAGC AGAGCGTAGTCTGCTGCTCTATGTCGTA CTCTTGGACCGCGCCCTGATA ACACCATGTAGCGCTGAGGAGGAGAAAACCTCCCATCAGCCCACTCAGCAA CTCTTTGTTGAGACACCATAACCTAGTCTATTCAACGTGCTCTAGAAGCG CTTCTCAGCGTCAAGAAGGTTACCTTCGACAGGCTGCAGGTGCTCGAC GACCATTACAAGACTGCATTAAGGAGGTAAGGAGCGAGCGTCTAGGGT AAAGGCTCGCATGCTCACCATCGAGGAAGCGTGCGCGCTCGTCCCTCCTC ACTCTGCCCCTCAAGGTTCCGGTATAGTGCGAAGGACGTTCCGCTCCTTG TCCAGCAAGGCCATTAACCAGATCCGCTCCGTCTGGGAGGACTTGCTGGA AGACACCACAACCAATTCCAACCACCATCATGGCGAAGAACGAGGTTT TTTGCGTAGACCCGCTAAAGGGGGCCGCAAGCCGCTCGCCTCATTGTT TACCCTGACCTGGGGTGCCTGTCTGTGAGAAACGCGCCCTATATGATGT GATAAAAAGTTGTCAATTGAGACGATGGGTTCCGCTTATGGATTCCAAT ACTCGCTCAGCAGCGGTGCAACGTCTGTTGAAGATGTGGACCTCAAAG AAAACCCCTTGGGGTCTCGTATGACACCCGCTGCTTTGACTCGACTGT CACTGAACAGGACATCAGGGTGAAGAGGAGATATACCAATGCTGTAACC TTGAACCGGAGGCCAAGAAGGTGATCTCCTCCCTCACGGAGCGGCTTTAC TGCGGGGGCCCTATGTTTAAACAGCAAAGGGGCCAGTGTGGTTATCGCCG TTGCCGTGCCAGTGGAGTTCTGCCTACCAGTTTCGGCAACACAATCACTT GTTACATCAAGGCCACAGCGGCTGCGAGGGCCGCGGGCTCCGGAACCCG GACTTTCTTGTCTGCGGAGATGATCTAGTCTGGTGGCTGAGAGTGACGG CGTCGACGAGGATAGAACAGCCCTGAGAGCCTTACGGAGGCTATGACCA GGTACTCTGCTCCACCCGAGATGCTCCACAGCCTACCTACGACCTTGGAG CTCATTACATCTTGTCTCTAACGTCTCCGTGGCACTGGACAATAAGGG GAAGAGGTATTATTACCTCACCCGTGATGCCACCACTCCCCTGGCCCGTG CGGCTTGGGAAACAGCTCGTCACTCCGGTTAACTCCTGGCTGGGCAAC ATCATCATGTACGCGCTACCATCTGGGTGCGCATGGTAATGATGACACA TTTTTCTCCATACTTCAATCCCAGGAGATACTTGACCGACCCCTTGACT TTGAAATGTACGGGGCCACTTACTCTGTCACTCCGCTGGATTTACCAGCT ATCATTGAAAGACTCCATGGTCTGAGCGGTTACGCTCCACAGTTATTC TCCAGTAGAGCTCAATAGGGTTGCGGGGACACTCAGGAAGCTTGGGTGCC CCCCCTACGGGCTTGGAGACATCGGGCACGAGCAGTGCAGCGCCAAGCTT ATCGCCAGGAGGGAAGGCCAAAACATGTGGCCTTTATCTCTTTAATTG GGCGGTACGCACCAAGACCAAACTCACTCCACTGCCGCCGCTGGCCAGC TGGATTTATCCAGTTGTTTACGGTTGGCGTCCGGGGAACGACATTTAT

CACAGCGgtcaCGTGCCCGAACCCGCCATTTGCTGCTTTGCCTACTCCT
ACTAACGGTAGGGGTAGGCATCTTTCTCCTGCCAGCTCGGTGAGGTGGTA
AGAAAACACTCCCTTCCCTTTTTGTTTTCCCCCTTTTTTTTTTTTTTTT

8.2 References

- Abida, K., de Gottardi, A., Rubbia-Brandt, L., Conne, B., Pugnale, P., Rossia C., Mangia, A and Negro, F. (2005) An in vitro model of hepatitis C virus genotype 3a-associated triglycerides accumulation. *Journal of Hepatology* 42(5), 744-751.
- Adhikari, R., and Novick, R. (2005) Subinhibitory cerulenin inhibits staphylococcal exoprotein production by blocking transcription rather than by blocking secretion. *Microbiology* 151(9), 3059-3069.
- Adinolfi, R., Andreana, A., Tripodi, M., Utili, R and Ruggiero, G. (2001) Steatosis accelerates the progression of liver damage of chronic hepatitis C patients and correlates with specific HCV genotype and visceral obesity. *Hepatology* 33(6), 1358-1364.
- Agnello, V., Abel, G., Elfahal, M., Knight, G and Zhang, Q. (1999) Hepatitis C virus and other Flaviviridae viruses enter cells via low-density lipoprotein receptor. *PNAS* 96(22), 12766-12771.
- Aizaki, H., Lee, K., Sung, V., Ishiko, H and Lai, M. (2004) Characterization of the hepatitis C virus RNA replication complex associated with lipid rafts. *Virology* 324(2), 450-461.
- Alter, H., Morrow, A., Purcell, R., Feinstone, S and Moritsugu, Y. (1975) Clinical and serological analysis of transfusion-associated hepatitis. *Lancet* 2(7940), 838-841.
- Asabe, S., Tanji, Y., Satoh, S., Kaneko, T., Kimura, K and Shimotohno, K. (1997) The N-terminal region of hepatitis C virus-encoded NS5A is important for NS4A-dependent phosphorylation. *J. Virol.* 71(1), 790-796.
- Asselah, T., Rubbia-Brandt, L., Marcellin, P and Negro, F. (2006) Steatosis in chronic hepatitis C: why does it really matter? *Gut* 55(1), 123-130.
- Bandyopadhyay, S., Watabe, M., Gross, S., Hirota, S., Hosobe, S., Tsukada, T., Miura, K., Saito, K., Markwell, S., Wang, Y., Huggenvik, J., Pauza, M., Iizumi, M and Watabe, K. (2005) FAS expression inversely correlates with PTEN level in prostate cancer and a PI 3-kinase inhibitor synergizes with FAS siRNA to induce apoptosis. *Oncogene* 24(34), 5389-5395.
- Banerjee, R and Dasgupta, A. (2001) Specific Interaction of Hepatitis C Virus Protease/Helicase NS3 with the 3'-Terminal Sequences of Viral Positive- and Negative-Strand RNA. *J. Virol.* 75(4), 1708-1721.

- Barba, G., Harper, F., Harada, T., Kohara, M., Goulinet, S., Matsuura, Y., Eder, G., Schaff, Z., Chapman, M., Miyamura, T and Brechot, C. (1997) Hepatitis C virus core protein shows a cytoplasmic localization and associates to cellular lipid storage droplets. *PNAS* 94(4), 1200-1205.
- Bartenschlager, R., Ahlborn-Laake, L., Mous, J and Jacobsen, H. (1993) Nonstructural protein 3 of the hepatitis C virus encodes a serine-type proteinase required for cleavage at the NS3/4 and NS4/5 junctions. *J. Virol.* 67(7), 3835-3844.
- Bartenschlager, R., Ahlborn-Laake, L., Mous, J and Jacobsen, H. (1994) Kinetic and structural analyses of hepatitis C virus polyprotein processing. *J. Virol.* 68(8), 5045-5055.
- Bartosch, B., Dubuisson, J and Cosset, F. (2003) Infectious Hepatitis C Virus Pseudo-particles Containing Functional E1-E2 Envelope Protein Complexes. *J. Exp. Med.* 197(5), 633-642.
- Beales, L., Holzenburg, A and Rowlands, D. (2003) Viral Internal Ribosome Entry Site Structures Segregate into Two Distinct Morphologies. *J. Virol.* 77(11), 6574-6579.
- Beard, M., Honda, H., Carroll, A., Gartland, M., Clarke, B., Suzuki, K., Lanford, R., Sangar, D and Lemon, S. (1999) An infectious molecular clone of a Japanese genotype 1b hepatitis C virus. *Hepatology* 30(1), 316-324.
- Behrens, S., and De Francesco, R. (1996) Identification and properties of the RNA-dependent RNA polymerase of hepatitis C virus. *EMBO J.* 15(1), 12-22.
- Bertile, F and Raclot, T. (2004) mRNA levels of SREBP-1c do not coincide with the changes in adipose lipogenic gene expression. *Biochemical and Biophysical Research Communications* 325(3), 827-834.
- Bigger, C., Brasky, K and Lanford, R. (2001) DNA Microarray Analysis of Chimpanzee Liver during Acute Resolving Hepatitis C Virus Infection. *J. Virol.* 75(15), 7059-7066.
- Bigger, C., Guerra, B., Brasky, K., Hubbard, G., Beard, M., Luxon, B., Lemon, S and Lanford, R. (2004) Intrahepatic Gene Expression during Chronic Hepatitis C Virus Infection in Chimpanzees. *J. Virol.* 78(24), 13779-13792.
- Bisceglie, A. (1997) Hepatitis C and Hepatocellular Carcinoma. *Hepatology* 26(3 Suppl. 1), 34 S - 38S.

- Blight, K and Rice, C. (1997) Secondary structure determination of the conserved 98-base sequence at the 3' terminus of hepatitis C virus genome RNA. *J. Virol.* 71(10), 7345-7352.
- Blight, K., McKeating, J., Marcotrigiano, J and Rice, C. (2003) Efficient Replication of Hepatitis C Virus Genotype 1a RNAs in Cell Culture. *J. Virol.* 77(5), 3181-3190.
- Blight, K., McKeating, J and Rice, C. (2002) Highly Permissive Cell Lines for Subgenomic and Genomic Hepatitis C Virus RNA Replication. *J. Virol.* 76(24), 13001-13014.
- Borowski, P., Oehlmann, K., Heiland, M and Laufs, R. (1997) Nonstructural protein 3 of hepatitis C virus blocks the distribution of the free catalytic subunit of cyclic AMP-dependent protein kinase. *J. Virol.* 71(4), 2838-2843.
- Boulestin, A., Payen, J., Alric, L., Dubois, M., Pasquier, C., Vinel, J., Pascal, J., Puel, J and Izopet, J. (2002) Genetic heterogeneity of the envelope 2 gene and eradication of hepatitis C virus after a second course of interferon-alpha. *Journal of Medical Virology* 68, 221-228.
- Brass, V., Bieck, E., Montserret, R., Wolk, B., Hellings, J.A., Blum, H.E., Penin, F and Moradpour, D. (2002) An Amino-terminal Amphipathic alpha -Helix Mediates Membrane Association of the Hepatitis C Virus Nonstructural Protein 5A. *J. Biol. Chem.* 277(10), 8130-8139.
- Brocard, M., Komarova, A., Deveaux, V and Kean, K. (2006) Evidence that PTB does not stimulate HCV IRES-driven translation *Virus Genes* 35(1), 5-15.
- Brown, E., Zhang, H., Ping, L and Lemon, S. (1992) Secondary structure of the 5' nontranslated regions of hepatitis C virus and pestivirus genomic RNAs. *Nucl. Acids Res.* 20(19), 5041-5045.
- Brown, M. (1997) The SREBP pathway: regulation of cholesterol metabolism by proteolysis of a membrane-bound transcription factor. *cell* 89, 331-340.
- Bugianesi, E., Gentilcore, E., Homer, H., Vanni, E., Rizzetto, M and George, J. (2006) Fibrosis in genotype 3 chronic hepatitis C and nonalcoholic fatty liver disease: Role of insulin resistance and hepatic steatosis. *Hepatology* 44(6), 1648-1655.
- Bukh, J., Pietschmann, T., Lohmann, V., Krieger, N., Faulk, K., Engle, R., Govindarajan, S., Shapiro, M., St. Claire, M and Bartenschlager, R. (2002) Mutations that permit efficient replication of hepatitis C virus RNA in Huh-7 cells prevent productive replication in chimpanzees. *PNAS* 99(22), 14416-14421.

- Bukh, J., Purcell, R and Miller, R. (1994) Sequence Analysis of the Core Gene of 14 Hepatitis C Virus Genotypes. *PNAS* 91(17), 8239-8243.
- Cai, Z., Zhang, C., Chang, K., Jiang, J., Ahn, B., Wakita, T., Liang, T and Luo, G. (2005) Robust Production of Infectious Hepatitis C Virus (HCV) from Stably HCV cDNA-Transfected Human Hepatoma Cells. *J. Virol.* 79(22), 13963-13973.
- Carrasco, L. (1991) Cerulenin, an inhibitor of lipid synthesis, blocks vesicular stomatitis virus RNA replication. *FEBS Letters* 280(1), 129-133.
- Carrasco, L. (1990) Phospholipid biosynthesis and poliovirus genome replication, two coupled phenomena. *EMBO J.* 9(6), 2011-2016.
- Carrere-Kremer, S., Montpellier-Pala, C., Cocquerel, L., Wychowski, C., Penin, F and Dubuisson, J. (2002) Subcellular Localization and Topology of the p7 Polypeptide of Hepatitis C Virus. *J. Virol.* 76(8), 3720-3730.
- Cha, T., Beall, E., Irvine, B., Kolberg, J., Chien, D and Urdea, M. (1992) At Least Five Related, but Distinct, Hepatitis C Viral Genotypes Exist. *PNAS* 89(15), 7144-7148.
- Chawla, R., Watson, W., Eastin, C., Lee, E., Schmidt, J and McClain, C. (1998) S-adenosylmethionine deficiency and TNF-alpha in lipopolysaccharide-induced hepatic injury. *Am J Physiol Gastrointest Liver Physiol* 275(1), G125-129.
- Chayama, K., Tsubota, A., Koida, I., Arase, Y., Saitoh, S., Ikeda, K and Kumada, H. (1994) Nucleotide sequence of hepatitis C virus (type 3b) isolated from a Japanese patient with chronic hepatitis C. *J Gen Virol* 75(12), 3623-3628.
- Chen, C., You, L., Hwang, L and Lee, Y. (1997) Direct interaction of hepatitis C virus core protein with the cellular lymphotoxin-beta receptor modulates the signal pathway of the lymphotoxin-beta receptor. *J. Virol.* 71(12), 9417-9426.
- Chen, S., Kao, C., Chen, C., Shih, C., Hsu, M., Chao, C., Wang, S., You, L and Lee, Y. (2003) Mechanisms for Inhibition of Hepatitis B Virus Gene Expression and Replication by Hepatitis C Virus Core Protein. *J. Biol. Chem.* 278(1), 591-607.
- Chomczynski, P. (1987) Single-step method of RNA isolation by acid guanidinium thiocyanate-phenol-chloroform extraction. *Analytical Biochemistry* 162(1), 156-9.

- Choo, Q., Richman, K., Han, J., Berger, K., Lee, C., Dong, C., Gallegos, C., Coit, D., Medina-Selby, A., Barr, P., Weiner, A., Bradley, D., Kuo, G and Houghton, M. (1991) Genetic Organization and Diversity of the Hepatitis C Virus. *PNAS* 88(6), 2451-2455.
- Clarke, S. (2001) Nonalcoholic Steatosis and Steatohepatitis.: I. Molecular mechanism for polyunsaturated fatty acid regulation of gene transcription. *Am J Physiol Gastrointest Liver Physiol* 281(4), G865-869.
- Cocquerel, L., Wychowski, C., Minner, F., Penin, F and Dubuisson, J. (2000) Charged Residues in the Transmembrane Domains of Hepatitis C Virus Glycoproteins Play a Major Role in the Processing, Subcellular Localization, and Assembly of These Envelope Proteins. *J. Virol.* 74(8), 3623-3633.
- Date, T., Kato, T., Miyamoto, M., Zhao, Z., Yasui, K., Mizokami, M and Wakita, T. (2004) Genotype 2a Hepatitis C Virus Subgenomic Replicon Can Replicate in HepG2 and IMY-N9 Cells. *J. Biol. Chem.* 279(21), 22371-22376.
- Diedrich, G. (2006) How does hepatitis C virus enter cells? *FEBS J* 273(17), 3871-3885.
- Dubuisson, J and Rice, C. (1996) Hepatitis C virus glycoprotein folding: disulfide bond formation and association with calnexin. *J. Virol.* 70(2), 778-786.
- Eckart, M., Masiarz, F., Lee, C., Berger, K., Crawford, K., Kuo, C., Kuo, G., Houghton, M and Choo, Q. (1993) The Hepatitis C Virus Encodes a Serine Protease Involved in Processing of the Putative Nonstructural Proteins from the Viral Polyprotein Precursor. *J. Virol.* 67(2), 399-406.
- Egger, D., Wolk, B., Gosert, R., Bianchi, L., Blum, H., Moradpour, D and Bienz, K. (2002) Expression of Hepatitis C Virus Proteins Induces Distinct Membrane Alterations Including a Candidate Viral Replication Complex. *J. Virol.* 76(12), 5974-5984.
- Elazar, M., Cheong, K., Liu, P., Greenberg, H., Rice, C and Glenn, J. (2003) Amphipathic Helix-Dependent Localization of NS5A Mediates Hepatitis C Virus RNA Replication. *J. Virol.* 77(10), 6055-6061.
- Elbrecht, A., Chen, Y., Cullinan, C., Hayes, N., Leibowitz, M., Moller, D and Berger, J. (1996) Molecular Cloning, Expression and Characterization of Human Peroxisome Proliferator Activated Receptors [γ]1 and [γ]2. *Biochemical and Biophysical Research Communications* 224(2), 431-437.

- Enomoto, N., Asahina, Y., Kurosaki, M., Murakami, T., Yamamoto, C., Izumi, N., Marumo, F and Sato, C. (1995) Comparison of full-length sequences of interferon-sensitive and resistant hepatitis C virus 1b. Sensitivity to interferon is conferred by amino acid substitutions in the NS5A region. *Journal of Clinical Investigation* 96(1), 224-230.
- Erhardt, A., Heintges, T and Haussinger, D. (2002) Hepatitis C Virus Core Protein Induces Cell Proliferation and Activates ERK, JNK, and p38 MAP Kinases Together with the MAP Kinase Phosphatase MKP-1 in a HepG2 Tet-Off Cell Line. *Virology* 292(2), 272-284.
- Fartoux, L., Poujol-Robert, A., Guechot, J., Wendum, D., Poupon, R and Serfaty, L. (2005) Insulin resistance is a cause of steatosis and fibrosis progression in chronic hepatitis C. *Gut* 54(7), 1003-1008.
- Feinman, C., Sinclair, J and Wrobel, D. (1980) Hepatitis non-A, non-B. *Canadian Medical Association Journal* 123(3), 181-184.
- Feinstone, S., Mihalik, K., Kamimura, T., Alter, H., London, W and Purcell, R. (1983) Inactivation of hepatitis B virus and non-A, non-B hepatitis by chloroform. *Infect. Immun.* 41(2), 816-821.
- Flamm, S. (2003) Chronic Hepatitis C Virus Infection. *Journal of American Medical Association* 289(18), 2413-2417.
- Folch, J. (1957) A simple method for the isolation and purification of total lipids from animal tissues. *J. Biol. Chem.* 226, 497-509.
- Foretz, M and Ferre, P. (1999) Polyunsaturated fatty acids inhibit fatty acid synthase and spot-14-protein gene *Biochem J.* 341 (2), 371-6.
- Forns, X and Burk, J. (1999) Quasispecies in viral persistence and pathogenesis of hepatitis C virus. *Trends of Microbiology* 7(10), 402-409.
- Frese, M., Pietschmann, T., Moradpour, D., Haller, O and Bartenschlager, R. (2001) Interferon- α inhibits hepatitis C virus subgenomic RNA replication by an MxA-independent pathway. *J Gen Virol* 82(4), 723-733.
- Friebe, P and Bartenschlager, R. (2002) Genetic Analysis of Sequences in the 3' Nontranslated Region of Hepatitis C Virus That Are Important for RNA Replication. *J. Virol.* 76(11), 5326-5338.
- Friebe, P., Boudet, J., Simorre, J and Bartenschlager, R. (2005) Kissing-Loop Interaction in the 3' End of the Hepatitis C Virus Genome Essential for RNA Replication. *J. Virol.* 79(1), 380-392.

- Fukushi, S., Okada, M., Stahl, J., Kageyama, T., Hoshino, F and Katayama, K. (2001) Ribosomal Protein S5 Interacts with the Internal Ribosomal Entry Site of Hepatitis C Virus. *J. Biol. Chem.* 276(24), 20824-20826.
- Gale, M., Norina, M., Tang, S., Hopkins D., Dever, T., Polyak, S., Gretch, D and Katze, M. (1997) Evidence That Hepatitis C Virus Resistance to Interferon Is Mediated through Repression of the PKR Protein Kinase by the Nonstructural 5A Protein. *Virology* 230(2), 217-227.
- Gallinari, P., Brennan, D., Nardi, C., Brunetti, M., Tomei, L., Steinkuhler, C and De Francesco, R. (1998) Multiple Enzymatic Activities Associated with Recombinant NS3 Protein of Hepatitis C Virus. *J. Virol.* 72(8), 6758-6769.
- Gardner, J., Durso, R., Arrigale, R., Donovan, G., Maddon, P., Dragic, T and Olson, W.C. (2003) L-SIGN (CD 209L) is a liver-specific capture receptor for hepatitis C virus. *PNAS* 100(8), 4498-4503.
- Gibbons, G. (2005) Old fat, make way for new fat. *Nature medicine* 11(7), 722-723.
- Gontarek, R., Gutshall, L., Herold, K., Tsai, J., Sathe, G., Mao, J., Prescott, C and Del Vecchio, A. (1999) hnRNP C and polypyrimidine tract-binding protein specifically interact with the pyrimidine-rich region within the 3'NTR of the HCV RNA genome. *Nucl. Acids Res.* 27(6), 1457-1463.
- Grakoui, A., McCourt, D., Wychowski, C., Feinstone, S and Rice, C. (1993a) A Second Hepatitis C Virus-Encoded Proteinase. *PNAS* 90(22), 10583-10587.
- Grakoui, A., Wychowski, C., Lin, C., Feinstone, S and Rice, C. (1993b) Expression and identification of hepatitis C virus polyprotein cleavage products. *J. Virol.* 67(3), 1385-1395.
- Green, R. (2003) NASH- hepatic metabolism and not simply the metabolic syndrome. *Hepatology* 38(1), 123-133.
- Gretton, S., Taylor, A and McLauchlan, J. (2005) Mobility of the hepatitis C virus NS4B protein on the endoplasmic reticulum membrane and membrane-associated foci. *Journal of General Virology* 86(5), 1415-1421.
- Griffin, S., Clarke, D., McCormick, C., Rowlands, D and Harris, M. (2005) Signal Peptide Cleavage and Internal Targeting Signals Direct the Hepatitis C Virus p7 Protein to Distinct Intracellular Membranes. *J. Virol.* 79(24), 15525-15536.
- Griffin, S., Beales, L., Clarke, D., Worsfold, O., Evans, S., Jaeger, J., Harris, M. and Rowlands, D. (2003) The p7 protein of hepatitis C virus forms an ion

channel that is blocked by the antiviral drug, Amantadine. FEBS Letters 535(1-3), 34-38.

Guo, J., Bichko, V and Seeger, C. (2001) Effect of Alpha Interferon on the Hepatitis C Virus Replicon. J. Virol. 75(18), 8516-8523.

Han, J., Shyamala, V., Richman, K., Brauer, M., Irvine, B., Urdea, M., Tekamp-Olson, P., Kuo, G., Choo, Q and Houghton, M. (1991) Characterization of the Terminal Regions of Hepatitis C Viral RNA: Identification of Conserved Sequences in the 5' Untranslated Region and Poly(A) Tails at the 3' End PNAS 88(5), 1711-1715.

Haraguchi, G., Kobayashi, Y., Brown, M., Tanaka, A., Isobe, M., Gianturco, S and Bradley, W. (2003) PPAR α and PPAR γ activators suppress the monocyte-macrophage apoB-48 receptor. J. Lipid Res. 44(6), 1224-1231.

He LF, A., Popkin, T., Shapiro, M., Alter, H and Purcell, R. (1987) Determining the size of non-A, non-B hepatitis virus by filtration. Journal of Infectious Disease 156(4), 636 - 640.

Hegarty, B., Bobard, A., Hainault, I., Ferre, P., Bossard, P and Fougelle, F. (2005) From The Cover: Distinct roles of insulin and liver X receptor in the induction and cleavage of sterol regulatory element-binding protein-1c. PNAS 102(3), 791-796.

Hickman, I., Clouston, A., Macdonald, G., Purdie, D., Prins, J., Ash, S., Jonsson, J and Powell, E. (2002) Effect of weight reduction on liver histology and biochemistry in patients with chronic hepatitis C. Gut 51(1), 89-94.

Hijikata, M., Kato, N., Ootsuyama, Y., Nakagawa, M and Shimotohno, K. (1991) Gene Mapping of the Putative Structural Region of the Hepatitis C Virus Genome by In Vitro Processing Analysis. PNAS 88(13), 5547-5551.

Hijikata, M., Shimizu, Y.K., Kato, H., Iwamoto, A., Shih, J., Alter, H., Purcell, R and Yoshikura, H. (1993) Equilibrium centrifugation studies of hepatitis C virus: evidence for circulating immune complexes. J. Virol. 67(4), 1953-1958.

Honda, M., Brown, E and Lemon, S. (1996) Stability of a stem-loop involving the initiator AUG controls the efficiency of internal initiation of translation on hepatitis C virus RNA. RNA 2(10), 955-968.

Horton, J. (2002) Sterol regulatory element-binding proteins: transcriptional activators of lipid synthesis. Biochem. Soc. Trans 30(6), 1091-1095.

- Horton, J., Bashmakov, Y., Shimomura, I and Shimano, H. (1998) Regulation of sterol regulatory element binding proteins in livers of fasted and refed mice. *PNAS* 95(11), 5987-5992.
- Horton, J., Goldstein, J and Brown, M. (2002) SREBPs: activators of the complete program of cholesterol and fatty acid synthesis in the liver. *J. Clin. Invest.* 109(9), 1125-1131.
- Hsu, M., Zhang, J., Flint, M., Logvinoff, C., Cheng-Mayer, C., Rice, C and McKeating, J (2003) Hepatitis C virus glycoproteins mediate pH-dependent cell entry of pseudotyped retroviral particles. *PNAS* 100(12), 7271-7276.
- Hu, X., Li, S., Wu, J., Xia, C and Lala, D. (2003) Liver X Receptors Interact with Corepressors to Regulate Gene Expression. *Mol Endocrinol* 17(6), 1019-1026.
- Hua, X., Goldstein, J and Brown, M. (1996) Sterol resistance in CHO cells traced to point mutation in SREBP cleavage-activating protein. *cell* 87(3), 415-426.
- Huang, H., Sun, F., Owen, D., Li, W., Chen, Y., Gale, M and Sun, F. (2007). From the Cover: Hepatitis C virus production by human hepatocytes dependent on assembly and secretion of very low-density lipoproteins. *Proceedings of the National Academy of Sciences* 104(14): 5848-5853
- Hugle, T., Bieck, E., Kohara, M., Krausslich, H., Rice, C and Blum, H. (2001) The Hepatitis C Virus Nonstructural Protein 4B Is an Integral Endoplasmic Reticulum Membrane Protein. *Virology* 284(1), 70-81.
- Hüssy, P., Mous, J and Jacobsen, H. (1994) Hepatitis C Virus Core Protein: Carboxy-Terminal Boundaries of Two Processed Species Suggest Cleavage by a Signal Peptide Peptidase. *Virology* 224(1), 93-194.
- Ide, T., Yahagi, N., Matsuzaka, T., Nakakuki, M., Yamamoto, T., Nakagawa, Y., Takahashi, A., Suzuki, H., Sone, H., Toyoshima, H., Fukamizu, A and Yamada, N. (2004) SREBPs suppress IRS-2-mediated insulin signalling in the liver. *Nature Cell Biology* 6(4), 351-357.
- Ide, T., Shimano, H., Yoshikawa, T., Yahagi, N., Amemiya-Kudo, M., Matsuzaka, T., Nakakuki, M., Yatoh, S., Iizuka, Y., Tomita, S., Ohashi, K., Takahashi, A., Sone, H., Gotoda, T., Osuga, J., Ishibashi, S and Yamada, N. (2003) Cross-Talk between Peroxisome Proliferator-Activated Receptor (PPAR) {alpha} and Liver X Receptor (LXR) in Nutritional Regulation of Fatty Acid Metabolism. II. LXRs Suppress Lipid Degradation Gene Promoters through Inhibition of PPAR Signaling. *Mol Endocrinol* 17(7), 1255-1267.

- Ip, E., Robertson, G., Hall, P., Kirsch, R and Leclercq, I. (2003) Central role of PPAR α -dependent hepatic lipid turnover in dietary steatohepatitis in mice. *Hepatology* 38(1), 123-132.
- Ito, T and Lai, M. (1997) Determination of the secondary structure of and cellular protein binding to the 3'-untranslated region of the hepatitis C virus RNA genome. *J. Virol.* 71(11), 8698-8706.
- Ito, T., Mukaigawa, J., Zuo, J., Hirabayashi, Y., Mitamura, K and Yasui, K. (1996) Cultivation of hepatitis C virus in primary hepatocyte culture from patients with chronic hepatitis C results in release of high titre infectious virus. *J Gen Virol* 77(5), 1043-1054.
- Ito, T., Tahara, S and Lai, M. (1998) The 3'-Untranslated Region of Hepatitis C Virus RNA Enhances Translation from an Internal Ribosomal Entry Site. *J. Virol.* 72(11), 8789-8796.
- Jump, D. (2004) Fatty Acid Regulation of Gene Transcription. *Critical Reviews in Clinical Laboratory Sciences* V41(1), 41-78.
- Kapadia, S and Chisari, F. (2005) Hepatitis C virus RNA replication is regulated by host geranylgeranylation and fatty acids. *PNAS* 102(7), 2561-2566.
- Kato, N., Ikeda, M., Mizutani, T., Sugiyama, K., Noguchi, M., Hirohashi, S and Shimotohno, K. (1996) Replication of Hepatitis C Virus in Cultured Non-neoplastic Human Hepatocytes. *Cancer Science* 87 787-792.
- Kato, T., Date, T., Miyamoto, M., Zhao, Z., Mizokami, M and Wakita, T. (2005) Nonhepatic Cell Lines HeLa and 293 Support Efficient Replication of the Hepatitis C Virus Genotype 2a Subgenomic Replicon. *J. Virol.* 79(1), 592-596.
- Kato, T., Akihiro, F., Miyamoto, Michiko., Date, T., Yasui, K., Hiramoto, J., Nagayama, K., Tanaka, Teruji and Wakita, T. (2001) Sequence analysis of hepatitis C virus isolated from a fulminant hepatitis patient. *Journal of Medical Virology* 64(3), 334-339.
- Kato, T., Miyamoto, M., Furusaka, A., Tokushige, K., Mizokami, M and Wakita, T. (2003) Efficient replication of the genotype 2a hepatitis C virus subgenomic replicon. *Gastroenterology* 125(6), 1808-1817.
- Kersten, S. (2002) Effects of fatty acids on gene expression: role of peroxisome proliferator-activated receptor , liver X receptor and sterol regulatory element-binding protein-1c. *Proceedings of the Nutrition Society* 61(3), 371-374.

- Kim, J., Lin, C., Fox, T., Dwyer, M., Landro, J., Chambers, S., Markland, W., Lepre, C and O'Malley, E. (1996) Crystal Structure of the Hepatitis C Virus NS3 Protease Domain Complexed with a Synthetic NS4A Cofactor Peptide. *Cell* 87(2), 343-355.
- Kim, D., Han, J and Choe, J. (1995) C-Terminal Domain of the Hepatitis C Virus NS3 Protein Contains an RNA Helicase Activity. *Biochemical and Biophysical Research Communications* 215(1), 160-166.
- Kliwer, K., Noonan, D., Heyman, R and Evans, R. (1992) Convergence of 9-cis retinoic acid and peroxisome proliferator signalling pathways through heterodimer formation of their receptors. *Nature* 358, 771-774.
- Kolykhalov, A., Agapov, E., Blight, K., Mihalik, K., Feinstone, S and Rice, C. (1997) Transmission of Hepatitis C by Intrahepatic Inoculation with Transcribed RNA. *Science* 277(5325), 570-574.
- Kolykhalov, A., Feinstone, S and Rice, C. (1996) Identification of a highly conserved sequence element at the 3' terminus of hepatitis C virus genome RNA. *J. Virol.* 70(6), 3363-3371.
- Kolykhalov, A., Mihalik, K., Feinstone, S and Rice, C. (2000) Hepatitis C Virus-Encoded Enzymatic Activities and Conserved RNA Elements in the 3' Nontranslated Region Are Essential for Virus Replication In Vivo. *J. Virol.* 74(4), 2046-2051.
- Koutsoudakis, G., Herrmann, E., Kallis, S., Bartenschlager, R and Pietschmann, T. (2006) The level of CD81 cell surface expression is a key determinant for productive entry of Hepatitis C Virus into host cells. *J. Virol.*, JVI1534-06.
- Krieger, N., Lohmann, V and Bartenschlager, R. (2001) Enhancement of Hepatitis C Virus RNA Replication by Cell Culture-Adaptive Mutations. *J. Virol.* 75(10), 4614-4624.
- Kruger, M., Beger, C., Li, Q., Welch, P., Tritz, R., Leavitt, M., Barber, J and Wong-Staal, F. (2000) Identification of eIF2B γ and eIF2 γ as cofactors of hepatitis C virus internal ribosome entry site-mediated translation using a functional genomics approach. *PNAS* 97(15), 8566-8571.
- Kuhajda, F., Jenner, K., Wood, F., Hennigar, R., Jacobs, L., Dick, J and Pasternack, G. (1994) Fatty Acid Synthesis: A Potential Selective Target for Antineoplastic Therapy. *PNAS* 91(14), 6379-6383.
- Kuhajda, F. (2000) Fatty-acid synthase and human cancer: new perspectives on its role in tumor biology. *Nutrition* 16(3), 202-208.

- Kuhajda, F. (2006) Fatty Acid Synthase and Cancer: New Application of an Old Pathway *Cancer Res* 66(12), 5977-5980.
- Kumar, D., Fung, C and George, J. (2002) Hepatitis C virus genotype 3 is cytopathic to hepatocytes: Reversal of hepatic steatosis after sustained therapeutic response. *Hepatology* 36(5), 1266-1272.
- Kwiterovich, P. (2000) The metabolic pathways of high-density lipoprotein, low-density lipoprotein, and triglycerides: a current review. *The American Journal of Cardiology* 86(12, Supplement 1), 5-10.
- Laemmli, U. (1970) Cleavage of structural proteins during the assembly of the head of bacteriophage T4. *Nature* 227, 570-574.
- Lanford, R., Sureau, C., Jacob, J., White, R and Fuerst, T. (1994) Demonstration of in vitro infection of chimpanzee hepatocytes with hepatitis C virus using strand-specific RT/PCR. *Virology* 202(2), 606-614.
- Le Jossic-Corcus, C., Zaghini, I., Logette, E., Shechter, I and Bournot, P. (2005) Hepatic farnesyl diphosphate synthase expression is suppressed by polyunsaturated fatty acids. *Biochem J.* 385(3), 787-94.
- Lee, W., Ishikawa, M and Ahlquist, P. (2001) Mutation of Host $\Delta 9$ Fatty Acid Desaturase Inhibits Brome Mosaic Virus RNA Replication between Template Recognition and RNA Synthesis. *J. Virol.* 75(5), 2097-2106.
- Leu, G., Lin, T and Hsu, J. (2004) Anti-HCV activities of selective polyunsaturated fatty acids. *Biochemical and Biophysical Research Communications* 318(1), 275-280.
- Lesburg, C., Ferrari, E., Hong, Z., Mannarino, A and Weber, P. (1999) Crystal structure of the RNA-dependent RNA polymerase from hepatitis C virus reveals a fully encircled active site. *Nature Structural and Molecular Biology* 6(10), 937-943.
- Lettéron, P., Sutton, A., Mansouri, A., Fromenty, B and Pessayre, D. (2003) Inhibition of microsomal triglyceride transfer protein: Another mechanism for drug-induced steatosis in mice. *Hepatology* 38(1), 133-140.
- Li, Y., Webster-Cyriaque, J., Tomlinson, C., Yohe, M and Kenney, S. (2004) Fatty Acid Synthase Expression Is Induced by the Epstein-Barr Virus Immediate-Early Protein BRLF1 and Is Required for Lytic Viral Gene Expression. *J. Virol.* 78(8), 4197-4206.
- Lin, C., Lindenbach, B., Pragai, B., McCourt, D and Rice, C. (1994) Processing in the hepatitis C virus E2-NS2 region: identification of p7 and two distinct E2-specific products with different C termini. *J. Virol.* 68(8), 5063-5073.

- Lin, C., Wu, J., Hsiao, K and Su, M. (1997) The hepatitis C virus NS4A protein: interactions with the NS4B and NS5A proteins. *J. Virol.* 71(9), 6465-6471.
- Lo S-Y, M.F., Hwang S.B, Lai M.M.C, Ou J-H. (1995) Differential subcellular localization of hepatitis C virus core gene products. *Virology* 213(2), 455-461.
- Lohmann, V., Hoffmann, S., Herian, U., Penin, F and Bartenschlager, R. (2003) Viral and Cellular Determinants of Hepatitis C Virus RNA Replication in Cell Culture. *J. Virol.* 77(5), 3007-3019.
- Lohmann, V., Körner, F., Koch, J., Herian, U., Theilmann, L and Bartenschlager, R. (1999) Replication of Subgenomic Hepatitis C Virus RNAs in a Hepatoma Cell Line. *Science* 285(5424), 110-113.
- Lopez, C., Moratorio, G., Lopez, L., Vasquez, S., Garcia-Aguirre, L and Chunga, A. (2005) Hepatitis C virus F protein sequence reveals a lack of functional constraints and a variable pattern of amino acid substitution. *J Gen Virol* 86(1), 115-120.
- Lundin, M., Lindstrom, H., Gronwall, C and Persson, M. (2006) Dual topology of the processed hepatitis C virus protein NS4B is influenced by the NS5A protein. *J Gen Virol* 87(11), 3263-3272.
- Luo, G. (1999) Cellular Proteins Bind to the Poly(U) Tract of the 3' Untranslated Region of Hepatitis C Virus RNA Genome. *Virology* 256(1), 105-118.
- Ma, D., Seo, J., Switzer, K., Fan, Y., McMurray, D., Lupton, J and Chapkin, R. (2004) n-3 PUFA and membrane microdomains: a new frontier in bioactive lipid research. *The Journal of Nutritional Biochemistry* 15(11), 700-706.
- Macdonald, A and Harris, M. (2004) Hepatitis C virus NS5A: tales of a promiscuous protein. *J Gen Virol* 85(9), 2485-2502.
- Macdonald, A., K. Crowder, A. Street, C. McCormick, K. Saksela and Harris M. 2003. The hepatitis C virus NS5A protein inhibits activating protein-1 function by perturbing Ras-ERK pathway signalling. *J. Biol. Chem.* 278:17775-17784
- Mamiya, N and Worman, H.J. (1999) Hepatitis C Virus Core Protein Binds to a DEAD Box RNA Helicase. *J. Biol. Chem.* 274(22), 15751-15756.
- Martin, A. (2006) Hepatitis A virus: From discovery to vaccines. *Hepatology* 43(S1), S164-S172.

- Mater, M., Thelen, A., Pan, D and Jump, D. (1999) Sterol Response Element-binding Protein 1c (SREBP1c) Is Involved in the Polyunsaturated Fatty Acid Suppression of Hepatic S14 Gene Transcription. *J. Biol. Chem.* 274(46), 32725-32732.
- Matsumoto, M., Jeng, K., Zhu, N and Lai, M. (1996) Homotypic Interaction and Multimerization of Hepatitis C Virus Core Protein. *Virology* 218(1), 43-51.
- McKechnie, V., Mills, P and McCrudden, E. (2000) The NS5a gene of hepatitis C virus in patients treated with interferon-alpha *Journal of Medical Virology* 60(4), 367-378.
- McLauchlan, J. (2000) Properties of the hepatitis C virus core protein: a structural protein that modulates cellular processes. *Journal of Viral Hepatitis* 7 2-14.
- McLauchlan, J., Lemberg, M., Hope, G and Martoglio, B. (2002) Intramembrane proteolysis promotes trafficking of hepatitis C virus core protein to lipid droplets. *EMBO J.* 21(15), 3980-3988.
- McOmish, F., Yap, P., Dow, B., Follett, E., Seed, C., Keller, A., Cobain, T., Krusius, T., Kolho, E and Naukkarinen, R. (1994) Geographical distribution of hepatitis C virus genotypes in blood donors: an international collaborative survey. *J. Clin. Microbiol.* 32(4), 884-892.
- Mei-Ling, T. (2006) Interaction of hepatitis C virus F protein with prefoldin 2 perturbs tubulin cytoskeleton organization. *Biochemical and Biophysical Research Communications* 348(1), 271-277.
- Menendez, J., Mehmi, I., Atlas, E., Colomer, R and Lupu, R. (2004) Overexpression and hyperactivity of breast cancer-associated fatty acid synthase (oncogenic antigen-519) is insensitive to normal arachidonic fatty acid-induced suppression in lipogenic tissues but it is selectively inhibited by tumoricidal alpha-linolenic and gamma-linolenic fatty acids: a novel mechanism by which dietary fat can alter mammary tumorigenesis. *Int J Oncol* 24(6), 1369-1383.
- Merola, M., Brazzoli, M., Cocchiarella, F., Heile, J., Helenius, A., Weiner, A., Houghton, M and Abrignani, S. (2001) Folding of Hepatitis C Virus E1 Glycoprotein in a Cell-Free System. *J. Virol.* 75(22), 11205-11217.
- Mihm, S., Hartmann, H and Ramadori, G. (1997) Analysis of Histopathological manifestations of chronic hepatitis C virus infection with respect to virus genotype. *Hepatology* 25, 735-739.

- Miller, R and Purcell, R. (1990) Hepatitis C Virus Shares Amino Acid Sequence Similarity with Pestiviruses and Flaviviruses as Well as Members of Two Plant Virus Supergroups. *PNAS* 87(6), 2057-2061.
- Moradpour, D and Penin, F. (2005) Function follows form: The structure of the N-terminal domain of HCV NS5A. *Hepatology* 42(3), 732-735.
- Moriya, K., Todoroki, T., Tsutsumi, T., Fujie, H., Shintani, Y., Miyoshi, H., Ishibashi, K., Takayama, T., Makuuchi, M and Watanabe, K. (2001) Increase in the Concentration of Carbon 18 Monounsaturated Fatty Acids in the Liver with Hepatitis C: Analysis in Transgenic Mice and Humans. *Biochemical and Biophysical Research Communications* 281(5), 1207-1212.
- Mosmann, T. (1983) Rapid colorimetric assay for cellular growth and survival: Application to proliferation and cytotoxicity assays. *Journal of Immunological Methods* 65(1-2), 55-63.
- Murakami, K., Kageyama, T., Kamoshita, N and Nomoto, A. (2001) Down-regulation of translation driven by hepatitis C virus internal ribosomal entry site by the 3' untranslated region of RNA. *Archives of Virology* V146(4), 729-741.
- Neddermann, P., Clementi, A and De Francesco, R. (1999) Hyperphosphorylation of the Hepatitis C Virus NS5A Protein Requires an Active NS3 Protease, NS4A, NS4B, and NS5A Encoded on the Same Polyprotein. *J. Virol.* 73(12), 9984-9991.
- Nielsen, S., Bassendine, M., Burt, A., Martin, C., Pumeechockchai, W and Toms, G. (2006) Association between Hepatitis C Virus and Very-Low-Density Lipoprotein (VLDL)/LDL Analyzed in Iodixanol Density Gradients 80 (5): 2418-2428
- Neuman, M., Benhamou, J., Malkiewicz, I., Ibrahim, A., Valla, D., Martinot-Peignoux, M., Asselah, T., Bourliere, M., Katz, G., Shear, N and Marcellin, P. (2002) Kinetics of serum cytokines reflect changes in the severity of chronic hepatitis C presenting minimal fibrosis. *Journal of Viral Hepatitis* 9 134-140.
- Noriko, Y., Akira, T., Tetsuya, Y., Mikihiro, T., Hiroyuki, S., Takao, T and Takayasu, D. (1996) Genetic Organization and Diversity of the 3' Noncoding Region of the Hepatitis C Virus Genome. *Virology* 223(1), 255-261.
- Owsianka, A and Patel, A. (1999) Hepatitis C Virus Core Protein Interacts with a Human DEAD Box Protein DDX3. *Virology* 257(2), 330-340.

- Pai, J., Guryev, O., Brown, M and Goldstein, J. (1998) Differential Stimulation of Cholesterol and Unsaturated Fatty Acid Biosynthesis in Cells Expressing Individual Nuclear Sterol Regulatory Element-binding Proteins. *J. Biol. Chem.* 273(40), 26138-26148.
- Pallaoro, M., Lahm, A., Biasiol, G., Brunetti, M., Nardella, C., Orsatti, L., Bonelli, F., Orru, S., Narjes, F and Steinkuhler, C. (2001) Characterization of the Hepatitis C Virus NS2/3 Processing Reaction by Using a Purified Precursor Protein. *J. Virol.* 75(20), 9939-9946.
- Palmer, C., Griffin, K., Raucy, J and Johnson, E. (1998) Peroxisome Proliferator Activated Receptor-alpha Expression in Human Liver. *Mol Pharmacol* 53(1), 14-22.
- Pan, M., Cederbaum, A., Zhang, Y., Ginsberg, H., Williams, K and Fisher, E. (2006) Lipid peroxidation and oxidant stress regulate hepatic apolipoprotein B degradation and VLDL production. *The Journal of Clinical Investigation* 113(9), 1277-1287.
- Patel, J., Patel, A and Mclauchlan, J. (2001) The Transmembrane Domain of the Hepatitis C Virus E2 Glycoprotein Is Required for Correct Folding of the E1 Glycoprotein and Native Complex Formation. *Virology* 279(1), 58-68.
- Patton, H., Behling, C., Bylund, D., Blatt, L., Vallée, M., Heaton, S., Conrad, A., Pockros P and McHutchison, J. (2004) The impact of steatosis on disease progression and early and sustained treatment response in chronic hepatitis C patients. *Journal of Hepatology* 40(3), 484-490. Pawlotsky, J.-M. (2004) Pathophysiology of hepatitis C virus infection and relates liver disease. *Trends in Microbiology* 12(2), 96 - 102.
- Pelletier, J., Racaniello, V and N, Sonenberg. (1988) Cap-independent translation of poliovirus mRNA is conferred by sequence elements within the 5' noncoding region. *Molecular and Cellular Biology* 8(3), 1103-1112.
- Perlemuter, G., Letteron, A., Vona, P., Topilco, G., Chretien, A., Koike, Y., Pessayre, K., Chapman, D., Barba, J and Brechot, C. (2002) Hepatitis C virus core protein inhibits microsomal triglyceride transfer protein activity and very low density lipoprotein secretion: a model of viral-related steatosis. *FASEB J.* 16(2), 185-194.
- Pietschmann, T., Lohmann, V., Rutter, G., Kurpanek, K and Bartenschlager, R. (2001) Characterization of Cell Lines Carrying Self-Replicating Hepatitis C Virus RNAs. *J. Virol.* 75(3), 1252-1264.
- Pileri, P., Uematsu, Y., Campagnoli, S., Galli, G., Falugi, F., Petracca, R., Weiner, A., Houghton, M., Rosa, D., Grandi, G and Abrignani, S. (1998) Binding of Hepatitis C Virus to CD81. *Science* 282(5390), 938-941.

- Pitman, M., Suits, F., MacKerell, A and Feller, S. (2004) Molecular-Level Organization of Saturated and Polyunsaturated Fatty Acids in a Phosphatidylcholine Bilayer Containing Cholesterol. *Biochemistry* 43(49), 15318-15328.
- Pizer, E., Thupari, J., Han, W., Pinn, M., Chrest, F., Frehywot, G., Townsend, C and Kuhajda, F. (2000) Malonyl-Coenzyme-A Is a Potential Mediator of Cytotoxicity Induced by Fatty-Acid Synthase Inhibition in Human Breast Cancer Cells and Xenografts. *Cancer Res* 60(2), 213-218.
- Pol, A., Luetterforst, R., Lindsay, M., Heino, S., Ikonen, E and Parton, R. (2001) A Caveolin Dominant Negative Mutant Associates with Lipid Bodies and Induces Intracellular Cholesterol Imbalance. *J. Cell Biol.* %R 10.1083/jcb.152.5.1057 152(5), 1057-1070.
- Polyak, S., McArdle, S., Liu, S., Sullivan, D., Chung, M., Hofgartner, W., Carithers, R., McMahon, B., Mullins, J., Corey, L and Gretch, D. (1998) Evolution of Hepatitis C Virus Quasispecies in Hypervariable Region 1 and the Putative Interferon Sensitivity-Determining Region during Interferon Therapy and Natural Infection. *J. Virol.* 72(5), 4288-4296.
- Quadri, R., Rubbia-Brandt, L., Abid, K and Negro, F. (2001) Detection of the negative-strand hepatitis C virus RNA in tissues: implications for pathogenesis. *Antiviral Research* 52(2), 161-171.
- Quinkert, D., Bartenschlager, R and Lohmann, V. (2005) Quantitative Analysis of the Hepatitis C Virus Replication Complex. *J. Virol.* 79(21), 13594-13605.
- Ray, R and Ranjit, R. (1996) Suppression of Apoptotic Cell Death by Hepatitis C Virus Core Protein. *Virology* 226(2), 176-182.
- Reed, K., Grakoui, A and Rice, C. (1995) Hepatitis C virus-encoded NS2-3 protease: cleavage-site mutagenesis and requirements for bimolecular cleavage. *J. Virol.* 69(7), 4127-4136.
- Reed, K., Xu, J and Rice, C. (1997) Phosphorylation of the hepatitis C virus NS5A protein in vitro and in vivo: properties of the NS5A-associated kinase. *J. Virol.* 71(10), 7187-7197.
- Reynolds, J., Kettinen, H., Grace, K., Clarke, B., Carroll, A., Rowlands, D and Jackson, R. (1995) Unique features of internal initiation of hepatitis C virus RNA translation. *EMBO J.* 14(23), 6010-6020.
- Robertson B., Howard, C., Brettin, T., Bukh, J., Gaschen, B., Gojobori, T., Maertens, G., Mizokami, M., Nainan, O., Netesov, S., Nishioka, K., Shin-i, T., Simmonds, P., Smith, D., Stuyver, L and Weiner, A. (1998) Classification, nomenclature, and database development for hepatitis C

virus (HCV) and related viruses: proposals for standardization. *Archives of Virology* V143(12), 2493-2503.

- Rubbia-Brandt, L., Leandro, G., Spahr, L., Giostra, E., Quadri, R., Male, P and Negro, F. (2001) Liver steatosis in chronic hepatitis C: a morphological sign suggesting infection with HCV genotype 3. *Histopathology* 39(2), 119-124.
- Sakai, A., Claire, M., Faulk, K., Govindarajan, S., Emerson, S., Purcell, R and Bukh, J. (2003) The p7 polypeptide of hepatitis C virus is critical for infectivity and contains functionally important genotype-specific sequences. *PNAS* 100(20), 11646-11651.
- Sakai, J., Nohturfft, A., Cheng, D., Ho, Y., Brown, M and Goldstein, J. (1997) Identification of Complexes between the COOH-terminal Domains of Sterol Regulatory Element-binding Proteins (SREBPs) and SREBP Cleavage-Activating Protein. *J. Biol. Chem.* 272(32), 20213-20221.
- Sakamoto, M., Akahane, Y., Tsuda, F., Tanaka, T., Woodfield, D and Okamoto, H. (1994) Entire nucleotide sequence and characterization of a hepatitis C virus of genotype V/3a. *J Gen Virol* 75(7), 1761-1768.
- Sambrook, J and Maniatis. (1989) *Molecular Cloning: A laboratory manual*, Second Edition edn. Edited by N. Ford, C Nolan and M. Ferguson: Cold Spring Harbor Laboratory Press, USA.
- Santolini, E., Migliaccio, G and La Monica, N. (1994) Biosynthesis and biochemical properties of the hepatitis C virus core protein. *J. Virol.* 68(6), 3631-3641.
- Santolini, E., Pacini, L., Fipaldini, C., Migliaccio, G and Monica, N. (1995) The NS2 protein of hepatitis C virus is a transmembrane polypeptide. *J. Virol.* 69(12), 7461-7471.
- Scarselli, E., Cerino, R., Roccasecca, R., Acali, S., Filocamo, G., Traboni, C., Nicosia, A., Cortese, R and Vitelli, A. (2002) The human scavenger receptor class B type I is a novel candidate receptor for the hepatitis C virus. *EMBO J.* 21(19), 5017-5025.
- Schiffrin, E., Benkirane, K., Iglarz, M and Diep, Q. (2003) Peroxisome Proliferator-Activated Receptors: Vascular and Cardiac Effects in Hypertension. *Hypertension* 42(2), 1-5.
- Schlesinger, M and Malfer, C. (1982) Cerulenin blocks fatty acid acylation of glycoproteins and inhibits vesicular stomatitis and Sindbis virus particle formation. *J. Biol. Chem.* 257(17), 9887-9890.

- Schley, P., Jijon, H., Robinson, L and Field, C. (2005) Mechanisms of omega-3 fatty acid-induced growth inhibition in MDA-MB-231 human breast cancer cells. *Breast Cancer Research and Treatment* 92(2), 187-195.
- Schmidt-Mende, J., Bieck, E., Hugle, T., Penin, F., Rice, C., Blum, H and Moradpour, D. (2001) Determinants for Membrane Association of the Hepatitis C Virus RNA-dependent RNA Polymerase. *J. Biol. Chem.* 276(47), 44052-44063.
- Schoonjans, K., Staels, B and Auwerx, J. (1996) The peroxisome proliferator activated receptors (PPARs) and their effects on lipid metabolism and adipocyte differentiation. *Biochimica et Biophysica Acta (BBA) - Lipids and Lipid Metabolism* 1302(2), 93-109.
- Schwer, B., Ren, S., Pietschmann, T., Kartenbeck, J., Kaehlcke, K., Bartenschlager, R., Yen, T and Ott, M. (2004) Targeting of Hepatitis C Virus Core Protein to Mitochondria through a Novel C-Terminal Localization Motif. *J. Virol.* 78(15), 7958-7968.
- Seeff, L. (1997) Natural History of Hepatitis C. *Hepatology* 26(3 Suppl.1), 21S-28S.
- Seipp, S., Mueller, H., Pfaff, E., Stremmel, W., Theilmann, L and Goeser, T. (1997) Establishment of persistent hepatitis C virus infection and replication in vitro. *J Gen Virol* 78(10), 2467-2476.
- Shelness, G., Ingram, M., Huang, X and DeLozier, J. (1999) Apolipoprotein B in the Rough Endoplasmic Reticulum: Translation, Translocation and the Initiation of Lipoprotein Assembly. *J. Nutr.* 129(2), 456.
- Shepard, C., Simard, E., Finelli, L., Fiore, A and Bell, B. (2006) Hepatitis B Virus Infection: Epidemiology and Vaccination. *Epidemiol Rev* 28(1), 112-125.
- Shi, S., Lee, K., Aizaki, H., Hwang, S and Lai, M. (2003) Hepatitis C Virus RNA Replication Occurs on a Detergent-Resistant Membrane That Cofractionates with Caveolin-2. *J. Virol.* 77(7), 4160-4168.
- Shi, S., Polyak, S., Tu, H., Taylor, D., Gretch, D and Lai, M. (2002) Hepatitis C Virus NS5A Colocalizes with the Core Protein on Lipid Droplets and Interacts with Apolipoproteins. *Virology* 292(2), 198-210.
- Shimano, H. (2001) Sterol regulatory element-binding proteins (SREBPs): transcriptional regulators of lipid synthetic genes. *Progress in Lipid Research* 40(6), 439-452.

- Shimizu, Y., Igarashi, H., Kiyohara, T., Shapiro, M., Wong, D.C., Purcell, R and Yoshikura, H. (1998) Infection of a chimpanzee with hepatitis C virus grown in cell culture. *J Gen Virol* 79(6), 1383-1386.
- Shimomura, I., Shimano, H., Horton, J., Goldstein, J and Brown, M. (1997) Differential Expression of Exons 1a and 1c in mRNAs for Sterol Regulatory Element Binding Protein-1 in Human and Mouse Organs and Cultured Cells. *J. Clin. Invest.* 99(5), 838-845.
- Shimomura, I., Shimano, H., Korn, B., Bashmakov, Y and Horton, J. (1998) Nuclear Sterol Regulatory Element-binding Proteins Activate Genes Responsible for the Entire Program of Unsaturated Fatty Acid Biosynthesis in Transgenic Mouse Liver. *J. Biol. Chem.* 273(52), 35299-35306.
- Shinya, S., Tohru, N., Makoto, H., Hiroshi, H and Kunitada, S. (2000) Cleavage of Hepatitis C Virus Nonstructural Protein 5A by a Caspase-like Protease(s) in Mammalian Cells. *Virology* 270(2), 476-487.
- Shirota, Y., Luo, H., Qin, W., Kaneko, S., Yamashita, T., Kobayashi, K and Murakami, S. (2002) Hepatitis C Virus (HCV) NS5A Binds RNA-dependent RNA Polymerase (RdRP) NS5B and Modulates RNA-dependent RNA Polymerase Activity. *J. Biol. Chem.* 277(13), 11149-11155.
- Shukla, D., Chaturvedi, S., Cao, J and Hoyne, P. (1998) Complete Nucleotide Sequence of the genome of Hepatitis C Virus type 3a (CB). Unpublished AF046866.
- Simmonds, P., Alter, H., Bonino, F., Bradley, D., Brechot, C., Brouwer, J., Chan, S-W., Chayama, K., Chen, D-S., Choo, Q-L., Colombo, M., Cuypers, H., Date, T., Dusheiko, G., Esteban, J., Fay, O., Hadziyannis, S., Han, J., Hatzakis, A., Holmes, E., Hotta, H., Houghton, M., Irvine, B., Kohara, M., Kolberg, J., Kuo, G., Lau, J., Lelie, P., Maertens, G., McOmish, F., Miyamura, T., Mizokami, M., Nomoto, A., Prince, A., Reesink, H., Rice, C., Roggendorf, M., Schalm, S., Shikata, T., Shimotohno, K., Stuyver, L., Trépo, C., Weiner, A., Yap, P and Urdea, M. (1994) A proposed system for the nomenclature of hepatitis C viral genotypes. *Hepatology* 19(5), 1321-1324.
- Smith, S. (2002) Peroxisome proliferator-activated receptors and the regulation of mammalian lipid metabolism. *Biochem. Soc. Trans.* 30(6), 1086-1090.
- Spangberg, K., Wiklund, L and Schwartz, S. (2001) Binding of the La autoantigen to the hepatitis C virus 3' untranslated region protects the RNA from rapid degradation in vitro. *J Gen Virol* 82(1), 113-120.
- Stapleton, J., Williams, C and Xiang, J. (2004) GB Virus Type C: a Beneficial Infection? *J. Clin. Microbiol.* 42(9), 3915-3919.

- Steinmann, E., Penin, F., Kallis, S., Patel, A., Bartenschlager, R and Pietschmann, T. (2007) Hepatitis C Virus p7 Protein Is Crucial for Assembly and Release of Infectious Virions. *PLoS Pathogens* 3(7), e103.
- Stillwell, W and Wassall, S. (2003) Docosahexaenoic acid: membrane properties of a unique fatty acid. *Chemistry and Physics of Lipids* 126(1), 1-27.
- Stulnig, T., Huber, J., Leitinger, N., Imre, E., Angelisova, P., Nowotny, P and Waldhausl, W. (2001) Polyunsaturated Eicosapentaenoic Acid Displaces Proteins from Membrane Rafts by Altering Raft Lipid Composition. *J. Biol. Chem.* 276(40), 37335-37340.
- Su, A., Pezacki, J., Wodicka, L., Brideau, A., Supekova, L., Thimme, R., Wieland, S., Bukh, J., Purcell, R., Schultz, P and Chisari, F. (2002) Genomic analysis of the host response to hepatitis C virus infection. *PNAS* 99(24), 15669-15674.
- Subrat, K. (2006) Hepatitis E virus. *Reviews in Medical Virology* 9999(9999), n/a.
- Suzich, J., Tamura, J., Palmer-Hill, F., Warrener, P., Grakoui, A., Rice, C., Feinstone, S and Collett, M. (1993) Hepatitis C virus NS3 protein polynucleotide-stimulated nucleoside triphosphatase and comparison with the related pestivirus and flavivirus enzymes. *J. Virol.* 67(10), 6152-6158.
- Tada, H., Shiho, O., Kuroshima, K., Koyama, M and Tsukamoto, K. (1986) An improved colorimetric assay for interleukin 2. *Journal of Immunological Methods* 93(2), 157-165.
- Tai, C., Chi, W., Chen, D and Hwang, L. (1996) The helicase activity associated with hepatitis C virus nonstructural protein 3 (NS3). *J. Virol.* 70(12), 8477-8484.
- Takuya, U., Fumihiko, Y., Chiho, M., Yukiko, H., Kazuaki, C and Michinori, K. (2006) Serine palmitoyltransferase inhibitor suppresses HCV replication in a mouse model. *Biochemical and Biophysical Research Communications* 346(1), 67-73.
- Tanaka, T., Kato, N., Cho, M., Sugiyama, K and Shimotohno, K. (1996) Structure of the 3' terminus of the hepatitis C virus genome. *J. Virol.* 70(5), 3307-3312.
- Tanabe, Y and Sakamoto, N. (2004). Synergistic Inhibition of Intracellular Hepatitis C Virus Replication by Combination of Ribavirin and Interferon. *The Journal of Infectious Diseases* 189(7): 1129-1139.

- Takamizawa, A., Fuke, I., Manabe, S., Murakami, S., Fujita, J., Onishi, E., Andoh, T., Yoshida, I and Okayama, H. (1991) Structure and organization of the hepatitis C virus genome isolated from human carriers. *Journal of Virology* 65(3), 1105-1113.
- Tanji, Y., Kaneko, T., Satoh, S and Shimotohno, K. (1995) Phosphorylation of hepatitis C virus-encoded nonstructural protein NS5A. *J. Virol.* 69(7), 3980-3986.
- Tarantino, G., Saldalamacchia, G., Conca, P and Arena, A. (2007) Non-alcoholic fatty liver disease: Further expression of the metabolic syndrome. *Journal of Gastroenterology and Hepatology* 22 293-303.
- Targett-Adams, P., Chambers, D., Gledhill, S., Hope, R., Coy, J., Girod, A and McLauchlan, J. (2003) Live Cell Analysis and Targeting of the Lipid Droplet-binding Adipocyte Differentiation-related Protein. *J. Biol. Chem.* 278(18), 15998-16007.
- Targett-Adams, P and McLauchlan, J. (2005) Development and characterization of a transient-replication assay for the genotype 2a hepatitis C virus subgenomic replicon *J Gen Virol* 86(11), 3075-3080.
- Taylor, J. (2006) Hepatitis delta virus. *Virology 50th Anniversary Issue* 344(1), 71-76.
- Tetsuya, S., Seiji, H., Mitsuo, Y., Takuya, I., Toshiharu, H., Yoshifumi, T., Hitoshi, S and Harumasa, O. (2005) Apoptosis in human pancreatic cancer cells induced by eicosapentaenoic acid. *21(10)*, 1010-1017.
- Tomei, L., Failla, C., Santolini, E., De Francesco, R and La Monica, N. (1993) NS3 is a serine protease required for processing of hepatitis C virus polyprotein. *J. Virol.* 67(7), 4017-4026.
- Towbin, H. (1979) Electrophoretic transfer of proteins from polyacrylamide gels to nitrocellulose sheets: procedure and some applications. *PNAS* 76, 4350-4354.
- Tsuchihara, K., Tanaka, T., Hijikata, M., Kuge, S., Toyoda, H., Nomoto, A., Yamamoto, N and Shimotohno, K. (1997) Specific interaction of polypyrimidine tract-binding protein with the extreme 3'-terminal structure of the hepatitis C virus genome, the 3'X. *J. Virol.* 71(9), 6720-6726.
- Uysal, T., Marino, M and Hotamisligil, G. (1997) Protection from obesity-induced insulin resistance in mice lacking TNF- function. *Nature* 389(6651), 610-614.

- van 't Wout, A., Swain, J., Schindler, M., Rao, U., Pathmajeyan, M., Mullins, J and Kirchhoff, F. (2005) Nef Induces Multiple Genes Involved in Cholesterol Synthesis and Uptake in Human Immunodeficiency Virus Type 1-Infected T Cells. *J. Virol.* 79(15), 10053-10058.
- van Doorn, L., Capriles, I., Maertens, G., DeLeys, R., Murray, K., Kos, T., Schellekens, H and Quint, W. (1995) Sequence evolution of the hypervariable region in the putative envelope region E2/NS1 of hepatitis C virus is correlated with specific humoral immune responses. *J. Virol.* 69(2), 773-778.
- Wakita, T., Kato, T., Date, T., Miyamoto, M., Zhao, Z., Murthy, K., Habermann, A., Kräusslich, H-G., Mizokami, M., Bartenschlager, R and Liang, Jake. (2005) Production of infectious hepatitis C virus in tissue culture from a cloned viral genome. *Nature medicine* 11(7), 791-796.
- Wang, A-G., Kim, J-M., Hwang, S-B., Yu, D-Y and Lee, D-S. (2006) Expression of hepatitis C virus nonstructural 4B in transgenic mice *Experimental and Molecular Medicine* 38(3), 241-246.
- Wang, C., Keller, B., Huang, H., Brown, M., Goldstein, J and Ye, J. (2005) Identification of FBL2 As a Geranylgeranylated Cellular Protein Required for Hepatitis C Virus RNA Replication. *Molecular Cell* 18(4), 425-434.
- Wang, T., Rijnbrand, R and Lemon, S. (2000) Core Protein-Coding Sequence, but Not Core Protein, Modulates the Efficiency of Cap-Independent Translation Directed by the Internal Ribosome Entry Site of Hepatitis C Virus. *J. Virol.* 74(23), 11347-11358.
- Wang, C., Ali, N and Siddiqui, A. (1995) An RNA pseudoknot is an essential structural element of the internal ribosome entry site located within the hepatitis C virus 5' noncoding region. *RNA* 1(5), 526-537.
- Wejstal, R. (1995) Immune-mediated liver damage in chronic hepatitis C. *Scandinavian Journal of Gastroenterology* 30, 609-613.
- Westin, J., Nordlinder, H., Lagging, M., Norkrans, G and Wejstal, R. (2002) Steatosis accelerates fibrosis development over time in hepatitis C virus genotype 3 infected patients. *Journal of Hepatology* 37(6), 837-842.
- Wiese, M., Güthoff, W., Lafrenz, M., Oesen, U., Porst, H and for the East German Hepatitis C Study Group. (2005) Outcome in a hepatitis C (genotype 1b) single source outbreak in Germany--a 25-year multicenter study. *Journal of Hepatology* 43(4), 590-598.
- Wolfrum, C., Borrmann, C., Borchers, T and Spener, F. (2001) Fatty acids and hypolipidemic drugs regulate peroxisome proliferator-activated receptors

alpha - and gamma -mediated gene expression via liver fatty acid binding protein: A signaling path to the nucleus. *PNAS* 98(5), 2323-2328.

Wolk, B., Sansonno, D., Krausslich, H., Dammacco, F., Rice, C., Blum, H and Moradpour, D. (2000) Subcellular Localization, Stability, and trans-Cleavage Competence of the Hepatitis C Virus NS3-NS4A Complex Expressed in Tetracycline-Regulated Cell Lines. *J. Virol.* 74(5), 2293-2304.

Wood, J., Frederickson, R., Fields, S and Patel, A. (2001) Hepatitis C Virus 3'X Region Interacts with Human Ribosomal Proteins. *J. Virol.* 75(3), 1348-1358.

Xavier, F., Govindarajan, S., Emerson, S., H. Purcell, R., Chisari, F and Bukh, J. (2000) Hepatitis C virus lacking the hypervariable region 1 of the second envelope protein is infectious and causes acute resolving or persistent infection in chimpanzees. *PNAS* 97(24), 13318 -13323.

Xinyue, L., Copeland, N., Gilbert, D., Jenkins, N., Londos, C and Kimmel, A. (2001) The murine perilipin gene: the lipid droplet-associated perilipins derive from tissue-specific, mRNA splice variants and define a gene family of ancient origin. *Mammalian Genome* V12(9), 741-749.

Yabe, D., Brown, M and Goldstein, J. (2002) Insig-2, a second endoplasmic reticulum protein that binds SCAP and blocks export of sterol regulatory element-binding proteins. *PNAS* 99(20), 12753-12758.

Yamada, N., Tanihara, K., Mizokami, M., Ohba, K., Takada, A., Tsutsumi, M and Date, T. (1994) Full-length Sequence of the Genome of Hepatitis C Virus Type 3a: Comparative Study With Different Genotypes. *J Gen Virol* 75(11), 3279-3284.

Yamaga, A and Ou, J. (2002) Membrane Topology of the Hepatitis C Virus NS2 Protein. *J. Biol. Chem.* 277(36), 33228-33234.

Yamaguchi, A., Tazuma, S., Nishioka, T., Ohishi, W., Hyogo, H., Nomura, S and Chayama, K. (2005) Hepatitis C Virus Core Protein Modulates Fatty Acid Metabolism and Thereby Causes Lipid Accumulation in the Liver. *Digestive Diseases and Sciences* 50(7), 1361-1371.

Yamashita, T., Kaneko, S., Shiota, Y., Qin, W., Nomura, T., Kobayashi, K and Murakami, S. (1998) RNA-dependent RNA Polymerase Activity of the Soluble Recombinant Hepatitis C Virus NS5B Protein Truncated at the C-terminal Region. *J. Biol. Chem.* 273(25), 15479-15486.

- Yanagi, M., Emerson, S and Bukh, J. (1999) Hepatitis C Virus: An Infectious Molecular Clone of a Second Major Genotype (2a) and Lack of Viability of Intertypic 1a and 2a Chimeras. *Virology* 262(1), 250-263.
- Yanagi, M., Purcell, R., Emerson, S and Bukh, J. (1997) Transcripts from a single full-length cDNA clone of hepatitis C virus are infectious when directly transfected into the liver of a chimpanzee *PNAS* 94(16), 8738-8743.
- Yanagi, M., St. Claire, M., Emerson, S., Purcell, R and Bukh, J. (1999) In vivo analysis of the 3' untranslated region of the hepatitis C virus after in vitro mutagenesis of an infectious cDNA clone. *PNAS* 96(5), 2291-2295.
- Yao, H and Ye, J. (2008) Long Chain Acyl-CoA Synthetase 3-mediated Phosphatidylcholine Synthesis Is Required for Assembly of Very Low Density Lipoproteins in Human Hepatoma Huh7 Cells *Journal of Biological Chemistry*. 283(2), 849-854,
- Yasui, K., Wakita, T., Tsukiyama-Kohara, K., Funahashi, S., Ichikawa, M., Kajita, T., Moradpour, D., Wands, J and Kohara, M. (1998) The Native Form and Maturation Process of Hepatitis C Virus Core Protein. *J. Virol.* 72(7), 6048-6055.
- Ye, J., Wang, C., Sumpter, R., Brown, M., Goldstein, J and Gale, M. (2003) Disruption of hepatitis C virus RNA replication through inhibition of host protein geranylgeranylation *PNAS* 100(26), 15865-15870.
- Yi, M and Lemon, S. (2003) 3' Nontranslated RNA Signals Required for Replication of Hepatitis C Virus RNA. *J. Virol.* 77(6), 3557-3568.
- Yoon Ki, K., Song, H and Sung, K. (2002) Domains I and II in the 5' Nontranslated Region of the HCV Genome Are Required for RNA Replication. *Biochemical and Biophysical Research Communications* 290(1), 105-112.
- Yoshida, T., Hanada, T., Tokuhisa, T., Kosai, K., Sata, M., Kohara, M and Yoshimura, A. (2002) Activation of STAT3 by the Hepatitis C Virus Core Protein Leads to Cellular Transformation. *J. Exp. Med.* 196(5), 641-653.
- Yoshikawa, T., Ide, T., Shimano, H., Yahagi, N., Amemiya-Kudo, M., Matsuzaka, T., Yatoh, S., Kitamine, T., Okazaki, H., Tamura, Y., Sekiya, M., Takahashi, A., Hasty, A., Sato, R., Sone, H., Osuga, J., Ishibashi, S and Yamada, N. (2003) Cross-Talk between Peroxisome Proliferator-Activated Receptor (PPAR) α and Liver X Receptor (LXR) in Nutritional Regulation of Fatty Acid Metabolism. I. PPARs Suppress Sterol Regulatory Element Binding Protein-1c Promoter through Inhibition of LXR Signaling. *Mol Endocrinol* 17(7), 1240-1254.
- You, S., Stump, D., Branch, A and Rice, C. (2004) A cis-Acting Replication Element in the Sequence Encoding the NS5B RNA-Dependent RNA

Polymerase Is Required for Hepatitis C Virus RNA Replication. *J. Virol.* 78(3), 1352-1366.

Yu, G., Lee, K., Gao, L and Lai, M. (2006) Palmitoylation and Polymerization of Hepatitis C Virus NS4B Protein. *J. Virol.* 80(12), 6013-6023.

Zein, N. (2000) Clinical Significance of Hepatitis C Virus Genotypes. *Clin. Microbiol. Rev.* 13(2), 223-235.

Zein, N., Rakela, J., Krawitt, E., Reddy, K., Tominaga, T and Persing, D. (1996) Hepatitis C Virus Genotypes in the United States: Epidemiology, Pathogenicity, and Response to Interferon Therapy. *Ann Intern Med* 125(8), 634-639.

Zhong, J., Gastaminza, P., Cheng, G., Kapadia, S., Kato, T., Burton, D., Wieland, S., Uprichard, S., Wakita, T and Chisari, F. (2005) Robust hepatitis C virus infection in vitro. *PNAS* 102(26), 9294-9299.

Zhou, W., Simpson, P., McFadden, J., Townsend, C., Medghalchi, S., Vadlamudi, A., Pinn, M., Ronnett, G and Kuhajda, F. (2003) Fatty Acid Synthase Inhibition Triggers Apoptosis during S Phase in Human Cancer Cells. *Cancer Res* 63(21), 7330-7337.

Zhu, A. (2003) Hepatic steatosis in patients with chronic hepatitis C virus infection Another risk factor for hepatocellular carcinoma? *Cancer* 97(12), 2948-2950.

Zhuhui, H. (2006) Recent development of therapeutics for chronic HCV infection. Special Issue To Honour Professor Erik De Clercq 71(2-3), 351-362.